8-2014

World Wide Diversity of *Phytophthora capsici*

Dylan B. Storey
University of Tennessee - Knoxville, dstorey@utk.edu

To the Graduate Council:

I am submitting herewith a dissertation written by Dylan B. Storey entitled "World Wide Diversity of *Phytophthora capsici*." I have examined the final electronic copy of this dissertation for form and content and recommend that it be accepted in partial fulfillment of the requirements for the degree of Doctor of Philosophy, with a major in Life Sciences.

Kurt H. Lamour, Major Professor

We have read this dissertation and recommend its acceptance:

Albrecht Von Arnim, Todd Reynolds, Juan Luis Jurat Fuentes

Accepted for the Council:

Carolyn R. Hodges

Vice Provost and Dean of the Graduate School

(Original signatures are on file with official student records.)

8-2014

World Wide Diversity of *Phytophthora capsici*

Dylan B. Storey
University of Tennessee - Knoxville, dstorey@utk.edu

To the Graduate Council:

I am submitting herewith a dissertation written by Dylan B. Storey entitled "World Wide Diversity of *Phytophthora capsici*." I have examined the final electronic copy of this dissertation for form and content and recommend that it be accepted in partial fulfillment of the requirements for the degree of Doctor of Philosophy, with a major in Life Sciences.

Kurt H. Lamour, Major Professor

We have read this dissertation and recommend its acceptance:

Albrecht Von Arnim, Todd Reynolds, Juan Luis Jurat Fuentes

Accepted for the Council:
Carolyn R. Hodges

Vice Provost and Dean of the Graduate School

(Original signatures are on file with official student records.)

World Wide Diversity of *Phytophthora capsici*

A Dissertation Presented for the

Doctor of Philosophy

Degree

The University of Tennessee, Knoxville

Dylan B. Storey

August 2014

To the shoulder I have stood on.

Acknowledgements

I would like to thank: the University of Tennessee, Knoxville for providing me with a world class education; the Genome Sciences and Technology department for the opportunity to create and enact a non-traditional educational plan; the SCALE-IT program for providing unique professional development, education opportunities, and funding; and the USDA-NIFA programs for funding and supporting my research.

I would like to thank my committee (Dr. Albrecht Von Arnim, Dr. Todd Reynolds, Dr. Juan Luis Jurat-Fuentes) and committee chair (Dr. Kurt Lamour) for their time and input into the development and execution of this document.

I would like to thank the director of the SCALE-IT program (Dr. Harry Richards) for providing constant mentoring, support, and friendship.

I would like to thank the following members of the SCALE-IT program : Rick Weber, David Jenkins, Nick Lineback, Joe Hughs, Doug Kaylor, Sally Ellingson. Our chemically fuelled discussions were better than any class room for learning.

Finally, I would like to thank Christina Sellers for never doubting that I would finish.

"There is a single light of science, and to brighten it anywhere is to brighten it everywhere." - Isaac Asimov

Abstract

The plant pathogen *Phytophthora capsici* is a genetically diverse organism that is a global problem. It effects many crops across the *Solanacea*, *Cucurbitacea*, and*Leguminosea*. As a result of the large diversity between individuals (and by extension populations) it has been previously near impossible to make meaningful comparisons between individuals of geographically distinct locations. Here we present the results of applying Next Generation Sequencing (NGS) technologies to a representative panel of isolates. This information and data is further used to demonstrate how this diversity has a functionally relevent effect on a class of proteins responsible for the infectious process. We also demonstrate the application of these technologies and techniques to even lesser studied plant pathogen systems and how they can be used to make intelligent decisions about isolate selection for future studies.

Table of Contents

List of Tables

List of Figures

Chapter 1

Literature Review

1.1 The Plant Pathogen *Phytophthora Capsici*

1.1.1 Basic Biology

Phytophthora capsici is an aggressive filamentous plant pathogen belonging to the class Oomycota, in Clade 2b of the *Phytophthora* genus [1]. It is the cause of significant crop loss in the United States where it threatens an estimated one-billion dollars in crops annually [2]. First described on a New Mexico agricultural research station in 1922 [3]; it is the causal agent of root, crown, and fruit rot on a number of economically important crops [4]. While it was initially thought to only infect chili peppers; it has been since described on: tomato, eggplant, cucurbits, lima, and snap beans [5–11].

Phytophthora capsici is a heterothallic species where each isolate has one mating type (A1 or A2). When both mating types are in close proximity, sexual reproduction can occur [12]. Sexual reproduction results in the production of thick walled oospores that can survive harsh environmental conditions for greater than 5 years [13–15]. While this cycle is important for the pathogen to survive fallow periods and produce recombinant offspring, when under favorable conditions the pathogen produces asexual sporangia that release motile zoospores into standing water [15,16].

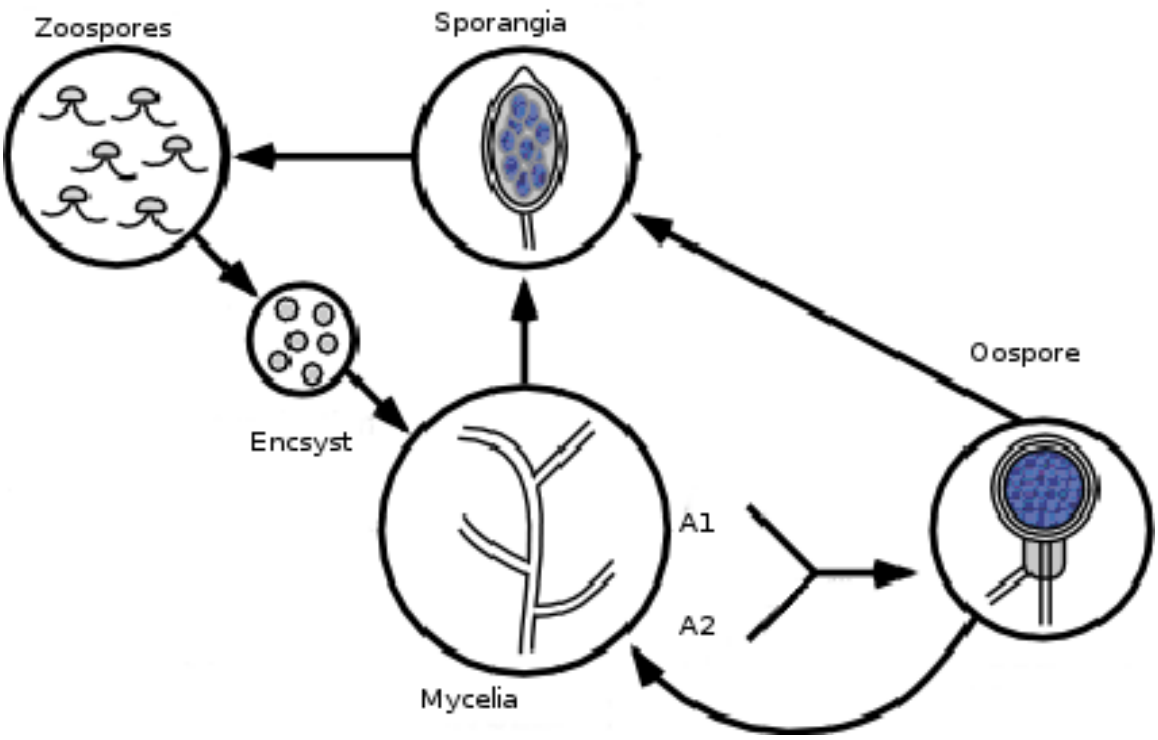

Figure 1.1: The life cycle of *Phytophthora capsici*. The pathogen grows as mycelia in the field. If it encounters mycelia of another mating type the two individuals will undergo meiosis and produce thick walled oospores. These structures allow the pathogen to survive fallow periods. Upon germination, an oospore can create both sporangia and mycelia. Both of these structures are capable of infecting new plant tissue. In the case of sporangia, the structure contains and release motile bi-flagellated zoo-spores that will encyst onto plant tissue prior to forming mycellial tissue.

This allows the pathogen to produce a poly-cyclic infection cycle and can cause entire crops to be lost in a few days [17].

1.1.2 Infection

The infectious process can start in one of two ways : the germination of an oospore, or adherence of a zoospore. In the first method, an oospore germinates resulting in the production of mycellia and sporangia. These sporangia then go on to produce and release 20-40 flagellated zoospores. These zoospores demonstrate chemotactic responses toward plants and a negative geotropism. Once these zoospores encounter

plant tissue they adhere and produce a germ-tube. This germ tube penetrates the host cuticle using secreted enzymes and colonizes the host tissue [18, 19]. Infection then goes through two distinct stages : biotrophy and necrotrophy. Early on in infection host cells do not appear to be largely affected indicating there is a local suppression of host defense responses. As the pathogen continues to develop and mature the pathogen kills infected cells and causes significant tissue damage. Upon tissue collapse, new sporangia begin emerge allowing the pathogen to disperse and begin a poly-cyclic infection cycle. In the presence of warm weather (25-30) and high relative humidity the time period between initial infection by a germ tube and sporulation is 2-3 days [17]. While the necrotrophic phase of infection causes obvious crop loss by damaging the host plant, the biotrophic phase is responsible for post harvest losses. This loss occurs because biotrophic infection may not be readily apparent during harvest and necrotrophic symptoms will not become obvious until fruit reaches a packing plant [15].

1.1.3 Pathogen Control

Genetic Resistance: Currently only a few varieties of *C. annuum* have been found to have natural host resistance to *Phytophthora capsici*. Specifically in pepper a number of studies on the genetics and inheritence of resistance have led to the identification of numerous Quantitative Trait Loci (QTLs) for resistance. Unfortunately only one land race of *Capsicum annuum*, var. Criollo de Morelos, has demonstrated near absolute resistance to all isolates of *Phytopthora capsici*. This variety of *C. annum* is not a commercial variety and the broad pathogen resistance trait appears to be complex; this means that there are currently no crops with any appreciable durable resistance to this pathogen at this time and there are not likely to be any soon as pyramiding multiple resistance QTLs requires long periods for breeding and verification.

Crop Rotation: Crop rotation strategies ,while still advisable [20], are likely non-function for control as oospores are able to go dormant for long periods of time [21] and the pathogen has been associated with non canonical species both in the field [22,23] and lab [24]. This long term oospore survival coupled with continual reports [5–11,24] of host expansion and association with weed species [22,23] indicate that this pathogen may be much better at surviving crop rotation than previously expected.

Exclusion: Exclusion practices when executed properly and maintained are capable of controlling the introduction of *P. capsici* to crop land. Irrigation water [4, 25, 26] and field run off [15, 27, 28] have been demonstrated as common routes by which spores may enter a field, providing several obvious targets on which exclusionary practices may be employed.

Cultural Methods: With the infectious cycle, dispersal, and biology of *P.capsici* being so tightly linked with standing water it should come as no surprise that cultural methods that limit this resource are highly effective at control. General recommendations for controlling the pathogen include: using raised planting beds [20], bedding in soil that allows for good drainage, using irrigation drip tape [29] , wide row and plant spacing, and grading fields to ensure water isn't allowed to stand [30]. Unsurprisingly, these methods work especially well in arid areas with little rainfall (Central California and New Mexico), but are often harder to implement in areas that are generally wetter and may receive significant rainfall (Michigan, Tennessee, North Carolina).

Chemical: There are a limited number of chemicals registered for use in controlling *P. capsici*: dimethomorph (Acrobat) , metalaxyl(MetaStar) , mefanoxam (Ridomil), cynofamid (Ranman), propamocarb (Previcur Flex) [31,32]. Usage of these chemicals along with good cultural practices and crop rotation has been successful at controlling serious outbreaks. As a result of *P. capsici*'s high diversity, mitotic recombination, and the high selection pressure of these chemicals, resistance often develops quickly and absolutely if care is not taken [**?**, 33]. While in the past methyl-bromide fumigation was an efficacious method for protecting a field it has been in the

process of being phased-out of usage and is now only available through critical use exemptions.

1.1.4 Population Structures

The structure of individual populations of *P. capsici* has been studied globally using a number of marker systems (SSR,AFLP,SNP,SSR, physiological race systems etc.) and study designs (spatio-temporal, survey , etc). These studies demonstrate that the population structure and genetic compostition varies greatly by geographic location and potentially on the availability of hosts. It is important to note that while physiological race systems have been used to describe and classify populations of*P. capsici* these systems are reliant on plant host interactions and environmental conditions making calculating a proper distance metric impossible [34–36].

In the United States and South Africa, populations are diverse, short lived, narrowly dispersed, and out-crossing. Furthermore spatio-temporal studies of U.S. populations have demonstrated that during initial stages of an epidemic a population is genetically very diverse and as time progresses the population becomes genetically pure. These populations are generally confined to individual growers or fields and do not survive fallow periods as the following year a new group of competitive genotypes germinates from infectious materials in the soil [21, 37–41].

In Peru and Argentina populations are characterized as being clonal, long lived, and widely dispersed [42–44]. It is thought that this population structure primarily arises from the wet and humid climate combined with a perennial cropping system.

In China it appears that there may be four populations that are long lived and clonal along with a considerable reservoir of highly unique long lived genotypes present [45, 46]. This situation may be similar to that described in South America masquerading as something more complex due to geographic scale.

1.2 Oomycete Effectors

1.2.1 Biology and Function

Effectors are secreted by plant pathogens and are broadly defined as: a protein or small molecule that alters the host cell structure or function [47–51]. These molecules can : facilitate infection through the modulation of resistance pathways or cell function, trigger host defense responses by being recognized, or potentially do both [52–55]. These effectors provide an extended phenotype for the pathogen as their physical manifestation of the origin of the phenotype [51, 56]. This broad definition of effectors while very convienient means that a number of small molecules, toxins, enzymes, and pathogen associated molecular patterns (PAMPs) are all sub-terms that may fit into this class. This means that with the acceleration of next generation sequencing technologies the identification of putative effectors is increasing, actual identification of function can be difficult as it requires isolating and measuring phenotypes in a second host plant [50, 51].

Effectors are important for the pathogens ability to subvert and suppress the host cell function [52–54, 57–59]. Many effectors have been identified as being avirulence factors ; being identified by resistance genes (R-genes) inside of plants and triggering hypersensitive responses to the pathogen. This duality of effectors as being required for infection and responsible for host detection of the pathogen has kicked off a molecular arms race between host and pathogen [47] resulting in the expansion of most effector families and plant resistance genes.

This detection of effectors by plant cells have also provided a number of very specific targets for breeders to use in the development of genetically resistant strains of crops [60, 61] and the identification of important R genes in resistant germ-plasm.

Figure 1.2: The basic structure of an RxLR effector. An RxLR effector is defined by a signal peptide within 30 amino acids of a start codon, followed by a linear RxLR motif between 30 and 60 amino acids from the signal peptide, the dEER motif is usually within 20-40 amino acids of the RxLR and is within the effector domain.

1.2.2 RxLR Effectors

This class of effectors has been historically very important in the field mainly as several members from this group were the first described avirulence genes in the *Phytophthora* genus [59,62,63] and has recently been studied and reviewed in a number of publications [51,64,65]. Of all described Oomycete effectors, this class is the largest.

The oomycete RxLR effectors are a class of cytoplasmic effectors that are defined by an signal peptide followed by: an immutable RxLR motif (Arginine-Anything-Leucine-Arginine), a high frequency of acidic residues(D/E), and a diverse effector domain that is responsible for function (Figure 1.2). This conserved RxLR motif has allowed for the use of bio-informatic pipelines that screen potential proteins for the preceeding criteria and allow the *ab initio* prediction of these proteins [66,67]. In brief these workflows take the six frame translation of a genome and search for sequences greater than 70 amino acids that have: a signal peptide within 30 amino acids of the start codon and an RxLR sequence between 30 and 60 amino acids of the start and behind the signal peptide.

RxLR effectors display signatures of strong positive (diversifying) selection, especially on the C-terminal end [61, 66]. This is believed to be primarily due to the fact that this family is under pressure to evolve away from plant resistance genes in order to survive. This information paired with a crystal structure for several effectors [68–70] has provided new insight into how these mutational events may allow an effector to evade detection while maintaining function. Based on the highly

conserved helical bundle structure of many of these proteins it is believed that these proteins mutate away from R genes by extending N and C terminal lengths, inserting loops between conserved helical bundles, and limiting mutations to exposed amino acids.

While initial reports indicated that the RxLR domain was solely responsible as a host cell targeting motif [67, 71] and responsible for the entrance of the protein into cells, later reports have demonstrated that other higher order structures in the N terminal domain are likely to be playing a more important role [68, 72] in directly binding specific lipids presented at the cytoplasmic surface. A recent thorough review of this problem has come to the conclusion that the delivery of these effectors is a complex process that involves multiple steps and may go through multiple different pathways in order to arrive at their destination [73].

1.2.3 CRN Effectors

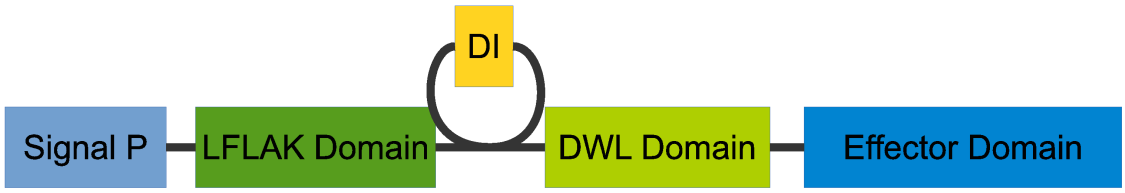

Figure 1.3: The modular structure of the CRN Family. A CRN has a signal peptide, and LFLAK domain, a potential DI domain, a DWL domain, and a trailing effector domain [74].

The Crinkler(CRN) effector family is another highly redundant group of cytoplasmic effectors highly conserved across the *Phytopthora* genus. This family of effectors was named based on a crinkling leaf phenotype observed during ectopic expression of these proteins in plant [75].

The CRNs also share the RxLR effectors modularity but are generally larger and are sequentially much more complex (Figure 1.3). A typical CRN protein is

compromised of a signal peptide, followed by an LFLAK domain, possibly a DI domain, a DWL domain, and an effector domain.

Currently the best method of annotating CRN effectors from genomic sequences is to : generate a library of open reading frames greater than 300 amino acids in length, detect secreted proteins , search for an LFLAK domain that is behind the signal peptide and within 66 amino acids of the start, search for a DWL domain down stream of the LFLAK domain followed by an effector domain. This pipeline has shown to be both sensitive and specific within *P. capsici* [74].

1.3 Next Generation Sequencing - The Illumina Platform

Sequencing starts with the preparation of raw material and generation of a sequencing library. In the case of genomic samples this means the extraction of high quality molecular weight DNA, followed by shearing and size selection of fragments between 200-500 base pairs in length, and the ligation of Illumina specific adapters. In RNA-Seq experiments samples go through either poly-A enrichment or rRNA depletion to enrich transcripts. After this enrichment : a cDNA library is generated and then the following processing steps are the exact same as the steps required for genomic re-sequencing.

Libraries are then loaded onto a glass flow cell and attached to its surface. Each of these single molecules then goes through an amplification step that creates a cluster of several million identical sequences directly surrounding the originally bound DNA molecule. The free end is then bound to the flow cell as well creating a bridged molecule.

A sequencing by synthesis approach is then used to determine the sequence of each cluster. In such an approach, a DNA polymerase and all four nucleotides are added to a flow channel at every step. These nucleotides include fluorescent labels.

After incorporation of nucleotides onto a cluster, an image of the flow cell is taken. After imaging a blocking group is removed from all molecules and the next round of nucleotides is applied and another image is taken for a defined number of times. If a single end sequencing experiment is all that was required, the sequencing process ends at the completion of this step. In the event that a paired end approach is required, the clusters are regenerated so that the opposite side of the original molecule is now being visualized and the sequencing reaction is carried out again.

1.4 Processing NGS Data

1.4.1 Common File Formats

FASTA: The fasta format is a format for the description of nucleotide and protein sequences. In the format each sequences consists of a header denoted with a ">" symbol followed by a descriptor of the following sequence. While early versions of this format were strict about a 72 character per line format because of computational needs, this standard is rarely if ever forced in modern formats.

FASTQ: The fastq format is a format that describes sequencing data using four lines per sequence. Line one begins with an "@" symbol and is followed by a sequence identifier and/or description. Line two contains the raw sequence called by whatever technology generated the read. Line 3 begins with a "+" symbol and may have the same sequence identifier as line 1. Line 4 contains the phred quality values that correspond to each nucleotide of line 2. The phred score of a base is determined by converting the ascii character of a symbol into its corresponding integer and subtracting the vendor specific offset(Figure 1.4).

GFF: The Generic Feature Format are used to annotate features within a genome. It consists of 9 columns of data that are tab delimited: Sequence ID, Source, Type, Start, End, Score, Strand, Phase, and Attributes. Any feature in a sequence can

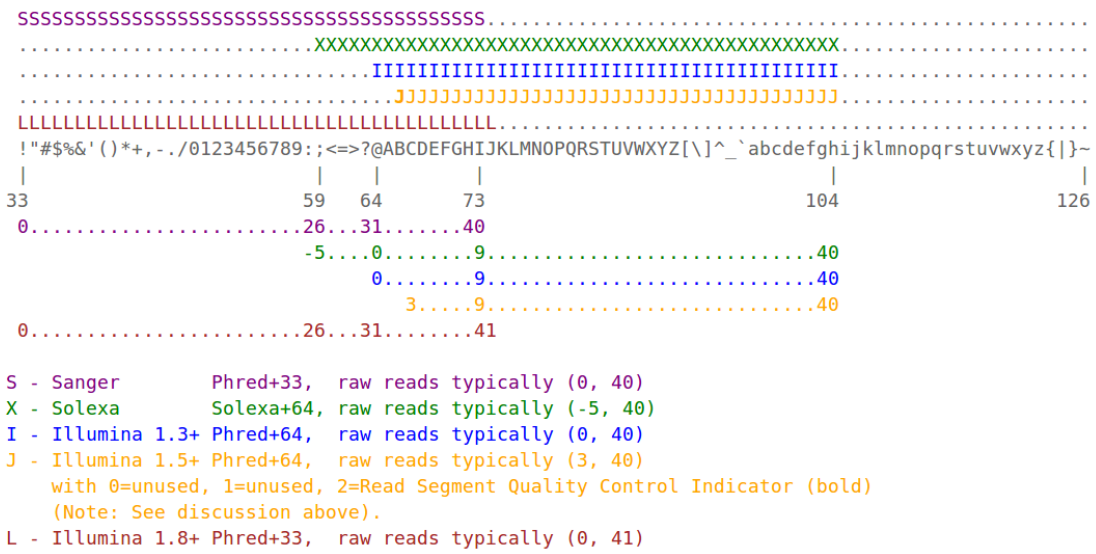

Figure 1.4: The phred quality score for different sequencing vendors. The integer value of valid ascii characters used to encode this information, and the resulting quality score after offset.

be described using this format and it is generally very flexible to individual users applying internal lab ontologies to gene features.

GTF: The Gene Transfer Format is a based partially on the GFF format but has additional structure and requirements. While the individual fields in a line are the same as that of a GFF, the GTF has increased requirement for descriptions that must be present for each annotated feature. In this case a start codon, stop codon, and CDS feature type must be attributed to each sequence identifier provided.

SAM/BAM Format: The SAM format is specified in the samtools [76] package and has been widely adopted as being the format to describe how a read aligns to a reference genome. The minimal record identifies on a single line: the query name, a bitwise flag, reference sequence name, 1 base left most mapping position, mapping quality, a CIGAR string, Reference name of the mate if paired, observed template length, the segment sequence, and a 33 offset phred score for the sequence. The BAM format is simply a binary version of the SAM format that is compressed and can be indexed for quick sequence lookup and retrieval.

1.4.2 Short Read Aligners

The alignment of DNA and protein sequences is an old and well described problem in bio-informatics. In this problem, two strings are presented for comparison. By applying a user defined set of rewards for matches and penalties for mismatches and gaps alignment algorithms compare the possible ways that any two sequences could be related two each other and alignment with the best score is selected as being correct.

In bio-informatics there are two basic alignment methods: the Needleman-Wunsch [77] and Smith-Waterman [78] algorithms for alignment. Both are considered classic examples of dynamic programming algorithms and are used to report an optimal alignment between two sequences. The major difference between these two algorithms is that the Needleman-Wunsch is a globally optimized algorithm while Smith-Waterman is a locally optimizing algorithm.

Global alignment methods attempt to align the two sequences over the entire length of the sequence and only work well when two sequences are highly related to each other with few mismatches. Local alignment methods find regions of high similarity and minimize scores over those regions allowing them to be used on sequences that are potentially divergent or only have small regions of similarity.

The alignment of short reads from high throughput sequencing technologies to a genome provide a similar if different sort of problem in aligning two sequences together. Because the two previously described algorithms are quadratic in nature more advanced methods to limit search spaces or modify search parameters are required to align millions of reads to genomes in a useful time. As a result of this need more than 30 alignment algorithms have been described to solve this informatics problem. These aligners broadly fall into two categories and attempt to increase search speeds by limiting the amount of space required to search for best matches. A summary of popular open source search tools is presented in Table 1.1. Please keep in mind that this is a brief list of only the most commonly used software and is by no means a complete or comprehensive list.

Table 1.1: Summary of popular short read aligners, the underlying technique used for computing matches, and available features.

	Algorithm	Allows Gaps	Paired End	Junction Splicing	Reference
Bfast	Hashing ref	Yes	Yes	No	[79]
Bowtie2	Trie	Yes	Yes	No	[80]
Blat	Hashing ref	Yes	No	No	[81]
BWA	Trie	Yes	Yes	No	[82]
MAQ	Hashing reads	Yes	Yes	No	[83]
SOAP2	Trie	No	Yes	No	[84]
Tophat2	Trie	Yes	Yes	Yes	[85]

Hash table aligners: The hash aligner has its roots in the BLAST algorithm [86]. In the BLAST algorithm a series of sub words of length k are generated from a query, the algorithm then uses the words from the query and words from each potential match to find subjects with many word pairs in common and define where alignments may exist between two strings, from each of these seeds alignments are locally extended until their alignment score decreases. This process is completed for all sequences in a database of subject sequences, alignments are refined using a Smith-Waterman alignment and significant outputs are reported. This allows the algorithm to first limit its search space to likely candidates before executing computationally expensive exact alignments. Hash table aligners follow a similar pattern of seeding many small alignments from a short read and then extending them in order to match a short read against the genome. In this scheme a hash table is generated for the genome and held in memory and local alignments are only done when a query sequence has many words that hit near each other within the hash table of the genome. As a class these aligners are highly sensitive but, suffer from severe performance considerations when the detection of indels and mismatches is required.

Trie tree aligners: Aligners in this group identify exact matches within a genome and then build inexact alignments that are supported by many exact matches. In order to do this, these algorithms first build a suffix trie for the genome. A suffix tree is a representation of all of the possible suffixes of a word, this tree is usually compressed

into a structure to make indexed searching feasible. A search is then started by taking a single letter from the end of a query and eliminating any indexed positions that it does not match to. The next letter from the query is added to the search and the search is repeated to find eliminate any sequences that do not match. In this way an exact string match can be found in any database, in order to do mismatches searches must be repetitively seeded with mismatches allowed at individual and/or multiple sites and final alignment scores calculated upon completion of a search. From this list the best score is reported.

As a group these aligners tend to use less memory as a result of compression on the suffix trie and are quick to run but suffer from issues of sensitivity as they require the reseeding of queries against the tree in order to ensure that all possible mismatches and indels are taken into consideration before reporting a best alignment.

1.4.3 Intron Junction Mappers

The mapping of reads originating from transcripts is a particularly difficult problem as it combines all of the normal problems associated with the above mappers with the added wrinkle that proper alignments may have large gaps of several thousand letters in them as the result of intron splicing. One method of dealing with this problem is to simply extract and generate all of the known (or predicted) transcripts from a genome and then searching your reads against this database. This method is great because it is computationally trivial and intuitive for most people to understand but requires that researchers have great confidence in their prior knowledge of the gene structure and content of an organism. Another method is to make a two pass approach to mapping. In this approach reads are mapped against the genome as previously described and any unmapped reads are then used in the second round of mapping. This second round of mapping splits each read into two reads in order to simulate a splice event. Both of these reads are then mapped to the genome and any

alignments in which the left read and the right read map in a linear fashion within a set number of base pairs is kept.

1.4.4 Genotype and SNP Calling from NGS Sequencing Data

NGS data can suffer from high error rates due to errors in the actual sequencing of data and down stream errors in mis-alignment during mapping. Furthermore, low coverage regions (<5x coverage) have a high probability of having only one chromosome in a diploid individual being sequenced [87]. These conditions make the accurate calling of genotypes a difficult problem that imparts high levels of uncertainty in results.

A common method of reducing these compounding errors is to only consider sites that have "deep coverage" (>19x). Unfortunately for many studies, this criteria makes the usage of next generation sequencing a prohibitively costly venture. It is much more cost effective to reduce the uncertainty of resulting genotpe and SNP calls in lower coverage regions than to over sequence samples.

Criteria Based

Early methods of base calling were heuristic models in which researchers would filter sites based on a number of criteria. Commonly pipelines would: filter out all "low quality sites" , check for a minimum depth of coverage, and use the ratios of bases called to assign a genotype. Common practice is to call a site homozygous if any allele is more than 80% of all alleles seen and heterozygous if any two alleles are both between 20% and 80% of all alleles seen. An example of this process is presented in Figure 1.5.

These methods are simple to understand, calculate, and work well in high coverage areas. Unfortunately, in low coverage areas these methods result in either: no call being made or a high proportion of heterozygous sites being mis identified as homozygotes. These methods can be improved using empirically estimated cut-offs but still suffer in low coverage experiments [88].

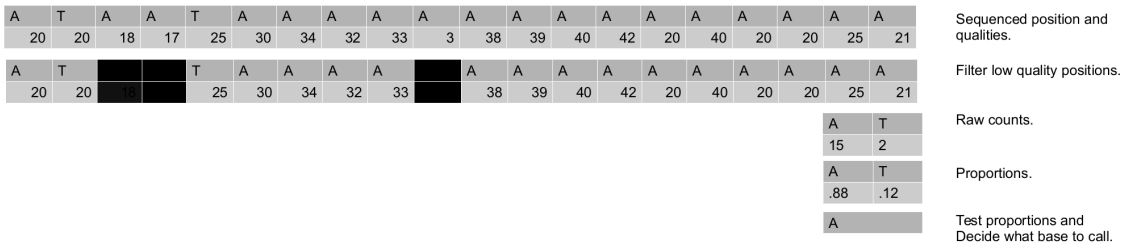

Figure 1.5: An example of a criteria based genotype method. A positions bases and associated qualities are read. Positions that have a low quality (score of < 20) are removed. The read depth (17x) is calculated as are the proportions of all sequenced bases. The position is called A because proportion of A $> .8$ and T $< .2$.

Bayesian Methods

For low sequencing depth samples , using criteria based methods results in: a large number of heterozygous sites mis-identified as homozygous and the loss of information from read qualities. Criteria based methods also do not allow for any measurement of uncertainty in a called genotype.

Bayesian methods , apply Bayes Theorem to this problem by calculating the likelihood of an observed allele and utilizing prior probability of a variant to calculate the posterior probability of the genotype given the data. The general model [89, 90] for genotype G given the reads D (where $D = d_1, d_2, ...d_n$) in individual i is :

$$P(G \mid D) = \frac{P(G)P(D \mid G)}{\sum_{i=1}^{n} P(G_i)P(D \mid G_i)}$$

$$P(D \mid G) = \prod_j \left(\frac{P(D_j \mid H_1)}{2} + \frac{P(D_j \mid H_2)}{2} \right)$$

$$P(D_j|H) = PrD_j|b$$

$$P(D_j|b) = \begin{matrix} 1 - e_j \text{ if } D_j = b \\ e_j \text{ else} \end{matrix}$$

In the case that an insertion or deletion is to be called at a site: haplotypes H_i are discovered from reads at a position, the diploid genotypes G of all possible haplotype

combinations H_iH_j is created , for each haplotype the likelihood of each read D_j over all possible π alignments.

$$P(D_j \mid H) = \sum_{\pi} P(D_j, \pi)$$

Genotype likelihoods ($P(D \mid G)$) can be improved by: re-calibrating per base quality scores [89,91], filtering used reads based on base and mapping quality, [90,92]. Prior probabilities ($P(G)$) can be assigned as being completely naive (all genotypes having an equal weight) , assigned based from allele frequencies of previous studies [84,89], or incorporating calls from other individuals in the same study [76] assuming Hardy-Weinberg equilibrium.

Other Statistical Methods

The assignment of genotype from sequencing data can also be completed through the application of Fischer's Exact Test or Pearson's chi-squared test [93, 94]. These two tests are both for a 2x2 contingency table in which the probability of the observed table is calculated compared to any that are more extreme. Fischer's Exact Test is particularly useful in these situations as sequencing data is often sparse enough that a chi-squared test is inappropriate.

Given the table:

$$\begin{pmatrix} a & b & r_1 = a + b \\ c & d & r_2 = c + d \\ c_1 = a + c & c_2 = b + c & n = (a + b + c + d) \end{pmatrix}$$

The probability of obtaining a set of values can be calculated as:

$$p = \frac{r_1! r_2! c_1! c_2!}{a! b! c! d! n!}$$

This equation gives the exact probability of observing this arrangement of marginal totals against the null hypothesis that columns are equally distributed. In the case of genotype calling we are also interested in the probabilities associated with more extreme conditions. This is done by calculating all potential p-values for tables that have the same marginal values and calculating the sum of all p-values that are less than or equal to the first test. This is clearly a non trivial matter in the case that there are large numbers of observations. The final significance level can be calculated in a simpler matter by organizing the table such that $c1$ is the smallest of the four marginal totals and a can be increased in the direction specified by the alternative hypothesis. In this case the generalized equation:

$$\alpha = \sum_{x=a}^{x=min(r_1,c_1)} \frac{\begin{pmatrix} r_1 \\ x \end{pmatrix} \begin{pmatrix} r_2 \\ c_1 - x \end{pmatrix}}{\begin{pmatrix} n \\ c_1 \end{pmatrix}}$$

This computation is still non trivial for a large number of observations and is the cause of computational bottle necks when using these methods to make genotype calls.

1.5 *Phytophthora tropicalis* a brief history and overview

It has always been clear that *Phytopthora capsici* is a diverse species and carries large levels of variation between individuals [95–97].

Prior to the extensive use of molecular tools in species identification, *P. capsici* was described using isozymes and morphological data. These descriptions classified *P. capsci* into three groups: CAP1,CAP2, and CAP3 [95]. The CAP1 group contained individuals that were primarily from vegetable plants with some from black pepper

and cacao, the CAP2 were primarily from tropical woody plants , and CAP3 was exclusively populated by individuals isolated from Brazilian cacao. This classification was later revised to merge CAP2 and CAP3 into a single group, CAPB, and CAP1 was re-designated CAPA [96]. As more data and markers have been applied to this problem the description of *Phytophthora tropicalis* emerged [98]. This reclassification redefined isolates of from CAPA (CAP1) and *Phytopthora palmivora* MF4 into the species [98].

This species description relies heavily on previous studies morphological and isozyme descriptions and adds to it the addition of host range and avirulence measurements. *Phytophthora tropicalis* being isolated from perennial woody species such as : *Piper nigrum* , *Macademia itergrifolia* , and *Theobroma cacao*.

The generation of molecular phylogenies within the genus *Phytopthora* using the ITS region of the genome, cytochrome oxidase genes from the mitochondria, and other genomic loci has further muddied the waters by providing evidence that isolates from tropical and temperate regions have a high continuity of relatedness based on the observed morphological and molecular markers. [27, 99–101]. Furthermore, it has been demonstrated that in some rare cases *P. capsici* and *P. tropicalis* are capable of producing viable offspring [102]. Taken in total, it is clear that while *P. tropicalis* is a distinct, albeit related, species from *P.capsici* but current molecular markers have a difficult time distinguishing both inter and intra specific variation.

Chapter 2

Population Structures of *Phytophthora capsici*: A Global Context

2.1 Introduction

Phytophthora capsici, first described on chili peppers in 1922 New Mexico [3], has since been reported in most cucurbits , tomato, eggplant, snap , and lima beans. *P. capsici* is a worldwide problem. *P.capsici* is a heterothallic organism that has two mating types (A1 and A2); when these mating types encounter each other it results in the creation of a thick walled , genetically recombinant, oospore. This pathogen also produces large numbers of deciduous sporangia on the surface of infected tissue; capable of directly infecting tissue or releasing many motile zoospores into standing water. In warm wet conditions the pathogen is capable of destroying a field within days of introduction.

The epidemiology and genetic structure of *P.capsici* has been investigated at locations around the globe using a number of genetic markers and it is clear that populations vary greatly. In the US and South Africa both mating types are

commonly found in the same field and infectious material does not appear to survive fallow periods. This results in populations that are short lived, genetically diverse, and are spatially restricted. In contrast in Argentina, Peru, and China populations are spatially large, long lived, and clonal.

With the publication of a high quality genome in 2012 [103], it has become possible to begin leveraging high throughput sequencing technologies in order to asses and measure genome scale diversity in this pathogen. This publication was also the first to document mitotic recombination; while the mechanism for such a process is unclear signatures of it are easily detected as the switching of heterozygous regions to homozygous. This loss of heterozygosity has been linked with physical growth characteristics, change of mating type, and virulence in lab populations. This process has been suggested as a major driver for the pathogens clonal profile in a number of studies and causes issues in biological replication of sequencing results.

This makes the application of high throughput sequencing technologies especially exciting as it gives an approach that allows for the comparison of all sites in the genome, a method to measure events of mitotic recombination, and the development of informative markers between geographically distinct isolates. These resources are especially needed as there is obvious need to develop prior knowledge of allele frequencies so that researchers do not need to rely on heuristic criteria based methods or frequentest approaches that require high depth of sequencing.

In this study we present a comparison in the genetic diversity, distance, and structure of a global panel of *Phytophthora capsici* isolates. Because of the inclusion of transcriptomic samples taken while isolates were infecting plant material, it is especially suited for dissecting the population structure using SNP markers that are functionally linked to the survival of the pathogen. By considering a greater number of markers than previously used in these types of studies we also avoid extreme calculations of distance that arise from only a few differences in between individuals. This approach demonstrates that isolates from Chinese regions are genomically distinct from their western counterparts both in absolute distance and

based on regional patterns of variation. The presence of fine grained population structures within western populations is also discussed.

2.2 Materials and Methods

2.2.1 Isolate Growth and Genomic DNA Extraction:

Tufts of mycelia were placed into 50mL Falcon tubes of liquid V8-PARP media (160 mL of V8, 3g CaCo3, 960 mL of ddH2O, 25ppm pimaricin, 25ppm rifampacin, 25ppm PCNB, 100ppm ampacillin). Tubes were grown with agitation at 28 degrees Celsius for 3 days. Tissue was harvested and lyopholized; then powdered using liquid nitrogen, mortar, and pestle. Genomic DNA was extracted using standard phenol/chloroform extraction methods. All sample concentrations were checked via 260/280 absorption readings using a NanoDrop ND-1000 and high molecular weight DNA verified using 1% agarose gel.

2.2.2 Infection Assays and Total RNA Extraction:

Tufts of mycelia were placed onto V8-PARP agar and allowed to grow for 3 days at room temperature under fluorescent light. A 6mm punch was then used to take multiple plugs from fully covered portions of agar. 4 plugs were placed mycelia side down on the underside of 6 week old tomato plants (var. Moneymaker). At 24 and 72 hours post inoculation infected tissue was taken from the area directly under the agar plug from 4 separate sites (2 separate leaves), frozen in liquid nitrogen, and stored for later extraction. Total RNA was then extracted using RNA-Easy (Qiagen) extraction kit using the manufacturer's instructions. All samples were treated with DNAse (Ambion) on the column prior to final elution. Sample quality was assessed using a NanoDrop ND-100 and 1.5% agarose gel.

2.2.3 Library Construction and Sequencing (Genomic) :

Genomic sequencing was carried out on an Illumina HiSeq 2000 with 100bp single end reads being output. All sample and library preparation was carried out by staff at Children's Mercy Hospital (Kansas City, MO, USA) as per manufacturers instructions.

2.2.4 Library Construction and Sequencing (Transcript) :

RNA sequencing was carried out on an Illumina HiSeq 2000 with 100bp paired end reads being output. All sample and library preperation was carried out by staff at GeneWiz Inc (South Plainfield , NJ, USA) as per manufacturers instructions.

2.2.5 Read Mapping (Genomic):

Reads were mapped to the Phytophthora capsici genome [103] using Bowtie2 [80]. Bowtie was employed using the end-to-end high sensitivity mode and the following modifications: -D 40 -R 10 -L10 -N1. Only uniquely mapping reads were used for consensus sequence determination and SNP calling. Potential PCR duplicates were then removed from these mapped reads using the samtools utility [76].

2.2.6 Read Mapping (Transcript):

Reads originating from transcript sequences were mapped to a concatenation of the Phytophothora capsici and Solanum lycopersicum genomes [103, 104] using the program TopHat2 [**?**]. TopHat2 was employed with the following settings : read mismatches 8 , read gap length 8, microexon search True, splice mismatches 2, mate inner distance 100, mate standard deviation 100, read edit distance 8, read realign edit distance 0, max insertion length 8, max deletion length 8, min anchor length 15, GFF guided mapping True, max multi hits 40. Bowtie 2 settings were : N 1 , L 10,

I S,1,1.5 , D 20 , R 10. Only uniquely mapping ,conchordant, reads were used for consensus sequence determination and SNP calling.

2.2.7 Consensus Sequence Determination (Transcriptomic and Genomic) and SNP calling:

SNPs were called using the VarScan2 (ver 2.3.4) program [93] with the following settings: 8x coverage , 3x alternate allele minimum coverage, minimum quality score of 20, minimum variant frequency of 0.1, and a P-value threshold of 0.01.

2.2.8 Between Isolate Distance and Clustering:

All sites in which mapping data was available for all samples were considered for calculating distance.The distance between two individuals being defined as :

$$D_{ij} = \frac{1}{L} \sum_{l=1}^{L} d_{ij}^{l}$$

Where L is the number of sites observed for comparison and was set to 1 base calls with no overlap, 0 for matching consensus base calls, 0.5 for heterozygous/homozygous overlap (i.e. : A to [W,M], T to [Y,K], G to [S,K], C to [Y,S]), or 0.83 for heterozygous/heterozygous overlap (i.e. : R to [Y,S,W,K,M] , Y to [S,W,K,M] , S to [R,Y,K,M], W to [R,Y,K,M], M to [R,Y,S,W,M]).

Hierarchical clustering was performed on the calculated distance matrix using euclidean distances and complete linkage in R.

2.2.9 SNP Matrix Construction and PCA analysis:

SNP data was transformed into a numerical matrix and a PCA analysis was performed by the EIGENSOFT (ver 5.1) suite of programs [105,106]. SNP data was transformed by comparing each site against the re-sequenced LT1534 genomic sequence and assigning a score between 0-2 where: 0 is a match , 1 is a heterozygous match , 2 is

a mismatch. The significance of eigenvectors was determined by the Tracey-Widom test , also implemented in the EIGENSOFT package.

2.3 Results and Discussion

2.3.1 Sequencing

Individual files were concatenated into single files for each library and summary statistics were calculated using internally developed scripts and programs. Cumulative quality scores (Figure 2.1, Figure 2.2, Figure 2.3) for genomic and transcriptomic samples showed a large number of good to high quality bases in each sample and for each run overall. Nucleotide proportions at each position (Figure 2.4, Figure 2.5, Figure 2.6) showed a near even distribution at most reported positions. Quality scores (Figure 2.7, Figure 2.8, Figure 2.9) at demonstrated that >95% of position qualities were over 30 in the transcriptomic samples and >80% of position quality scores were over 30 in the genomic samples.

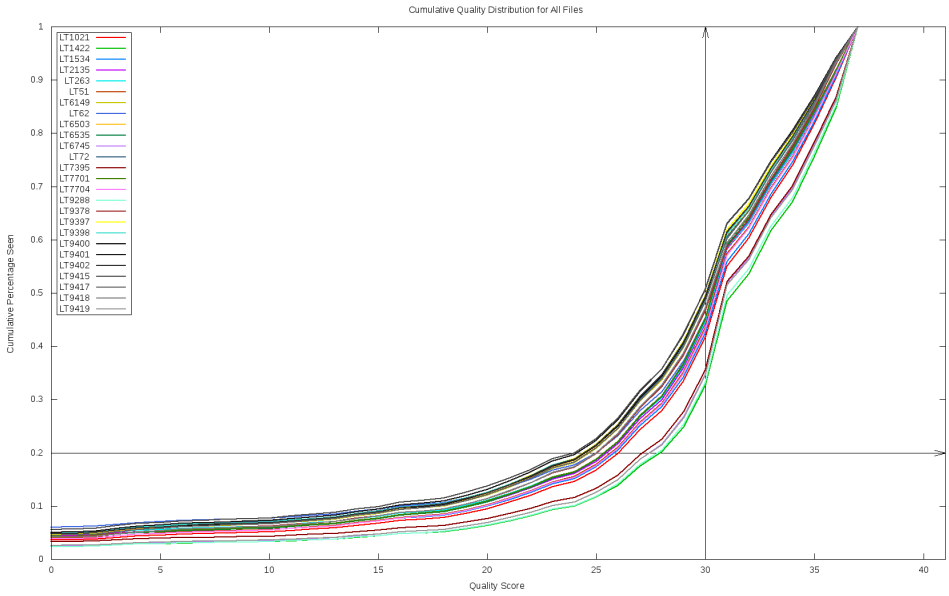

Figure 2.1: Cumulative proportion of sequencing quality scores for the genomic re-sequencing run.

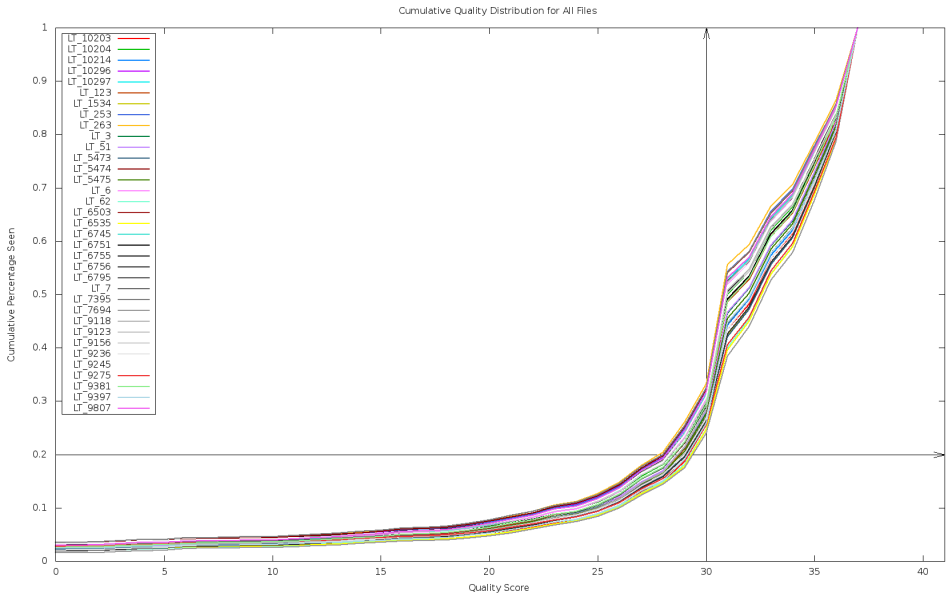

Figure 2.2: Cumulative proportion of sequencing quality scores for the biotrophic nucleotide sample.

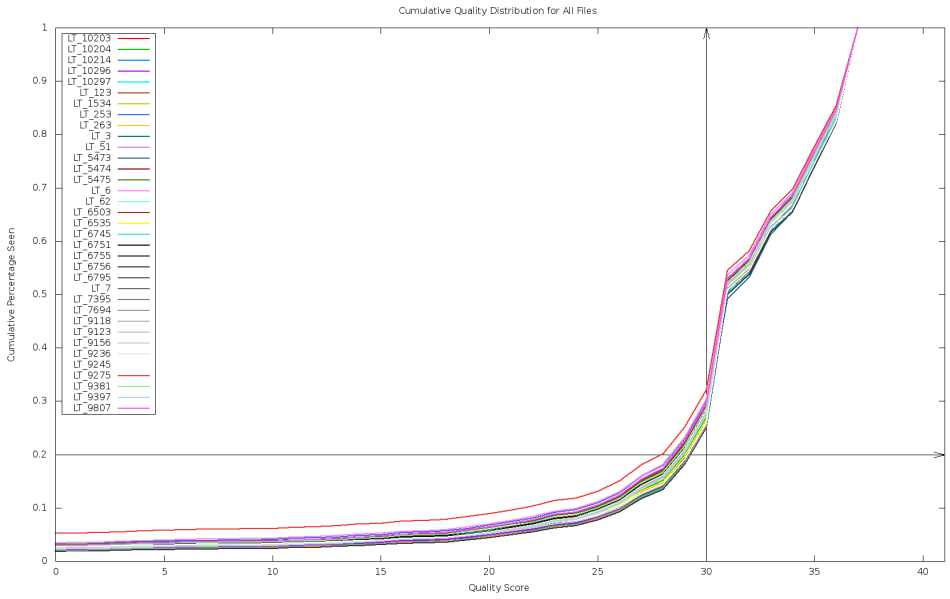

Figure 2.3: Cumulative proportion of sequencing quality scores for the necrotrophic nucleotide sample.

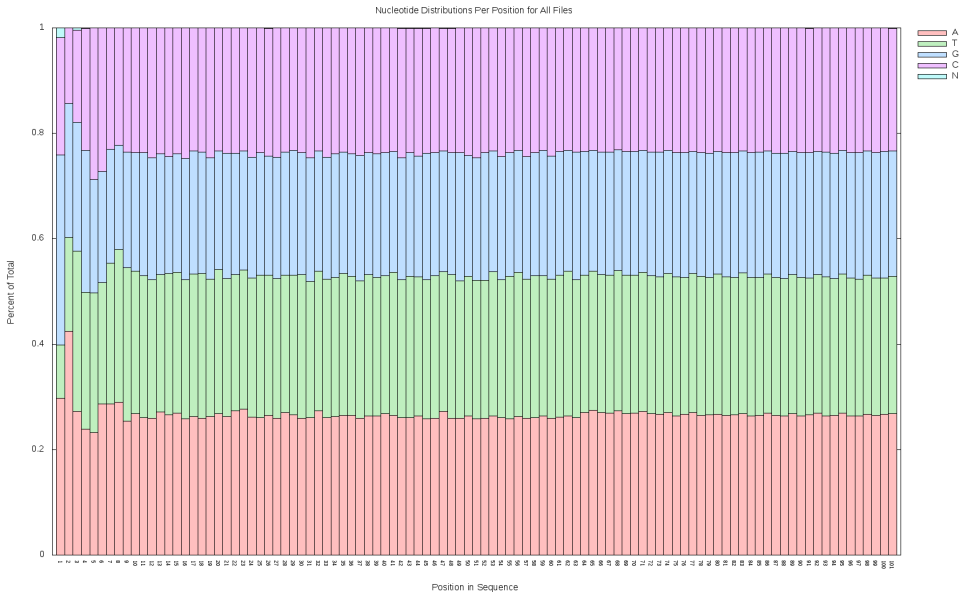

Figure 2.4: Proportion of nucleotides reported at each position in the genomic sequencing run.

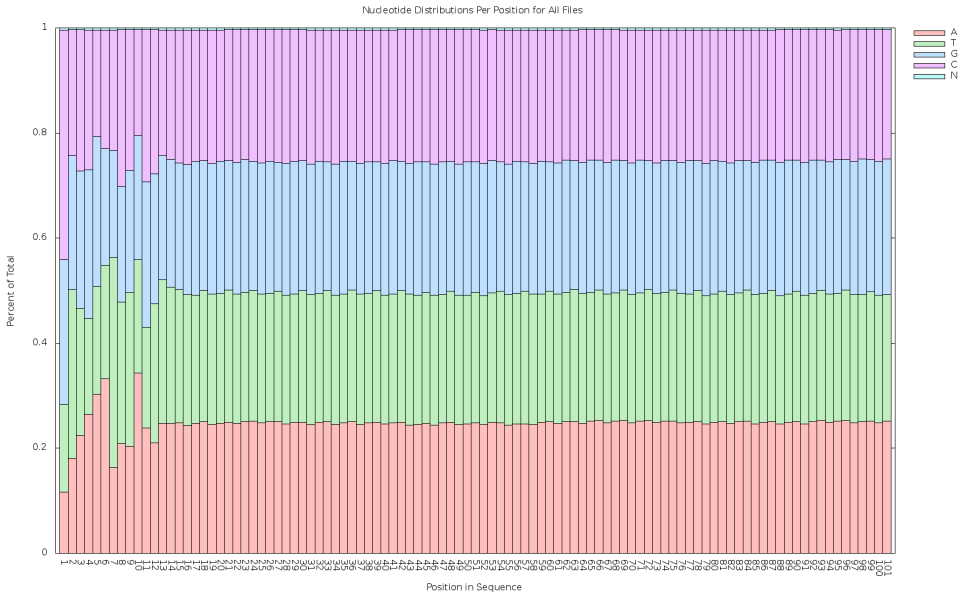

Figure 2.5: Proportion of nucleotides reported at each position in the biotrophic nucleotide sample.

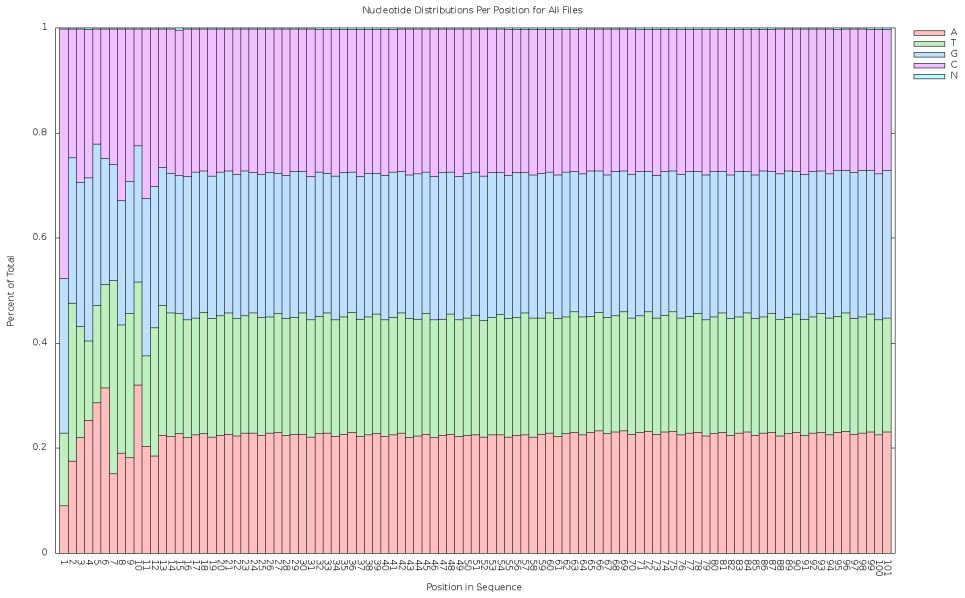

Figure 2.6: Proportion of nucleotides reported at each position in the necrotrophic nucleotide sample.

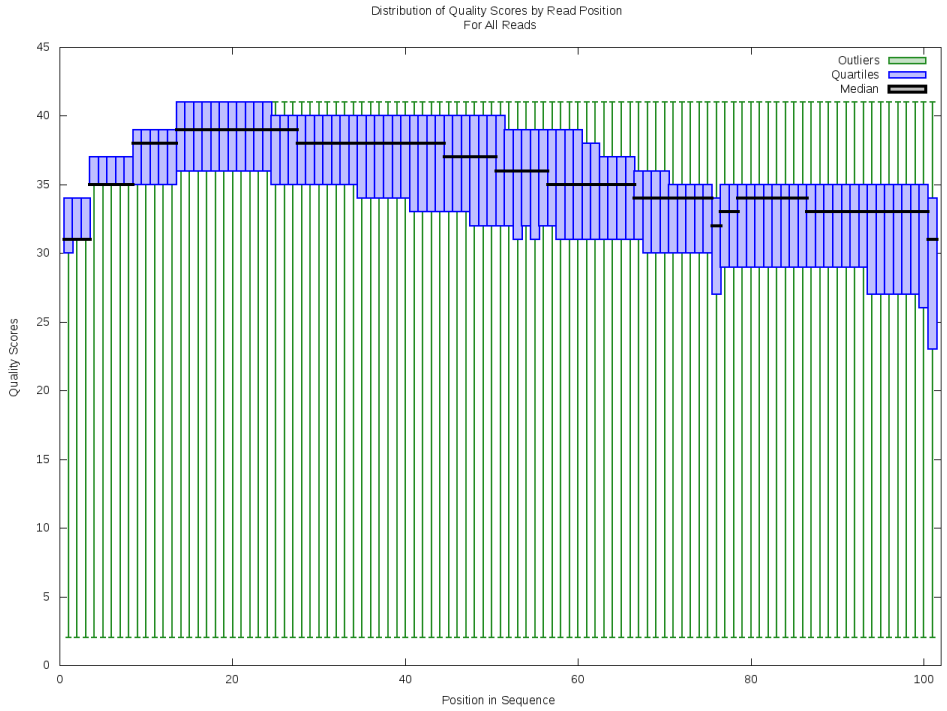

Figure 2.7: Distribution of quality scores at each position in the genomic sequencing run.

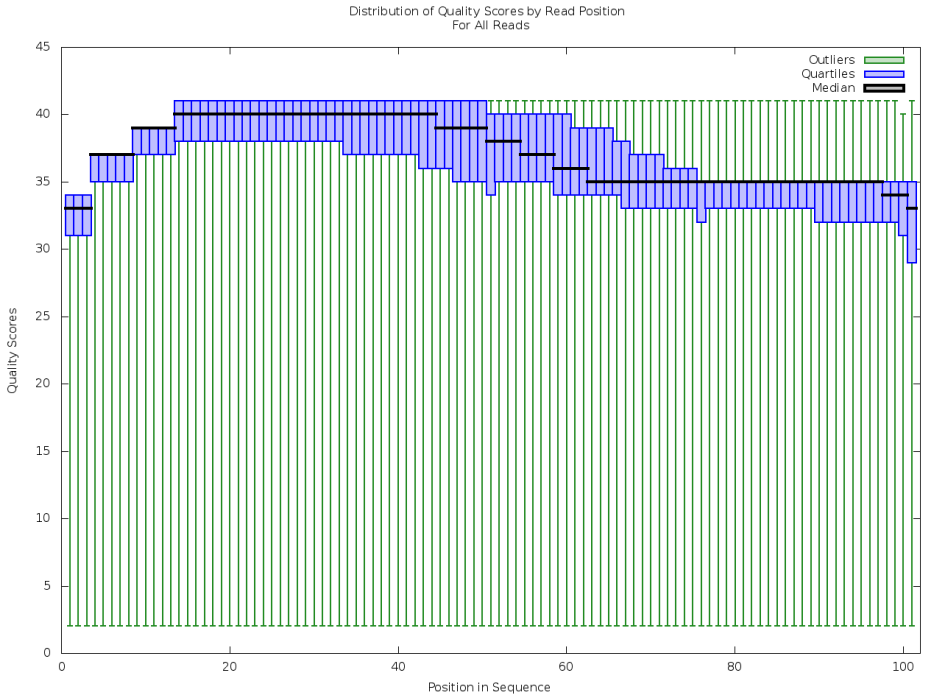

Figure 2.8: Distribution of quality scores at each position in the biotrophic nucleotide sample.

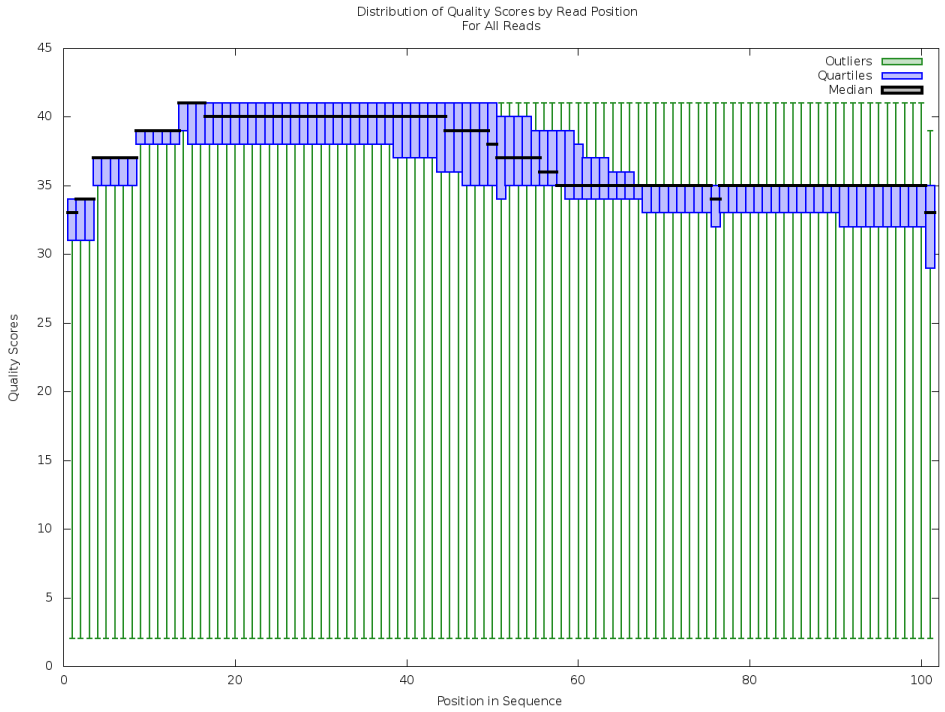

Figure 2.9: Distribution of quality scores at each position in the necrotrophic nucleotide sample.

2.3.2 Mapping and SNP Calling

Mapping was completed using either the Bowtie2 [80] or TopHat2 [**?**] programs using the NewtonHPC cluster at the University of Tennessee, Knoxville. Initial mapping rates for genomic samples were curiously low (64-86%). As isolates were grown in a rich medium to promote growth, it was decided to take the initially unmapped reads and map them against the mitochondrial genome of *Phytophthora capsici*. Final mapping rates after this step were much higher (2.10). Transcriptomic samples showed a generally high mapping rate (69-91%, 2.11). In order to ascertain how many of these reads were mapped properly to *P.capsici* counts of primary concordant reads against each genome were gathered. While it was clear that there were different proportions depending on what stage in the life cycle the transcript was taken (data not presented here), overall a large proportion of high quality reads mapped to the *Phytophthora capsici* genome(53-99% , 2.12).

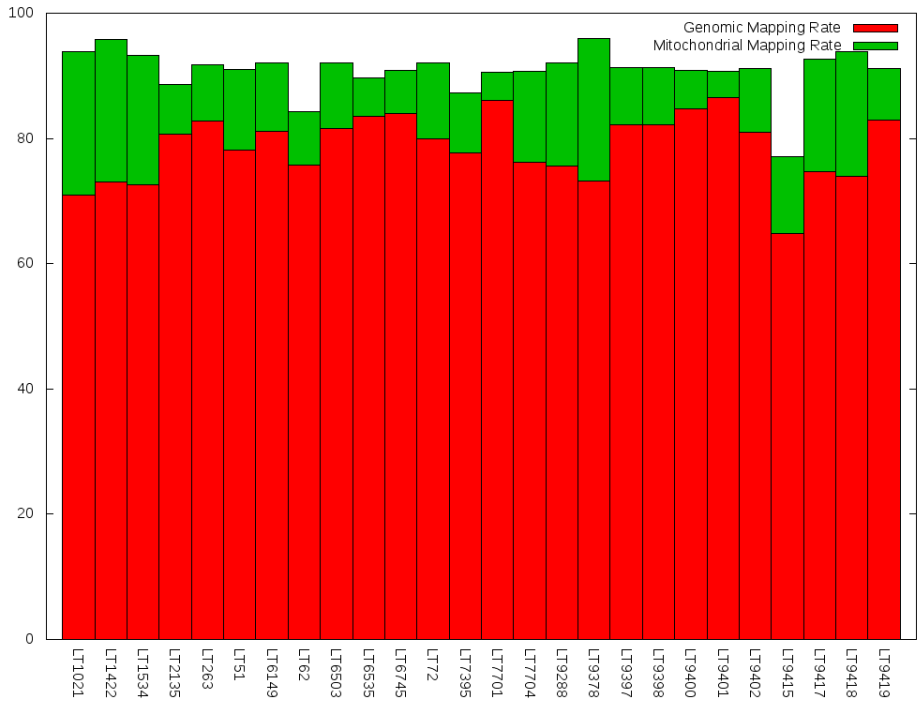

Figure 2.10: Mapping rate of genomic samples as reported by Bowtie2.

BAM files for the biotrophic and necrotrophic life stages of each isolate were merged into a single file. This file was then filtered to only include primary concordant reads that mapped to the *P.capsici* genome. Reads that sat across exon junction were then removed to ensure that ambiguous bases were not included in the pileup file. A pileup file was produced using samtools [76] for all genomic samples, all transcriptomic samples, and all samples combined.

SNP calling was carried out on each pileup file using the VarScan2 [93] program's mpileup2snp command. Table 2.1 contains a summary of the number of sites considered for SNP calling, number of SNPs called in each pool, and the number of sites shared across all isolates. In order to asses the effects of using transcriptomic samples for SNP calling comparisons between identical isolates used in both data collection sets was completed (Table 2.2). These comparisons showed that while pairwise samples had a calculated distance between 0.05 and 0.081 from each other, absolute differences(homozygous mismatch, heterozygous mismatch) in SNP calls did

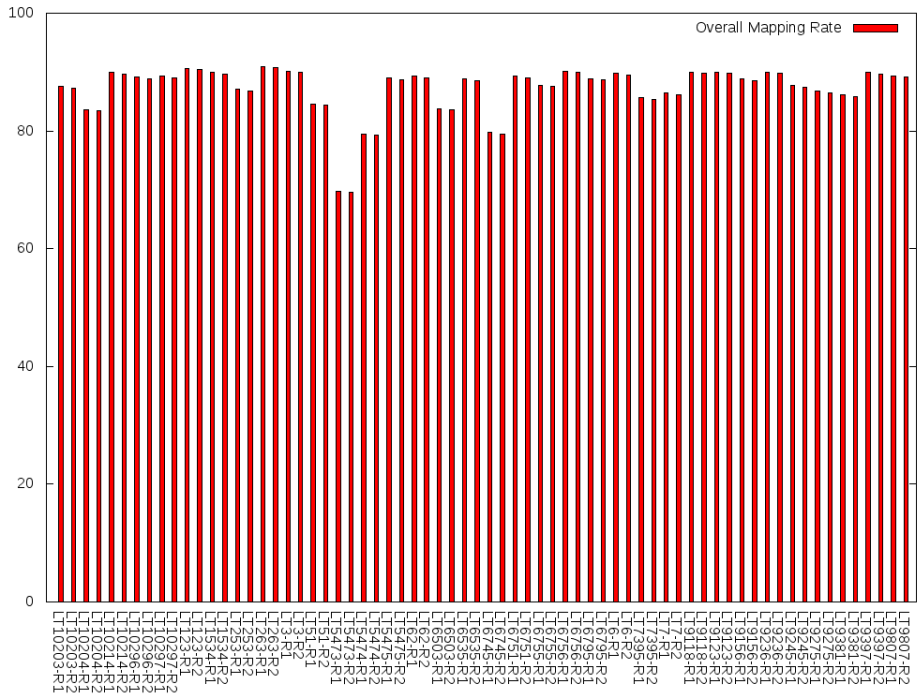

Figure 2.11: Average overall mapping rate of transcriptomic samples. Reported mapping statistics as reported by TopHat2 were arithmetically averaged between each isolate.

not make up many of the disagreements. A number of the disagreements generated came from calls switching from heterozygous to homozygous sites. This may be a statistical artifact of low coverage, the conversion of heterozygous sites has been described as a normally occurring event in *P. capsici* [103] and may also be driving a portion of these disagreements. While these type of errors may be problematic, it is more important for the community that the allele frequency at each site for a large number of individuals is available in order to allow for the usage of Bayesian methods of SNP calling in low coverage samples. This will help future projects by allowing more individuals to be sampled and the usage of low coverage sites in a statistically sound manner.

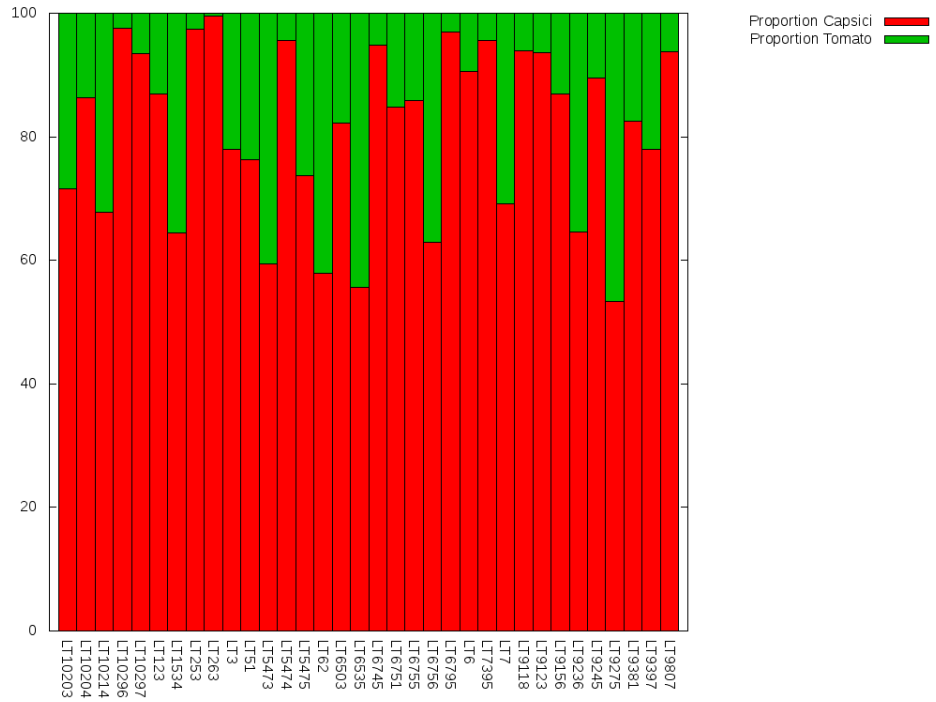

Figure 2.12: Average overall mapping rate of transcriptomic samples for each genome. The proportion of primary, concordant was calculated for each sample. These proportions were then arithmetically averaged for each isolate.

Table 2.1: SNP calling statistics for each pool of called individuals.

	Sites Considered	SNPs Called	Completely Shared
Transcriptomic Individuals	42,143,345	1,505,241	377,832
Genomic Individuals	56,178,139	2,740,759	287,301
All Individuals	56,178,139	3,522,934	12,507

Table 2.2: Comparison of Transcriptomic and Genomic SNP calls from re-sequenced isolates. Isolate - Isolate Identifier, Distance - Distance between Transcriptomic and Genomic samples, Total Mismatch - Total number of loci not in agreement, Hom-Hom - Number of Alleles that showed two different homozygous calls, Het-Het - Number of alleles that showed two different heterozygous alleles, Het-Hom - Number of loci that switched from heterozygous-homozygous. T(het)-G(hom) - The number of loci that were heterozygous in the transcriptomic sample and homozygous in the genomic sample, G(het)-T(hom) - The number of loci that went from heterozygous in the genome-homozygous in the transcriptome, Ratio - The ratio of events between T(het)-G(hom) and G(het)-T(hom).

Isolate	Distance	Total Mis-Match	Hom-Hom	Het-Het	Het-Hom	T(het)-G(hom)	G(het)-T(hom)	Ratio
7395	.050	1170	3	14	1155	153	1002	13.25% : 86.75%
6745	.050	1144	10	8	1129	451	678	39.95% : 60.05%
6503	.062	1471	10	10	1456	875	581	60.10% : 39.90%
51	.061	1485	8	12	1470	475	995	32.31% : 67.69%
263	.061	1460	13	5	1445	1183	262	81.87% : 18.13%
1534	.040	961	8	9	947	374	573	39.49% : 60.51%
9397	.081	1962	25	11	1931	1504	426	77.89% : 22.06%

2.3.3 Hierarchical Clustering and Principle Component Analysis on Populations

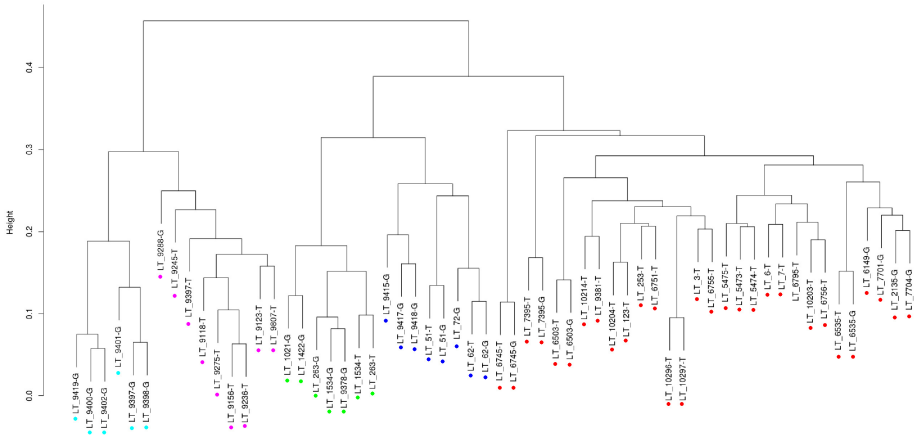

Figure 2.13: Dendogram of all samples distance matrix based on euclidean distance and complete linkage. Colored dots indicate which group an individual was assigned to based on this dendogram. Cyan - China A, Pink - China B, Blue - Western A, Red - Western B, Green - Lab

VarScan2 native output was transformed into a distance matrix using an internally developed script (Appendix A). It was decided to only use sites where all individuals had a base called for this operation.

Hierarchical clustering was performed on the calculated distance matrices for each pooled set using R, between row distances were calculated using a euclidean method and complete linkage was used for merging groups (Figure 2.13). The resulting dendogram shows that: all of the isolates originating from western countries are closer to each other than to those from China, the Chinese group most likely has at least two major groups, the western group has at least three major groups. When a heatmap (Figure 2.14) is produced by applying the dendogram to order the initial distance matrix some of the drivers of the clustering become more apparent.

While no re sampled isolates were identical, there was only one instance where they were merged with another isolates before their counterpart (LT_1534-T and LT_263-T). While this was unexpected it is not terribly surprising as LT263 is

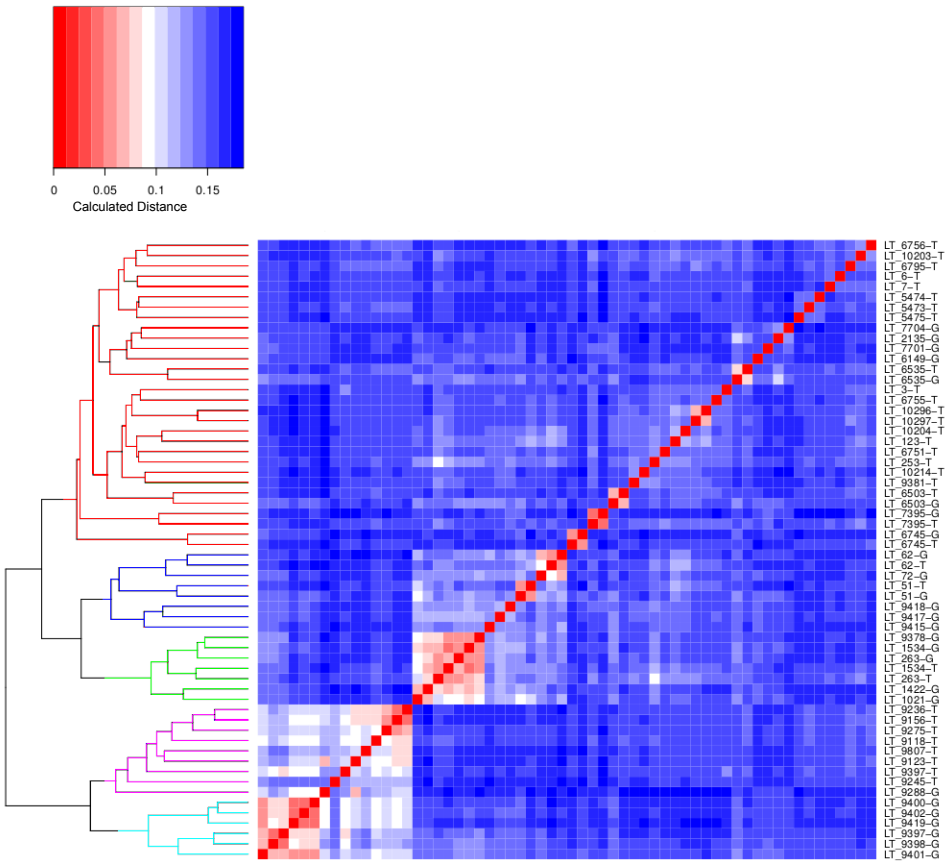

Figure 2.14: Clustered heat map of all individuals. The dendogram has been colored to match the dendogram colors in Figure 2.13.

the primary parent in the back-cross that created LT1534 and in the event that transcriptional bias is driving genotype calls one would expect them to have a small calculated distance from each other. It should be noted that a group of isolates (LT1021,LT1422,LT263,LT1534) formed a very distinct group far away from the other western samples. These isolates are all lab strains that were created for the building of the draft genome of *P. capsici* [107] or LT1534 with TD-TOM fluorescent label (LT9378). These isolates are derivatives of LT263. This brings up some concerns about the usefulness of these lab strains for translative based studies as they are

genetically distinct and have a life history that is wholly unique and artificial to the species.

If you look at the largest western population (Western B), it is clear that all of these individuals are largely distant from all other isolates and show little similarity to any other individuals. This group comprises a broad geographic range and while geographically linked isolates do appear to be more closely related to eachother (LT5473,LT5474,LT5475 ; LT10296,10297), distance calculations and clustering alone are incapable of resolving higher order differentiations.

Western A shows a higher level of internal similarity. This group contains individuals who: are the other parent of the back cross scheme (LT51,Michigan), geographically close (Wisconsin/Michigan), or from a research field in North Carolina. Whether this decrease in distance is due to inbreeding or similar selection pressures; it is clear that there is a difference from Western B.

The Chinese isolates are very distant from western and Lab groups and split into two distinct sub-groups: China A and China B. This dichotomy is due to the over representation of a genotype in China A; LT9401,LT9402,and LT9419 are all sectors of LT9400 that demonstrated major shifts while growing under lab conditions on V8-agar. These types of extreme phenotype shifts while under vegetative growth are indicitive of loss of heterozygosity. These samples give us a measurement for how much distance between individuals could be ascribed to this event. The China B clade is comprised of several related individuals that show very little similarity to any western or Lab Strains. These measurements parallel observations from previous studies [45, 46] but are not replicated enough to support the idea that a few highly clonal lineages exist in China.

Calculating distances and then clustering based on the resulting patterns of relationships means that differences are aggregated before any sort of group assignment occurs. In order to gain more fine scaled groupings based on the genomic location and pattern of SNPs principle component analysis was applied to this dataset using the EIGENSOFT 5.1 software package. Native Varscan2 outputs were transformed

into inputs for the EIGENSOFT package [105] using an internally developed script (Appendix B). The EIGENSOFT analysis was run with individuals binned into a number of groups: groups as defined by hierarchical clustering, country of origin, and state of origin(For US Samples).

Table 2.3: Statistical significance of eigenvectors based on Tracy-Widdom test statistic. Calculated using twstats from the EIGENSOFT software package.

Number	Eigenvalue	TW-pvalue
1	4.984158	4.83E-018
2	3.223916	6.69E-008
3	2.46997	0.0231457
4	2.276269	0.0748581
5	2.072959	0.330732
6	1.883087	0.819575
7	1.804541	0.863314
8	1.63595	0.99796
9	1.557456	0.999759
10	1.552837	0.997547

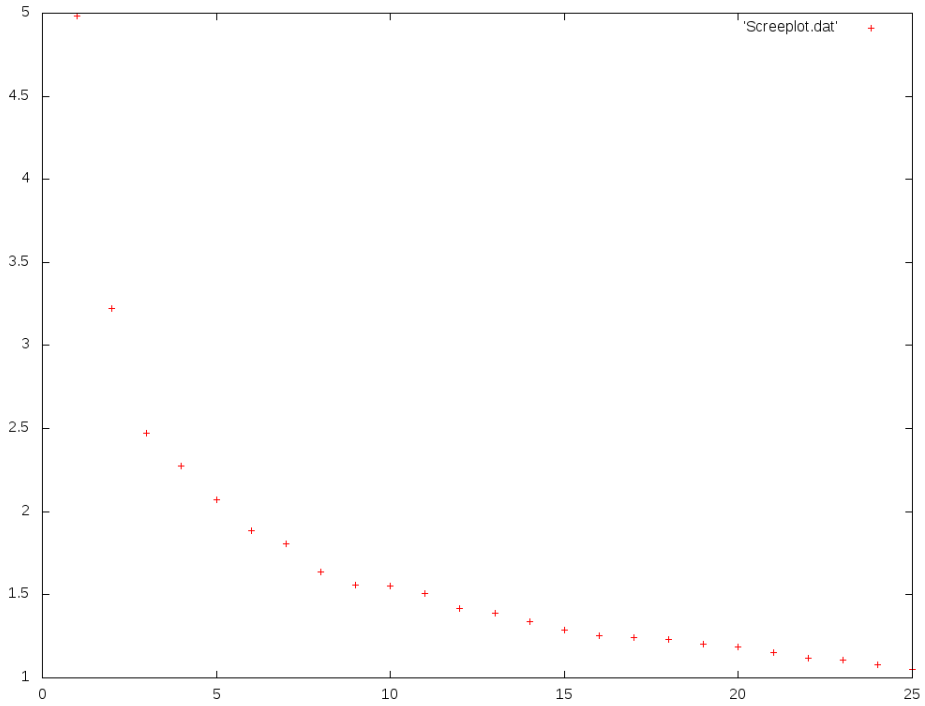

Figure 2.15: A screeplot of the eigenvalues calculated from principle component analysis.

The Tracy-Widom statistic was calculated and a scree plot generated on the resulting eigenvalues from the PCA analysis (Table 2.3 , Figure 2.15). While the output from calculating Tracy-Widom test statistics indicates that only the first three factors are significant, the scree plot indicates that more factors may still be informative. As a result of this it was decided to continue all resulting analyses in EIGENSOFT while keeping the top ten principle components. The ten SNPs with the highest singular value decomposition for each eigenvector are presented in Appendix C.

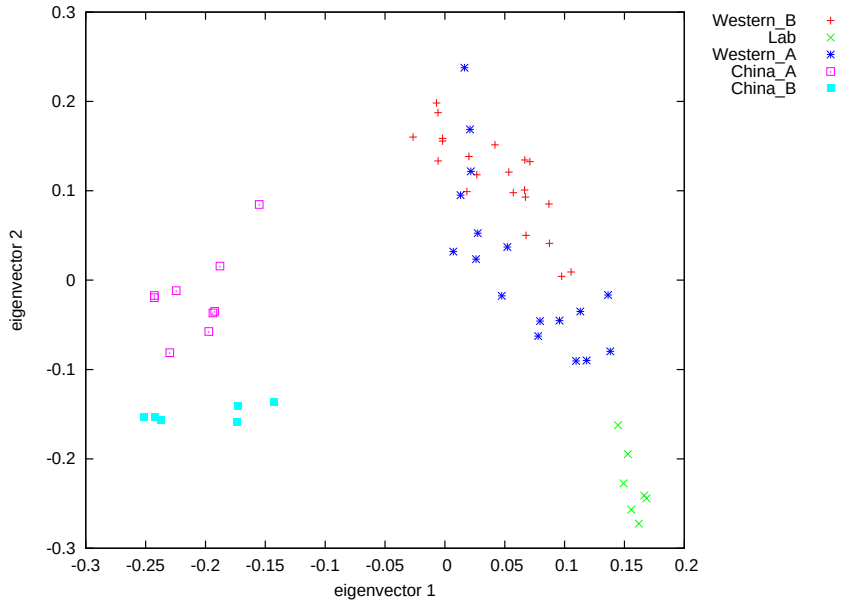

Figure 2.16: Plot of the first two Eigenvectors of PCA analysis; populations based on hierarchical clustering coloring corresponds to 2.13.

Table 2.4: Statistical significance of differences between populations as defined on groups found during hierarchical clustering are shown on the upper triangle. The statistically significant (pvalue <1e-3)eigenvectors between each group is on the lower triangle.

	Lab	Western_A	Western_B	China_A	China_B
Lab	x	5.5441e-19	1.02768e-21	2.86361e-49	6.79034e-30
Western_A	1,2,4,5	x	1.40091e-12	3.12257e-22	1.23574e-24
Western_B	1,2	1,2,5	x	1.51584e-22	1.34019e-19
China_A	1,2,3,4,7,8,9,10	1,2,8	1,2	x	2.99121e-30
China_B	1,2,5,8	1,2,4	1,2	2,3,4,7,8,9,10	x

When labeling samples by the large groups defined during hierarchical clustering, it is apparent that the populations are readily identifiable along the first two

eigenvectors of analysis and all groups are statistically significant from eachother along a number of components and in overall space (Table 3.4,Fig 2.16).

These results are interesting but hardly surprising based on previously measured genetic distances. The Chinese isolates show low within group variation. This may be indicative of long term inbreeding and/or mitotic recombination combined with a lack of introduced allelic diversity from outside sources. What is unclear is whether this has resulted in previously reported clonal populations ([45, 46]) or simply reduced allelic complexity, the variance along eigen vectors within the Chinese population would seem to indicate the latter. the Chinese population would seem to indicate the latter.

Lab strains of the pathogen continue to show that they are infact highly distinct from all other individuals in the analysis (including their parents) and very unique when compared to Chinese isolates. This should help serve as a strong reminder that the strain sequenced for the published genome has a unique life history resulting in what is a comparatively abnormal genomic landscape.

WesternA continues to show that while similar to Western B , it is statistically unique. Western B also showed the highest within group variance in eigenvalues along each vector indicating that it may be comprised of many smaller groups.

In order to determine if there are differences at different levels of geographic granularity, individuals were relabeled on first a country (Table 2.5,Fig 2.17) then for US isolates a state basis(Table 2.6,Fig 2.18). Based on these results is evident that there is a distinct difference between individuals from different countries and even between states in the US. Because this partitioning of data results in a lower sample number for subsequent statistical tests, only samples with at least n=3 have been reported. These results demonstrate that the WesternB group is made up of a large number of smaller groups that contain local similarities but between group variability.

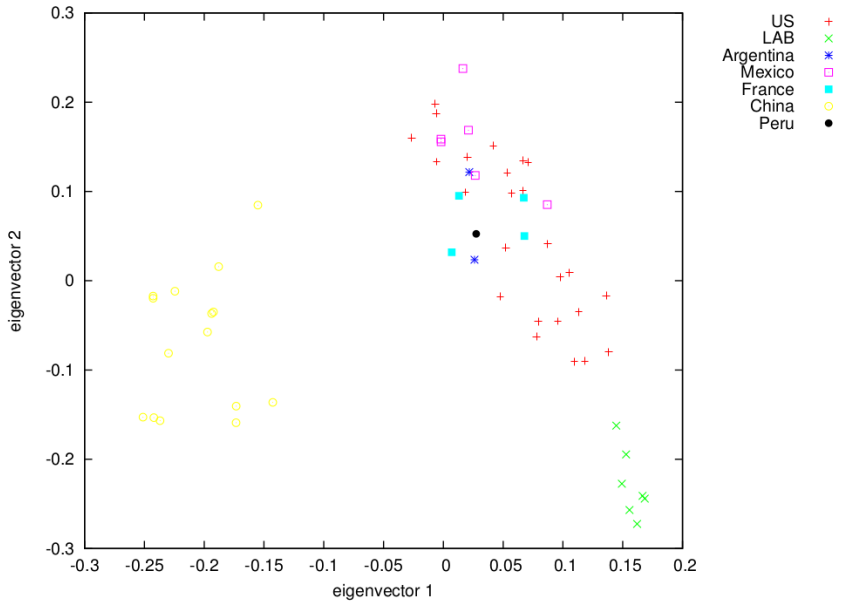

Figure 2.17: Plot of the first two Eigenvectors of PCA analysis; populations defined by country.

Table 2.5: Statistical significance of differences between countries. Significant Chi-Squared tests are on the upper triangle. The statistically significant (p-value <1e-3) eigenvectors between each group is on the lower triangle.

	US	Lab	Mexico	France	China
US	x	1.57E-14	0.00024	1.68E-10	8.01E-21
Lab	1,2,4	x	1.29E-16	6.75E-19	2.16E-26
Mexico	4	1,2,5	x	2.59E-8	1.45E-15
France	3,4	1,2,4	4,5	x	9.17E-28
China	1,2	1,2,4,5	1,2	1,4,5	x

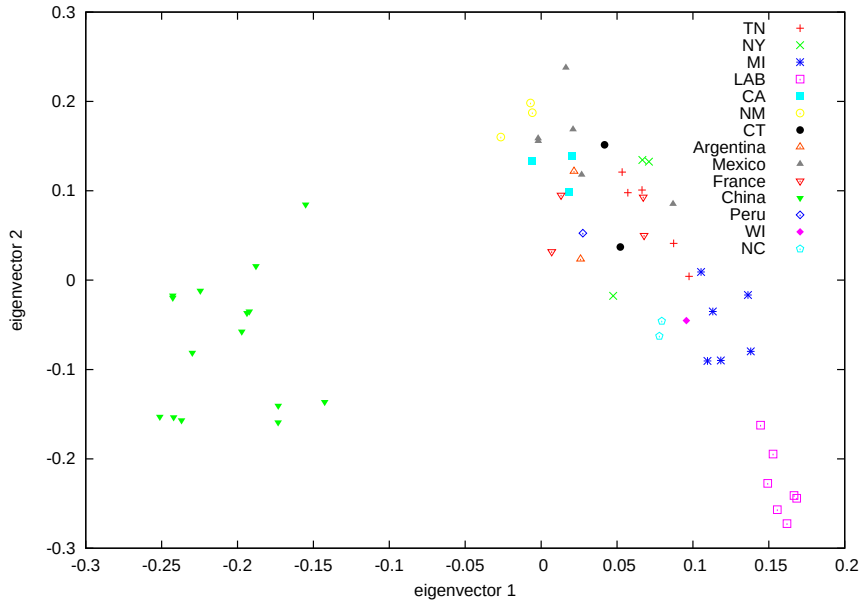

Figure 2.18: Plot of the first two Eigenvectors of PCA analysis; populations defined by country and state.

Table 2.6: Statistical significance of differences between states. States without enough samples to be considered are not included in this table. Significance as a result of a Chi-Squared test is on the upper triangle, significant eigenvectore (p-value <1e-3) are on the lower triangle.

	TN	NY	MI	CA	NM	CT	NC
TN	X	0.00102285	2.17E-10	7.20E-6	1.27E-11	2.71E-9	0.000821334
NY		X	1.06E-16	1.02E-10	9.75E-11	0.000112663	1.87E-8
MI	1	1,7,9	X	2.15E-17	3.87E-22	2.60E-19	5.43E-11
CA		5	1,2,5	X	2.97E-10	6.84E-9	1.20E-9
NM	1		1,2,4,5		X	3.09E-11	8.19E-15
CT	8		1,7,8			X	2.19E-15
NC			10		2		X

This first ever comparasion of isolates across distinct geographic locations provides a number of insights into the life history of the pathogen *Phytophthora capsici*. While the within population variation of this pathogen has been studied numerous times [21, 37–46], markers used in these studies were not conserved across studies making it impossible to do a global comparison. With the application of next generation sequencing it becomes a relatively trivial matter make these comparasions using a unified marker set.

This is the first time it has been possible to make direct comparisons between isolates of different countries. These comparisons make it quite obvious that there are definte large scale differences between countries (Table 2.5); the most considerable difference being between that of China and Western countries. This difference is not just the result of relative distance (Figure 2.14) but also genetic content (Figure 2.17) and may be the result of a founder effect coupled with inbreeding loss of heterozygosity and the lack of gene flow coming into the Chinese region. This type of situation means that the use of genetic resistance in crops to control this pathogen is tenable but that breeders need to ensure that they are developing these crops using isolates from the area. This lack of genetic diversity, signatures of inbreeding, and lack of gene flow also mean that genetic resistance is more likely to be robust and long lasting.

On the other hand, the Western isolates continue to show that they are genetically distant when compared to each other even when coming from the same region(Figure 2.14). This variability is patterned enough to allow regions to be statistically separated from each other (Table 2.6) indicating that there is some underlying structure to what appears to be a homogeneous group of individuals. This may create a more difficult situation when it comes to using genetic control in the pathogen in these areas and if there is any sort of drift between these populations make generating plant germ-lines with robust resistance an intractable problem.

This study demonstrates the relative and absolute differences between individuals drawn from a global panel of *P. capsici* isolates. These similarities and differences are especially important when thought of from the context of effector based breading

strategies that are becoming increasingly popular in an effort to exploit genetic resistance for control. While not directly addressed in this study , it is highly probable and likely that a number of these differences fall within avirulence factors that are important for infection and are detected by host R genes. These levels of absolute difference between isolates and conservation at a local regional level indicate that great care needs to be made in these breeding schemes to either : identify and target highly conserved breeding targets in the pathogen or develop multiple strains of resistant plants that can be targeted to the local genetic structure of the pathogen.

Chapter 3

Molecular description of *Phytopthora tropicalis*

3.1 Introduction

Phytophthora tropicalis is relatively recently described species in the *Phytophthora* genus [98]. The original description included certain isolates that were originally classified as *Phytophthora capsici* and *Phytophthora palmivora* MF4 [4]. Initial characteristics that were used to differentiate *P.tropicalis* from *P. capsici* were morphological in nature and included: the production of chlamydospores, poor to no growth at 35 degrees Celsius, a lack of pathogenicity on *Capsicum* seedlings, and narrow sporangia. Most isolates of *P. tropicalis* were also isolated from woody perennial plants like : *Piper nigrum* , *Macademia itergrifolia* , and *Theobroma cacao* [98].

Before *P. tropicalis* was formally described there was evidence that there were extreme levels of variation within the *P. capsici* species, and through the usage of morphological data and isozymes the species was initially described as having three and later two subgroups [95–97].

The development of multiple gene molecular phylogenies in the genus *Phytophthora* using the internal transcribed spacer (ITS) sequence [99], mitochondrial cytochrome oxidase genes [100], and other molecular [27, 101, 108] markers has created a situation where while it is clear that *P. tropicalis* is a distinct species its classification is difficult due to the continuum of variation that spans between both species [102, 109, 110].

One of the objectives of our laboratory is to develop and describe molecular tools for the identification and classification of *Phytophthora capsici*. As a result of historically fluid description of this species it has also become important for us to be able to quickly and succinctly identify if an isolate is instead *Phytophthora tropicalis* so that we may properly include or exclude it in relevant studies. Here we present evidence for the continued description of *P. tropicalis* as at least one species and molecular data that can be used to distinguish isolates.

3.2 Materials and Methods

3.2.1 Isolate Selection:

Isolates were selected based on geographic diversity and host range. Please note that *P. subnubulus* has not been described and was named such due to its host of collection but lack of *P. capscici* characteristics. Table 3.1 contains a description of isolates used in this study.

Isolate	Species	Location	Host	Citation
LT_5230	P. subnubulus	Oxapampa, Peru	*C. Pubescens*	[43, 44]
LT_5287	P. subnubulus	Oxapampa, Peru	*C. Pubescens*	[43, 44]
LT_5395	P. subnubulus	Oxapampa, Peru	*C. Pubescens*	[43, 44]
LT_5761	P. tropicalis	Oahu	*C. papaya*	[98]
LT_35	P. tropicalis	Brazil	*T. cacao*	[96]

LT_232	P. tropicalis	Murfreesboro, TN	*Rhododendron*	[102]
LT_29	P. tropicalis	Brazil	*T. cacao*	[96]
LT_5762	P. tropicalis	Hawaii	*Anthurium*	[98]
LT_5763	P. tropicalis	Oahu	*D. caryophylus*	[98]
LT_1021	P. capsici	Lab		[107]
LT_1422	P. capsici	Lab		[107]
LT_1534	P. capsici	Lab		[103]
LT_2135	P. capsici	Lab		[107]
LT_263	P. capsici	Tennessee	*Cucurbita*	
LT_51	P. capsici	Michigan	*Cucurbita*	[38]
LT_6149	P. capsici	NY	*Cucurbita*	
LT_62	P. capsici	Michigan	*Cucurbita*	[38]
LT_6503	P. capsici	Conneticut	*P. vulgaris*	
LT_6535	P. capsici	Argentina	*C. Annuum*	
LT_6745	P. capsici	Mexico	*C. Annuum*	
LT_72	P. capsici	Michigan	*Cucurbita*	[38]
LT_7395	P. capsici	France	*C. Annuum*	
LT_7701	P. capsici	France	*C. Annuum*	
LT_7704	P. capsici	France	*C. Annuum*	
LT_9288	P. capsici	China	*C. Annuum*	[45, 46]
LT_9378	P. capsici	Lab		[103]
LT_9397	P. capsici	China	*C. Annuum*	[45, 46]
LT_9398	P. capsici	China	*C. Annuum*	[45, 46]
LT_9400	P. capsici	China	*C. Annuum*	[45, 46]
LT_9401	P. capsici	China	*C. Annuum*	[45, 46]
LT_9402	P. capsici	China	*C. Annuum*	[45, 46]
LT_9415	P. capsici	Wisconsin	*Cucurbita*	

LT_9417	P. capsici	North Carolina	*C. lanatus*	
LT_9418	P. capsici	North Carolina	*C. lanatus*	
LT_9419	P. capsici	China	*C. Annuum*	[45, 46]

Table 3.1: A brief description of isolates used in this study, their initial species description, collection location, and host collected from.

3.2.2 Isolate Growth and Genomic DNA extraction:

Tufts of mycellia were placed into 50mL Falcon tubes of liquid V8-PARP media (160 mL of V8, 3g CaCo3, 960 mL of ddH2O, 25ppm pimaricin, 25ppm rifampacin, 25ppm PCNB, 100ppm ampacillin). Tubes were grown with agitation at 28 degrees Celsius for 3 days. Tissue was harvested and lyopholized; then powdered using liquid nitrogen, mortar, and pestle. Genomic DNA was extracted using standard phenol/chloroform extraction methods. All sample concentrations were checked via 260/280 absorption readings using a NanoDrop ND-1000 and high molecular weight DNA verified using 1% agarose gel.

3.2.3 Library Construction and Sequencing:

Genomic sequencing was carried out on an Illumina HiSeq 2000 with 100bp single end reads being output. All sample and library preperation was carried out by staff at Children's Mercy Hospital (Kansas City, MO, USA) as per manufacturers instructions.

3.2.4 Read Mapping:

Reads were mapped to the Phytophthora capsici genome [103] using Bowtie2 [80]. Bowtie was employed using the end-to-end high sensitivity mode and the following modifications: -D 40 -R 10 -L10 -N1. Only uniquely mapping reads were used for

consensus sequence determination and SNP calling. Potential PCR duplicates were then removed from these mapped reads using the samtools utility [76].

3.2.5 Consensus Sequence Determination (Transcriptomic and Genomic) and SNP calling:

SNPs were called using the VarScan2 (ver 2.3.4) program [93] with the following settings: 8x coverage , 3x alternate allele minimum coverage, minimum quality score of 20, minimum variant frequency of 0.1, and a P-value threshold of 0.01.

3.2.6 Between Isolate Distance and Clustering:

All sites in which mapping data was available for all samples were considered for calculating distance.The distance between two individuals being defined as :

$$D_{ij} = \frac{1}{L} \sum_{l=1}^{L} d_{ij}^{l}$$

Where L is the number of sites observed for comparison and was set to 1 base calls with no overlap, 0 for matching consensus base calls, 0.5 for heterozygous/homozygous overlap (i.e. : A to [W,M], T to [Y,K], G to [S,K], C to [Y,S]), or 0.83 for heterozygous/heterozygous overlap (i.e. : R to [Y,S,W,K,M] , Y to [S,W,K,M] , S to [R,Y,K,M], W to [R,Y,K,M], M to [R,Y,S,W,M]).

Hierarchical clustering was performed on the calculated distance matrix using euclidean distances and complete linkage in R.

3.2.7 SNP Matrix Construction and PCA analysis:

SNP data was transformed into a numerical matrix and a PCA analysis was performed by the EIGENSOFT (ver 5.1) suite of programs [105,106]. SNP data was transformed by comparing each site against the re-sequenced LT1534 genomic sequence and assigning a score between 0-2 where: 0 is a match , 1 is a heterozygous match , 2 is

a mismatch. The significance of eigenvectors was determined by the Tracey-Widom test , also implemented in the EIGENSOFT package.

3.3 Results and Discussion

3.3.1 Raw Sequencing, Mapping of Data, and SNP calling

Individual files were combined into single files for each library library and summary statistics were calculated using internally developed scripts and programs. Cumulative quality scores (Figure 3.1) for all samples showed a large number of good to high quality bases in each sample and for each run overall. Nucleotide proportions at each position (Figure 3.2) showed a near even distribution at most reported positions. Quality scores (Figure 3.3) showed >80% of position quality scores were over 30 in all samples.

Mapping rates were expectedly low for *P.tropicalis* and *P. subnubulu* isolates, between 15% and 20%, while *P.capsci* rates were at levels from 70-90% (data not shown). All mapping files had potential PCR duplicates removed using the samtools package [76].

Variant calling was carried out on pileup files of all samples using the VarScan2 utility. Of 56,174,635 considiered bases in pileup file 2,766,390 SNP positions were called and 2,740,759 positions were maintained after filtering for strand bias.

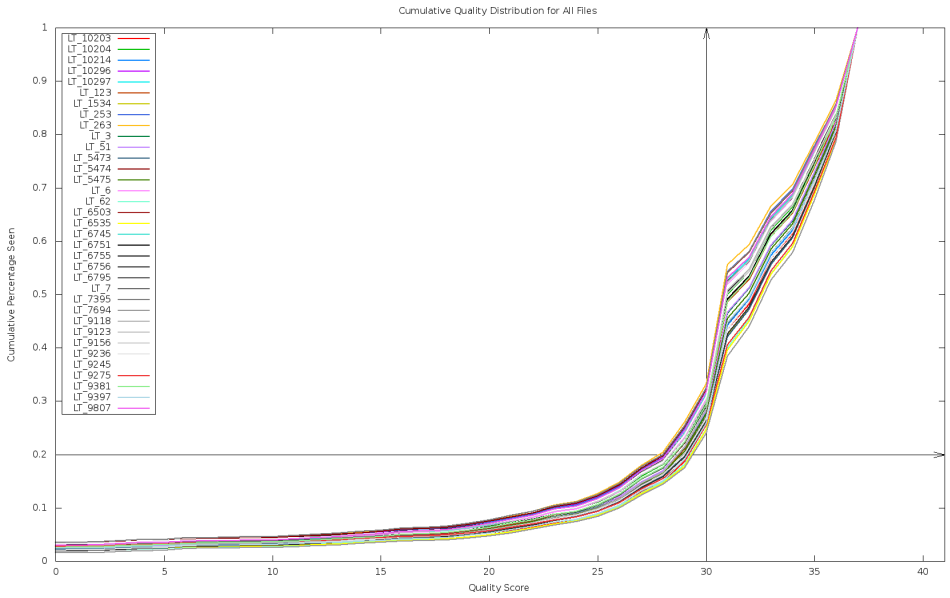

Figure 3.1: Cumulative proportion of sequencing quality scores for the run.

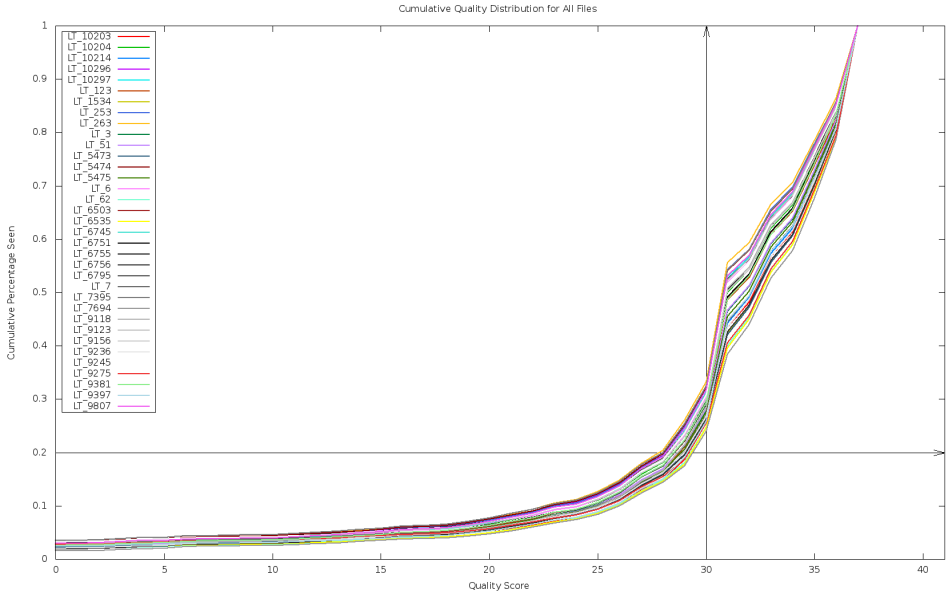

Figure 3.2: Cumulative proportion of sequencing quality scores for the run.

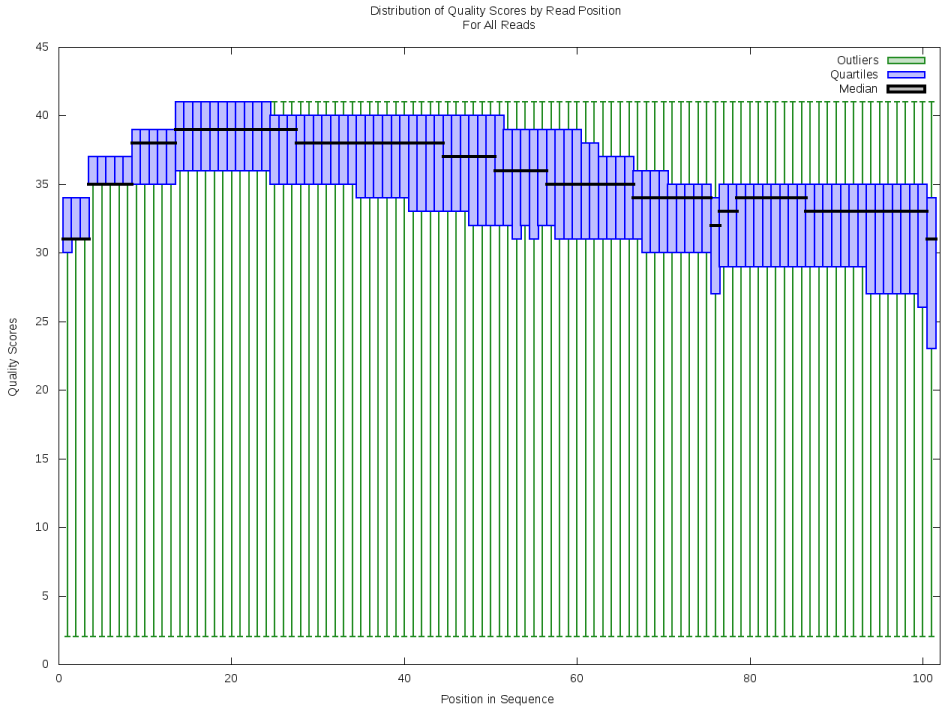

Figure 3.3: Distribution of quality scores at each position in the run.

3.3.2 Hierarchical Clustering and Principle Component Analysis

VarScan2 native output was transformed into a distance matrix using internally developed scripts (Appendix A). It was decided to only use sites where all individuals had a base called for this operation. After this filtering step 35,163 sites were used for all further analysis.

Hierarchical clustering was performed on the calculated distance matrix in R, between row distances were calculated using a euclidean method and complete linkage was used for merging groups (Figure 3.4). The resulting dendrogram shows that: all *P. capsici* isolates predictably cluster together, these isolates are predictably distant from other isolates, the *P. tropicalis* isolates break into two distinct clades, and the *P. subnublus* sample form a grouping next to but relatively distant from *P.tropicalis samples*. When a heatmap (Figure 3.5) is produced with this dendrogram it is

apparent that there are at least three sub-groups of individuals in the *P. tropicalis* / *P. subnubulus* line and the group comprised of LT5762 , LT5761 , LT5763 , LT232 may be comprised of even more sub groups.

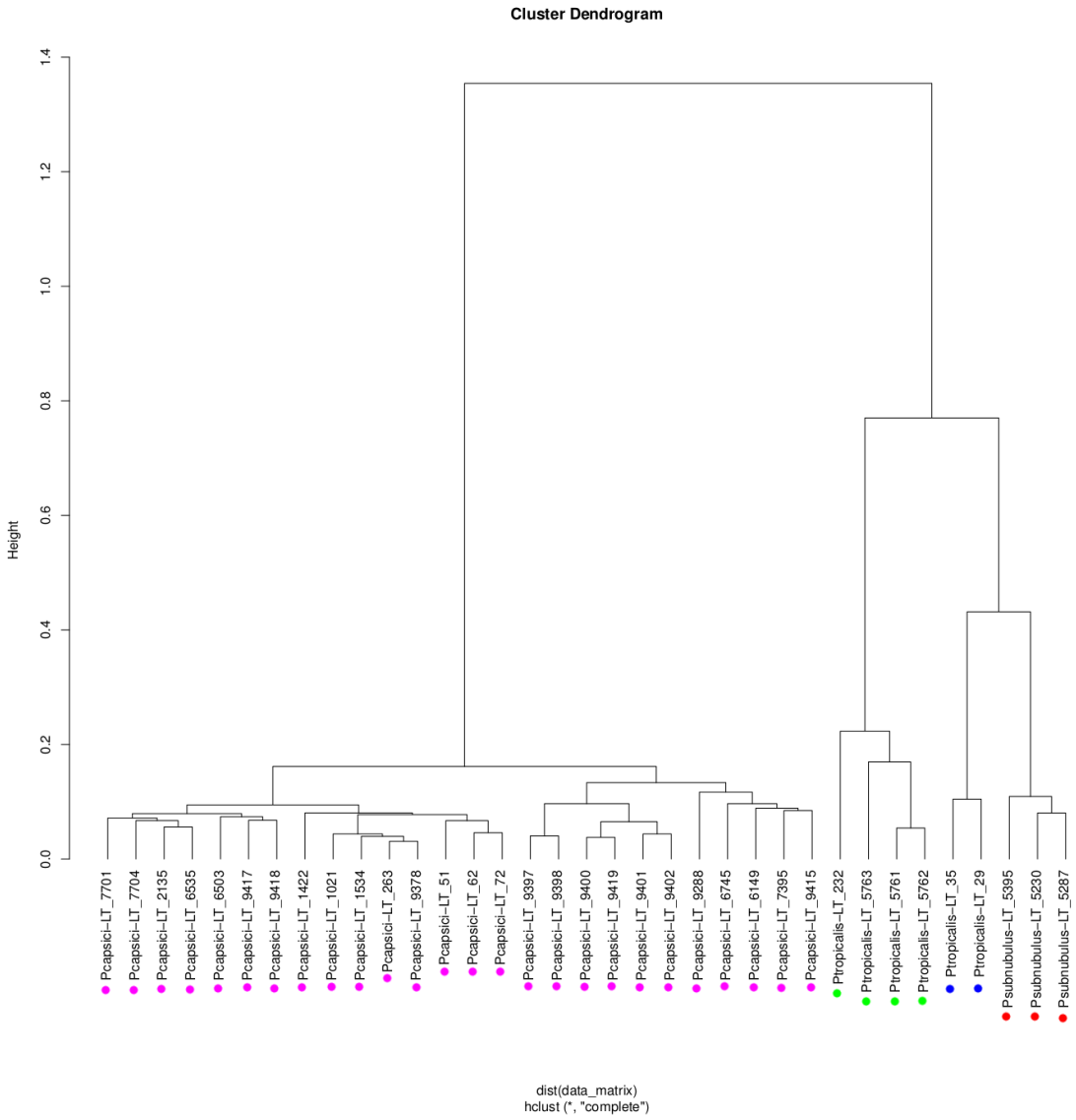

Figure 3.4: Dendrogram of all individuals calculated from the SNP distance matrix. Generated using complete language and the euclidean distance between all samples.

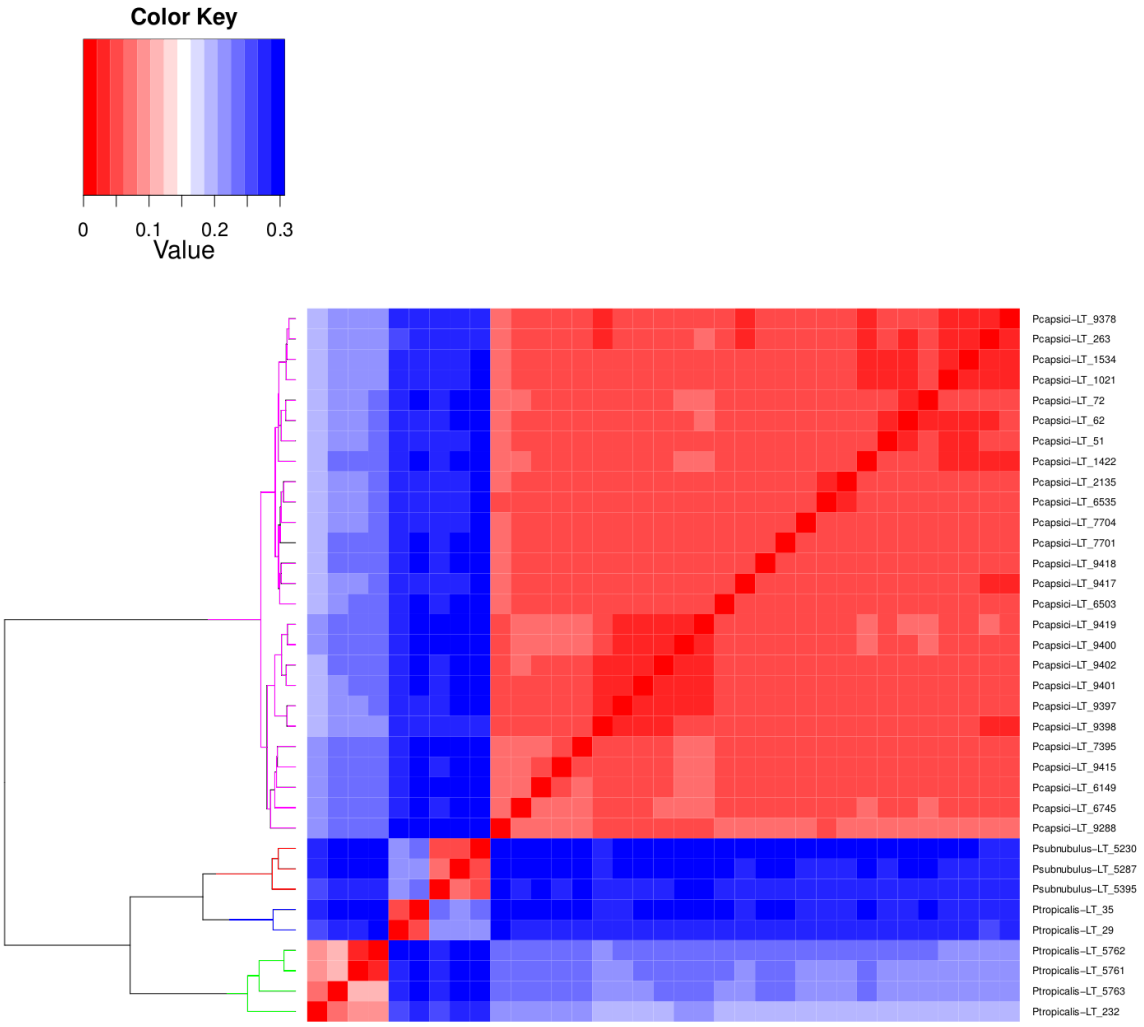

Figure 3.5: Heatmap of all individuals.

SNP data was transformed into a matrix suitable for PCA analysis using internally developed scripts (B). PCA was carried out using the EIGENSOFT software package with population labels applied derived from both presumed species name and hierarchical clustering groups. Tracy-Widom statistics were calculated on the resultant eigenvectors of analysis and show that the first four eigenvectors were of statistical significance, a screeplot on the same data shows the same (Table 3.2 and Figure 3.6).

PCA plots of the first three eigenvectors were plotted using labels either garnered from hierarchical clustering or assigned species name (Figures 3.7, 3.8 and Figures 3.9, 3.10 respectively). These plots show that while it is clear on a genomic level that *P.capsci* and *P.tropicalis* are distinct from eachother , there may be at least 2 sub groups of *P. tropicalis* and the tenatively named *P. subnubulus* is also its own group. Interestingly, the isolates identified as *P. subnubulus* demonstrate a number of morphological and genomic similarites to *P. tropicalis* but were collected from pepper plants in Peruvian farms near the jungle. This may indicate that like *P. capsici* this species may be capable of jumping to new hosts, or more likely simply was in an environment provided it with an environment that was conducive to growth. *P. tropicalis* group B also warrants further attention as this grouping shows a high level of within group variation and may harbor multiple sub-populations.

Calculations of significance between both plots was also performed and is reported on Tables 3.4 and 3.3 for both sets of labels. It is clear both from the PCA and these calculations that while *P. tropicalis* is clearly its own species compared to *P. capcisi*, there may be further sub groups or species left to describe.

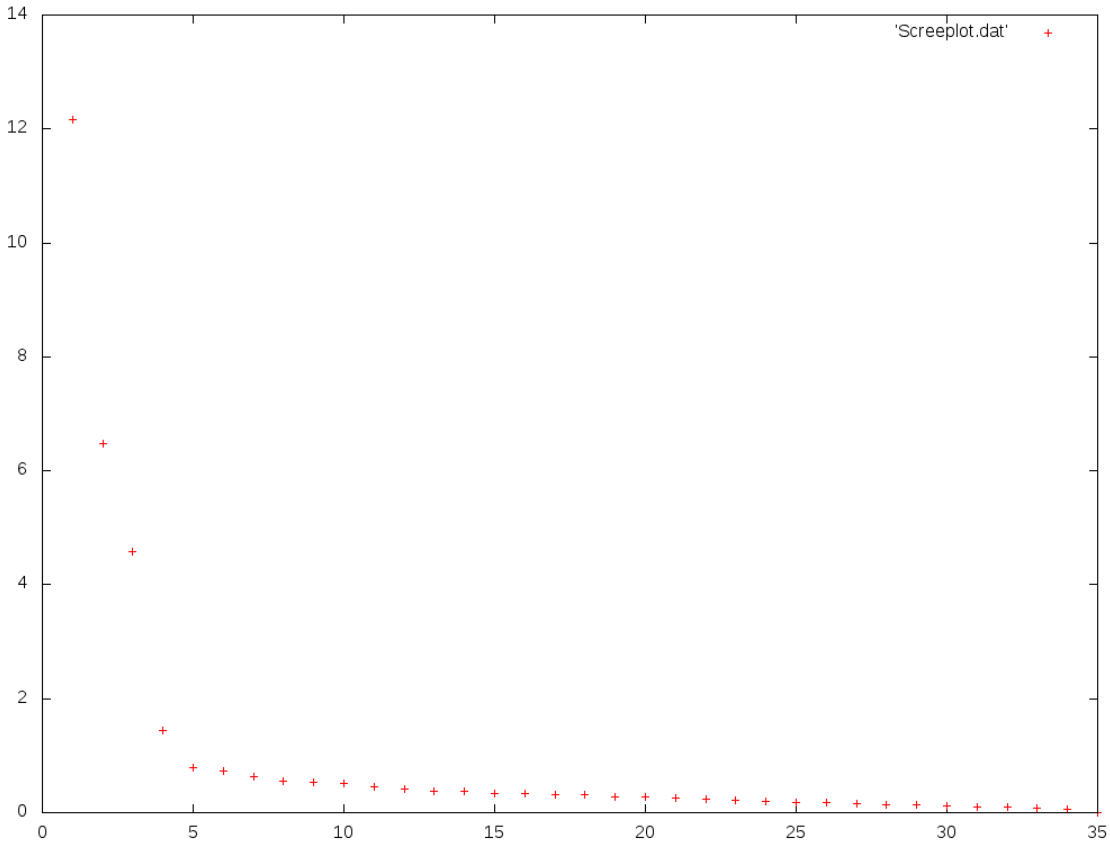

Figure 3.6

Table 3.2: Statistical significance of eigenvectors generated during PCA, calculated using the twstats package from EIGENSOFT.

#N	eigenvalue	p-value
1	12.158865	0.01587
2	6.476862	0.00778839
3	4.580823	8.61E-006
4	1.437583	5.26E-007
5	0.786518	0.154235

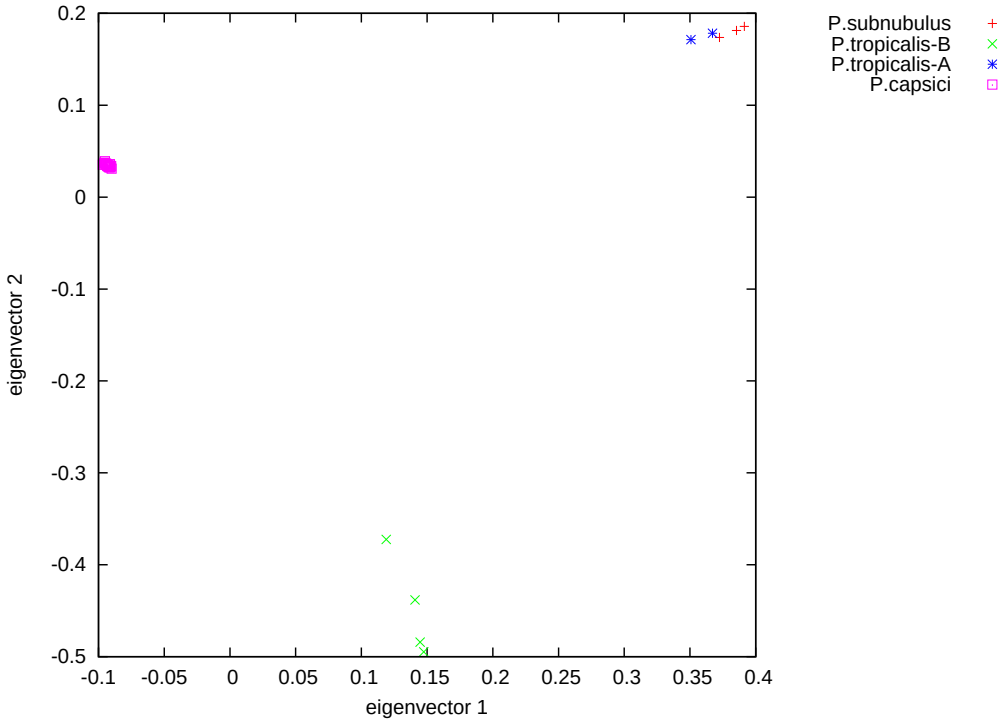

Figure 3.7: Plot of the first two Eigenvectors of PCA analysis,groups assigned by herarchical clustering.

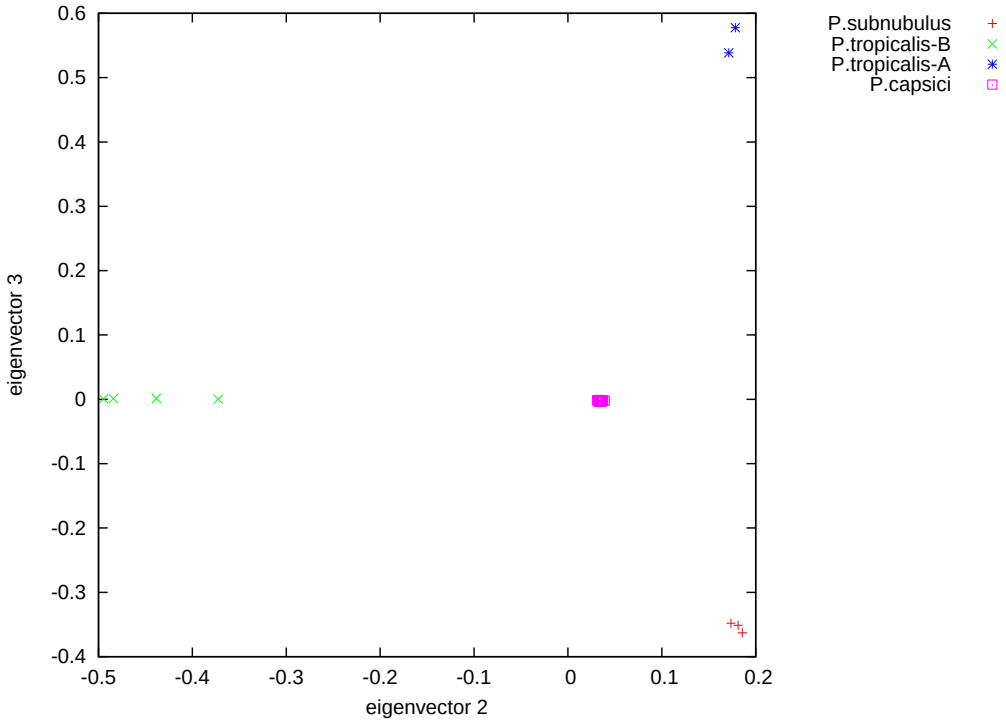

Figure 3.8: Plot of the Second two Eigenvectors of PCA analysis, groups assigned by hierarchical clustering.

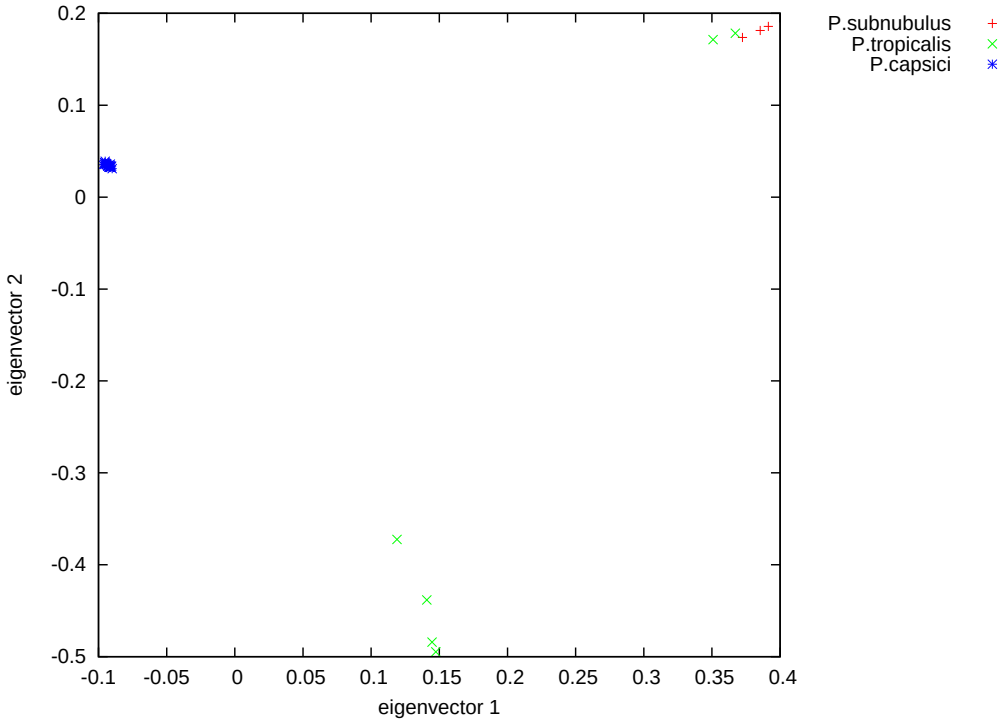

Figure 3.9: Plot of the first two Eigenvectors of PCA analysis, groups assigned by species.

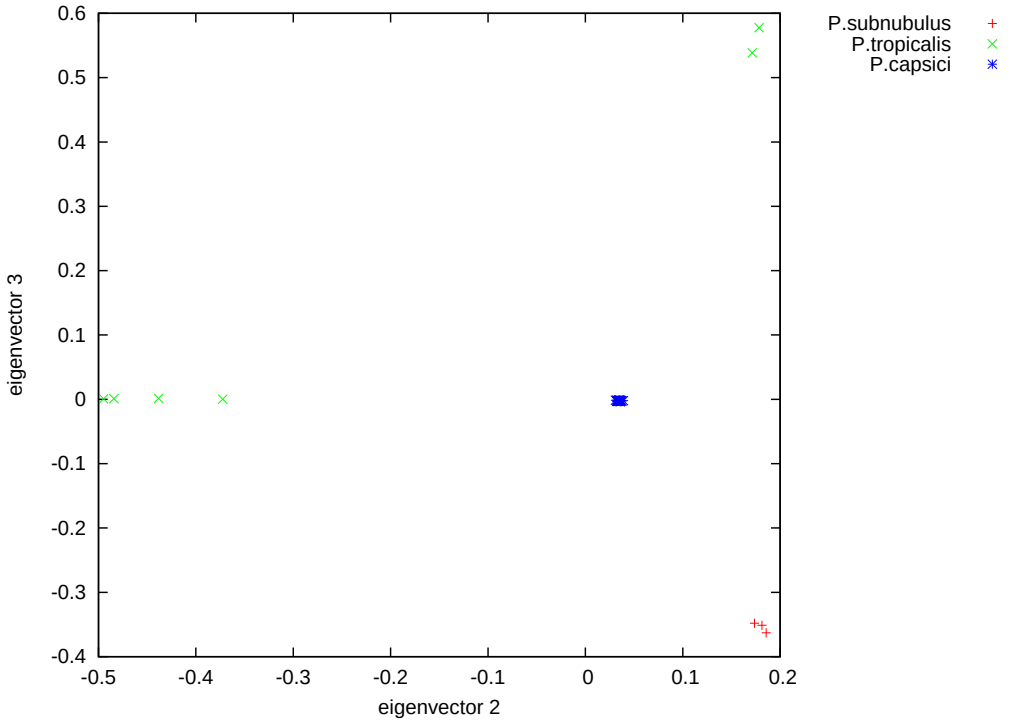

Figure 3.10: Plot of the Second two Eigenvectors of PCA analysis, groups assigned by species.

Table 3.3: Statistical significance of differences between species. Significance as a result of a Chi-Squared test is on the upper triangle, significant eigenvectors (p-value <1e-3) are on the lower triangle.

	P. tropicalis	*P. subnubulus*	*P. capsici*
P. tropicalis	x	0.00259772	8.37168e-19
P. subnubulus		X	5.24046e-137
P. capsici	1,2,3,4	1,2	X

These results taken as a whole strongly support the continued separation of *P.tropicalis* from *P. capsici* and continue to support previous findings that suggest that there is reason to re-structure the *P. tropicalis* species into more sub groups [102]. They further point to a need to further study this species as it is clear that while there

Table 3.4: Statistical significance of differences between groups assigned by hierarchical clustering. Significance as a result of a Chi-Squared test is on the upper triangle, significant eigenvectors (p-value <1e-3) are on the lower triangle.

	P. Tropicalis-A	*P. Tropicalis*-B	*P. Subnubulus*	*P. Capsici*	
P. Tropicalis-A	X	7.48e-18	4.75e-08	3.48E-122	
P. Tropicalis-B	1,2,3	X	1.14e-23	7.82E-073	
P. Subnubulus	1,3	1,2,3	X	5.24E-137	
P. Capsici	1,2,3	1,2,3	1,2,3	X	

are potentially highly divergent groups within *P. tropicalis* there was not enough data in this group to adequately describe it.

It has been clear for some time that the usage of standard highly conserved molecular markers for phylogeny reconstruction while powerful offers little in situations where highly divergent species show overlapping variations at the same loci [27, 95–102, 108–110]. In order to properly measure and determine the structure of groups from each other it is important that data collection be done in a more agnostic matter, allowing for the sampling of sites that are not classically used (such as ITS and COX)and instead using sites that maximize chances of observing variation.

We further demonstrate the power of applying NGS technologies and population level analysis to non model organisms that have historically been overlooked in these fields. As the costs associated with these techniques continues to drop it is crucial that researchers of these less studied (but still highly important) species begin adopting and utilizing these tools. As we have demonstrated here it is possible to apply these techniques and technologies even without classically needed resources such as a reference genome. These technologies have already allowed for us to provide a series of SNP markers that allow researchers to assign isolates to these provisional groups D.

Chapter 4

Effector Diversity in *Phytophthora capsici*

4.1 Introduction

Plant pathogens secrete proteins that target host proteins within the host cytoplasm and directly modify host cell processes in order to promote infection [47, 49, 51, 111]. Within the oomycetes there are two large and widely studied classes of effectors: the RxLR so named because of a linear Arginine-Anything-Leucine-Arginine motif [66, 67], and the Crinkler (CRN) intially named after their demonstrated phenotype of leaf crinkling [112, 113]. These effector classes have been widely studied in the *Phytophthora infestans* and *Phytophthora sojae* patho systems and have been demonstrated to play a large role in the pathogens ability to infect a host. They have also been demonstrated as being responsible for host recognition by host R genes [53, 54, 114].

As potential agents for a hosts ability to recognize a pathogen, effectors have held the promise of providing strong breeding targets in the screening and development of pathogen resistant germplasm [115, 116]. This method has proven to be a successful strategy in creating crop lines resistant to *P. infestans* [60, 61] and is in varying levels

of development in other *Phytophthora* patho-systems.The physical assaying of protein in plant/pathogen pathosystems continues to be a major bottle neck in the description and functional classification of effector proteins [117] and as our ability to describe potential effectors in a genome is ever increasing this problem has been exacerbated.

Phytophthora capsici is a globally important plant pathogen known to infect a broad range of hosts in the field [36]. It has also been demonstrated that it has high levels of between isolate variation and likely uses a number of mechanisms to quickly both quickly fix alleles and maintain population diversity [46, 103]. The diversifying selection pressure placed on these families of effectors coupled with the natural diversity of *P. capsici* potentially compounds the problem of too many effectors and not enough time by providing more unique targets than a lab could reasonably expect to assay.

Here we describe a set of effectors based on the reference guided assembly of a panel of *P. capsici* isolates and a systematic classification system by which effectors can be assigned to a larger paralog family. These paralog families can then serve as proxies of core conserved effectors. This approach allows researchers to bypass the lack of physical syntenic conservation absent between most effectors in *P. capsici* and instead utilize sequence identities and patterns of conservation to assign proteins to groups.This approach allows for increased power in the detection of sites that are under varying levels of selection and guide future interrogations of effector functionality. We use the Avr3a effector protein as a case study in how this classification may be used to determine the relative importance of a molecule.

4.2 Methods and Materials

4.2.1 Isolate Growth and Genomic DNA extraction:

Tufts of mycellia were placed into 50mL Falcon tubes of liquid V8-PARP media (160 mL of V8, 3g CaCo3, 960 mL of ddH2O, 25ppm pimaricin, 25ppm rifampacin, 25ppm

PCNB, 100ppm ampacillin). Tubes were grown with agitation at 28 degrees Celsius for 3 days. Tissue was harvested and lyophilized; then powdered using liquid nitrogen, mortar, and pestle. Genomic DNA was extracted using standard phenol/chloroform extraction methods. All sample concentrations were checked via 260/280 absorption readings using a NanoDrop ND-1000 and high molecular weight DNA verified using 1% agarose gel.

4.2.2 Library Construction and Sequencing:

Genomic sequencing was carried out on an Illumina HiSeq 2000 with 100bp single end reads being output. All sample and library preperation was carried out by staff at Children's Mercy Hospital (Kansas City, MO, USA) as per manufacturers instructions.

4.2.3 Read Mapping:

Reads were mapped to the Phytophthora capsici genome [103] using Bowtie2 [80]. Bowtie was employed using the end-to-end high sensitivity mode and the following modifications: -D 40 -R 10 -L10 -N1. Only uniquely mapping reads were used for consensus sequence determination and SNP calling. Potential PCR duplicates were then removed from these mapped reads using the samtools utility [76].

4.2.4 Consensus Sequence Determination sequence construction:

SNPs were called using the VarScan2 (ver 2.3.4) program [93] with the following settings: 8x coverage , 3x alternate allele minimum coverage, minimum quality score of 20, minimum variant frequency of 0.1, and a P-value threshold of 0.01. Resulting VCF files were then used to modify the reported *P.capsici* genome using the vcftools command vcf-consensus.

4.2.5 ORF Detection, Local Phasing, and Translation:

Six frame translation was carried out on resulting genomes for each sample using an internally developed program (Appendix E). Open reading frames were defined as any set of sequences that had an in frame start and stop codon and were at least 213 nucleotides in length. In the event that an open reading frame had multiple start codons , the longest open reading frame was retained. We also allowed for a maximum of six missing amino acids within an open reading frame before an ORF was excluded from consideration.

4.2.6 RxLR Effector Detection:

The RxLR effector pipeline described by Win et al [66] was implemented and used to detect RxLR like effectors. In brief, translated open reading frames from a genome were scanned for a signal peptide within 30 amino acids of a start site and RxLR motif within the first 60 amino acids of a start site and behind the signal peptide cleavage point.

4.2.7 CRN Effector Detection:

An RxLR effector pipeline described by Stam et al was [74] implemented and used to dect CRN effectors. In brief: translated open reading frames were filtered for records longer than 300 amino acids in length and then scanned for a secretion signal. This sub set of records is then subjected to a search of the LFLAK and DWL domains using previously developed hidden markov models. This sub-set is further subjected to searches for effector domains using another set of previously described hidden markov models for effector domains [118].

4.3 Results and Discussion

4.3.1 Sequencing and Mapping Results:

Mapping was completed using the Bowtie2 program [80] against the *Phytophthora capsci* genome as a reference [103]. Mapping rates were between 60% and 80% (data not shown)for all samples and after subsequent filtering of PCR duplicates using the samtools [76] package estimates of total genome coverage showed generally favorable results (Table 4.1). Mapped reads were then compiled into locally phased genomes and entered effector detection pipelines.

Table 4.1: Total number of uniquely aligning reads for each sample and estimated genome coverage based on a 64Mb genome of *Phytophthora capsici* for each isolate in this study.

Isolate	Reads	Estimated Coverage (64Mb)
LT 263	11448613	17.9
LT 7395	40535291	63.3
LT 62	13007162	20.3
LT 2135	18141183	28.3
LT 6535	14696770	23
LT 51	22039048	34.4
LT 7704	18311991	28.6
LT 7701	19914895	31.1
LT 9397	8004572	12.5
LT 6503	12563504	19.6
LT 9417	10729665	16.8
LT 9418	14258492	22.3
LT 9415	18268665	28.5
LT 6745	14686079	22.9
LT 9288	23995631	37.5

4.3.2 Effector Detection:

The RxLR effector pipeline detected a total number of 31,175 mature sequences across all sampled isolates; 15,083 were completely unique at an amino acid level. The

detected RxLR effectors had a median length of 145 amino acids and a mean length of 296 amino acids.

The CRN effector pipeline detected a total number of 3575 mature sequences across all isolates; 2,629 of which were complete unique at the amino acid level. The detected mature CRN effetors had a median length of 285 amino acids and mean length of 322 amino acids.

This raw number of unique sequences demonstrates the need for a classification system that can assign effectors to larger groups with potentially similar function for future study.

4.3.3 Effector Relatedness and Clustering:

In order to assess the relatedness of all sequences within a family, iterative clustering of records was performed using the USEARCH [119] program and for each inclusion identity measuring the resulting values: number of clusters, the number of records in the largest cluster, number of records in the smallest cluster, the average number of records per cluster, the number of individual sequences that formed their own cluster. These measures provide estimates of the relatedness of sequences within each of these families.

In the case of the RxLR effectors, it is clear that clusters form at low similarities and remain stable until high (>95%) measures of similarity are reached. This is indicative that there are a large number of groups that have high internal similarity and low between group similarities(Fig 4.1). In contrast to the RxLR effectors, CRN effectors steadily break into groups as percent identities for group inclusion are increased. This is indicative of CRN effectors groups having high internal similarity and moderate levels of between group similarity (Fig **??**).

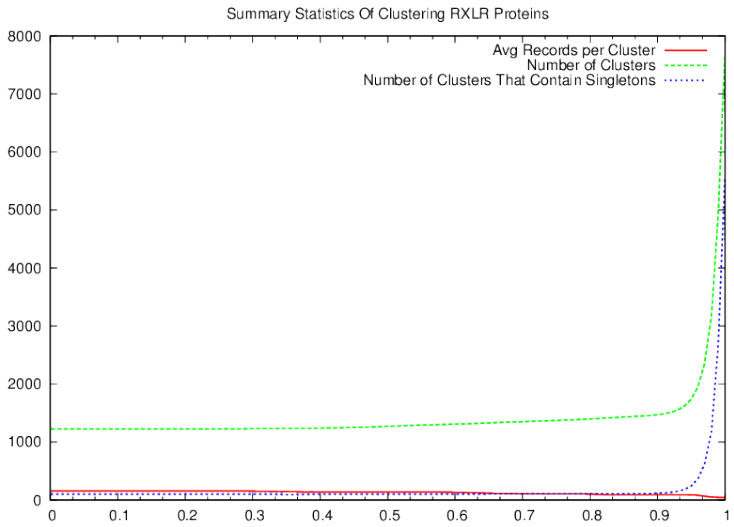

Figure 4.1: Distribution of quality scores at each position in the run. The X axis the simmilarity measures used to determine if an individual belonged in a group, and the y-axis is the measure of the corresponding value.

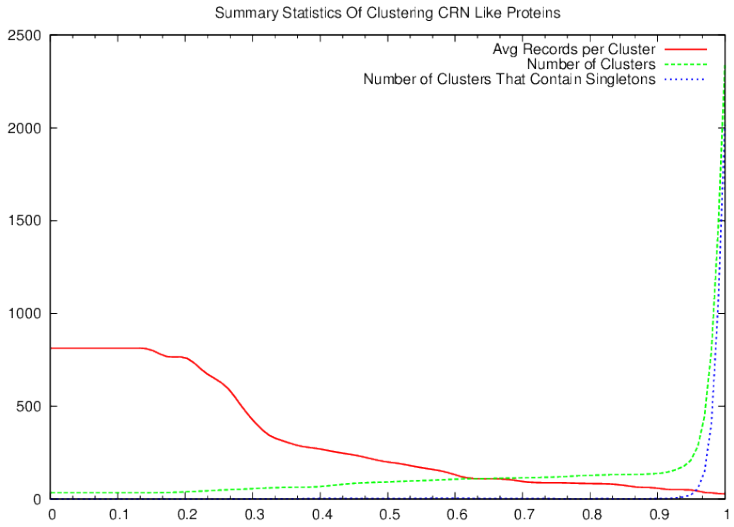

Figure 4.2: Distribution of quality scores at each position in the run.The X axis the the simmilarity measures used to determine if an individual belonged in a group, and the y-axis is the measure of the corresponding value.

While this high level overview is useful in describing the relatedness of individual sequences to each other, it was decided to perform a less naive approach to clustering related sequences. Effectors were merged into "nodes" by combining any described

effector that demonstrated an overlap in physical location within the genome. In order to be considered valid a node had to have at least three effectors associated with it. These nodes are described in Appendix F. The RxLR effectors mapped to a total of 1,936 nodes ; 1,051 of which had at least 3 sequences. The CRN effectors mapped to a total of 140 loci; 139 of which had at least 3 sequences. No nodes in either family were found in all resequenced isolates.

4.3.4 Determining Paralagous Effector Groups:

As no nodes were completely conserved across all sampled isolates it was impossible to determine a core set of conserved effectors for either family. As these proteins are known to be highly modular [74, 118], exist within transposable elements [113, 120], and have undergone recent duplication events [120–122] , the definition of broader paralagous group that contain many nodes may provide a better description of core effector groups.

The average sequence similarity between each node was calculated for each family. In order to do this the similarities of all sequences in one node was calculated by comparison to all of the sequences in a second node. These similarities were calculated by global alignment using a BLOSUM62 matrix [123]. Each query was required to be half the length of the target and the final alignment must cover 60% of the query. This was carried out for all pair-wise combinations of nodes. The average similarity was then calculated by the arithmetic mean of distances between each node. This resulting matrix of average similarity measures was then filtered to include only values of great than or equal to 60% so that only potentially homologous values would be included in down stream analysis.

The minimum spanning tree of the matrix was calculated using Chu-Liu-Edmods algorithm for computing shortest routes of a directed graph [124, 125]. Because only connections with a weight of greater than 60% were considered , each family resulted in a forest of minimum spanning trees. Each of these trees can be considered to be

a paralogous group of sequences.The RxLR family has 121 total paralagous groups containing between 2 and 12 nodes each. The CRN family has 24 total paralagous groups containing between 2 and 14 nodes in each graph. These results show good agreement of the clustering patterns previously described based on just sequence data. These trees are presented in Appendix G and Appendix H for the RxLR and CRN families respectively.

By using both the physical location of described effectors in combination with average sequence identity as a proxy for evolutionary distance some conclusions about the evolutionary history of each of these families can be made.

In the case of RxLR effectors, most (68 groups , 57% of total described), of the paralagous groups contain only 2 nodes. Many of the paralagous groups extracted from the RxLR effector group also demonstrated a contiguous relation ship existing on the same scaffold in a linear fashion. This observation combined with high similarity measures may indicate evolutionarily recent duplication events. It should be noted as well that the paralagous groups with 5 or more nodes all are made up of sequences from each of the sampled isolates which may indicate sequence within these groups are important for virulence.

In contrast the CRN family of effectors paralagous groups contain on average many more nodes and a nodes most similar neighbor is most likely to be on a different scaffold than on the same scaffold. These observations combined with the much more consistent discovery of sequences from each isolate belonging to individual nodes would indicate that this family of effectors is necessary for the pathogen to successfully infect a host.

4.3.5 Selection Pressure Calculations:

In order to more effectively determine the types of selection pressures on each paralagous group (and loci under selection pressure) all mature sequences from paralagous groups were aligned into a multiple sequence alignment in an automated

fashion using MUSCLE [126]. Corresponding nucleotide sequences were fetched and aligned based on MUSCLE alignments using pal2nal [127]. These alignements were then tested for codon level selection pressures using the HyPhy package FUBAR [128, 129].

Graphs of codon level selection pressures and amino acids present at loci are included as part of Appendix I and Appendix J for RxLR and CRN families respectively. Measures of overall selection pressure in the RxLR family indicate that few residues in any paralagous group are under strong purifying pressure.

P. capsici is a pathogen that shows great diversity between individuals and the RxLR family of effectors has been described as being highly diverse within genomes of the *Phytophthora* genus [66,67]. It should therefore come as no surprise that there is an extreme level of diversity in this class of proteins when comparisons are made between individuals of *P. capsci*. What is surprising is that if this if this class of proteins is also crucial for the pathogen's ability to infect host plants, no RxLR effectors were conserved based on physical location. This is highly problematic if breeders and researchers wish to use these proteins as breeding targets to generate resistant lines as there does not appear to be a core conserved set of effectors that is shared across all isolates. This may indicate that while *P. capsici* still carries a relatively large number of RxLR effectors in it's genome they may not be as functionally important to infection. While the CRN family shows much higher levels of conservation based both on selection levels and physical conservation between isolates; it still does not provide any candidates that demonstrate absolute physical conservation.

By further systematically defining paralagous families of effectors we have provided a system by which effectors can be assigned to a paralagous group through sequence identity and access this information to determine potentially significant residues. This classification system provides a frame work through which a core set of effectors can be described and assigned.

Based on previous observations that *P. capsici* has 4 major sub groups the possibility exists that each major group would have its own set of core effectors.

This may be especially true in China where it is clear that there is much less diversity between isolates. The inclusion of more isolates into this classification system coupled with division of data based on population may provide a more reasonable and powerful classification system for effectors. While the research presented here paints a fairly bleak picture in the application of effector based screening programs in *P. capsci*, it should be noted that the limited number of isolates included in this sample coupled with the extreme diversity of this organism is likely the cause.

4.3.6 The Avr3a Effector Group:

The Avr3a effector has been widely studied in a number of *Phytophthora* species as it is a locus that has been long associated with virulence in *Phytopthora* pathosystems. With the publication of a crystal structure of this effector [69] and subsequent controversy surrounding which portion of the protein is responsible for binding external cell lipids [68, 72, 130–132] it was decided to investigate this specific effector in depth.

A hidden markov model based on previously described Avr3a sequences was used to identify which paralagous group was comprised of the most Avr3a like sequences(Figure 4.3). This sequence fell into a paralagous group containing at least one sequence from each individual. As a representative sequence from each isolate sequenced is contained within this group , it is likely a core effector and important for infection.

The previously calculated selection pressure for group 51 was then mapped onto the three dimensional structure of Avr3a (Figure 4.4 and Figure 4.4). These explorations demonstrate that residues predicted and demonstrated to have importance in the entry of Avr3a to host cells are under high (red) to absolute (yellow) levels of purifying selection [68]. There are a number of residues on the back side that have also been predicted to of importance for the structural integrity of the protein that are under strong levels of purifying selection [70]. Interestingly regions of the

protein that are disordered loops and that if mutated could break certain turns are under diversifying selection. It has been hypothesized that this protein may undergo conformational shifts to escape cell detection and the placement of these diversifying sites would indicate that many potenially structurally important sites are under such pressures.

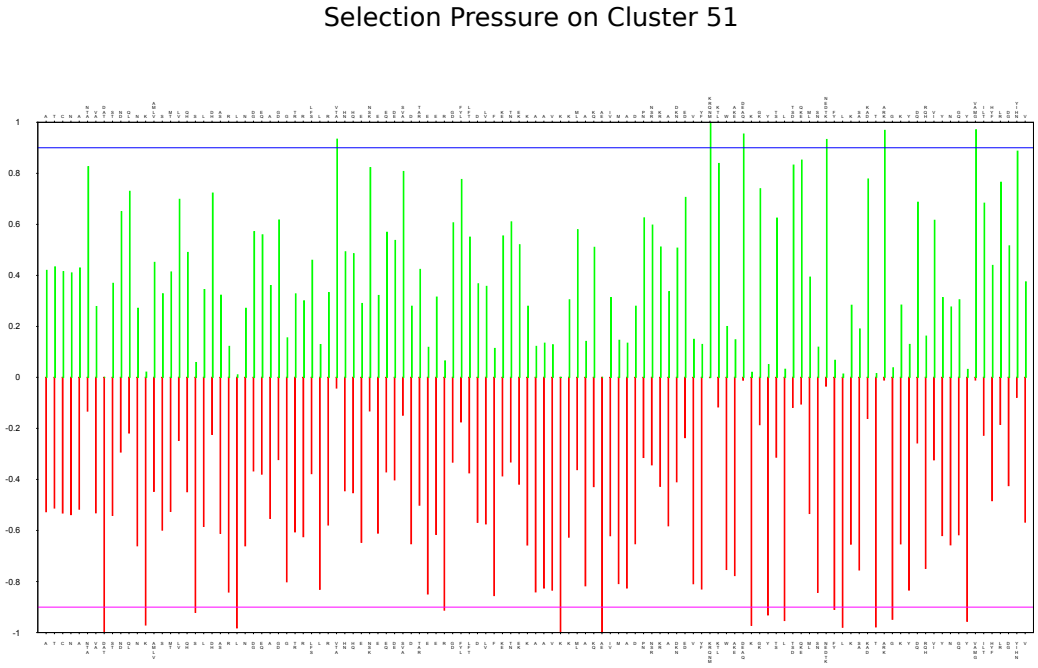

Figure 4.3: The calculated codon level selection levels on RxLR paralagous group 51.

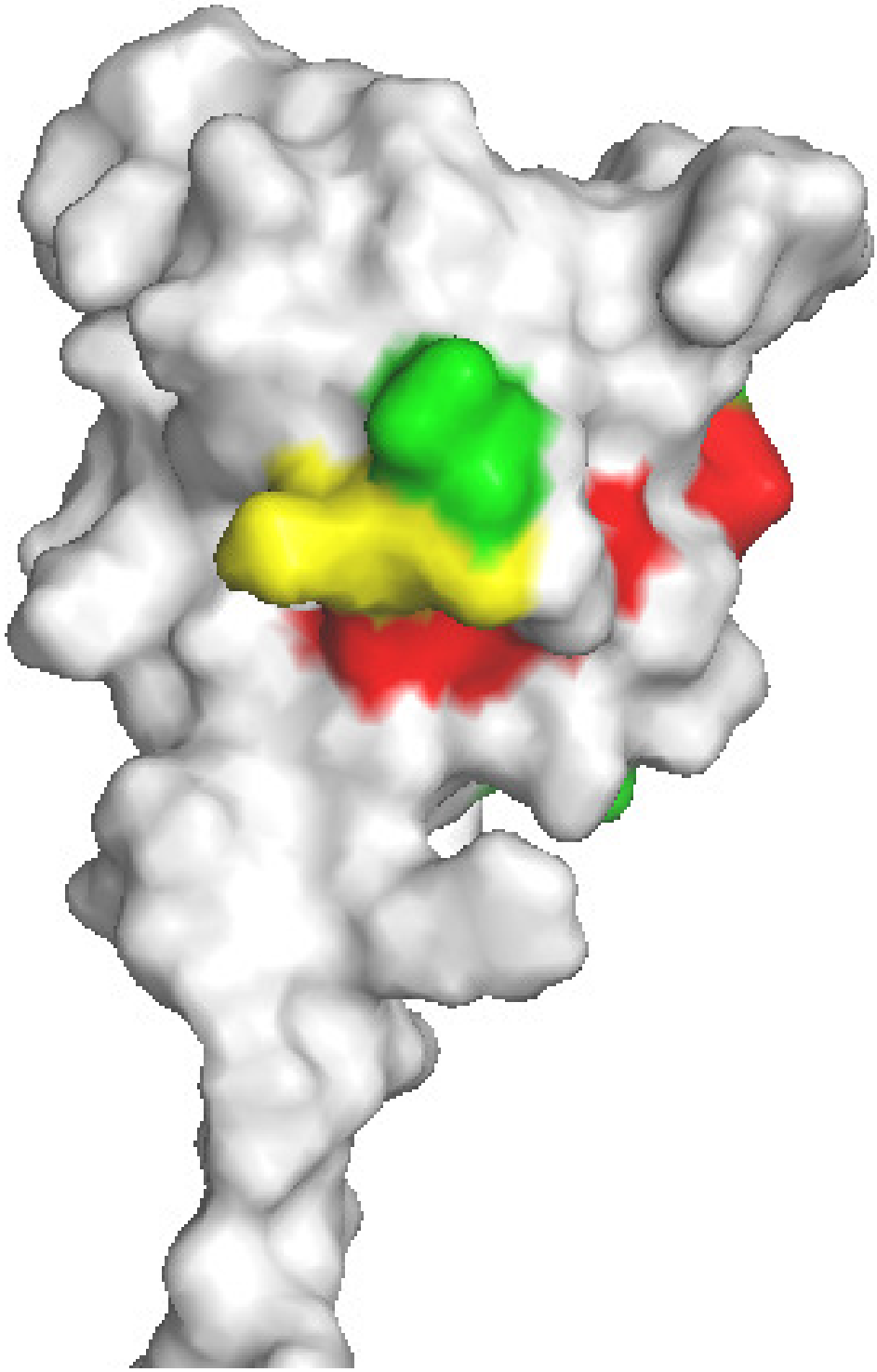

Figure 4.4: The positive charged face of the Avr3a effector with amino acids colored as red or yellow for negative selection pressures and green for positive selection pressures.

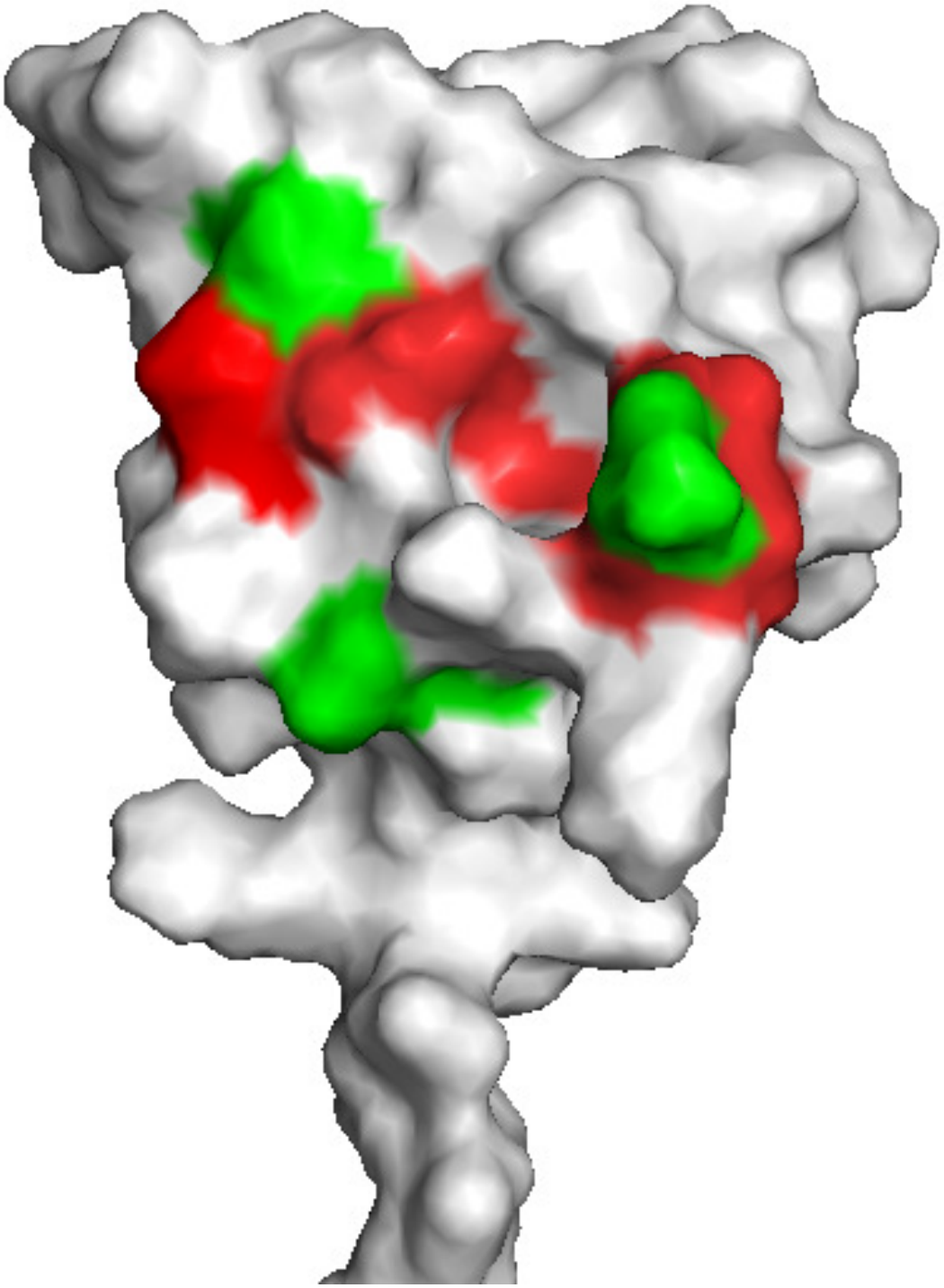

Figure 4.5: The face opposite of the positively charged face on the Avr3a effector with amino acids colored as red for negative selection pressures and green for positive selection pressures.

Chapter 5

Conclusions

This dissertation demonstrates: the variation present within *P. capsici*, the genetic structure of the organism based on geographic location, the effects that diversity has on expanding gene families, and how next generation sequencing technologies can be applied to clarify the classification cryptic non-model organisms.

While it has been demonstrated by multiple studies that this pathogen shows high levels of diversity within locally sampled populations, this is the first time that individuals between geographic locations have been compared. The application of next generation sequencing technologies to this problem provides the ability to select a high number of sites that are both conserved and variable across the entire genome of organism. This increased power allows for very granular measurements of variation based on calculations of raw distance and fine scaled measurements based on patterns of inheritance within the genome. These measures have resulted in the observation that there may be multiple distinct sub groups of individuals across the globe and that even within the United States there are signatures of local selection pressures and allele fixation. We now also have a number of markers that have a quantified ability to distinguish these groups from each other allowing for the quick screening and identification of samples with unknown origin. While this study benefited from large sample size, it did demonstrate the problems associated with low coverage samples

and the use of criteria based SNP callers and the issues of bad prior assumption in bayesian classifiers. Future research creating, curating and maintaining a SNP data base based on these initial observations and the re-calibration of priors for higher heterozygous rates should prove to be a valuable resource for the community as a whole.

We applied the same technologies and analyses to a closely related but separate sister species *P. tropicalis* and potentially un-described species *P. subnubulus*. By doing this we help clarify that *P. tropicalis* is in fact its own distinct species and that it may be comprised of multiple subgroups. We were also able to demonstrate that while *P. subnubulus* may not be its own species it is at least a distinct sub group of *P. tropicalis*. Because these two species are morphologically very similar to *P. capsici* and commonly used sequences such as ITS and COX often are unable to differentiate between them the addition of loci that can be easily assayed is of great value to the community. While initial sampling of *P. tropicalis* should have provided enough samples for stronger statistical analyses, the realization that there may be multiple sub populations within this described species created a dearth of individuals in each group. Never the less this provides a strong indication that further investigation into genome wide variation within isolates that have been classified to this species will provide be valuable and that the species classification within this group needs to be revisited.

Finally, by using reference guided genome construction techniques we have been able to generate a number of resequenced genomes of reasonable quality. Because of the high rate of heterozygous sites within the organism we have also been able to apply read backed phasing to short areas of interest a practice that has been developed for some time but because of biological limitations is rarely feasible. By applying this method to the description of an biologically important class of effectors we were able to measure and demonstrate the lack of a conserved set of proteins within this species and have put forward a different classification system that can be used to assign proteins to larger groups.This last study provides a good look at how low sample size,

high variability, and diverse between group population structures within *P. capsici* stymies common tasks in comparative genomics.

Taken *in toto* these findings illustrate the need for future research to refine these observations with increased sampling of isolates, to identify and measure population stratification based on whole genome measures, and to take into account the population strucutre of samples when conducting both comparative and translational.

Bibliography

[1] Blair JE, Coffey MD, Park SY, Geiser DM, Kang S (2008) A multi-locus phylogeny for phytophthora utilizing markers derived from complete genome sequences. Fungal Genetics and Biology 45: 266–277. 1

[2] (2007). Usda: National agricultural statistics service. URL http://www.nass.usda.gov. 1

[3] Leonian L (1922) Stem and fruit blight of pepper caused by phytophthora capsici species nov. Phytopathology 12: 401-418. 1, 20

[4] Erwin DC, Ribeiro OK, et al. (1996) Phytophthora diseases worldwide. American Phytopathological Society (APS Press). 1, 4, 46

[5] Davidson CR, Carroll RB, Evans TA, Mulrooney RP, Kim SH (2002) First report of phytophthora capsici infecting lima bean (phaseolus lunatus) in the mid-atlantic region. Plant Disease 86: 1049–1049. 1, 4

[6] Gevens A, Hausbeck M (2005) Phytophthora capsici isolated from snap beans is pathogenic to cucumber fruit and soybean. Phytopathology 95. 1, 4

[7] Kreutzer W (1937) A phytophthora rot of cucumber fruit. Phytopathology 27: 955. 1, 4

[8] Kreutzer W, Bryant L (1946) Certain aspects of the epiphytology and control of tomato fruit rot caused by phytophthora-capsici leonian. Phytopathology 36: 329–339. 1, 4

[9] Kreutzer W, Bodine E, Durrell L, et al. (1940) Cucurbit diseases and rot of tomato fruit caused by phytophthora capsici. Phytopathology 30: 972–975. 1, 4

[10] Tompkins CM, Tucker C, et al. (1937) Phytophthora rot of honeydew melon. Journal of Agricultural Research 54: 933–944. 1

[11] Wiant J, Tucker C, et al. (1940) A rot of winter queen water-melons caused by phytophthora capsici. Journal of Agricultural Research 9: 73–88. 1, 4

[12] Ko Wh (1988) Hormonal heterothallism and homothallism in phytophthora. Annual Review of Phytopathology 26: 57–73. 1

[13] Bowers J, Papavizas G, Johnston S, et al. (1990) Effect of soil temperature and soil-water matric potential on the survival of phytophthora capsici in natural soil. Plant disease 74: 771–777. 1

[14] Lamour K, Hausbeck MK (2003) Effect of crop rotation on the survival of phytophthora capsici in michigan. Plant Disease 87: 841–845. 1

[15] Hausbeck MK, Lamour KH (2004) Phytophthora capsici on vegetable crops: research progress and management challenges. Plant Disease 88: 1292–1303. 1, 3, 4

[16] Granke L, Windstam S, Hoch H, Smart C, Hausbeck M (2009) Dispersal and movement mechanisms of phytophthora capsici sporangia. Phytopathology 99: 1258–1264. 1

[17] Lamour KH, Stam R, Jupe J, Huitema E (2012) The oomycete broad-host-range pathogen phytophthora capsici. Molecular Plant Pathology 13: 329–337. 2, 3

[18] Feng B, Li P, Wang H, Zhang X (2010) Functional analysis of¡ i¿ pcpme¡/i¿ 6 from oomycete plant pathogen¡ i¿ phytophthora capsici¡/i¿. Microbial pathogenesis 49: 23–31. 3

[19] Li P, Feng B, Wang H, Tooley PW, Zhang X (2011) Isolation of nine phytophthora capsici pectin methylesterase genes which are differentially expressed in various plant species. Journal of basic microbiology 51: 61–70. 3

[20] Ristaino JB, Johnston SA (1999) Ecologically based approaches to management of phytophthora blight on bell pepper. Plant Disease 83: 1080–1089. 4

[21] Lamour K, Hausbeck M (2001) The dynamics of mefenoxam insensitivity in a recombining population of phytophthora capsici characterized with amplified fragment length polymorphism markers. Phytopathology 91: 553–557. 4, 5, 44

[22] French-Monar RD, Jones JB, Roberts PD (2006) Characterization of phytophthora capsici associated with roots of weeds on florida vegetable farms. Plant disease 90: 345–350. 4

[23] Ploetz R, Haynes J, Heine G, Watson M (2001) Investigating factors that may contribute to the increased prevalence of phytophthora capsci-induced diseases in south florida. In: Abstr.) Phytopathology. volume 91, p. S72. 4

[24] Wang Y, Bouwmeester K, MORTEL JE, Shan W, Govers F (2013) A novel arabidopsis–oomycete pathosystem: differential interactions with phytophthora capsici reveal a role for camalexin, indole glucosinolates and salicylic acid in defence. Plant, cell & environment 36: 1192–1203. 4

[25] Gevens A, Donahoo R, Lamour K, Hausbeck M (2007) Characterization of phytophthora capsici from michigan surface irrigation water. Phytopathology 97: 421–428. 4

[26] Quesada-Ocampo L, Granke L, Hausbeck M (2011) Temporal genetic structure of phytophthora capsici populations from a creek used for irrigation in michigan. Plant Disease 95: 1358–1369.

[27] Donahoo RS, Lamour KH (2008) Characterization of phytophthora species from leaves of nursery woody ornamentals in tennessee. HortScience 43: 1833–1837. 4, 19, 47, 62

[28] Granke LL, Quesada-Ocampo L, Lamour K, Hausbeck MK (2012) Advances in research on phytophthora capsici on vegetable crops in the united states. Plant Disease 96: 1588–1600.

[29] Café-Filho A, Duniway J, et al. (1996) Effect of location of drip irrigation emitters and position of phytophthora capsici infections in roots on phytophthora root rot of pepper. Phytopathology 86: 1364–1369. 4

[30] Café-Filho A, Duniway J, Davis R (1995) Effects of the frequency of furrow irrigation on root and fruit rots of squash caused by phytophthora capsici. Plant disease 79: 44–48. 4

[31] Babadoost M, Tian D, Islam S, Pavon C, Pitrat M (2008) Challenges and options in managing phytophthora blight (phytophthora capsici) of cucurbits . 4

[32] Babadoost M, Islam S (2003) Fungicide seed treatment effects on seedling damping-off of pumpkin caused by phytophthora capsici. Plant disease 87: 63–68. 4

[33] Lamour K, Hausbeck M (2003) Susceptibility of mefenoxam-treated cucurbits to isolates of phytophthora capsici sensitive and insensitive to mefenoxam. Plant disease 87: 920–922. 4

[34] Oelke LM, Bosland PW, Steiner R (2003) Differentiation of race specific resistance to phytophthora root rot and foliar blight in capsicum annuum. Journal of the American Society for Horticultural Science 128: 213–218. 5

[35] Glosier BR, Ogundiwin EA, Sidhu GS, Sischo DR, Prince JP (2008) A differential series of pepper (capsicum annuum) lines delineates fourteen physiological races of phytophthora capsici. Euphytica 162: 23–30. 5

[36] Sanogo S, Bosland PW, Lamour K, et al. (2013) Biology and management of phytophthora capsici in the southwestern usa. Phytophthora: A Global Perspective 2: 87. 5, 64

[37] Gobena D, McGrath MT, Lamour K (2012) Survival and spread of phytophthora capsici on long island, new york. Mycological Progress 11: 761–768. 5, 44

[38] Lamour K, Hausbeck M (2001) Investigating the spatiotemporal genetic structure of phytophthora capsici in michigan. Phytopathology 91: 973–980. 5, 44, 48

[39] Dunn A, Milgroom M, Meitz J, McLeod A, Fry W, et al. (2010) Population structure and resistance to mefenoxam of phytophthora capsici in new york state. Plant Disease 94: 1461–1468. 44

[40] Meitz JC, Linde CC, Thompson A, Langenhoven S, McLeod A (2010) Phytophthora capsici on vegetable hosts in south africa: distribution, host range and genetic diversity. Australasian Plant Pathology 39: 431–439. 5, 44

[41] Lamour K, Hausbeck M (2002) The spatiotemporal genetic structure of phytophthora capsici in michigan and implications for disease management. Phytopathology 92: 681–684. 5, 44

[42] Gobena D, Roig J, Galmarini C, Hulvey J, Lamour K (2012) Genetic diversity of phytophthora capsici isolates from pepper and pumpkin in argentina. Mycologia 104: 102–107. 5, 44

[43] Hurtado-Gonzales O, Aragon-Caballero L, Apaza-Tapia W, Donahoo R, Lamour K (2008) Survival and spread of phytophthora capsici in coastal peru. Phytopathology 98: 688–694. 5, 44

[44] Hulvey J, Hurtado-Gonzalez O, Aragón-Caballero L, Gobena D, Storey D, et al. (2011) Genetic diversity of the pepper pathogen phytophthora capsici on farms in the amazonian high jungle of peru. American Journal of Plant Sciences 2: 461. 5, 44, 47

[45] Hu J, Pang Z, Bi Y, Shao J, Diao Y, et al. (2013) Genetically diverse long-lived clonal lineages of phytophthora capsici from pepper in gansu, china. Phytopathology 103: 920–926. 5, 37, 41, 44, 48, 49

[46] Hu J, Diao Y, Zhou Y, Lin D, Bi Y, et al. (2013) Loss of heterozygosity drives clonal diversity of phytophthora capsici in china. PloS one 8: e82691. 5, 37, 41, 44, 48, 49, 64

[47] Birch PR, Rehmany AP, Pritchard L, Kamoun S, Beynon JL (2006) Trafficking arms: oomycete effectors enter host plant cells. Trends in microbiology 14: 8–11. 6, 63

[48] Boch J, Landgraf A, Krause J, Kunkel B, Bonas U (2003) Identification of virulence factors from pseudomonas syringae. In: Pseudomonas syringae and related pathogens, Springer. pp. 225–231. 6

[49] Chisholm ST, Coaker G, Day B, Staskawicz BJ (2006) Host-microbe interactions: shaping the evolution of the plant immune response. Cell 124: 803–814. 6, 63

[50] van der Hoorn RA, Kamoun S (2008) From guard to decoy: a new model for perception of plant pathogen effectors. The Plant Cell Online 20: 2009–2017. 6

[51] Kamoun S (2006) A catalogue of the effector secretome of plant pathogenic oomycetes. Annu Rev Phytopathol 44: 41–60. 6, 7, 63

[52] Evangelisti E, Govetto B, Minet-Kebdani N, Kuhn ML, Attard A, et al. (2013) The phytophthora parasitica rxlr effector penetration-specific effector 1 favours arabidopsis thaliana infection by interfering with auxin physiology. New Phytologist 199: 476–489. 6

[53] Bos JI, Armstrong MR, Gilroy EM, Boevink PC, Hein I, et al. (2010) Phytophthora infestans effector avr3a is essential for virulence and manipulates plant immunity by stabilizing host e3 ligase cmpg1. Proceedings of the National Academy of Sciences 107: 9909–9914. 6, 63

[54] Bos JI, Kanneganti TD, Young C, Cakir C, Huitema E, et al. (2006) The c-terminal half of phytophthora infestans rxlr effector avr3a is sufficient to trigger r3a-mediated hypersensitivity and suppress inf1-induced cell death in nicotiana benthamiana. The Plant Journal 48: 165–176. 6, 63

[55] Huitema E, Bos JI, Tian M, Win J, Waugh ME, et al. (2004) Linking sequence to phenotype in phytophthora–plant interactions. Trends in microbiology 12: 193–200. 6

[56] Dawkins R (1999) The extended phenotype: The long reach of the gene. Oxford University Press. 6

[57] Damasceno CM, Bishop JG, Ripoll DR, Win J, Kamoun S, et al. (2008) Structure of the glucanase inhibitor protein (gip) family from phytophthora species suggests coevolution with plant endo-β-1, 3-glucanases. Molecular plant-microbe interactions 21: 820–830. 6

[58] Rose JK, Ham KS, Darvill AG, Albersheim P (2002) Molecular cloning and characterization of glucanase inhibitor proteins coevolution of a counterdefense mechanism by plant pathogens. The Plant Cell Online 14: 1329–1345. 6

[59] Armstrong MR, Whisson SC, Pritchard L, Bos JI, Venter E, et al. (2005) An ancestral oomycete locus contains late blight avirulence gene avr3a, encoding a protein that is recognized in the host cytoplasm. Proceedings of the National Academy of Sciences of the United States of America 102: 7766–7771. 6, 7

[60] Vleeshouwers VG, Rietman H, Krenek P, Champouret N, Young C, et al. (2008) Effector genomics accelerates discovery and functional profiling of potato disease resistance and phytophthora infestans avirulence genes. PLoS One 3: e2875. 6, 63

[61] Oh SK, Young C, Lee M, Oliva R, Bozkurt TO, et al. (2009) In planta expression screens of phytophthora infestans rxlr effectors reveal diverse phenotypes, including activation of the solanum bulbocastanum disease resistance protein rpi-blb2. The Plant Cell Online 21: 2928–2947. 6, 7, 63

[62] Rehmany AP, Gordon A, Rose LE, Allen RL, Armstrong MR, et al. (2005) Differential recognition of highly divergent downy mildew avirulence gene alleles by rpp1 resistance genes from two arabidopsis lines. The Plant Cell Online 17: 1839–1850. 7

[63] Shan W, Cao M, Leung D, Tyler BM (2004) The avr1b locus of phytophthora sojae encodes an elicitor and a regulator required for avirulence on soybean plants carrying resistance gene rps 1b. Molecular Plant-Microbe Interactions 17: 394–403. 7

[64] Kale SD, Tyler BM (2011) Entry of oomycete and fungal effectors into plant and animal host cells. Cellular microbiology 13: 1839–1848. 7

[65] Tyler BM (2009) Entering and breaking: virulence effector proteins of oomycete plant pathogens. Cellular microbiology 11: 13–20. 7

[66] Win J, Morgan W, Bos J, Krasileva KV, Cano LM, et al. (2007) Adaptive evolution has targeted the c-terminal domain of the rxlr effectors of plant pathogenic oomycetes. The Plant Cell Online 19: 2349–2369. 7, 63, 66, 72

[67] Whisson SC, Boevink PC, Moleleki L, Avrova AO, Morales JG, et al. (2007) A translocation signal for delivery of oomycete effector proteins into host plant cells. Nature 450: 115–118. 7, 8, 63, 72

[68] Yaeno T, Li H, Chaparro-Garcia A, Schornack S, Koshiba S, et al. (2011) Phosphatidylinositol monophosphate-binding interface in the oomycete rxlr effector avr3a is required for its stability in host cells to modulate plant immunity. Proceedings of the National Academy of Sciences 108: 14682–14687. 7, 8, 73

[69] Boutemy LS, King SR, Win J, Hughes RK, Clarke TA, et al. (2011) Structures of phytophthora rxlr effector proteins a conserved but adaptable fold underpins functional diversity. Journal of Biological Chemistry 286: 35834–35842. 7, 73

[70] Win J, Krasileva KV, Kamoun S, Shirasu K, Staskawicz BJ, et al. (2012) Sequence divergent rxlr effectors share a structural fold conserved across plant pathogenic oomycete species. PLoS pathogens 8: e1002400. 7, 73

[71] Dou D, Kale SD, Wang X, Chen Y, Wang Q, et al. (2008) Conserved c-terminal motifs required for avirulence and suppression of cell death by phytophthora sojae effector avr1b. The Plant Cell Online 20: 1118–1133. 8

[72] Ellis JG, Dodds PN (2011) Showdown at the rxlr motif: Serious differences of opinion in how effector proteins from filamentous eukaryotic pathogens enter plant cells. Proceedings of the National Academy of Sciences 108: 14381–14382. 8, 73

[73] Petre B, Kamoun S (2014) How do filamentous pathogens deliver effector proteins into plant cells? PLoS Biol 12: e1001801. 8

[74] Stam R, Jupe J, Howden AJM, Morris JA, Boevink PC, et al. (2013) Identification and characterisation crn effectors in ¡italic¿phytophthora capsici¡/italic¿ shows modularity and functional diversity. PLoS ONE 8: e59517. 8, 9, 66, 70

[75] Torto-Alalibo TA, Tripathy S, Smith BM, Arredondo FD, Zhou L, et al. (2007) Expressed sequence tags from phytophthora sojae reveal genes specific to development and infection. Molecular plant-microbe interactions 20: 781–793. 8

[76] Li H, Handsaker B, Wysoker A, Fennell T, Ruan J, et al. (2009) The sequence alignment/map format and samtools. Bioinformatics 25: 2078–2079. 11, 17, 23, 31, 50, 51, 65, 67

[77] Needleman SB, Wunsch CD (1970) A general method applicable to the search for similarities in the amino acid sequence of two proteins. Journal of molecular biology 48: 443–453. 12

[78] Smith TF, Waterman MS (1981) Comparison of biosequences. Advances in applied mathematics 2: 482–489. 12

[79] Homer N, Merriman B, Nelson SF (2009) Bfast: an alignment tool for large scale genome resequencing. PloS one 4: e7767. 13

[80] Langmead B, Salzberg SL (2012) Fast gapped-read alignment with bowtie 2. Nat Meth 9: 357–359. 13, 23, 30, 49, 65, 67

[81] Kent WJ (2002) Blat:the blast-like alignment tool. Genome research 12: 656–664. 13

[82] Li H, Durbin R (2009) Fast and accurate short read alignment with burrows–wheeler transform. Bioinformatics 25: 1754–1760. 13

[83] Li H, Ruan J, Durbin R (2008) Mapping short dna sequencing reads and calling variants using mapping quality scores. Genome research 18: 1851–1858. 13

[84] Li R, Yu C, Li Y, Lam TW, Yiu SM, et al. (2009) Soap2: an improved ultrafast tool for short read alignment. Bioinformatics 25: 1966–1967. 13, 17

[85] Kim D, Pertea G, Trapnell C, Pimentel H, Kelley R, et al. (2013) Tophat2: accurate alignment of transcriptomes in the presence of insertions, deletions and gene fusions. Genome Biology 14: R36. 13

[86] Altschul SF, Madden TL, Schäffer AA, Zhang J, Zhang Z, et al. (1997) Gapped blast and psi-blast: a new generation of protein database search programs. Nucleic acids research 25: 3389–3402. 13

[87] Nielsen R, Paul JS, Albrechtsen A, Song YS (2011) Genotype and snp calling from next-generation sequencing data. Nature Reviews Genetics 12: 443–451. 15

[88] Hedges D, Burges D, Powell E, Almonte C, Huang J, et al. (2009) Exome sequencing of a multigenerational human pedigree. PLoS One 4: e8232. 15

[89] Li R, Li Y, Fang X, Yang H, Wang J, et al. (2009) Snp detection for massively parallel whole-genome resequencing. Genome research 19: 1124–1132. 16, 17

[90] McKenna A, Hanna M, Banks E, Sivachenko A, Cibulskis K, et al. (2010) The genome analysis toolkit: a mapreduce framework for analyzing next-generation dna sequencing data. Genome research 20: 1297–1303. 16, 17

[91] Auwera GA, Carneiro MO, Hartl C, Poplin R, del Angel G, et al. (2013) From fastq data to high-confidence variant calls: The genome analysis toolkit best practices pipeline. Current Protocols in Bioinformatics : 11–10. 17

[92] DePristo MA, Banks E, Poplin R, Garimella KV, Maguire JR, et al. (2011) A framework for variation discovery and genotyping using next-generation dna sequencing data. Nature genetics 43: 491–498. 17

[93] Koboldt DC, Zhang Q, Larson DE, Shen D, McLellan MD, et al. (2012) Varscan 2: Somatic mutation and copy number alteration discovery in cancer by exome sequencing. Genome Research 22: 568-576. 17, 24, 31, 50, 65

[94] Koboldt DC, Chen K, Wylie T, Larson DE, McLellan MD, et al. (2009) Varscan: variant detection in massively parallel sequencing of individual and pooled samples. Bioinformatics 25: 2283–2285. 17

[95] Oudemans P, Coffey MD (1991) A revised systematics of twelve papillate phytophthora species based on isozyme analysis. Mycological Research 95: 1025 - 1046. 18, 46, 62

[96] Mchau GR, Coffey MD (1995) Evidence for the existence of two subpopulations in phytophthora capsici and a redescription of the species. Mycological Research 99: 89 - 102. 18, 19, 46, 47, 48, 62

[97] Forster H, Oudemans P, Coffey MD (1990) Mitochondrial and nuclear {DNA} diversity within six species ofphytophthora. Experimental Mycology 14: 18 - 31. 18, 46, 62

[98] Aragaki M, Uchida JY, et al. (2001) Morphological distinctions between phytophthora capsici and p. tropicalis sp. nov. Mycologia 93: 137–145. 19, 46, 47, 48, 62

[99] Kroon L, Bakker F, Van Den Bosch G, Bonants P, Flier W (2004) Phylogenetic analysis of *Phytophthora* species based on mitochondrial and nuclear dna sequences. Fungal Genetics and Biology 41: 766–782. 19, 47, 62

[100] Martin FN, Tooley PW (2003) Phylogenetic relationships among phytophthora species inferred from sequence analysis of mitochondrially encoded cytochrome oxidase i and ii genes. Mycologia 95: 269–284. 19, 47, 62

[101] Bowers J, Martin F, Tooley P, Luz E (2007) Genetic and morphological diversity of temperate and tropical isolates of phytophthora capsici. Phytopathology 97: 492–503. 19, 47, 62

[102] Donahoo RS, Lamour KH (2008) Interspecific hybridization and apomixis between phytophthora capsici and phytophthora tropicalis. Mycologia 100: 911–920. 19, 47, 48, 61, 62

[103] Lamour KH, Mudge J, Gobena D, Hurtado-Gonzales OP, Schmutz J, et al. (2012) Genome sequencing and mapping reveal loss of heterozygosity as a mechanism for rapid adaptation in the vegetable pathogen phytophthora capsici. Molecular Plant-Microbe Interactions 25: 1350–1360. 21, 23, 32, 48, 49, 64, 65, 67

[104] (2012) The tomato genome sequence provides insights into fleshy fruit evolution. Nature 485: 635–641. 23

[105] Patterson N, Price AL, Reich D (2006) Population structure and eigenanalysis. PLoS Genet 2: e190. 24, 38, 50

[106] Price AL, Patterson NJ, Plenge RM, Weinblatt ME, Shadick NA, et al. (2006) Principal components analysis corrects for stratification in genome-wide association studies. Nat Genet 38: 904–909. 24, 50

[107] Hurtado-Gonzales O, Lamour K (2009) Evidence for inbreeding and apomixis in close crosses of phytophthora capsici. Plant pathology 58: 715–722. 36, 48

[108] Zhang Z, Zhang J, Zheng X, Yang Y, Ko W (2004) Molecular distinctions between phytophthora capsici and ph. tropicalis based on its sequences of ribosomal dna. Journal of phytopathology 152: 358–364. 62

[109] Truong NV, Liew EC, Burgess LW (2010) Characterisation of¡ i¿ phytophthora capsici¡/i¿ isolates from black pepper in vietnam. Fungal biology 114: 160–170. 47

[110] Truong NV, Burgess LW, Liew EC (2012) Cross-infectivity and genetic variation of phytophthora capsici isolates from chilli and black pepper in vietnam. Australasian Plant Pathology 41: 439–447. 47, 62

[111] Hogenhout SA, Van der Hoorn RA, Terauchi R, Kamoun S (2009) Emerging concepts in effector biology of plant-associated organisms. Molecular plant-microbe interactions 22: 115–122. 63

[112] Torto TA, Li S, Styer A, Huitema E, Testa A, et al. (2003) Est mining and functional expression assays identify extracellular effector proteins from the plant pathogen phytophthora. Genome research 13: 1675–1685. 63

[113] Haas BJ, Kamoun S, Zody MC, Jiang RH, Handsaker RE, et al. (2009) Genome sequence and analysis of the irish potato famine pathogen phytophthora infestans. Nature 461: 393–398. 63, 70

[114] Li G, Huang S, Guo X, Li Y, Yang Y, et al. (2011) Cloning and characterization of r3b; members of the r3 superfamily of late blight resistance genes show sequence and functional divergence. Molecular Plant-Microbe Interactions 24: 1132–1142. 63

[115] Morgan W, Kamoun S (2007) Rxlr effectors of plant pathogenic oomycetes. Current opinion in microbiology 10: 332–338. 63

[116] Kamoun S (2007) Groovy times: filamentous pathogen effectors revealed. Current opinion in plant biology 10: 358–365. 63

[117] Bozkurt TO, Schornack S, Banfield MJ, Kamoun S (2012) Oomycetes, effectors, and all that jazz. Current opinion in plant biology 15: 483–492. 64

[118] Schornack S, Van Damme M, Bozkurt TO, Cano LM, Smoker M, et al. (2010) Ancient class of translocated oomycete effectors targets the host nucleus. Proceedings of the National Academy of Sciences 107: 17421–17426. 66, 70

[119] Edgar RC (2010) Search and clustering orders of magnitude faster than blast. Bioinformatics 26: 2460–2461. 68

[120] Jiang RH, Tripathy S, Govers F, Tyler BM (2008) Rxlr effector reservoir in two phytophthora species is dominated by a single rapidly evolving superfamily with more than 700 members. Proceedings of the National Academy of Sciences 105: 4874–4879. 70

[121] Oliva R, Win J, Raffaele S, Boutemy L, Bozkurt TO, et al. (2010) Recent developments in effector biology of filamentous plant pathogens. Cellular microbiology 12: 705–715. 70

[122] Ellis JG, Rafiqi M, Gan P, Chakrabarti A, Dodds PN (2009) Recent progress in discovery and functional analysis of effector proteins of fungal and oomycete plant pathogens. Current opinion in plant biology 12: 399–405. 70

[123] Henikoff S, Henikoff JG (1992) Amino acid substitution matrices from protein blocks. Proceedings of the National Academy of Sciences 89: 10915–10919. 70

[124] Edmonds J (1967) Optimum branchings. JOURNAL OF RESEARCH OF THE NATIONAL BUREAU OF STANDARDS SECTION B-MATHEMATICAL SCIENCES : 233–+. 70

[125] Chu YJ, Liu TH (1965) On shortest arborescence of a directed graph. Scientia Sinica 14: 1396. 70

[126] Edgar RC (2004) Muscle: multiple sequence alignment with high accuracy and high throughput. Nucleic acids research 32: 1792–1797. 72

[127] Suyama M, Torrents D, Bork P (2006) Pal2nal: robust conversion of protein sequence alignments into the corresponding codon alignments. Nucleic acids research 34: W609–W612. 72

[128] Murrell B, Moola S, Mabona A, Weighill T, Sheward D, et al. (2013) Fubar: a fast, unconstrained bayesian approximation for inferring selection. Molecular biology and evolution 30: 1196–1205. 72

[129] Pond SLK, Muse SV (2005) Hyphy: hypothesis testing using phylogenies. In: Statistical methods in molecular evolution, Springer. pp. 125–181. 72

[130] Taeno T, Shirasu K (2013). The rxlr motif of oomycete effectors is not a sufficient element for binding to phosphatidylinositol monophosphates. 73

[131] Kale SD, Gu B, Capelluto DG, Dou D, Feldman E, et al. (2010) External lipid pi3p mediates entry of eukaryotic pathogen effectors into plant and animal host cells. Cell 142: 284–295. 73

[132] Dou D, Kale SD, Wang X, Jiang RH, Bruce NA, et al. (2008) Rxlr-mediated entry of phytophthora sojae effector avr1b into soybean cells does not require pathogen-encoded machinery. The Plant Cell Online 20: 1930–1947. 73

Appendix

Appendix A

Varscan2 to Distance Utilility

```
#!/usr/bin/perl

use warnings;
use strict;

#indel comparisons using Levenshtein distance;
use Text::Levenshtein qw(fastdistance);
use Getopt::Long;

#Global_Variables
my @file_names;
my %distance_matrix;
my %number_comparisons_matrix;

my $allowed_missing = 0;
my $varscan_file;
my $inventory_file;
my $snps_only = 0;
my $file_prefix;
my $help = 0;
```

```
GetOptions("missing=i"    => \$allowed_missing,
           "varscan=s"    => \$varscan_file,
           "inventory=s" => \$inventory_file,
           "snps_only+"   => \$snps_only,
           "prefix=s"     => \$file_prefix,
           "help+"        => \$help
         ) or die usage();

usage() if $help == 1;



open(INVENTORY, "<" , $inventory_file) || die $!;
open(VARSCAN ,"<",$varscan_file) || die $!;

while (my $line = <INVENTORY>){
    chomp $line;
    if ($line eq ''){
        next;
        }
    else{
        my ($prefix , $suffix) = split (/\./ , $line);
        push @file_names , $prefix;
        }
    }

close INVENTORY;

print "loading file \n";
my $line_counter = 0;
my @lines =<VARSCAN>;
print " . . . in\n";
```

```
open (KEPT , ">", 'kept_lines.txt') || die $!;

foreach my $line (@lines){
    chomp $line;
    $line_counter++;
    if ($line_counter%1000000 ==0){
        print STDOUT $line_counter . " completed\n";
        }
    if ($line eq "Chrom    Position    Ref Var Cons:Cov:Reads1:Reads2:
       Freq:P-value StrandFilter:R1+:R1-:R2+:R2-:pval   SamplesRef
       SamplesHet   SamplesHom   SamplesNC   Cons:Cov:Reads1:Reads2:Freq:
       P-value"){
        next;
        }

    my @tmp = split (/\s+/,$line);
    my @individual_info = @tmp[10..$#tmp]; #taking an array slice so its
         less maths to adjust indices

    my $number_of_Ns = count_missing(\@individual_info);

    if (($tmp[9] <= $allowed_missing)&&($number_of_Ns <=
       $allowed_missing)){
        print KEPT $line . "\n";
        for(my $x = 0; $x <=$#individual_info; $x++){
            for (my $y = $x; $y<=$#individual_info ; $y++){
                my $info_string_1 = $individual_info[$x];
                my $info_string_2 = $individual_info[$y];

                if (($info_string_1 eq 'N') || ($info_string_2 eq 'N')
                   || ($info_string_2 eq '') || ($info_string_2 eq ''))
                   { #non informative comparisons are dumped.

                    }
```

```
elsif( ($info_string_1 =~/\+|\-[ATGC]+/) && (
    $info_string_2 =~/\+|\-[ATGC]+/)){ #two indel type
    positions
     if ($snps_only == 0){
          $distance_matrix{$file_names[$x]}{$file_names[$y
              ]} += ($info_string_1 eq $info_string_2) ? 0
               : compare_indel_indel($info_string_1,
              $info_string_2);
          $number_comparisons_matrix{$file_names[$x]}{
              $file_names[$y]} += ($info_string_1 =~/\*/
              || $info_string_2=~/\*/) ? 2 : 1; ##if there
               is a * in any of the string it technically
              represents two positions for comparison)
          }
     }
elsif( ($info_string_1 =~/\+|\-[ATGC]+/) || (
    $info_string_2 =~/\+|\-[ATGC]+/)){ #indel to non
    indel
     if ($snps_only == 0){
          $distance_matrix{$file_names[$x]}{$file_names[$y
              ]} += compare_indel_base($info_string_1,
              $info_string_2);
          $number_comparisons_matrix{$file_names[$x]}{
              $file_names[$y]} += ($info_string_1 =~/\*/
              || $info_string_2=~/\*/) ? 2 : 1; ##if there
               is a * in any of the string it technically
              represents two positions)
          }
     }
else{
     (my $position_call1,my @trash) =split (/\:/,
         $info_string_1);
     (my $position_call2,    @trash) =split (/\:/ ,
         $info_string_2);
```

```
                    $distance_matrix{$file_names[$x]}{$file_names[$y]}
                        += ($position_call1 eq $position_call2) ? 0 :
                        compare_bases($position_call1,$position_call2);
                    $number_comparisons_matrix{$file_names[$x]}{
                        $file_names[$y]} += 1;

                    }
                }
            }
        }
    }


my %weighted_distance;

foreach my $x(@file_names){
    foreach my $y(@file_names){
        if ((exists $distance_matrix{$x}{$y}) && (exists
            $number_comparisons_matrix{$x}{$y})){
            my $avg = $distance_matrix{$x}{$y} /
                $number_comparisons_matrix{$x}{$y};
            $weighted_distance{$x}{$y} = $avg;
            }
        }
    }


my $dout = $file_prefix . '_distance.matrix';
my $wout = $file_prefix . '_weighted.matrix';
my $cout = $file_prefix . '_comparisons.matrix';


pretty_printer ($dout, \%distance_matrix , \@file_names);
```

```
pretty_printer ($wout , \%weighted_distance,\@file_names);
pretty_printer ($cout, \%number_comparisons_matrix,\@file_names);
pretty_printer_complete ("$wout\.complete",\%weighted_distance,\
    @file_names);
print "Run complete \n";

exit;


sub compare_bases{
    my ($base1 , $base2) = @_;


    if ($base1 eq $base2) {
        return 0;
        }


    ## Both Items are homozygous ##
    if ((($base1 eq 'A')||($base1 eq 'T')||($base1 eq 'G')||($base1 eq '
       C')) &&(($base2 eq 'A')||($base2 eq 'T')||($base2 eq 'G')||(
       $base2 eq 'C'))){
            return 1;
            }

    ## base1 is homozygous base2 is heterozygous
    if ((($base1 eq 'A')||($base1 eq 'T')||($base1 eq 'G')||($base1 eq '
       C')) && (($base2 eq 'Y')||($base2 eq 'R')||($base2 eq 'W')||(
       $base2 eq 'S')||($base2 eq 'K')||($base2 eq 'M'))){
        #Make our comparisons#
        if($base2 eq 'Y' && ($base1 eq 'C'||$base1 eq 'T') ){
            return 0.5;
            }
        if($base2 eq 'R' && ($base1 eq 'A'||$base1 eq 'G') ){
```

```
        return 0.5;
        }
    if($base2 eq 'W' && ($base1 eq 'A'||$base1 eq 'T') ){
        return 0.5;
        }
    if($base2 eq 'S' && ($base1 eq 'G'||$base1 eq 'C') ){
        return 0.5;
        }
    if($base2 eq 'K' && ($base1 eq 'T'||$base1 eq 'G') ){
        return 0.5;
        }
    if($base2 eq 'M' && ($base1 eq 'C'||$base1 eq 'A') ){
        return 0.5;
        }
        return 1;
    }


## base2 is homozygous base1 is heterozygous
if ((($base2 eq 'A')||($base2 eq 'T')||($base2 eq 'G')||($base2 eq '
   C')) && (($base1 eq 'Y')||($base1 eq 'R')||($base1 eq 'W')||(
   $base1 eq 'S')||($base1 eq 'K')||($base1 eq 'M'))){
    return compare_bases($base2 , $base1); #swap our variable and
       call the subroutine again;
    }

## both bases are heterozygotes ##
if (($base1 eq 'Y') && ($base2 eq 'R')){
        return 1;
    }
if (($base1 eq 'W') && ($base2 eq 'S')){
        return 1;
    }
if (($base1 eq 'M') && ($base2 eq 'K')){
```

```
            return 1;
        }
    if (($base1 eq 'R') && ($base2 eq 'Y')){
            return 1;
        }
    if (($base1 eq 'S') && ($base2 eq 'W')){
            return 1;
        }
    if (($base1 eq 'K') && ($base2 eq 'M')){
            return 1;
        }

    return 0.83;

}

sub compare_indel_indel{
    (my $insert_1  , my @trash)= split (/\:/ ,$_[0]); #grab the sequence
    (my $insert_2  ,    @trash)= split (/\:/ ,$_[1]); #grab the sequence

    if ($insert_1 eq $insert_2){
        return 0; #perfect match == zero distance;
        }
    if ($insert_1 =~ /\// && $insert_2 =~ /\//){ #handles all het/het
       comparisons
        ## average levenstein distance between all everything
        my ($string_1_a,$string_1_b)= split (/\//,$insert_1);
        my ($string_2_a,$string_2_b)= split (/\//,$insert_2);

        my $distance = 0;
        my $comparisons = 0;
        foreach my $x($string_1_a,$string_1_b){
            foreach my $y ($string_2_a,$string_2_b){
                $distance += fastdistance ($x , $y);
```

```
                $comparisons++;
                }
            }
        return ($distance / $comparisons);
        }

    }

sub compare_indel_base{
    (my $insert_1 , my @trash)= split (/\:/ ,$_[0]); #grab the sequence
    (my $insert_2 ,    @trash)= split (/\:/ ,$_[1]); #grab the sequence

    ($insert_1,$insert_2) =($insert_1 =~/\+|-/)? ($insert_1,$insert_2) :
        ($insert_2,$insert_1); # Check our string 1 has the indel , if
       it doesnt flip them;
    my ($string_1_a , $string_1_b)=split (/\//,$insert_1);
    $string_1_a =~ s/\+|-//;
    $string_1_b =~ s/\+|-//;

    if ($string_1_a eq $string_1_b){
        return fastdistance($string_1_a,$insert_2);
        }
    elsif($string_1_a ne $string_1_b){
        my $distance = 0;
        my $comparisons =       0;
        foreach ($string_1_a , $string_1_b){
            $distance += fastdistance($_ , $insert_2);
            $comparisons ++;
            }
        ($distance==0) ? (return 0) : (return ($distance/$comparisons));
        }
}

sub pretty_printer{
```

```
    my $file_out = $_[0];
    my %hash = %{$_[1]};
    my @files = @{$_[2]};

    open (OUT , ">" , $file_out) || die $!;

    #HEADER
    print OUT"\t" .scalar(@files)."\n";
    #END HEADER

    for(my $x = 0; $x <= $#files; $x++){
            print OUT $files[$x] ."\t";
            for (my $y = $x; $y<= $#files ; $y++){
            if (exists $hash{$files[$x]}{$files[$y]}) {
                print OUT $hash{$files[$x]}{$files[$y]} ."\t"
                }
            else {print OUT $hash{$files[$y]}{$files[$x]} ."\t";}

            }
            print OUT "\n";
        }
    return;
    }

sub pretty_printer_complete{
    my $file_out = $_[0];
    my %hash = %{$_[1]};
    my @files = @{$_[2]};

    open (OUT , ">" , $file_out) || die $!;

    #HEADER
    print OUT"\t" .scalar(@files)."\n";
    #END HEADER
```

```
    for(my $x = 0; $x <= $#files; $x++){
            print OUT $files[$x] ."\t";
            for (my $y = 0; $y<= $#files ; $y++){
            if (exists $hash{$files[$x]}{$files[$y]}) {
                print OUT $hash{$files[$x]}{$files[$y]} ."\t"
                }
            else {print OUT $hash{$files[$y]}{$files[$x]} ."\t";}

            }
            print OUT "\n";
        }
    return;
    }

sub usage{
    print "\n\nBasic Usage: \n";
    print "./Varscan2_to_Distance.pl --varscan <varscan_file> --
       inventory <list of isolates> --prefix <string>\n";
    print "\t\t--varscan <string> mpileup2cns file from varscan2\n";
    print "\t\t--inventory <string> inventory file for the pileups (
       isolate name on each line)\n";
    print "\t\t--prefix <string> prefix you want for out put files\n";
    print "optional arguments:\n";
    print "\t\t--missing <int> number of isolates with missing data
       allowed for a locus\n";
    print "\t\t--snps_only     Only compare snp sites , this will skip
       over calculations of levenstein distance between sites with
       indels\n";
    print "\n";

    print "This program take two files:\n";
    print "\t\t 1) Standard Varscan mpileup2cns output\n";
    print "\t\t 2) The inventory list from that mpileup2cns run\n";
```

```
    print "It will then process the lines to calulate distance between
        each individual using the following rules:\n";
    print "\t\t Homozygous match = 0 \n";
    print "\t\t Homozygous mismatch = 1 \n";
    print "\t\t Homozygous/Heterozygous overlap = 0.5\n";
    print "\t\t Heterozygous/Heterozygous overlap = 0.83 \n";
    print "\t\t Indel/Indel = Levenshtein distance between the two
        strings\n";
    print "Scores are summed up for all comparisons made then averaged
        out by the number of comparisons made\n";

    print "The program then outputs 3 files , the upper right triangle
        of : \n";
    print "\t\tTotal scores\n \t\tTotal comparisons\n \t\tWeighted
        distance\n\n";
    print "All files are formatted for immediate use in the Phylip
        program\n";

    print "Some notes:\n";
    print "\t\t Its recommended to only input variant sites from
        varscan2 (--variants_only option)\n";



    exit;
    }

sub count_missing {
    my @array = @{$_[0]};
    my $missing = 0;
    foreach my $test(@array){
        (my $position_call,my @trash) =split (/\:/, $test);
        if ($position_call=~/N/g){ #skip lines with N positions calls
                    $missing++;
                    }
```

```
    }
return $missing;
}
```

Appendix B

VarScan2 to EIGENSOFT Utility

```
#!/usr/bin/perl

use warnings;
use strict;
use Getopt::Long;


#Global_Variables
my @file_names;
my %matrix;

my $allowed_missing = 0;
my $compare_to = "ref";
my $line_counter = 0;
my $output_prefix;
my $varscan_file;
my $inventory_file;
my $help = 0;
my $index = -1; #holds the position of the column to compare to.

GetOptions("missing=i"    => \$allowed_missing,
           "varscan=s"    => \$varscan_file,
```

```
            "inventory=s" => \$inventory_file,
            "prefix=s"    => \$output_prefix,
            "help+"       => \$help,
            "compare_to=s"  => \$compare_to
        ) or usage();

usage () if $help == 1;

#output files
my $snp_out = $output_prefix . ".snp";
my $geno_out = $output_prefix . ".geno";

foreach ($inventory_file, $varscan_file,$compare_to,$output_prefix) {
    usage() if $_ eq '';
    }


open(VARSCAN ,"<",$varscan_file) || die $!;
open (GEN , ">" , $geno_out) || die $!;
open (SNP , ">" , $snp_out ) || die $!;


    open(INVENTORY , "<" , $inventory_file) || die $!;
    while (my $line = <INVENTORY>){
        chomp $line;
        push @file_names , $line;
        }
    close INVENTORY;

#inventory to list of file names
if ($compare_to ne "ref"){
    ## get the index number for the inventory list
    for (my $i = 0; $i < @file_names; ++$i){
        if ($file_names[$i] eq $compare_to){
```

```
            $index = $i;
        }
    }
die "couldn't find the column you want me to compare to" if ($index ==
    -1);
}




print "loading varscan file ...\n";
my @lines =<VARSCAN>;
print "\t\t\t...loaded\n\n";

foreach my $line (@lines){
    chomp $line;
    $line_counter++;
    if ($line_counter%1e6 ==0){
        print STDOUT $line_counter . " completed\n";
        }
    if ($line eq "Chrom    Position    Ref Var Cons:Cov:Reads1:Reads2:
        Freq:P-value StrandFilter:R1+:R1-:R2+:R2-:pval    SamplesRef
        SamplesHet  SamplesHom  SamplesNC    Cons:Cov:Reads1:Reads2:Freq:
        P-value"){
        next;
        }

    my @tmp = split (/\s+/,$line);
    my @individual_info = @tmp[10..$#tmp]; #taking an array slice so its
        less maths to adjust indices


    if ($tmp[9] == 0){
```

```
if (check_for_indels_or_missing(\@individual_info) == 42){

    my $position_scaff = $1 if ($tmp[0] =~/(\d+)/);
    my $position_name = $position_scaff . "_" . $tmp[1];
    my $i = 0;

    my %local_hash;
    print SNP $position_name . "\t". $position_scaff . "\t0.0\t"
        . $tmp[1]."\n";
    foreach (@individual_info){
        (my $position_call1 ,my @trash) =split (/\:/, $_);
        my $position_call2;
        if ($compare_to ne "ref"){
            ( $position_call2 ,   @trash) =split (/\:/ ,
                $individual_info[$index]);
            }
        else{
            $position_call2 = $tmp[2];
            }
        my $value = compare_bases($position_call1 ,
            $position_call2);
        if ($value > -1){
            print GEN $position_name . "\t" . $file_names[$i] .
                "\t" . $value . "\n";
            }
        else{
            die "WAKA WAKA WAKA\n";
            }
        $i++;
        }

    }

}
```

```
    }



exit;

sub usage{
    print "\n\nBasic Usage: \n";
    print "./Varscan2_to_Matrix.pl --varscan <varscan_file> --compare_to
        <isolate_to_compare_to> --missing <missing> --inventory <list
       of isolates> --prefix <string>\n";
    print "\t\t--varscan <string> mpileup2cns file from varscan2\n";
    print "\t\t--inventory <string> inventory file for the pileups (
       isolate name on each line)\n";
    print "\t\t--prefix <string> prefix you want for output files\n";
    print "\n";

    print "This program take two files:\n";
    print "\t\t 1) Standard Varscan mpileup2cns output\n";
    print "\t\t 2) The inventory list from that mpileup2cns run\n";
    print "It will then process the lines and encode snps against the
       chosen individual using the following scheme\n";
    print "\t\t Homozygous match = 0\n";
    print "\t\t Homozygous mismatch = 2\n";
    print "\t\t Homozygous/Heterozygous overlap = 1\n";
    print "\t\t Heterozygous/Heterozygous overlap = 1\n\n";

    print "The program then outputs 2 files  : \n";
    print "\t\tList of all snps scored\n";
    print "\t\tScores for all individuals for all snps\n";
    print "\t\tAll files are formatted for the EigenSNP software\n\n";

    print "Some notes:\n";
```

```
    print "\t\t Its recommended to only input variant sites from
        varscan2 (--variants_only option)\n";


    exit;
    }

sub compare_bases{
    my ($base1 , $base2) = @_;


    if ($base1 eq $base2) {
        return 0;
        }
    if ((($base1 eq 'A')||($base1 eq 'T')||($base1 eq 'G')||($base1 eq '
        C')) &&(($base2 eq 'A')||($base2 eq 'T')||($base2 eq 'G')||(
        $base2 eq 'C'))){
        return 2;
        }
    ## base1 is homozygous base2 is heterozygous all of these cases are
        for when only one base needs to change for them to match
    if ((($base1 eq 'A')||($base1 eq 'T')||($base1 eq 'G')||($base1 eq '
        C')) && (($base2 eq 'Y')||($base2 eq 'R')||($base2 eq 'W')||(
        $base2 eq 'S')||($base2 eq 'K')||($base2 eq 'M'))){
        #Make our comparisons#
        if($base2 eq 'Y' && ($base1 eq 'C'||$base1 eq 'T') ){
            return 1;
            }
        if($base2 eq 'R' && ($base1 eq 'A'||$base1 eq 'G') ){
            return 1;
            }
        if($base2 eq 'W' && ($base1 eq 'A'||$base1 eq 'T') ){
            return 1;
            }
```

```
if($base2 eq 'S' && ($base1 eq 'G'||$base1 eq 'C') ){
    return 1;
    }
if($base2 eq 'K' && ($base1 eq 'T'||$base1 eq 'G') ){
    return 1;
    }
if($base2 eq 'M' && ($base1 eq 'C'||$base1 eq 'A') ){
    return 1;
    }


if($base2 eq 'R' && ($base1 eq 'C'||$base1 eq 'T') ){
    return 2;
    }
if($base2 eq 'Y' && ($base1 eq 'A'||$base1 eq 'G') ){
    return 2;
    }
if($base2 eq 'S' && ($base1 eq 'A'||$base1 eq 'T') ){
    return 2;
    }
if($base2 eq 'W' && ($base1 eq 'G'||$base1 eq 'C') ){
    return 2;
    }
if($base2 eq 'M' && ($base1 eq 'T'||$base1 eq 'G') ){
    return 2;
    }
if($base2 eq 'K' && ($base1 eq 'C'||$base1 eq 'A') ){
    return 2;
    }
```

```
        }

    ## base2 is homozygous base1 is heterozygous
    if (((($base2 eq 'A')||($base2 eq 'T')||($base2 eq 'G')||($base2 eq '
       C')) && (($base1 eq 'Y')||($base1 eq 'R')||($base1 eq 'W')||(
       $base1 eq 'S')||($base1 eq 'K')||($base1 eq 'M'))){
        return compare_bases($base2 , $base1); #swap our variable and
           call the subroutine again;
        }
    if (((($base1 eq 'Y')||($base1 eq 'R')||($base1 eq 'W')||($base1 eq '
       S')||($base1 eq 'K')||($base1 eq 'M')) && (($base2 eq 'Y')||(
       $base2 eq 'R')||($base2 eq 'W')||($base2 eq 'S')||($base2 eq 'K'
       )||($base2 eq 'M')) )  {
    ## both bases are heterozygotes with no overlap ##
        if (($base1 eq 'R') && ($base2 eq 'Y')){
            return 2;
            }
        if (($base1 eq 'Y') && ($base2 eq 'R')){
            return 2;
            }
        if (($base1 eq 'S') && ($base2 eq 'W')){
            return 2;
            }
        if (($base1 eq 'W') && ($base2 eq 'S')){
            return 2;
            }
        return 1; # default behavior
    }

return -1;
}

sub check_for_indels_or_missing {
```

```
my @array = @{$_[0]};

foreach my $test(@array){
    (my $position_call,my @trash) =split (/\:/, $test);

    if ($position_call=~/\+|\-|\*/g || $position_call eq ''){ #non
       informative comparisons are dumped.
                return -1;
                }
    if ($position_call=~/N/g){ #skip lines with N positions calls
                return -1;
                }

    }

return 42;
}
```

Appendix C

High Value SNPs within *P. capsici.*

The ten SNPs with the highest singular value decomposition for each eigenvector as reported by the EIGENSOFT package.

EigenVector	SNP Name	Scaffold	Position	SVD	Alleles Present
1	14_552797	14	552797	4.867	A,M,C
1	14_526491	14	526491	4.782	A,R,G
1	17_12019	17	12019	4.209	T,C,Y
1	6_998905	6	998905	4.171	A,W,T
1	9_287111	9	287111	4.168	T,C,Y
1	20_559866	20	559866	4.093	T,C,Y
1	6_460442	6	460442	4.089	A,R,G
1	2_1616779	2	1616779	3.99	A,R,G
1	2_1616861	2	1616861	3.986	T,C,Y
1	20_572811	20	572811	3.863	T,K,G
2	15_726217	15	726217	3.791	A,R,G
2	11_182933	11	182933	3.618	S,C,G
2	7_693612	7	693612	3.613	A,R,G

2	13_1028113	13	1028113	3.603	A,R,G
2	3_880189	3	880189	3.596	T,C,Y
2	21_227318	21	227318	3.583	A,R,G
2	18_914098	18	914098	3.577	T,C,Y
2	10_1087317	10	1087317	3.557	T,C,Y
2	8_732616	8	732616	3.534	A,R,G
2	15_681752	15	681752	3.509	T,C,Y
3	1_1640307	1	1640307	5.608	A,G
3	2_1003184	2	1003184	5.608	C,G
3	4_1413785	4	1413785	5.608	A,G
3	8_1125200	8	1125200	5.608	T,C
3	2_463967	2	463967	4.576	A,R,G
3	13_596134	13	596134	4.576	A,R,G
3	13_596135	13	596135	4.576	A,R,G
3	2_1325240	2	1325240	4.165	A,W,T
3	2_1379175	2	1379175	3.993	T,C,Y
3	2_782680	2	782680	3.966	A,T,W
4	13_597579	13	597579	4.758	T,C,Y
4	13_597576	13	597576	4.563	T,C,Y
4	1_55802	1	55802	3.986	A,R,G
4	13_595983	13	595983	3.963	T,C,Y
4	2_439383	2	439383	3.789	T,C,Y
4	22_239274	22	239274	3.651	R,G
4	22_240165	22	240165	3.651	R,G
4	5_1163140	5	1163140	3.362	R,G
4	6_551821	6	551821	3.362	R,G
4	16_655190	16	655190	3.357	T,K,G

5	11_765770	11	765770	5.292	T,C,Y
5	17_323455	17	323455	4.934	T,K,G
5	17_440448	17	440448	4.836	A,R,G
5	13_610564	13	610564	4.672	A,R,G
5	7_93053	7	93053	4.59	A,R,G
5	17_309213	17	309213	4.533	A,G
5	10_449580	10	449580	4.431	A,R,G
5	4_166065	4	166065	4.344	A,R,G
5	15_855110	15	855110	4.305	A,R,G
5	17_440452	17	440452	4.302	A,M,C
6	22_782188	22	782188	4.155	S,C,G
6	6_440129	6	440129	3.855	T,C,Y
6	1_606386	1	606386	3.803	C,Y
6	17_170207	17	170207	3.775	T,C,Y
6	17_170216	17	170216	3.775	A,T,W
6	15_595665	15	595665	3.741	S,C,GY
6	4_332284	4	332284	3.65	T,C,Y
6	21_101774	21	101774	3.591	A,R,G
6	10_884017	10	884017	3.493	A,R,G
6	22_789496	22	789496	3.464	A,R,G
7	19_356721	19	356721	4.444	A,R,G
7	9_185259	9	185259	3.718	A,R,G
7	21_245518	21	245518	3.649	T,K,G
7	11_187518	11	187518	3.541	A,M,C
7	19_356894	19	356894	3.432	S,C,G
7	11_318193	11	318193	3.419	R,G
7	4_45737	4	45737	3.41	S,C,G

7	11_186176	11	186176	3.395	R,G
7	6_770682	6	770682	3.352	T,C,Y
7	18_916283	18	916283	3.342	T,Y
8	5_677190	5	677190	4.54	A,R,G
8	21_429359	21	429359	4.459	A,R,G
8	21_501247	21	501247	4.246	A,R,G
8	14_555854	14	555854	3.973	R,G
8	6_931389	6	931389	3.804	A,R,G
8	13_940310	13	940310	3.581	T,C,Y
8	4_214861	4	214861	3.552	A,R,G
8	9_453826	9	453826	3.532	S,C,G
8	10_353315	10	353315	3.519	A,M,C
8	16_936671	16	936671	3.443	S,C,G
9	17_321960	17	321960	5.015	T,C,Y
9	17_323751	17	323751	4.281	T,C,Y
9	3_1019857	3	1019857	4.259	A,R,G
9	3_1019864	3	1019864	4.259	A,R,G
9	3_1026294	3	1026294	4.259	T,C,Y
9	8_180944	8	180944	4.109	A,M,C
9	1_68897	1	68897	3.96	A,G
9	4_353869	4	353869	3.96	A,T
9	5_1314613	5	1314613	3.96	A,G
9	7_680173	7	680173	3.96	A,C
10	1_68897	1	68897	4.285	A,G
10	4_353869	4	353869	4.285	A,T
10	5_1314613	5	1314613	4.285	A,G
10	7_680173	7	680173	4.285	A,C

10	7_693648	7	693648	4.285	T,G
10	5_665315	5	665315	3.959	T,C,Y
10	4_274962	4	274962	3.953	A,R,G
10	4_169465	4	169465	3.855	A,T,W
10	14_489467	14	489467	3.8	A,R,G
10	7_702402	7	702402	3.796	T,K,G

Table C.1: SNP markers that explain the most variation along each eigenvector,and the alleles present at these loci.

Appendix D

High Value SNPs between *P. capsici* and *P. tropicalis*

The ten SNPs with the highest singular value decomposition for each eigenvector as reported by the EIGENSOFT package.

EigenVector	SNP Name	Scaffold	Position	SVD	*P. Subnubulis*	*P. Tropicalis*	*P. Capsici*
1	1_73805	1	73805	2.169	T	T,C	G
1	1_99952	1	99952	2.169	C	C	T
1	1_140290	1	140290	2.169	T	T	C
1	1_140304	1	140304	2.169	C	C	G
1	1_258552	1	258552	2.169	T	T	C
1	1_258568	1	258568	2.169	T	T	C
1	1_287061	1	287061	2.169	C	C	T
1	1_406498	1	406498	2.169	C	C	T
1	1_409267	1	409267	2.169	C	C	A
1	1_421573	1	421573	2.169	T	T	C
2	1_59737	1	59737	2.93	A	G,A	A
2	1_59741	1	59741	2.93	G	G,A	G
2	1_59743	1	59743	2.93	G	G,C	G

2	1_59758	1	59758	2.93	A	C,A	A
2	1_59761	1	59761	2.93	G	G,A	G
2	1_59769	1	59769	2.93	G	G,A	G
2	1_75994	1	75994	2.93	C	C,T	C
2	1_75996	1	75996	2.93	C	C,G	C
2	1_228922	1	228922	2.93	G	G,T	G
2	1_287058	1	287058	2.93	T	T,C	T
3	1_55810	1	55810	2.827	G	A,G	G
3	1_59772	1	59772	2.827	A	T,A	A
3	1_59773	1	59773	2.827	C	T,C	C
3	1_73692	1	73692	2.827	A	C,A	A
3	1_73697	1	73697	2.827	C	T,C	C
3	1_89603	1	89603	2.827	C	T,C	C
3	1_89632	1	89632	2.827	C	T,C	C
3	1_115845	1	115845	2.827	G	A,G	G
3	1_136920	1	136920	2.827	T	A,G	T
3	1_148635	1	148635	2.827	T	C,T	T
4	1_644862	1	644862	4.689	A	A,G	A
4	1_1147588	1	1147588	4.689	G	A,G	G
4	1_1256579	1	1256579	4.689	T	T,C	T
4	1_1258758	1	1258758	4.689	C	C,G	C
4	1_1841529	1	1841529	4.689	T	T,C	T
4	1_1864629	1	1864629	4.689	A	A,G	A
4	2_581994	2	581994	4.689	T	T,A	T
4	3_1183603	3	1183603	4.689	A	A,G	A
4	6_1104888	6	1104888	4.689	C	C,T	C
4	16_637463	16	637463	4.689	C	C,T	C

5	2_1374321	2	1374321	7.731	G	G	G,K,T
5	9_277144	9	277144	7.652	C	C	C,Y,T
5	7_962612	7	962612	7.562	C	C	C,Y,T
5	9_211073	9	211073	7.562	C	C	C,S,G
5	18_89948	18	89948	7.365	T	T	C,Y,T
5	4_87070	4	87070	7.297	C	C	C,Y,T
5	14_597493	14	597493	7.297	A	A	A,R,G
5	2_1502322	2	1502322	6.976	C	T,C	C,Y,T
5	21_497740	21	497740	6.96	G	G	A,R,G
5	22_575348	22	575348	6.918	G	G	G,R,A

Table D.1: SNP markers that explain the most variation along each eigenvector,and the alleles present at these loci.

Appendix E

Six Frame and Translation Utility

```
#!/usr/bin/perl
use warnings;
use strict;
use threads;
use Config;
use Getopt::Long;

#compiling our regular expressions#

# Get our settings #
my $threads = 4;
my $orf_size = 70;
my $informatic_stops = 0;
my @files =();
my $missing_max = 6;

GetOptions(
'threads|i' => \$threads,
'orf_size|i' => \$orf_size,
'informatic_stops' => \$informatic_stops,
'missing_data'=> \$missing_max,
'<>' => \&file_or_something
```

```
);

#load our codon table
my %g = load_codon_table();


#Check Dependencies#
$Config{useithreads} || die "Recompile Perl with threads in order to use
     this program";

#checking for files to work on#
if (@files < 0){
     die "You didn't provide files to work on.\n";
     usage();
     }
print "Current settings are: \n\tthreads -> $threads\n\torfsize ->
    $orf_size\n\tinformatic stops -> $informatic_stops\n\tMissing
    Information -> $missing_max\n\tfiles -> " .join(', ' , @files) ."\n\
    n";

## Main Program

my $terminator = $/; #saving our EOL

foreach my $file (@files){
     (my $filename = $file) =~ s/\.[^.]+$//; ## get the prefix
     local $/ = ">"; #splitting file on > character now Scoped to  this
        loop and all sub_routines called from here.
     open (FASTA , '<', $file) || die $!;
     open (AAOUT , '>' , "$filename\.sfaa" ) || die $!;
     open (NTOUT , '>' , "$filename\.sfnt") || die $!;
     my @records = <FASTA>; #slurp
     shift @records;
     my @executing_threads = (); #list of executing threads
```

```
    while (@records) {
        for(my $i = 0 ;$i < $threads ; $i++){ ## only want to execute
            threads that we can actually work on
             if (@records){ ## assuming we have stuff to work on
                 push @executing_threads , (threads->create(\&
                     six_frame_translate , pop(@records))); ## execute a
                     thread to do the work , denote the return variable
                     as an array by encasing the create in ()
                 }
             }
        while (@executing_threads){ # while I have threads to clean up
             (my $nt_print ,my $aa_print) = (pop(@executing_threads)->
                 join()); ## clean the threads and get our print returns
                 back
             print NTOUT uc $nt_print; ## we're doing this out of the
                 thread so that we don't have buffer flushes screwing up
                 prints
             print AAOUT uc $aa_print;
             }


        }

    }
exit;



sub usage{
    return;
    }
```

```
sub file_or_something{
    if (-f $_[0]){
        push @files , shift @_;
        }
    else{
        print "@_ either doesn't exist or an unknown option !\n";
        }
    }

sub load_codon_table{
    #simply returns a hash containing an extended table of codon => AA
        converstions

    my %g=(
        'GCA' => 'A',
        'GCT' => 'A',
        'GCG' => 'A',
        'GCC' => 'A',
        'GCW' => 'A',
        'GCS' => 'A',
        'GCM' => 'A',
        'GCK' => 'A',
        'GCR' => 'A',
        'GCY' => 'A',
        'GCB' => 'A',
        'GCD' => 'A',
        'GCH' => 'A',
        'GCV' => 'A',
        'GCN' => 'A',

        'CGT' => 'R',
        'CGC' => 'R',
        'CGA' => 'R',
        'CGG' => 'R',
```

```
'AGA' => 'R',
'AGG' => 'R',
'CGN' => 'R',
'CGW' => 'R',
'CGS' => 'R',
'CGM' => 'R',
'CGK' => 'R',
'CGR' => 'R',
'CGY' => 'R',
'CGB' => 'R',
'CGD' => 'R',
'CGH' => 'R',
'CGV' => 'R',
'MGR' => 'R',

'AAT' => 'N',
'AAC' => 'N',
'AAY' => 'N',

'GAT' => 'D',
'GAC' => 'D',
'GAY' => 'D',

'TGT' => 'C',
'TGC' => 'C',
'TGY' => 'C',

'CAA' => 'Q',
'CAG' => 'Q',
'CAR' => 'Q',

'GAA' => 'E',
'GAG' => 'E',
'GAR' => 'E',
```

```
'GGT' => 'G',
'GGC' => 'G',
'GGA' => 'G',
'GGG' => 'G',
'GGN' => 'G',
'GGW' => 'G',
'GGS' => 'G',
'GGM' => 'G',
'GGK' => 'G',
'GGR' => 'G',
'GGY' => 'G',
'GGB' => 'G',
'GGD' => 'G',
'GGH' => 'G',
'GGV' => 'G',

'CAT' => 'H',
'CAC' => 'H',
'CAY' => 'H',

'ATT' => 'I',
'ATC' => 'I',
'ATA' => 'I',
'ATH' => 'I',
'ATM' => 'I',
'ATW' => 'I',
'ATY' => 'I',

'ATG' => 'M',

'TTA' => 'L',
'TTG' => 'L',
'CTT' => 'L',
```

```
'CTC' => 'L',
'CTA' => 'L',
'CTG' => 'L',
'YTR' => 'L',
'CTN' => 'L',
'CTW' => 'L',
'CTS' => 'L',
'CTM' => 'L',
'CTK' => 'L',
'CTR' => 'L',
'CTY' => 'L',
'CTB' => 'L',
'CTD' => 'L',
'CTH' => 'L',
'CTV' => 'L',

'AAA' => 'K',
'AAG' => 'K',
'AAR' => 'K',

'TTT' => 'F',
'TTC' => 'F',
'TTY' => 'F',

'CCT' => 'P',
'CCC' => 'P',
'CCA' => 'P',
'CCG' => 'P',
'CCN' => 'P',
'CCW' => 'P',
'CCS' => 'P',
'CCM' => 'P',
'CCK' => 'P',
'CCR' => 'P',
```

```
'CCY' => 'P',
'CCB' => 'P',
'CCD' => 'P',
'CCH' => 'P',
'CCV' => 'P',

'TCT' => 'S',
'TCC' => 'S',
'TCA' => 'S',
'TCG' => 'S',
'AGT' => 'S',
'AGC' => 'S',
'AGY' => 'S',
'TCN' => 'S',
'TCW' => 'S',
'TCS' => 'S',
'TCM' => 'S',
'TCK' => 'S',
'TCR' => 'S',
'TCY' => 'S',
'TCB' => 'S',
'TCD' => 'S',
'TCH' => 'S',
'TCV' => 'S',

'ACT' => 'T',
'ACC' => 'T',
'ACA' => 'T',
'ACG' => 'T',
'ACN' => 'T',
'ACW' => 'T',
'ACS' => 'T',
'ACM' => 'T',
'ACK' => 'T',
```

```
'ACR' => 'T',
'ACY' => 'T',
'ACB' => 'T',
'ACD' => 'T',
'ACH' => 'T',
'ACV' => 'T',

'TGG' => 'W',

'TAT' => 'Y',
'TAC' => 'Y',
'TAY' => 'Y',

'GTT' => 'V',
'GTC' => 'V',
'GTA' => 'V',
'GTG' => 'V',
'GTN' => 'V',
'GTW' => 'V',
'GTS' => 'V',
'GTM' => 'V',
'GTK' => 'V',
'GTR' => 'V',
'GTY' => 'V',
'GTB' => 'V',
'GTD' => 'V',
'GTH' => 'V',
'GTV' => 'V',

'TAA' => '*',
'TGA' => '*',
'TAG' => '*',
'TAR' => '*',
'TRA' => '*'
```

```
    );
    return %g;
    }

sub six_frame_translate{
    my $aa_return ;
    my $nt_return;
    #process our record into a header and sequence and our reverse
        compliment
    (my $header , my @tmp) = split (/\n/,shift @_);
    my $sequence  = uc join '' , @tmp ;
    my $r_sequence = reverse $sequence; #reverse
    $r_sequence =~ tr/ATGC/TACG/; #compliment
    my @starts=([0],[1],[2],[0],[1],[2]); # declare our array of arrays;
    my @stops =([],[],[],[],[],[]); #declare our array of arrays;

    my $nt_length = $orf_size*3 + 3; #  add three for the stop codon

    if ($header =~ /(\d+)/){
    $header = $1; ## if our header has a number in it ( ie scaffold
        number we'll use it)
        }
    if ($informatic_stops == 0){
    while ($sequence =~ /ATG/ig){
        push (@starts[(pos($sequence)%3)] , pos ($sequence)-3);
        }
    while ($sequence =~ /TAG|TAA|TAR|TRA|TGA/ig){
        push (@stops[(pos($sequence)%3)] , pos ($sequence));
        }
    while ($r_sequence =~ /ATG/ig){
        push (@starts[(pos($r_sequence)%3) + 3] , pos ($r_sequence)-3);
        }
    while ($r_sequence =~ /TAG|TAA|TAR|TRA|TGA/ig){
        push (@stops[(pos($r_sequence)%3) +3] , pos ($r_sequence));
```

```
    }



foreach (0..2){
    push (@stops[(length($sequence)-$_)%3] , length($sequence)-$_);
    push (@stops[(length($sequence)-$_)%3 +3] , length($sequence)-$_
        )
    }
foreach my $frame (0,1,2){
    my $current_start = shift @{$starts[$frame]};
    my $current_stop = shift @{$stops[$frame]};

    while (@{$starts[$frame]}){ # while I have starts
        if(!(@{$stops[$frame]})){ # check if I have any stops , if
            no more stops clear out starts
            @{$starts[$frame]} =();
            }
        my $length = ($current_stop-$current_start);
        if ($length >= $nt_length){ #our current start/stop pair are
             far enough apart
            #print out our sequences to the correct files;
            my $translated = translate(substr($sequence,
                $current_start,$length));

            $nt_return .= ">scaf_$header"."_frame_". ($frame+1) . "
                _start_".$current_start."_stop_".$current_stop."\n".
                substr($sequence,$current_start,$length)."\n";
            $aa_return .= ">scaf_$header"."_frame_". ($frame+1) . "
                _start_".$current_start."_stop_".$current_stop."\n".
                $translated."\n";

            while ($current_start < $current_stop){ # while my start
                 is in front of my stop
```

```
                if (!@{$starts[$frame]}){ # if I'm out of start
                    codons
                    $current_start = $current_stop +1; # make a fake
                        start that's beyond my current stop
                    }
                else{
                    $current_start = shift @{$starts[$frame]}; #
                        other wise get the next start codon
                    }
                }

            }
        elsif (($length < $nt_length) && ($length >= 3)){ ## too
            short
            $current_start = shift @{$starts[$frame]};
            }
        elsif (($length <= 0)){
            $current_stop = shift @{$stops[$frame]};
            }
        }
    }


## now the reverse side
foreach my $frame (3,4,5){
    my $current_start = shift @{$starts[$frame]};
    my $current_stop = shift @{$stops[$frame]};

    while (@{$starts[$frame]}){ # while I have starts
        if(!(@{$stops[$frame]})){ # check if I have any stops , if
            no more stops clear out starts
            @{$starts[$frame]} =();
            }
        my $length = ($current_stop-$current_start);
```

```
if ($length >= $nt_length){ #our current start/stop pair are
    far enough apart
   #print out our sequences to the correct files;
   my $translated = translate(substr($r_sequence,
       $current_start,$length) , $_[2]);

   $nt_return .= ">scaf_"."$header" . "_frame_". ($frame+1)
       . "_start_" . (length($r_sequence)-$current_start
   +1) . "_stop_" . (length($r_sequence)-$current_stop
   +1) ."\n".substr($r_sequence,$current_start,$length)
   ."\n";
   $aa_return .= ">scaf_"."$header" . "_frame_". ($frame+1)
       . "_start_" . (length($r_sequence)-$current_start
   +1) . "_stop_" . (length($r_sequence)-$current_stop
   +1) ."\n". $translated ."\n";


   ## this loop bleeds off start codons so we dont get
       multiple sub strings
   while ($current_start < $current_stop){ # while my start
       is in front of my stop
       if (!@{$starts[$frame]}){ # if I'm out of start
           codons
           $current_start = $current_stop +1; # make a fake
               start that's beyond my current stop
           }
       else{
           $current_start = shift @{$starts[$frame]}; #
               other wise get the next start codon
           }
       }

   }
```

```
            elsif (($length < $nt_length) && ($length >= 3)){ ## too
                short
                $current_start = shift @{$starts[$frame]};
                }
            elsif (($length <= 0)){
                $current_stop = shift @{$stops[$frame]};
                }
            }
        }
    return ($nt_return , $aa_return);
}

    if($informatic_stops == 1){

        }


    }

sub translate{
    #accepts a nucleotide sequence and returns an AA
    my $sequence_in = $_[0];
    my @DNA = split(//,$sequence_in);
    my $protein;
    while (@DNA){
        my $codon = join( "",(splice(@DNA,0,3)));
        if (exists($g{$codon})){
            $protein .= $g{$codon};
            }
        else{
            $protein .= 'X';
            }
        }
    return($protein);
```

```
}
```

Appendix F

RxLR and CRN Node Descriptions

F.1 RxLR Node Descriptions

PHYCAScaffold_25 DSRXLR CDS 323402 323764 . + . ID=name"RXLR_0"

PHYCAScaffold_8 DSRXLR CDS 247029 247274 . - . ID=name"RXLR_1"

PHYCAScaffold_18 DSRXLR CDS 388085 388681 . + . ID=name"RXLR_2"

PHYCAScaffold_48 DSRXLR CDS 137619 139427 . - . ID=name"RXLR_3"

PHYCAScaffold_6 DSRXLR CDS 1303307 1303645 . + . ID=name"RXLR_4"

PHYCAScaffold_17 DSRXLR CDS 419015 420544 . - . ID=name"RXLR_5"

PHYCAScaffold_32 DSRXLR CDS 390473 390856 . + . ID=name"RXLR_6"

PHYCAScaffold_40 DSRXLR CDS 393862 394293 . - . ID=name"RXLR_7"

PHYCAScaffold_55 DSRXLR CDS 246914 249292 . - . ID=name"RXLR_8"

PHYCAScaffold_41 DSRXLR CDS 225282 225803 . - . ID=name"RXLR_9"

PHYCAScaffold_24 DSRXLR CDS 612902 613150 . + . ID=name"RXLR_10"

PHYCAScaffold_37 DSRXLR CDS 175084 176634 . - . ID=name"RXLR_11"

PHYCAScaffold_3 DSRXLR CDS 1504049 1508131 . - . ID=name"RXLR_12"

PHYCAScaffold_92 DSRXLR CDS 71763 72062 . - . ID=name"RXLR_13"

PHYCAScaffold_106 DSRXLR CDS 72831 73556 . + . ID=name"RXLR_14"

PHYCAScaffold_38 DSRXLR CDS 229809 230123 . - . ID=name"RXLR_15"

PHYCAScaffold_431 DSRXLR CDS 2654 2914 . - . ID=name"RXLR_16"

PHYCAScaffold_53 DSRXLR CDS 47793 48248 . - . ID=name"RXLR_17"

PHYCAScaffold_28 DSRXLR CDS 357593 360748 . + . ID=name"RXLR_18"

PHYCAScaffold_64 DSRXLR CDS 34971 36383 . + . ID=name"RXLR_19"

PHYCAScaffold_10 DSRXLR CDS 1141669 1142448 . - . ID=name"RXLR_20"

PHYCAScaffold_68 DSRXLR CDS 117067 117285 . - . ID=name"RXLR_21"

PHYCAScaffold_31 DSRXLR CDS 505883 506356 . + . ID=name"RXLR_22"

PHYCAScaffold_103 DSRXLR CDS 129318 129734 . + . ID=name"RXLR_23"

PHYCAScaffold_2 DSRXLR CDS 323335 324462 . + . ID=name"RXLR_24"

PHYCAScaffold_60 DSRXLR CDS 162527 164635 . - . ID=name"RXLR_25"

PHYCAScaffold_21 DSRXLR CDS 666958 668031 . + . ID=name"RXLR_26"

PHYCAScaffold_13 DSRXLR CDS 1004702 1008061 . + . ID=name"RXLR_27"

PHYCAScaffold_5 DSRXLR CDS 378003 378584 . + . ID=name"RXLR_28"

PHYCAScaffold_36 DSRXLR CDS 601248 602570 . + . ID=name"RXLR_29"

PHYCAScaffold_8 DSRXLR CDS 2097 2474 . - . ID=name"RXLR_30"

PHYCAScaffold_19 DSRXLR CDS 637850 639442 . + . ID=name"RXLR_31"

PHYCAScaffold_108 DSRXLR CDS 44392 46107 . - . ID=name"RXLR_32"

PHYCAScaffold_62 DSRXLR CDS 271547 272839 . + . ID=name"RXLR_33"

PHYCAScaffold_10 DSRXLR CDS 716479 716982 . + . ID=name"RXLR_34"

PHYCAScaffold_11 DSRXLR CDS 87993 88256 . + . ID=name"RXLR_35"

PHYCAScaffold_16 DSRXLR CDS 449616 452552 . + . ID=name"RXLR_36"

PHYCAScaffold_50 DSRXLR CDS 102935 103612 . - . ID=name"RXLR_37"

PHYCAScaffold_40 DSRXLR CDS 445614 446174 . - . ID=name"RXLR_38"

PHYCAScaffold_70 DSRXLR CDS 118220 118888 . - . ID=name"RXLR_39"

PHYCAScaffold_40 DSRXLR CDS 247798 248127 . - . ID=name"RXLR_40"

PHYCAScaffold_19 DSRXLR CDS 460491 462089 . - . ID=name"RXLR_41"

PHYCAScaffold_27 DSRXLR CDS 691216 692610 . + . ID=name"RXLR_42"

PHYCAScaffold_87 DSRXLR CDS 4072 4518 . - . ID=name"RXLR_43"

PHYCAScaffold_2 DSRXLR CDS 1312901 1313387 . - . ID=name"RXLR_44"

PHYCAScaffold_2 DSRXLR CDS 1212053 1212397 . - . ID=name"RXLR_45"

PHYCAScaffold_1 DSRXLR CDS 629240 629965 . - . ID=name"RXLR_46"

PHYCAScaffold_7 DSRXLR CDS 169457 169729 . + . ID=name"RXLR_47"

PHYCAScaffold_13 DSRXLR CDS 314756 315094 . + . ID=name"RXLR_48"

PHYCAScaffold_18 DSRXLR CDS 882491 882712 . + . ID=name"RXLR_49"

PHYCAScaffold_19 DSRXLR CDS 724778 725227 . + . ID=name"RXLR_50"

PHYCAScaffold_53 DSRXLR CDS 170437 173070 . + . ID=name"RXLR_51"

PHYCAScaffold_2 DSRXLR CDS 315335 315790 . - . ID=name"RXLR_52"

PHYCAScaffold_23 DSRXLR CDS 345130 347379 . - . ID=name"RXLR_53"

PHYCAScaffold_20 DSRXLR CDS 354427 354654 . + . ID=name"RXLR_54"

PHYCAScaffold_30 DSRXLR CDS 28196 29137 . + . ID=name"RXLR_55"

PHYCAScaffold_29 DSRXLR CDS 321243 321641 . - . ID=name"RXLR_56"

PHYCAScaffold_21 DSRXLR CDS 423578 423841 . + . ID=name"RXLR_57"

PHYCAScaffold_4 DSRXLR CDS 355630 357201 . - . ID=name"RXLR_58"

PHYCAScaffold_5 DSRXLR CDS 997091 997765 . - . ID=name"RXLR_59"

PHYCAScaffold_104 DSRXLR CDS 75737 76348 . - . ID=name"RXLR_60"

PHYCAScaffold_39 DSRXLR CDS 272413 272784 . - . ID=name"RXLR_61"

PHYCAScaffold_11 DSRXLR CDS 221929 222540 . + . ID=name"RXLR_62"

PHYCAScaffold_8 DSRXLR CDS 599681 600712 . - . ID=name"RXLR_63"

PHYCAScaffold_52 DSRXLR CDS 67634 68023 . - . ID=name"RXLR_64"

PHYCAScaffold_49 DSRXLR CDS 304665 306644 . - . ID=name"RXLR_65"

PHYCAScaffold_2 DSRXLR CDS 1499362 1499717 . - . ID=name"RXLR_66"

PHYCAScaffold_96 DSRXLR CDS 13378 14031 . + . ID=name"RXLR_67"

PHYCAScaffold_2 DSRXLR CDS 317937 318323 . + . ID=name"RXLR_68"

PHYCAScaffold_57 DSRXLR CDS 325662 325874 . - . ID=name"RXLR_69"

PHYCAScaffold_21 DSRXLR CDS 90428 93247 . - . ID=name"RXLR_70"

PHYCAScaffold_6 DSRXLR CDS 905322 905768 . - . ID=name"RXLR_71"

PHYCAScaffold_80 DSRXLR CDS 37097 37423 . - . ID=name"RXLR_72"

PHYCAScaffold_48 DSRXLR CDS 65003 68284 . + . ID=name"RXLR_73"

PHYCAScaffold_2 DSRXLR CDS 157778 158170 . - . ID=name"RXLR_74"

PHYCAScaffold_42 DSRXLR CDS 21524 21796 . + . ID=name"RXLR_75"

PHYCAScaffold_4 DSRXLR CDS 43700 44113 . - . ID=name"RXLR_76"

PHYCAScaffold_2 DSRXLR CDS 156932 157300 . - . ID=name"RXLR_77"

PHYCAScaffold_9 DSRXLR CDS 684380 685951 . - . ID=name"RXLR_78"

PHYCAScaffold_7 DSRXLR CDS 881413 881802 . - . ID=name"RXLR_79"

PHYCAScaffold_38 DSRXLR CDS 498080 498781 . - . ID=name"RXLR_80"

PHYCAScaffold_87 DSRXLR CDS 66144 66452 . - . ID=name"RXLR_81"

PHYCAScaffold_12 DSRXLR CDS 813376 818256 . + . ID=name"RXLR_82"

PHYCAScaffold_6 DSRXLR CDS 1317937 1318254 . - . ID=name"RXLR_83"

PHYCAScaffold_33 DSRXLR CDS 276962 278917 . - . ID=name"RXLR_84"

PHYCAScaffold_29 DSRXLR CDS 346894 348741 . - . ID=name"RXLR_85"

PHYCAScaffold_1 DSRXLR CDS 773946 774881 . + . ID=name"RXLR_86"

PHYCAScaffold_30 DSRXLR CDS 60704 61219 . - . ID=name"RXLR_87"

PHYCAScaffold_16 DSRXLR CDS 320249 321379 . - . ID=name"RXLR_88"

PHYCAScaffold_29 DSRXLR CDS 607577 608101 . + . ID=name"RXLR_89"

PHYCAScaffold_12 DSRXLR CDS 192776 193192 . + . ID=name"RXLR_90"

PHYCAScaffold_50 DSRXLR CDS 361564 361791 . - . ID=name"RXLR_91"

PHYCAScaffold_4 DSRXLR CDS 237951 238235 . - . ID=name"RXLR_92"

PHYCAScaffold_536 DSRXLR CDS 2814 3098 . - . ID=name"RXLR_93"

PHYCAScaffold_2 DSRXLR CDS 588637 588933 . + . ID=name"RXLR_94"

PHYCAScaffold_14 DSRXLR CDS 851114 851455 . + . ID=name"RXLR_95"

PHYCAScaffold_72 DSRXLR CDS 25279 25596 . + . ID=name"RXLR_96"

PHYCAScaffold_47 DSRXLR CDS 197853 198869 . + . ID=name"RXLR_97"

PHYCAScaffold_3 DSRXLR CDS 1266965 1268998 . - . ID=name"RXLR_98"

PHYCAScaffold_43 DSRXLR CDS 44187 44411 . + . ID=name"RXLR_99"

PHYCAScaffold_86 DSRXLR CDS 45554 46108 . - . ID=name"RXLR_100"

PHYCAScaffold_48 DSRXLR CDS 407397 407654 . + . ID=name"RXLR_101"

PHYCAScaffold_27 DSRXLR CDS 256683 258155 . + . ID=name"RXLR_102"

PHYCAScaffold_18 DSRXLR CDS 930295 930546 . + . ID=name"RXLR_103"

PHYCAScaffold_1 DSRXLR CDS 1240114 1240698 . - . ID=name"RXLR_104"

PHYCAScaffold_7 DSRXLR CDS 787456 787866 . - . ID=name"RXLR_105"

PHYCAScaffold_46 DSRXLR CDS 238173 238667 . - . ID=name"RXLR_106"

PHYCAScaffold_29 DSRXLR CDS 263020 263517 . + . ID=name"RXLR_107"

PHYCAScaffold_25 DSRXLR CDS 329087 329506 . - . ID=name"RXLR_108"

PHYCAScaffold_20 DSRXLR CDS 832772 833359 . + . ID=name"RXLR_109"

PHYCAScaffold_14 DSRXLR CDS 1005147 1008800 . + . ID=name"RXLR_110"

PHYCAScaffold_26 DSRXLR CDS 244038 244904 . - . ID=name"RXLR_111"

PHYCAScaffold_37 DSRXLR CDS 221168 222031 . - . ID=name"RXLR_112"

PHYCAScaffold_3 DSRXLR CDS 256453 256878 . - . ID=name"RXLR_113"

PHYCAScaffold_65 DSRXLR CDS 135948 136790 . - . ID=name"RXLR_114"

PHYCAScaffold_1 DSRXLR CDS 154552 154764 . + . ID=name"RXLR_115"

PHYCAScaffold_37 DSRXLR CDS 451785 454598 . - . ID=name"RXLR_116"

PHYCAScaffold_7 DSRXLR CDS 608505 609764 . + . ID=name"RXLR_117"

PHYCAScaffold_104 DSRXLR CDS 65629 66234 . - . ID=name"RXLR_118"

PHYCAScaffold_3 DSRXLR CDS 533356 534846 . - . ID=name"RXLR_119"

PHYCAScaffold_2 DSRXLR CDS 1322482 1323174 . + . ID=name"RXLR_120"

PHYCAScaffold_55 DSRXLR CDS 82084 82464 . + . ID=name"RXLR_121"

PHYCAScaffold_81 DSRXLR CDS 103693 104391 . - . ID=name"RXLR_122"

PHYCAScaffold_40 DSRXLR CDS 335532 336290 . - . ID=name"RXLR_123"

PHYCAScaffold_17 DSRXLR CDS 839188 839529 . - . ID=name"RXLR_124"

PHYCAScaffold_11 DSRXLR CDS 396067 396351 . + . ID=name"RXLR_125"

PHYCAScaffold_14 DSRXLR CDS 758513 758863 . + . ID=name"RXLR_126"

PHYCAScaffold_51 DSRXLR CDS 405525 407660 . + . ID=name"RXLR_127"

PHYCAScaffold_2 DSRXLR CDS 705106 706329 . + . ID=name"RXLR_128"

PHYCAScaffold_12 DSRXLR CDS 1116105 1116563 . - . ID=name"RXLR_129"

PHYCAScaffold_7 DSRXLR CDS 865807 866112 . - . ID=name"RXLR_130"

PHYCAScaffold_21 DSRXLR CDS 183799 185793 . - . ID=name"RXLR_131"

PHYCAScaffold_3 DSRXLR CDS 697798 699396 . - . ID=name"RXLR_132"

PHYCAScaffold_38 DSRXLR CDS 467057 468412 . - . ID=name"RXLR_133"

PHYCAScaffold_9 DSRXLR CDS 730927 731655 . - . ID=name"RXLR_134"

PHYCAScaffold_74 DSRXLR CDS 54007 54294 . - . ID=name"RXLR_135"

PHYCAScaffold_102 DSRXLR CDS 85621 86358 . + . ID=name"RXLR_136"

PHYCAScaffold_87 DSRXLR CDS 161140 161775 . + . ID=name"RXLR_137"

PHYCAScaffold_86 DSRXLR CDS 75819 76898 . + . ID=name"RXLR_138"

PHYCAScaffold_12 DSRXLR CDS 706366 706833 . - . ID=name"RXLR_139"

PHYCAScaffold_12 DSRXLR CDS 931251 931553 . + . ID=name"RXLR_140"

PHYCAScaffold_4 DSRXLR CDS 390259 390531 . - . ID=name"RXLR_141"

PHYCAScaffold_37 DSRXLR CDS 498072 498491 . + . ID=name"RXLR_142"

PHYCAScaffold_4 DSRXLR CDS 1141843 1142124 . + . ID=name"RXLR_143"

PHYCAScaffold_46 DSRXLR CDS 234864 235526 . + . ID=name"RXLR_144"

PHYCAScaffold_3 DSRXLR CDS 539108 541129 . + . ID=name"RXLR_145"

PHYCAScaffold_32 DSRXLR CDS 251798 255175 . - . ID=name"RXLR_146"

PHYCAScaffold_15 DSRXLR CDS 801631 802014 . + . ID=name"RXLR_147"

PHYCAScaffold_5 DSRXLR CDS 1108202 1108510 . - . ID=name"RXLR_148"

PHYCAScaffold_1 DSRXLR CDS 491235 491879 . - . ID=name"RXLR_149"

PHYCAScaffold_6 DSRXLR CDS 1116718 1117008 . + . ID=name"RXLR_150"

PHYCAScaffold_17 DSRXLR CDS 94628 95146 . + . ID=name"RXLR_151"

PHYCAScaffold_7 DSRXLR CDS 125582 125848 . + . ID=name"RXLR_152"

PHYCAScaffold_36 DSRXLR CDS 110317 110766 . - . ID=name"RXLR_153"

PHYCAScaffold_90 DSRXLR CDS 118929 119171 . - . ID=name"RXLR_154"

PHYCAScaffold_27 DSRXLR CDS 348452 348694 . - . ID=name"RXLR_155"

PHYCAScaffold_6 DSRXLR CDS 633546 634535 . - . ID=name"RXLR_156"

PHYCAScaffold_105 DSRXLR CDS 38332 40374 . + . ID=name"RXLR_157"

PHYCAScaffold_46 DSRXLR CDS 65100 65543 . - . ID=name"RXLR_158"

PHYCAScaffold_37 DSRXLR CDS 178093 180252 . - . ID=name"RXLR_159"

PHYCAScaffold_34 DSRXLR CDS 450662 455890 . + . ID=name"RXLR_160"

PHYCAScaffold_25 DSRXLR CDS 705132 705512 . + . ID=name"RXLR_161"

PHYCAScaffold_76 DSRXLR CDS 98571 99077 . + . ID=name"RXLR_162"

PHYCAScaffold_11 DSRXLR CDS 295183 297129 . + . ID=name"RXLR_163"

PHYCAScaffold_18 DSRXLR CDS 856163 856591 . - . ID=name"RXLR_164"

PHYCAScaffold_5 DSRXLR CDS 5402 5824 . - . ID=name"RXLR_165"

PHYCAScaffold_26 DSRXLR CDS 109723 110064 . + . ID=name"RXLR_166"

PHYCAScaffold_640 DSRXLR CDS 1810 2082 . - . ID=name"RXLR_167"

PHYCAScaffold_53 DSRXLR CDS 44454 44855 . + . ID=name"RXLR_168"

PHYCAScaffold_121 DSRXLR CDS 50519 50785 . + . ID=name"RXLR_169"

PHYCAScaffold_592 DSRXLR CDS 3266 3478 . + . ID=name"RXLR_170"

PHYCAScaffold_47 DSRXLR CDS 216197 216628 . - . ID=name"RXLR_171"

PHYCAScaffold_8 DSRXLR CDS 1124521 1125948 . - . ID=name"RXLR_172"

PHYCAScaffold_4 DSRXLR CDS 1083030 1083308 . - . ID=name"RXLR_173"

PHYCAScaffold_11 DSRXLR CDS 1063702 1065099 . - . ID=name"RXLR_174"

PHYCAScaffold_35 DSRXLR CDS 413375 415471 . + . ID=name"RXLR_175"

PHYCAScaffold_36 DSRXLR CDS 242708 244201 . + . ID=name"RXLR_176"

PHYCAScaffold_30 DSRXLR CDS 328116 328367 . - . ID=name"RXLR_177"

PHYCAScaffold_4 DSRXLR CDS 1470348 1470599 . - . ID=name"RXLR_178"

PHYCAScaffold_4 DSRXLR CDS 1285842 1286090 . + . ID=name"RXLR_179"

PHYCAScaffold_100 DSRXLR CDS 80285 80593 . - . ID=name"RXLR_180"

PHYCAScaffold_2 DSRXLR CDS 479198 479608 . - . ID=name"RXLR_181"

PHYCAScaffold_5 DSRXLR CDS 844151 845401 . + . ID=name"RXLR_182"

PHYCAScaffold_40 DSRXLR CDS 242698 244503 . + . ID=name"RXLR_183"

PHYCAScaffold_9 DSRXLR CDS 1035173 1035751 . + . ID=name"RXLR_184"

PHYCAScaffold_3 DSRXLR CDS 535599 537218 . - . ID=name"RXLR_185"

PHYCAScaffold_1 DSRXLR CDS 929114 929813 . + . ID=name"RXLR_186"

PHYCAScaffold_18 DSRXLR CDS 788069 788467 . + . ID=name"RXLR_187"

PHYCAScaffold_1 DSRXLR CDS 2010182 2011090 . - . ID=name"RXLR_188"

PHYCAScaffold_2 DSRXLR CDS 1037099 1037365 . + . ID=name"RXLR_189"

PHYCAScaffold_21 DSRXLR CDS 81481 82236 . + . ID=name"RXLR_190"

PHYCAScaffold_25 DSRXLR CDS 771328 771894 . - . ID=name"RXLR_191"

PHYCAScaffold_1 DSRXLR CDS 2027470 2027745 . + . ID=name"RXLR_192"

PHYCAScaffold_37 DSRXLR CDS 104105 104998 . + . ID=name"RXLR_193"

PHYCAScaffold_9 DSRXLR CDS 955046 955810 . + . ID=name"RXLR_194"

PHYCAScaffold_15 DSRXLR CDS 443355 446510 . - . ID=name"RXLR_195"

PHYCAScaffold_82 DSRXLR CDS 118308 118961 . - . ID=name"RXLR_196"

PHYCAScaffold_25 DSRXLR CDS 356900 357550 . + . ID=name"RXLR_197"

PHYCAScaffold_111 DSRXLR CDS 28885 29109 . + . ID=name"RXLR_198"

PHYCAScaffold_111 DSRXLR CDS 74859 75383 . + . ID=name"RXLR_199"

PHYCAScaffold_7 DSRXLR CDS 171968 172378 . - . ID=name"RXLR_200"

PHYCAScaffold_27 DSRXLR CDS 21951 26951 . + . ID=name"RXLR_201"

PHYCAScaffold_41 DSRXLR CDS 223367 223744 . + . ID=name"RXLR_202"

PHYCAScaffold_48 DSRXLR CDS 420624 421199 . + . ID=name"RXLR_203"

PHYCAScaffold_8 DSRXLR CDS 1156246 1160307 . - . ID=name"RXLR_204"

PHYCAScaffold_29 DSRXLR CDS 257568 257807 . + . ID=name"RXLR_205"

PHYCAScaffold_2 DSRXLR CDS 541581 542585 . + . ID=name"RXLR_206"

PHYCAScaffold_1 DSRXLR CDS 439295 439609 . + . ID=name"RXLR_207"

PHYCAScaffold_19 DSRXLR CDS 596651 598480 . - . ID=name"RXLR_208"

PHYCAScaffold_53 DSRXLR CDS 334297 335220 . + . ID=name"RXLR_209"

PHYCAScaffold_46 DSRXLR CDS 254174 254767 . + . ID=name"RXLR_210"

PHYCAScaffold_12 DSRXLR CDS 473192 474175 . - . ID=name"RXLR_211"

PHYCAScaffold_13 DSRXLR CDS 312245 312583 . - . ID=name"RXLR_212"

PHYCAScaffold_42 DSRXLR CDS 486648 487049 . - . ID=name"RXLR_213"

PHYCAScaffold_20 DSRXLR CDS 32885 33142 . + . ID=name"RXLR_214"

PHYCAScaffold_7 DSRXLR CDS 1057776 1058249 . + . ID=name"RXLR_215"

PHYCAScaffold_77 DSRXLR CDS 135242 135538 . - . ID=name"RXLR_216"

PHYCAScaffold_37 DSRXLR CDS 214948 215397 . - . ID=name"RXLR_217"

PHYCAScaffold_57 DSRXLR CDS 56415 57692 . + . ID=name"RXLR_218"

PHYCAScaffold_7 DSRXLR CDS 876213 876800 . - . ID=name"RXLR_219"

PHYCAScaffold_17 DSRXLR CDS 531552 534035 . + . ID=name"RXLR_220"

PHYCAScaffold_65 DSRXLR CDS 121117 121545 . + . ID=name"RXLR_221"

PHYCAScaffold_6 DSRXLR CDS 1201165 1201413 . + . ID=name"RXLR_222"

PHYCAScaffold_104 DSRXLR CDS 102289 102708 . - . ID=name"RXLR_223"

PHYCAScaffold_14 DSRXLR CDS 363216 363869 . + . ID=name"RXLR_224"

PHYCAScaffold_36 DSRXLR CDS 646254 646724 . + . ID=name"RXLR_225"

PHYCAScaffold_21 DSRXLR CDS 494368 497733 . - . ID=name"RXLR_226"

PHYCAScaffold_1 DSRXLR CDS 2052038 2052655 . - . ID=name"RXLR_227"

PHYCAScaffold_21 DSRXLR CDS 523642 525390 . + . ID=name"RXLR_228"

PHYCAScaffold_5 DSRXLR CDS 64716 65867 . - . ID=name"RXLR_229"

PHYCAScaffold_37 DSRXLR CDS 89155 90048 . - . ID=name"RXLR_230"

PHYCAScaffold_10 DSRXLR CDS 432741 433787 . + . ID=name"RXLR_231"

PHYCAScaffold_22 DSRXLR CDS 378423 379244 . - . ID=name"RXLR_232"

PHYCAScaffold_17 DSRXLR CDS 219024 219305 . - . ID=name"RXLR_233"

PHYCAScaffold_26 DSRXLR CDS 335958 336992 . + . ID=name"RXLR_234"

PHYCAScaffold_46 DSRXLR CDS 177459 177860 . - . ID=name"RXLR_235"

PHYCAScaffold_92 DSRXLR CDS 4962 5408 . + . ID=name"RXLR_236"

PHYCAScaffold_10 DSRXLR CDS 320141 320359 . + . ID=name"RXLR_237"

PHYCAScaffold_9 DSRXLR CDS 207320 209557 . + . ID=name"RXLR_238"

PHYCAScaffold_1 DSRXLR CDS 2019607 2020503 . - . ID=name"RXLR_239"

PHYCAScaffold_1 DSRXLR CDS 1152011 1152448 . + . ID=name"RXLR_240"

PHYCAScaffold_99 DSRXLR CDS 138321 138686 . - . ID=name"RXLR_241"

PHYCAScaffold_22 DSRXLR CDS 570874 571125 . + . ID=name"RXLR_242"

PHYCAScaffold_35 DSRXLR CDS 91394 91693 . - . ID=name"RXLR_243"

PHYCAScaffold_1 DSRXLR CDS 2053894 2054235 . + . ID=name"RXLR_244"

PHYCAScaffold_10 DSRXLR CDS 718749 719252 . + . ID=name"RXLR_245"

PHYCAScaffold_42 DSRXLR CDS 400887 404054 . - . ID=name"RXLR_246"

PHYCAScaffold_13 DSRXLR CDS 1026619 1026975 . - . ID=name"RXLR_247"

PHYCAScaffold_14 DSRXLR CDS 602115 603005 . + . ID=name"RXLR_248"

PHYCAScaffold_29 DSRXLR CDS 264023 264430 . + . ID=name"RXLR_249"

PHYCAScaffold_7 DSRXLR CDS 980416 980697 . + . ID=name"RXLR_250"

PHYCAScaffold_5 DSRXLR CDS 1435222 1435731 . + . ID=name"RXLR_251"

PHYCAScaffold_11 DSRXLR CDS 394859 395125 . + . ID=name"RXLR_252"

PHYCAScaffold_444 DSRXLR CDS 3356 4582 . + . ID=name"RXLR_253"

PHYCAScaffold_18 DSRXLR CDS 950501 950884 . + . ID=name"RXLR_254"

PHYCAScaffold_17 DSRXLR CDS 755422 755943 . - . ID=name"RXLR_255"

PHYCAScaffold_32 DSRXLR CDS 131384 133522 . + . ID=name"RXLR_256"

PHYCAScaffold_25 DSRXLR CDS 371593 373725 . - . ID=name"RXLR_257"

PHYCAScaffold_4 DSRXLR CDS 1365629 1366516 . + . ID=name"RXLR_258"

PHYCAScaffold_73 DSRXLR CDS 156733 156981 . - . ID=name"RXLR_259"

PHYCAScaffold_54 DSRXLR CDS 311910 312929 . + . ID=name"RXLR_260"

PHYCAScaffold_7 DSRXLR CDS 354339 354683 . - . ID=name"RXLR_261"

PHYCAScaffold_38 DSRXLR CDS 143402 143995 . - . ID=name"RXLR_262"

PHYCAScaffold_5 DSRXLR CDS 167847 168614 . + . ID=name"RXLR_263"

PHYCAScaffold_13 DSRXLR CDS 972015 973151 . - . ID=name"RXLR_264"

PHYCAScaffold_6 DSRXLR CDS 841379 841633 . + . ID=name"RXLR_265"

PHYCAScaffold_1 DSRXLR CDS 1531955 1532326 . + . ID=name"RXLR_266"

PHYCAScaffold_162 DSRXLR CDS 10216 10527 . + . ID=name"RXLR_267"

PHYCAScaffold_97 DSRXLR CDS 72347 72562 . + . ID=name"RXLR_268"

PHYCAScaffold_51 DSRXLR CDS 313668 314555 . - . ID=name"RXLR_269"

PHYCAScaffold_60 DSRXLR CDS 58248 58499 . - . ID=name"RXLR_270"

PHYCAScaffold_37 DSRXLR CDS 448613 448918 . - . ID=name"RXLR_271"

PHYCAScaffold_9 DSRXLR CDS 769807 778068 . + . ID=name"RXLR_272"

PHYCAScaffold_52 DSRXLR CDS 172152 172571 . - . ID=name"RXLR_273"

PHYCAScaffold_95 DSRXLR CDS 57495 58370 . - . ID=name"RXLR_274"

PHYCAScaffold_9 DSRXLR CDS 752761 753297 . + . ID=name"RXLR_275"

PHYCAScaffold_19 DSRXLR CDS 268222 268443 . - . ID=name"RXLR_276"

PHYCAScaffold_48 DSRXLR CDS 231650 231919 . + . ID=name"RXLR_277"

PHYCAScaffold_6 DSRXLR CDS 128730 129938 . + . ID=name"RXLR_278"

PHYCAScaffold_66 DSRXLR CDS 91682 92188 . + . ID=name"RXLR_279"

PHYCAScaffold_1 DSRXLR CDS 1628297 1628743 . + . ID=name"RXLR_280"

PHYCAScaffold_25 DSRXLR CDS 290208 293318 . + . ID=name"RXLR_281"

PHYCAScaffold_27 DSRXLR CDS 190021 190326 . + . ID=name"RXLR_282"

PHYCAScaffold_2 DSRXLR CDS 316258 316668 . - . ID=name"RXLR_283"

PHYCAScaffold_57 DSRXLR CDS 165135 165380 . + . ID=name"RXLR_284"

PHYCAScaffold_237 DSRXLR CDS 5079 5366 . - . ID=name"RXLR_285"

PHYCAScaffold_73 DSRXLR CDS 194639 194995 . + . ID=name"RXLR_286"

PHYCAScaffold_15 DSRXLR CDS 69023 69595 . + . ID=name"RXLR_287"

PHYCAScaffold_6 DSRXLR CDS 180633 182348 . - . ID=name"RXLR_288"

PHYCAScaffold_7 DSRXLR CDS 1200651 1200869 . + . ID=name"RXLR_289"

PHYCAScaffold_70 DSRXLR CDS 91553 91867 . - . ID=name"RXLR_290"

PHYCAScaffold_48 DSRXLR CDS 69812 70858 . - . ID=name"RXLR_291"

PHYCAScaffold_3 DSRXLR CDS 447447 448238 . - . ID=name"RXLR_292"

PHYCAScaffold_11 DSRXLR CDS 265467 266468 . + . ID=name"RXLR_293"

PHYCAScaffold_15 DSRXLR CDS 873937 874362 . - . ID=name"RXLR_294"

PHYCAScaffold_13 DSRXLR CDS 929397 929690 . + . ID=name"RXLR_295"

PHYCAScaffold_3 DSRXLR CDS 476612 477079 . + . ID=name"RXLR_296"

PHYCAScaffold_10 DSRXLR CDS 151315 151572 . - . ID=name"RXLR_297"

PHYCAScaffold_1 DSRXLR CDS 1959435 1960472 . - . ID=name"RXLR_298"

PHYCAScaffold_41 DSRXLR CDS 133567 136524 . - . ID=name"RXLR_299"

PHYCAScaffold_25 DSRXLR CDS 528104 528502 . + . ID=name"RXLR_300"

PHYCAScaffold_7 DSRXLR CDS 140077 140460 . - . ID=name"RXLR_301"

PHYCAScaffold_2 DSRXLR CDS 191960 192295 . - . ID=name"RXLR_302"

PHYCAScaffold_5 DSRXLR CDS 704414 704839 . - . ID=name"RXLR_303"

PHYCAScaffold_44 DSRXLR CDS 380323 381774 . + . ID=name"RXLR_304"

PHYCAScaffold_1 DSRXLR CDS 1165829 1166266 . + . ID=name"RXLR_305"

PHYCAScaffold_42 DSRXLR CDS 445832 446422 . + . ID=name"RXLR_306"

PHYCAScaffold_47 DSRXLR CDS 266980 267321 . - . ID=name"RXLR_307"

PHYCAScaffold_31 DSRXLR CDS 322357 322941 . + . ID=name"RXLR_308"

PHYCAScaffold_79 DSRXLR CDS 52802 54565 . - . ID=name"RXLR_309"

PHYCAScaffold_3 DSRXLR CDS 531393 532706 . - . ID=name"RXLR_310"

PHYCAScaffold_8 DSRXLR CDS 150384 150710 . - . ID=name"RXLR_311"

PHYCAScaffold_17 DSRXLR CDS 75336 76355 . + . ID=name"RXLR_312"

PHYCAScaffold_3 DSRXLR CDS 1223861 1224076 . + . ID=name"RXLR_313"

PHYCAScaffold_33 DSRXLR CDS 440460 440966 . + . ID=name"RXLR_314"

PHYCAScaffold_6 DSRXLR CDS 613234 615537 . + . ID=name"RXLR_315"

PHYCAScaffold_19 DSRXLR CDS 698053 701541 . + . ID=name"RXLR_316"

PHYCAScaffold_53 DSRXLR CDS 45354 45794 . + . ID=name"RXLR_317"

PHYCAScaffold_101 DSRXLR CDS 51189 51614 . + . ID=name"RXLR_318"

PHYCAScaffold_6 DSRXLR CDS 463977 464804 . - . ID=name"RXLR_319"

PHYCAScaffold_106 DSRXLR CDS 36638 36886 . - . ID=name"RXLR_320"

PHYCAScaffold_494 DSRXLR CDS 745 1578 . + . ID=name"RXLR_321"

PHYCAScaffold_6 DSRXLR CDS 1135732 1135953 . - . ID=name"RXLR_322"

PHYCAScaffold_26 DSRXLR CDS 489888 491075 . + . ID=name"RXLR_323"

PHYCAScaffold_29 DSRXLR CDS 247983 248936 . + . ID=name"RXLR_324"

PHYCAScaffold_6 DSRXLR CDS 1308624 1308920 . - . ID=name"RXLR_325"

PHYCAScaffold_17 DSRXLR CDS 403482 403775 . + . ID=name"RXLR_326"

PHYCAScaffold_14 DSRXLR CDS 891564 892550 . + . ID=name"RXLR_327"

PHYCAScaffold_495 DSRXLR CDS 4033 4467 . - . ID=name"RXLR_328"

PHYCAScaffold_5 DSRXLR CDS 768937 769353 . + . ID=name"RXLR_329"

PHYCAScaffold_50 DSRXLR CDS 316199 316621 . - . ID=name"RXLR_330"

PHYCAScaffold_39 DSRXLR CDS 403827 405947 . - . ID=name"RXLR_331"

PHYCAScaffold_11 DSRXLR CDS 395392 395670 . + . ID=name"RXLR_332"

PHYCAScaffold_1 DSRXLR CDS 535596 535826 . - . ID=name"RXLR_333"

PHYCAScaffold_79 DSRXLR CDS 76013 79453 . - . ID=name"RXLR_334"

PHYCAScaffold_22 DSRXLR CDS 84762 87242 . - . ID=name"RXLR_335"

PHYCAScaffold_36 DSRXLR CDS 499212 500405 . - . ID=name"RXLR_336"

PHYCAScaffold_32 DSRXLR CDS 330137 330724 . + . ID=name"RXLR_337"

PHYCAScaffold_11 DSRXLR CDS 720322 720876 . - . ID=name"RXLR_338"

PHYCAScaffold_81 DSRXLR CDS 63248 64018 . + . ID=name"RXLR_339"

PHYCAScaffold_1 DSRXLR CDS 2049539 2050138 . - . ID=name"RXLR_340"

PHYCAScaffold_2 DSRXLR CDS 155819 156760 . - . ID=name"RXLR_341"

PHYCAScaffold_36 DSRXLR CDS 191571 191981 . - . ID=name"RXLR_342"

PHYCAScaffold_40 DSRXLR CDS 165289 165822 . + . ID=name"RXLR_343"

PHYCAScaffold_100 DSRXLR CDS 25640 26584 . + . ID=name"RXLR_344"

PHYCAScaffold_1 DSRXLR CDS 1673888 1674106 . + . ID=name"RXLR_345"

PHYCAScaffold_77 DSRXLR CDS 77348 77680 . + . ID=name"RXLR_346"

PHYCAScaffold_25 DSRXLR CDS 337072 339201 . - . ID=name"RXLR_347"

PHYCAScaffold_8 DSRXLR CDS 952194 952886 . + . ID=name"RXLR_348"

PHYCAScaffold_29 DSRXLR CDS 537904 538428 . + . ID=name"RXLR_349"

PHYCAScaffold_37 DSRXLR CDS 128309 128578 . - . ID=name"RXLR_350"

PHYCAScaffold_8 DSRXLR CDS 1118960 1123651 . + . ID=name"RXLR_351"

PHYCAScaffold_12 DSRXLR CDS 455256 457640 . + . ID=name"RXLR_352"

PHYCAScaffold_6 DSRXLR CDS 151997 152389 . - . ID=name"RXLR_353"

PHYCAScaffold_25 DSRXLR CDS 607387 607794 . + . ID=name"RXLR_354"

PHYCAScaffold_2 DSRXLR CDS 455597 456496 . - . ID=name"RXLR_355"

PHYCAScaffold_2 DSRXLR CDS 675198 675470 . + . ID=name"RXLR_356"

PHYCAScaffold_25 DSRXLR CDS 574602 574991 . + . ID=name"RXLR_357"

PHYCAScaffold_11 DSRXLR CDS 107696 108046 . - . ID=name"RXLR_358"

PHYCAScaffold_214 DSRXLR CDS 10325 10717 . - . ID=name"RXLR_359"

PHYCAScaffold_7 DSRXLR CDS 1323081 1323536 . - . ID=name"RXLR_360"

PHYCAScaffold_42 DSRXLR CDS 144827 146983 . + . ID=name"RXLR_361"

PHYCAScaffold_83 DSRXLR CDS 92896 93348 . + . ID=name"RXLR_362"

PHYCAScaffold_17 DSRXLR CDS 830340 830729 . + . ID=name"RXLR_363"

PHYCAScaffold_7 DSRXLR CDS 255303 255686 . + . ID=name"RXLR_364"

PHYCAScaffold_10 DSRXLR CDS 424815 425039 . + . ID=name"RXLR_365"

PHYCAScaffold_87 DSRXLR CDS 112320 112583 . + . ID=name"RXLR_366"

PHYCAScaffold_50 DSRXLR CDS 317280 317615 . + . ID=name"RXLR_367"

PHYCAScaffold_9 DSRXLR CDS 418797 419675 . + . ID=name"RXLR_368"

PHYCAScaffold_7 DSRXLR CDS 468940 469299 . - . ID=name"RXLR_369"

PHYCAScaffold_81 DSRXLR CDS 112786 113352 . + . ID=name"RXLR_370"

PHYCAScaffold_21 DSRXLR CDS 129668 137668 . + . ID=name"RXLR_371"

PHYCAScaffold_74 DSRXLR CDS 157008 157532 . + . ID=name"RXLR_372"

PHYCAScaffold_1 DSRXLR CDS 1665831 1668404 . + . ID=name"RXLR_373"

PHYCAScaffold_5 DSRXLR CDS 1367565 1369100 . + . ID=name"RXLR_374"

PHYCAScaffold_6 DSRXLR CDS 1373286 1374137 . + . ID=name"RXLR_375"

PHYCAScaffold_73 DSRXLR CDS 202049 204064 . - . ID=name"RXLR_376"

PHYCAScaffold_5 DSRXLR CDS 1546697 1547119 . + . ID=name"RXLR_377"

PHYCAScaffold_71 DSRXLR CDS 52171 52668 . + . ID=name"RXLR_378"

PHYCAScaffold_31 DSRXLR CDS 633947 634723 . - . ID=name"RXLR_379"

PHYCAScaffold_5 DSRXLR CDS 960759 961346 . + . ID=name"RXLR_380"

PHYCAScaffold_1 DSRXLR CDS 2013153 2016263 . - . ID=name"RXLR_381"

PHYCAScaffold_57 DSRXLR CDS 180136 181104 . - . ID=name"RXLR_382"

PHYCAScaffold_7 DSRXLR CDS 1077508 1077870 . - . ID=name"RXLR_383"

PHYCAScaffold_8 DSRXLR CDS 421213 422073 . - . ID=name"RXLR_384"

PHYCAScaffold_6 DSRXLR CDS 118835 119218 . + . ID=name"RXLR_385"

PHYCAScaffold_47 DSRXLR CDS 344225 344566 . - . ID=name"RXLR_386"

PHYCAScaffold_2 DSRXLR CDS 1435965 1443761 . + . ID=name"RXLR_387"

PHYCAScaffold_24 DSRXLR CDS 190809 191573 . + . ID=name"RXLR_388"

PHYCAScaffold_155 DSRXLR CDS 19091 19480 . - . ID=name"RXLR_389"

PHYCAScaffold_10 DSRXLR CDS 141378 141932 . + . ID=name"RXLR_390"

PHYCAScaffold_52 DSRXLR CDS 268778 269188 . + . ID=name"RXLR_391"

PHYCAScaffold_43 DSRXLR CDS 381859 382140 . + . ID=name"RXLR_392"

PHYCAScaffold_22 DSRXLR CDS 715037 716266 . + . ID=name"RXLR_393"

PHYCAScaffold_27 DSRXLR CDS 195639 198104 . - . ID=name"RXLR_394"

PHYCAScaffold_3 DSRXLR CDS 1404461 1405141 . - . ID=name"RXLR_395"

PHYCAScaffold_62 DSRXLR CDS 270142 270417 . - . ID=name"RXLR_396"

PHYCAScaffold_17 DSRXLR CDS 830393 835510 . - . ID=name"RXLR_397"

PHYCAScaffold_18 DSRXLR CDS 94600 96036 . + . ID=name"RXLR_398"

PHYCAScaffold_16 DSRXLR CDS 456414 456776 . + . ID=name"RXLR_399"

PHYCAScaffold_24 DSRXLR CDS 220066 220437 . + . ID=name"RXLR_400"

PHYCAScaffold_13 DSRXLR CDS 40719 42299 . - . ID=name"RXLR_401"

PHYCAScaffold_25 DSRXLR CDS 581645 582073 . + . ID=name"RXLR_402"

PHYCAScaffold_7 DSRXLR CDS 1095670 1096011 . + . ID=name"RXLR_403"

PHYCAScaffold_18 DSRXLR CDS 869239 871011 . - . ID=name"RXLR_404"

PHYCAScaffold_31 DSRXLR CDS 584263 584586 . + . ID=name"RXLR_405"

PHYCAScaffold_46 DSRXLR CDS 214487 215467 . + . ID=name"RXLR_406"

PHYCAScaffold_22 DSRXLR CDS 239210 239485 . - . ID=name"RXLR_407"

PHYCAScaffold_90 DSRXLR CDS 20149 24063 . + . ID=name"RXLR_408"

PHYCAScaffold_51 DSRXLR CDS 304401 305465 . + . ID=name"RXLR_409"

PHYCAScaffold_37 DSRXLR CDS 25778 26926 . + . ID=name"RXLR_410"

PHYCAScaffold_53 DSRXLR CDS 175264 175482 . + . ID=name"RXLR_411"

PHYCAScaffold_95 DSRXLR CDS 85518 86036 . - . ID=name"RXLR_412"

PHYCAScaffold_29 DSRXLR CDS 501158 502588 . + . ID=name"RXLR_413"

PHYCAScaffold_22 DSRXLR CDS 470726 471247 . + . ID=name"RXLR_414"

PHYCAScaffold_48 DSRXLR CDS 426041 426532 . + . ID=name"RXLR_415"

PHYCAScaffold_8 DSRXLR CDS 155537 156238 . - . ID=name"RXLR_416"

PHYCAScaffold_399 DSRXLR CDS 2819 3337 . - . ID=name"RXLR_417"

PHYCAScaffold_55 DSRXLR CDS 462045 462446 . - . ID=name"RXLR_418"

PHYCAScaffold_9 DSRXLR CDS 1014381 1014806 . - . ID=name"RXLR_419"

PHYCAScaffold_3 DSRXLR CDS 266960 267367 . - . ID=name"RXLR_420"

PHYCAScaffold_84 DSRXLR CDS 97265 97540 . - . ID=name"RXLR_421"

PHYCAScaffold_38 DSRXLR CDS 380578 381003 . + . ID=name"RXLR_422"

PHYCAScaffold_65 DSRXLR CDS 79096 79410 . - . ID=name"RXLR_423"

PHYCAScaffold_10 DSRXLR CDS 827135 827668 . + . ID=name"RXLR_424"

PHYCAScaffold_3 DSRXLR CDS 1044657 1045211 . + . ID=name"RXLR_425"

PHYCAScaffold_2 DSRXLR CDS 1324371 1324862 . + . ID=name"RXLR_426"

PHYCAScaffold_1 DSRXLR CDS 1821926 1822186 . - . ID=name"RXLR_427"

PHYCAScaffold_9 DSRXLR CDS 717213 717629 . - . ID=name"RXLR_428"

PHYCAScaffold_14 DSRXLR CDS 959521 960381 . - . ID=name"RXLR_429"

PHYCAScaffold_11 DSRXLR CDS 831732 834227 . - . ID=name"RXLR_430"

PHYCAScaffold_58 DSRXLR CDS 162409 162747 . + . ID=name"RXLR_431"

PHYCAScaffold_48 DSRXLR CDS 194739 195029 . + . ID=name"RXLR_432"

PHYCAScaffold_33 DSRXLR CDS 260464 263148 . + . ID=name"RXLR_433"

PHYCAScaffold_100 DSRXLR CDS 85441 85713 . + . ID=name"RXLR_434"

PHYCAScaffold_6 DSRXLR CDS 84270 84815 . + . ID=name"RXLR_435"

PHYCAScaffold_62 DSRXLR CDS 42353 42727 . - . ID=name"RXLR_436"

PHYCAScaffold_76 DSRXLR CDS 91716 91937 . + . ID=name"RXLR_437"

PHYCAScaffold_29 DSRXLR CDS 56475 56885 . + . ID=name"RXLR_438"

PHYCAScaffold_51 DSRXLR CDS 246203 246499 . + . ID=name"RXLR_439"

PHYCAScaffold_6 DSRXLR CDS 501553 502341 . - . ID=name"RXLR_440"

PHYCAScaffold_32 DSRXLR CDS 503592 503816 . + . ID=name"RXLR_441"

PHYCAScaffold_52 DSRXLR CDS 166596 166838 . - . ID=name"RXLR_442"

PHYCAScaffold_27 DSRXLR CDS 537016 537813 . - . ID=name"RXLR_443"

PHYCAScaffold_51 DSRXLR CDS 58338 58580 . + . ID=name"RXLR_444"

PHYCAScaffold_12 DSRXLR CDS 28369 29088 . + . ID=name"RXLR_445"

PHYCAScaffold_6 DSRXLR CDS 537553 537828 . + . ID=name"RXLR_446"

PHYCAScaffold_23 DSRXLR CDS 551650 551907 . + . ID=name"RXLR_447"

PHYCAScaffold_8 DSRXLR CDS 769165 769440 . - . ID=name"RXLR_448"

PHYCAScaffold_24 DSRXLR CDS 184601 184981 . + . ID=name"RXLR_449"

PHYCAScaffold_20 DSRXLR CDS 733911 735221 . + . ID=name"RXLR_450"

PHYCAScaffold_53 DSRXLR CDS 365708 366577 . + . ID=name"RXLR_451"

PHYCAScaffold_10 DSRXLR CDS 1178017 1179366 . + . ID=name"RXLR_452"

PHYCAScaffold_17 DSRXLR CDS 59067 59960 . - . ID=name"RXLR_453"

PHYCAScaffold_50 DSRXLR CDS 91856 93757 . + . ID=name"RXLR_454"

PHYCAScaffold_36 DSRXLR CDS 147554 148015 . - . ID=name"RXLR_455"

PHYCAScaffold_132 DSRXLR CDS 14590 14856 . + . ID=name"RXLR_456"

PHYCAScaffold_40 DSRXLR CDS 491708 492706 . + . ID=name"RXLR_457"

PHYCAScaffold_27 DSRXLR CDS 29945 32491 . + . ID=name"RXLR_458"

PHYCAScaffold_13 DSRXLR CDS 29750 30262 . + . ID=name"RXLR_459"

PHYCAScaffold_18 DSRXLR CDS 360391 360765 . - . ID=name"RXLR_460"

PHYCAScaffold_42 DSRXLR CDS 484760 485602 . + . ID=name"RXLR_461"

PHYCAScaffold_24 DSRXLR CDS 496767 497114 . + . ID=name"RXLR_462"

PHYCAScaffold_13 DSRXLR CDS 1023689 1025401 . - . ID=name"RXLR_463"

PHYCAScaffold_73 DSRXLR CDS 151586 152023 . - . ID=name"RXLR_464"

PHYCAScaffold_98 DSRXLR CDS 84649 85095 . + . ID=name"RXLR_465"

PHYCAScaffold_97 DSRXLR CDS 124806 125225 . - . ID=name"RXLR_466"

PHYCAScaffold_26 DSRXLR CDS 478664 482236 . + . ID=name"RXLR_467"

PHYCAScaffold_12 DSRXLR CDS 1113153 1114874 . + . ID=name"RXLR_468"

PHYCAScaffold_17 DSRXLR CDS 697430 697678 . - . ID=name"RXLR_469"

PHYCAScaffold_39 DSRXLR CDS 33074 33397 . - . ID=name"RXLR_470"

PHYCAScaffold_1 DSRXLR CDS 514133 515308 . + . ID=name"RXLR_471"

PHYCAScaffold_1 DSRXLR CDS 319697 320383 . - . ID=name"RXLR_472"

PHYCAScaffold_6 DSRXLR CDS 726276 727157 . - . ID=name"RXLR_473"

PHYCAScaffold_43 DSRXLR CDS 89396 89752 . + . ID=name"RXLR_474"

PHYCAScaffold_5 DSRXLR CDS 1552355 1553926 . - . ID=name"RXLR_475"

PHYCAScaffold_38 DSRXLR CDS 32630 33775 . + . ID=name"RXLR_476"

PHYCAScaffold_4 DSRXLR CDS 501106 503622 . - . ID=name"RXLR_477"

PHYCAScaffold_121 DSRXLR CDS 4022 4696 . - . ID=name"RXLR_478"

PHYCAScaffold_2 DSRXLR CDS 1135174 1136895 . - . ID=name"RXLR_479"

PHYCAScaffold_8 DSRXLR CDS 688533 688883 . - . ID=name"RXLR_480"

PHYCAScaffold_13 DSRXLR CDS 565047 566540 . + . ID=name"RXLR_481"

PHYCAScaffold_16 DSRXLR CDS 713083 719214 . - . ID=name"RXLR_482"

PHYCAScaffold_62 DSRXLR CDS 36477 36698 . + . ID=name"RXLR_483"

PHYCAScaffold_102 DSRXLR CDS 78719 78943 . - . ID=name"RXLR_484"

PHYCAScaffold_57 DSRXLR CDS 217147 217638 . - . ID=name"RXLR_485"

PHYCAScaffold_7 DSRXLR CDS 821872 822168 . - . ID=name"RXLR_486"

PHYCAScaffold_119 DSRXLR CDS 28114 28680 . - . ID=name"RXLR_487"

PHYCAScaffold_1 DSRXLR CDS 77862 78131 . - . ID=name"RXLR_488"

PHYCAScaffold_39 DSRXLR CDS 293501 293779 . + . ID=name"RXLR_489"

PHYCAScaffold_23 DSRXLR CDS 627147 627527 . - . ID=name"RXLR_490"

PHYCAScaffold_10 DSRXLR CDS 708802 709305 . - . ID=name"RXLR_491"

PHYCAScaffold_18 DSRXLR CDS 926495 926719 . + . ID=name"RXLR_492"

PHYCAScaffold_11 DSRXLR CDS 397054 397323 . + . ID=name"RXLR_493"

PHYCAScaffold_12 DSRXLR CDS 705857 706135 . + . ID=name"RXLR_494"

PHYCAScaffold_12 DSRXLR CDS 1110016 1110474 . + . ID=name"RXLR_495"

PHYCAScaffold_4 DSRXLR CDS 1453852 1454454 . + . ID=name"RXLR_496"

PHYCAScaffold_3 DSRXLR CDS 605129 605926 . + . ID=name"RXLR_497"

PHYCAScaffold_23 DSRXLR CDS 521955 522569 . - . ID=name"RXLR_498"

PHYCAScaffold_9 DSRXLR CDS 796209 796430 . + . ID=name"RXLR_499"

PHYCAScaffold_22 DSRXLR CDS 91462 91755 . - . ID=name"RXLR_500"

PHYCAScaffold_10 DSRXLR CDS 880172 882019 . - . ID=name"RXLR_501"

PHYCAScaffold_6 DSRXLR CDS 1350393 1350773 . + . ID=name"RXLR_502"

PHYCAScaffold_6 DSRXLR CDS 542035 542400 . + . ID=name"RXLR_503"

PHYCAScaffold_22 DSRXLR CDS 454513 454779 . - . ID=name"RXLR_504"

PHYCAScaffold_50 DSRXLR CDS 87290 88102 . + . ID=name"RXLR_505"

PHYCAScaffold_46 DSRXLR CDS 209453 210058 . + . ID=name"RXLR_506"

PHYCAScaffold_37 DSRXLR CDS 428027 428245 . + . ID=name"RXLR_507"

PHYCAScaffold_79 DSRXLR CDS 43669 45057 . - . ID=name"RXLR_508"

PHYCAScaffold_5 DSRXLR CDS 750394 750783 . - . ID=name"RXLR_509"

PHYCAScaffold_12 DSRXLR CDS 613377 613961 . - . ID=name"RXLR_510"

PHYCAScaffold_96 DSRXLR CDS 100445 100768 . + . ID=name"RXLR_511"

PHYCAScaffold_475 DSRXLR CDS 1662 2009 . - . ID=name"RXLR_512"

PHYCAScaffold_23 DSRXLR CDS 769043 770062 . - . ID=name"RXLR_513"

PHYCAScaffold_36 DSRXLR CDS 368335 369228 . - . ID=name"RXLR_514"

PHYCAScaffold_71 DSRXLR CDS 101711 102298 . - . ID=name"RXLR_515"

PHYCAScaffold_12 DSRXLR CDS 690845 691072 . + . ID=name"RXLR_516"

PHYCAScaffold_52 DSRXLR CDS 395374 395868 . + . ID=name"RXLR_517"

PHYCAScaffold_30 DSRXLR CDS 37183 37440 . - . ID=name"RXLR_518"

PHYCAScaffold_231 DSRXLR CDS 3841 4155 . - . ID=name"RXLR_519"

PHYCAScaffold_6 DSRXLR CDS 163387 164916 . + . ID=name"RXLR_520"

PHYCAScaffold_73 DSRXLR CDS 102430 103014 . - . ID=name"RXLR_521"

PHYCAScaffold_13 DSRXLR CDS 853862 854305 . - . ID=name"RXLR_522"

PHYCAScaffold_59 DSRXLR CDS 279500 280162 . + . ID=name"RXLR_523"

PHYCAScaffold_8 DSRXLR CDS 377339 377674 . + . ID=name"RXLR_524"

PHYCAScaffold_78 DSRXLR CDS 131597 133222 . + . ID=name"RXLR_525"

PHYCAScaffold_65 DSRXLR CDS 49349 49573 . + . ID=name"RXLR_526"

PHYCAScaffold_91 DSRXLR CDS 104125 105195 . - . ID=name"RXLR_527"

PHYCAScaffold_12 DSRXLR CDS 290845 291342 . + . ID=name"RXLR_528"

PHYCAScaffold_415 DSRXLR CDS 1362 2186 . - . ID=name"RXLR_529"

PHYCAScaffold_7 DSRXLR CDS 1137996 1138208 . - . ID=name"RXLR_530"

PHYCAScaffold_21 DSRXLR CDS 404487 405653 . + . ID=name"RXLR_531"

PHYCAScaffold_5 DSRXLR CDS 856565 858727 . - . ID=name"RXLR_532"

PHYCAScaffold_27 DSRXLR CDS 175006 175719 . + . ID=name"RXLR_533"

PHYCAScaffold_6 DSRXLR CDS 1181875 1183263 . + . ID=name"RXLR_534"

PHYCAScaffold_9 DSRXLR CDS 936797 937450 . + . ID=name"RXLR_535"

PHYCAScaffold_27 DSRXLR CDS 14810 15091 . + . ID=name"RXLR_536"

PHYCAScaffold_33 DSRXLR CDS 464536 467844 . - . ID=name"RXLR_537"

PHYCAScaffold_28 DSRXLR CDS 665930 667885 . + . ID=name"RXLR_538"

PHYCAScaffold_41 DSRXLR CDS 258785 261172 . + . ID=name"RXLR_539"

PHYCAScaffold_9 DSRXLR CDS 1094923 1095459 . + . ID=name"RXLR_540"

PHYCAScaffold_13 DSRXLR CDS 670589 672919 . + . ID=name"RXLR_541"

PHYCAScaffold_8 DSRXLR CDS 872438 872755 . + . ID=name"RXLR_542"

PHYCAScaffold_2 DSRXLR CDS 1373910 1374365 . - . ID=name"RXLR_543"

PHYCAScaffold_49 DSRXLR CDS 499440 501020 . + . ID=name"RXLR_544"

PHYCAScaffold_62 DSRXLR CDS 309422 309775 . + . ID=name"RXLR_545"

PHYCAScaffold_80 DSRXLR CDS 56575 56808 . + . ID=name"RXLR_546"

PHYCAScaffold_24 DSRXLR CDS 522957 523646 . + . ID=name"RXLR_547"

PHYCAScaffold_28 DSRXLR CDS 38681 40645 . + . ID=name"RXLR_548"

PHYCAScaffold_44 DSRXLR CDS 448995 449546 . + . ID=name"RXLR_549"

PHYCAScaffold_80 DSRXLR CDS 73547 73891 . + . ID=name"RXLR_550"

PHYCAScaffold_27 DSRXLR CDS 253740 254012 . + . ID=name"RXLR_551"

PHYCAScaffold_62 DSRXLR CDS 313496 313846 . - . ID=name"RXLR_552"

PHYCAScaffold_5 DSRXLR CDS 1024192 1026156 . + . ID=name"RXLR_553"

PHYCAScaffold_19 DSRXLR CDS 691629 691994 . - . ID=name"RXLR_554"

PHYCAScaffold_80 DSRXLR CDS 54455 54838 . + . ID=name"RXLR_555"

PHYCAScaffold_20 DSRXLR CDS 811560 811940 . + . ID=name"RXLR_556"

PHYCAScaffold_34 DSRXLR CDS 484065 486872 . + . ID=name"RXLR_557"

PHYCAScaffold_12 DSRXLR CDS 237608 239005 . + . ID=name"RXLR_558"

PHYCAScaffold_27 DSRXLR CDS 576991 577242 . + . ID=name"RXLR_559"

PHYCAScaffold_58 DSRXLR CDS 147701 147958 . - . ID=name"RXLR_560"

PHYCAScaffold_1 DSRXLR CDS 796279 797106 . + . ID=name"RXLR_561"

PHYCAScaffold_37 DSRXLR CDS 330165 330533 . - . ID=name"RXLR_562"

PHYCAScaffold_15 DSRXLR CDS 23630 24091 . - . ID=name"RXLR_563"

PHYCAScaffold_5 DSRXLR CDS 132230 136750 . - . ID=name"RXLR_564"

PHYCAScaffold_24 DSRXLR CDS 116131 116685 . - . ID=name"RXLR_565"

PHYCAScaffold_81 DSRXLR CDS 56718 57044 . + . ID=name"RXLR_566"

PHYCAScaffold_22 DSRXLR CDS 98161 99498 . - . ID=name"RXLR_567"

PHYCAScaffold_16 DSRXLR CDS 713763 714302 . - . ID=name"RXLR_568"

PHYCAScaffold_1 DSRXLR CDS 341813 342148 . - . ID=name"RXLR_569"

PHYCAScaffold_3 DSRXLR CDS 1084297 1084599 . + . ID=name"RXLR_570"

PHYCAScaffold_30 DSRXLR CDS 589685 590131 . + . ID=name"RXLR_571"

PHYCAScaffold_5 DSRXLR CDS 663492 663896 . + . ID=name"RXLR_572"

PHYCAScaffold_40 DSRXLR CDS 110202 110480 . + . ID=name"RXLR_573"

PHYCAScaffold_13 DSRXLR CDS 486647 486973 . + . ID=name"RXLR_574"

PHYCAScaffold_1 DSRXLR CDS 2059248 2059589 . + . ID=name"RXLR_575"

PHYCAScaffold_157 DSRXLR CDS 36018 36398 . + . ID=name"RXLR_576"

PHYCAScaffold_95 DSRXLR CDS 8549 8917 . - . ID=name"RXLR_577"

PHYCAScaffold_27 DSRXLR CDS 67505 68644 . - . ID=name"RXLR_578"

PHYCAScaffold_43 DSRXLR CDS 98885 99469 . - . ID=name"RXLR_579"

PHYCAScaffold_117 DSRXLR CDS 49312 51222 . - . ID=name"RXLR_580"

PHYCAScaffold_207 DSRXLR CDS 7004 7372 . + . ID=name"RXLR_581"

PHYCAScaffold_4 DSRXLR CDS 1224629 1224904 . - . ID=name"RXLR_582"

PHYCAScaffold_42 DSRXLR CDS 428965 429489 . - . ID=name"RXLR_583"

PHYCAScaffold_14 DSRXLR CDS 723533 727678 . - . ID=name"RXLR_584"

PHYCAScaffold_623 DSRXLR CDS 1396 2103 . + . ID=name"RXLR_585"

PHYCAScaffold_22 DSRXLR CDS 166813 167070 . + . ID=name"RXLR_586"

PHYCAScaffold_8 DSRXLR CDS 811193 812689 . - . ID=name"RXLR_587"

PHYCAScaffold_14 DSRXLR CDS 775321 775641 . + . ID=name"RXLR_588"

PHYCAScaffold_21 DSRXLR CDS 908122 909801 . + . ID=name"RXLR_589"

PHYCAScaffold_24 DSRXLR CDS 481306 482007 . - . ID=name"RXLR_590"

PHYCAScaffold_42 DSRXLR CDS 392232 392669 . - . ID=name"RXLR_591"

PHYCAScaffold_17 DSRXLR CDS 972551 973963 . - . ID=name"RXLR_592"

PHYCAScaffold_52 DSRXLR CDS 148311 148682 . - . ID=name"RXLR_593"

PHYCAScaffold_44 DSRXLR CDS 527477 527746 . - . ID=name"RXLR_594"

PHYCAScaffold_186 DSRXLR CDS 3824 6349 . - . ID=name"RXLR_595"

PHYCAScaffold_68 DSRXLR CDS 89357 89668 . + . ID=name"RXLR_596"

PHYCAScaffold_35 DSRXLR CDS 171458 172867 . + . ID=name"RXLR_597"

PHYCAScaffold_61 DSRXLR CDS 69700 70194 . + . ID=name"RXLR_598"

PHYCAScaffold_6 DSRXLR CDS 594042 594308 . + . ID=name"RXLR_599"

PHYCAScaffold_132 DSRXLR CDS 29634 30485 . - . ID=name"RXLR_600"

PHYCAScaffold_20 DSRXLR CDS 408914 409243 . - . ID=name"RXLR_601"

PHYCAScaffold_21 DSRXLR CDS 166604 167380 . - . ID=name"RXLR_602"

PHYCAScaffold_63 DSRXLR CDS 63663 63911 . + . ID=name"RXLR_603"

PHYCAScaffold_65 DSRXLR CDS 150452 151720 . - . ID=name"RXLR_604"

PHYCAScaffold_14 DSRXLR CDS 309736 310158 . + . ID=name"RXLR_605"

PHYCAScaffold_37 DSRXLR CDS 229673 230566 . - . ID=name"RXLR_606"

PHYCAScaffold_87 DSRXLR CDS 181751 182179 . - . ID=name"RXLR_607"

PHYCAScaffold_36 DSRXLR CDS 81867 82226 . - . ID=name"RXLR_608"

PHYCAScaffold_71 DSRXLR CDS 98995 99642 . - . ID=name"RXLR_609"

PHYCAScaffold_12 DSRXLR CDS 203926 204261 . + . ID=name"RXLR_610"

PHYCAScaffold_80 DSRXLR CDS 33793 34596 . - . ID=name"RXLR_611"

PHYCAScaffold_46 DSRXLR CDS 408020 408592 . + . ID=name"RXLR_612"

PHYCAScaffold_23 DSRXLR CDS 240115 240387 . - . ID=name"RXLR_613"

PHYCAScaffold_25 DSRXLR CDS 648180 648461 . - . ID=name"RXLR_614"

PHYCAScaffold_21 DSRXLR CDS 113938 119640 . - . ID=name"RXLR_615"

PHYCAScaffold_36 DSRXLR CDS 38163 39578 . - . ID=name"RXLR_616"

PHYCAScaffold_300 DSRXLR CDS 2314 2610 . + . ID=name"RXLR_617"

PHYCAScaffold_16 DSRXLR CDS 499034 499594 . + . ID=name"RXLR_618"

PHYCAScaffold_13 DSRXLR CDS 550284 552866 . - . ID=name"RXLR_619"

PHYCAScaffold_421 DSRXLR CDS 1168 1461 . - . ID=name"RXLR_620"

PHYCAScaffold_211 DSRXLR CDS 6943 7401 . - . ID=name"RXLR_621"

PHYCAScaffold_2 DSRXLR CDS 985135 985404 . - . ID=name"RXLR_622"

PHYCAScaffold_8 DSRXLR CDS 579417 580484 . - . ID=name"RXLR_623"

PHYCAScaffold_50 DSRXLR CDS 452446 452964 . + . ID=name"RXLR_624"

PHYCAScaffold_46 DSRXLR CDS 461468 462502 . + . ID=name"RXLR_625"

PHYCAScaffold_25 DSRXLR CDS 683541 684143 . + . ID=name"RXLR_626"

PHYCAScaffold_18 DSRXLR CDS 953526 958943 . - . ID=name"RXLR_627"

PHYCAScaffold_68 DSRXLR CDS 126115 126525 . - . ID=name"RXLR_628"

PHYCAScaffold_29 DSRXLR CDS 588650 588952 . + . ID=name"RXLR_629"

PHYCAScaffold_85 DSRXLR CDS 164159 164539 . - . ID=name"RXLR_630"

PHYCAScaffold_34 DSRXLR CDS 234354 236336 . - . ID=name"RXLR_631"

PHYCAScaffold_100 DSRXLR CDS 82964 84664 . + . ID=name"RXLR_632"

PHYCAScaffold_1 DSRXLR CDS 1923084 1924382 . + . ID=name"RXLR_633"

PHYCAScaffold_17 DSRXLR CDS 655773 664340 . - . ID=name"RXLR_634"

PHYCAScaffold_5 DSRXLR CDS 110327 110737 . - . ID=name"RXLR_635"

PHYCAScaffold_7 DSRXLR CDS 938487 940319 . - . ID=name"RXLR_636"

PHYCAScaffold_57 DSRXLR CDS 175969 177828 . + . ID=name"RXLR_637"

PHYCAScaffold_29 DSRXLR CDS 374705 375061 . - . ID=name"RXLR_638"

PHYCAScaffold_68 DSRXLR CDS 320566 320928 . + . ID=name"RXLR_639"

PHYCAScaffold_73 DSRXLR CDS 40903 41238 . + . ID=name"RXLR_640"

PHYCAScaffold_52 DSRXLR CDS 183444 184430 . - . ID=name"RXLR_641"

PHYCAScaffold_20 DSRXLR CDS 615716 616936 . + . ID=name"RXLR_642"

PHYCAScaffold_6 DSRXLR CDS 139967 140284 . - . ID=name"RXLR_643"

PHYCAScaffold_73 DSRXLR CDS 222910 223233 . - . ID=name"RXLR_644"

PHYCAScaffold_5 DSRXLR CDS 1474762 1475307 . - . ID=name"RXLR_645"

PHYCAScaffold_4 DSRXLR CDS 572132 578179 . - . ID=name"RXLR_646"

PHYCAScaffold_4 DSRXLR CDS 1305185 1305406 . + . ID=name"RXLR_647"

PHYCAScaffold_4 DSRXLR CDS 260883 264296 . - . ID=name"RXLR_648"

PHYCAScaffold_11 DSRXLR CDS 257536 264279 . + . ID=name"RXLR_649"

PHYCAScaffold_29 DSRXLR CDS 316852 317196 . + . ID=name"RXLR_650"

PHYCAScaffold_23 DSRXLR CDS 259640 261895 . - . ID=name"RXLR_651"

PHYCAScaffold_41 DSRXLR CDS 141714 142079 . + . ID=name"RXLR_652"

PHYCAScaffold_17 DSRXLR CDS 718777 722196 . + . ID=name"RXLR_653"

PHYCAScaffold_68 DSRXLR CDS 83218 83490 . + . ID=name"RXLR_654"

PHYCAScaffold_47 DSRXLR CDS 36962 37627 . - . ID=name"RXLR_655"

PHYCAScaffold_431 DSRXLR CDS 2508 3611 . + . ID=name"RXLR_656"

PHYCAScaffold_34 DSRXLR CDS 39616 40131 . - . ID=name"RXLR_657"

PHYCAScaffold_65 DSRXLR CDS 228747 228980 . + . ID=name"RXLR_658"

PHYCAScaffold_24 DSRXLR CDS 67285 68877 . - . ID=name"RXLR_659"

PHYCAScaffold_37 DSRXLR CDS 92664 93557 . - . ID=name"RXLR_660"

PHYCAScaffold_60 DSRXLR CDS 325161 327677 . + . ID=name"RXLR_661"

PHYCAScaffold_35 DSRXLR CDS 307836 310850 . - . ID=name"RXLR_662"

PHYCAScaffold_15 DSRXLR CDS 798711 799094 . + . ID=name"RXLR_663"

PHYCAScaffold_143 DSRXLR CDS 16576 17007 . - . ID=name"RXLR_664"

PHYCAScaffold_81 DSRXLR CDS 98738 99496 . + . ID=name"RXLR_665"

PHYCAScaffold_18 DSRXLR CDS 145054 145275 . - . ID=name"RXLR_666"

PHYCAScaffold_6 DSRXLR CDS 227786 228052 . - . ID=name"RXLR_667"

PHYCAScaffold_1 DSRXLR CDS 167648 169387 . - . ID=name"RXLR_668"

PHYCAScaffold_12 DSRXLR CDS 126671 126907 . + . ID=name"RXLR_669"

PHYCAScaffold_63 DSRXLR CDS 247632 247889 . - . ID=name"RXLR_670"

PHYCAScaffold_12 DSRXLR CDS 292556 292939 . + . ID=name"RXLR_671"

PHYCAScaffold_7 DSRXLR CDS 1112962 1116021 . - . ID=name"RXLR_672"

PHYCAScaffold_21 DSRXLR CDS 701487 701867 . + . ID=name"RXLR_673"

PHYCAScaffold_1 DSRXLR CDS 834167 834418 . + . ID=name"RXLR_674"

PHYCAScaffold_50 DSRXLR CDS 263364 265616 . + . ID=name"RXLR_675"

PHYCAScaffold_6 DSRXLR CDS 1081102 1081317 . + . ID=name"RXLR_676"

PHYCAScaffold_4 DSRXLR CDS 47981 48463 . - . ID=name"RXLR_677"

PHYCAScaffold_98 DSRXLR CDS 73226 73606 . + . ID=name"RXLR_678"

PHYCAScaffold_193 DSRXLR CDS 10125 10412 . - . ID=name"RXLR_679"

PHYCAScaffold_22 DSRXLR CDS 599790 600269 . + . ID=name"RXLR_680"

PHYCAScaffold_16 DSRXLR CDS 702728 705010 . - . ID=name"RXLR_681"

PHYCAScaffold_36 DSRXLR CDS 113700 114146 . + . ID=name"RXLR_682"

PHYCAScaffold_10 DSRXLR CDS 855301 855792 . - . ID=name"RXLR_683"

PHYCAScaffold_3 DSRXLR CDS 1503291 1503551 . + . ID=name"RXLR_684"

PHYCAScaffold_58 DSRXLR CDS 129396 130055 . - . ID=name"RXLR_685"

PHYCAScaffold_73 DSRXLR CDS 100292 100765 . - . ID=name"RXLR_686"

PHYCAScaffold_3 DSRXLR CDS 499618 499968 . + . ID=name"RXLR_687"

PHYCAScaffold_15 DSRXLR CDS 753396 753734 . + . ID=name"RXLR_688"

PHYCAScaffold_58 DSRXLR CDS 68623 71796 . + . ID=name"RXLR_689"

PHYCAScaffold_1 DSRXLR CDS 1770989 1772236 . + . ID=name"RXLR_690"

PHYCAScaffold_40 DSRXLR CDS 186685 192063 . + . ID=name"RXLR_691"

PHYCAScaffold_13 DSRXLR CDS 354300 354695 . + . ID=name"RXLR_692"

PHYCAScaffold_46 DSRXLR CDS 94053 94766 . - . ID=name"RXLR_693"

PHYCAScaffold_5 DSRXLR CDS 127971 128219 . - . ID=name"RXLR_694"

PHYCAScaffold_26 DSRXLR CDS 129345 129722 . + . ID=name"RXLR_695"

PHYCAScaffold_4 DSRXLR CDS 152485 154848 . + . ID=name"RXLR_696"

PHYCAScaffold_46 DSRXLR CDS 432519 433871 . + . ID=name"RXLR_697"

PHYCAScaffold_31 DSRXLR CDS 453885 454391 . + . ID=name"RXLR_698"

PHYCAScaffold_111 DSRXLR CDS 33350 33661 . - . ID=name"RXLR_699"

PHYCAScaffold_85 DSRXLR CDS 127630 129525 . + . ID=name"RXLR_700"

PHYCAScaffold_23 DSRXLR CDS 191351 191650 . - . ID=name"RXLR_701"

PHYCAScaffold_27 DSRXLR CDS 457337 458884 . + . ID=name"RXLR_702"

PHYCAScaffold_154 DSRXLR CDS 37906 40299 . - . ID=name"RXLR_703"

PHYCAScaffold_2 DSRXLR CDS 389304 390656 . + . ID=name"RXLR_704"

PHYCAScaffold_9 DSRXLR CDS 1012897 1013832 . + . ID=name"RXLR_705"

PHYCAScaffold_49 DSRXLR CDS 97510 97749 . + . ID=name"RXLR_706"

PHYCAScaffold_14 DSRXLR CDS 402047 402331 . + . ID=name"RXLR_707"

PHYCAScaffold_22 DSRXLR CDS 792609 793166 . + . ID=name"RXLR_708"

PHYCAScaffold_170 DSRXLR CDS 26296 26742 . + . ID=name"RXLR_709"

PHYCAScaffold_93 DSRXLR CDS 34460 34861 . + . ID=name"RXLR_710"

PHYCAScaffold_33 DSRXLR CDS 148537 150090 . + . ID=name"RXLR_711"

PHYCAScaffold_40 DSRXLR CDS 431226 431573 . + . ID=name"RXLR_712"

PHYCAScaffold_4 DSRXLR CDS 383970 384212 . - . ID=name"RXLR_713"

PHYCAScaffold_4 DSRXLR CDS 529945 530559 . + . ID=name"RXLR_714"

PHYCAScaffold_20 DSRXLR CDS 283136 283426 . + . ID=name"RXLR_715"

PHYCAScaffold_13 DSRXLR CDS 649574 651946 . - . ID=name"RXLR_716"

PHYCAScaffold_51 DSRXLR CDS 123069 124409 . - . ID=name"RXLR_717"

PHYCAScaffold_66 DSRXLR CDS 64796 65119 . - . ID=name"RXLR_718"

PHYCAScaffold_23 DSRXLR CDS 537260 537472 . + . ID=name"RXLR_719"

PHYCAScaffold_29 DSRXLR CDS 459320 459679 . - . ID=name"RXLR_720"

PHYCAScaffold_100 DSRXLR CDS 9682 10131 . - . ID=name"RXLR_721"

PHYCAScaffold_118 DSRXLR CDS 62148 62753 . - . ID=name"RXLR_722"

PHYCAScaffold_21 DSRXLR CDS 853035 854840 . - . ID=name"RXLR_723"

PHYCAScaffold_2 DSRXLR CDS 339154 339393 . + . ID=name"RXLR_724"

PHYCAScaffold_30 DSRXLR CDS 534647 534901 . - . ID=name"RXLR_725"

PHYCAScaffold_72 DSRXLR CDS 26567 27448 . + . ID=name"RXLR_726"

PHYCAScaffold_11 DSRXLR CDS 590527 590973 . + . ID=name"RXLR_727"

PHYCAScaffold_24 DSRXLR CDS 138930 139262 . - . ID=name"RXLR_728"

PHYCAScaffold_3 DSRXLR CDS 1269189 1269464 . + . ID=name"RXLR_729"

PHYCAScaffold_44 DSRXLR CDS 193992 194327 . + . ID=name"RXLR_730"

PHYCAScaffold_50 DSRXLR CDS 194691 195113 . + . ID=name"RXLR_731"

PHYCAScaffold_20 DSRXLR CDS 713975 714832 . - . ID=name"RXLR_732"

PHYCAScaffold_225 DSRXLR CDS 5283 5636 . - . ID=name"RXLR_733"

PHYCAScaffold_23 DSRXLR CDS 686311 686790 . + . ID=name"RXLR_734"

PHYCAScaffold_30 DSRXLR CDS 38346 39146 . - . ID=name"RXLR_735"

PHYCAScaffold_3 DSRXLR CDS 170214 170963 . + . ID=name"RXLR_736"

PHYCAScaffold_48 DSRXLR CDS 351654 351890 . + . ID=name"RXLR_737"

PHYCAScaffold_52 DSRXLR CDS 440539 440877 . - . ID=name"RXLR_738"

PHYCAScaffold_47 DSRXLR CDS 381599 382078 . + . ID=name"RXLR_739"

PHYCAScaffold_29 DSRXLR CDS 61792 62115 . + . ID=name"RXLR_740"

PHYCAScaffold_7 DSRXLR CDS 908685 909272 . + . ID=name"RXLR_741"

PHYCAScaffold_18 DSRXLR CDS 797545 797790 . + . ID=name"RXLR_742"

PHYCAScaffold_35 DSRXLR CDS 392909 393199 . + . ID=name"RXLR_743"

PHYCAScaffold_78 DSRXLR CDS 179365 179607 . - . ID=name"RXLR_744"

PHYCAScaffold_53 DSRXLR CDS 47292 47729 . + . ID=name"RXLR_745"

PHYCAScaffold_61 DSRXLR CDS 120660 121277 . - . ID=name"RXLR_746"

PHYCAScaffold_2 DSRXLR CDS 1359759 1360379 . - . ID=name"RXLR_747"

PHYCAScaffold_70 DSRXLR CDS 115325 117817 . - . ID=name"RXLR_748"

PHYCAScaffold_1 DSRXLR CDS 2021933 2022799 . + . ID=name"RXLR_749"

PHYCAScaffold_17 DSRXLR CDS 45911 46576 . + . ID=name"RXLR_750"

PHYCAScaffold_7 DSRXLR CDS 823586 823810 . - . ID=name"RXLR_751"

PHYCAScaffold_48 DSRXLR CDS 209587 215499 . + . ID=name"RXLR_752"

PHYCAScaffold_33 DSRXLR CDS 278542 278757 . + . ID=name"RXLR_753"

PHYCAScaffold_1 DSRXLR CDS 67337 68899 . + . ID=name"RXLR_754"

PHYCAScaffold_118 DSRXLR CDS 39134 40318 . + . ID=name"RXLR_755"

PHYCAScaffold_19 DSRXLR CDS 201101 203713 . + . ID=name"RXLR_756"

PHYCAScaffold_41 DSRXLR CDS 214512 215627 . - . ID=name"RXLR_757"

PHYCAScaffold_644 DSRXLR CDS 1643 1963 . + . ID=name"RXLR_758"

PHYCAScaffold_29 DSRXLR CDS 353337 353606 . - . ID=name"RXLR_759"

PHYCAScaffold_53 DSRXLR CDS 307471 309075 . - . ID=name"RXLR_760"

PHYCAScaffold_49 DSRXLR CDS 330805 332148 . - . ID=name"RXLR_761"

PHYCAScaffold_8 DSRXLR CDS 904913 905197 . + . ID=name"RXLR_762"

PHYCAScaffold_11 DSRXLR CDS 426486 426869 . + . ID=name"RXLR_763"

PHYCAScaffold_61 DSRXLR CDS 334755 335081 . - . ID=name"RXLR_764"

PHYCAScaffold_81 DSRXLR CDS 25 402 . - . ID=name"RXLR_765"

PHYCAScaffold_71 DSRXLR CDS 141778 142389 . + . ID=name"RXLR_766"

PHYCAScaffold_52 DSRXLR CDS 436461 436859 . - . ID=name"RXLR_767"

PHYCAScaffold_63 DSRXLR CDS 257258 257782 . - . ID=name"RXLR_768"

PHYCAScaffold_24 DSRXLR CDS 466245 466655 . - . ID=name"RXLR_769"

PHYCAScaffold_66 DSRXLR CDS 109837 110337 . + . ID=name"RXLR_770"

PHYCAScaffold_40 DSRXLR CDS 391599 392018 . - . ID=name"RXLR_771"

PHYCAScaffold_25 DSRXLR CDS 689118 689684 . - . ID=name"RXLR_772"

PHYCAScaffold_107 DSRXLR CDS 92381 92803 . + . ID=name"RXLR_773"

PHYCAScaffold_52 DSRXLR CDS 58586 58882 . - . ID=name"RXLR_774"

PHYCAScaffold_5 DSRXLR CDS 672614 673183 . + . ID=name"RXLR_775"

PHYCAScaffold_2 DSRXLR CDS 1743726 1744520 . + . ID=name"RXLR_776"

PHYCAScaffold_9 DSRXLR CDS 157873 158331 . + . ID=name"RXLR_777"

PHYCAScaffold_15 DSRXLR CDS 606511 606969 . - . ID=name"RXLR_778"

PHYCAScaffold_81 DSRXLR CDS 176252 177679 . - . ID=name"RXLR_779"

PHYCAScaffold_1 DSRXLR CDS 2004389 2004607 . + . ID=name"RXLR_780"

PHYCAScaffold_305 DSRXLR CDS 2507 2773 . + . ID=name"RXLR_781"

PHYCAScaffold_52 DSRXLR CDS 149233 149607 . - . ID=name"RXLR_782"

PHYCAScaffold_5 DSRXLR CDS 893767 894570 . + . ID=name"RXLR_783"

PHYCAScaffold_96 DSRXLR CDS 10737 10952 . + . ID=name"RXLR_784"

PHYCAScaffold_100 DSRXLR CDS 54179 54526 . + . ID=name"RXLR_785"

PHYCAScaffold_61 DSRXLR CDS 229809 230045 . + . ID=name"RXLR_786"

PHYCAScaffold_34 DSRXLR CDS 243775 243990 . + . ID=name"RXLR_787"

PHYCAScaffold_47 DSRXLR CDS 41330 42250 . + . ID=name"RXLR_788"

PHYCAScaffold_27 DSRXLR CDS 686765 687229 . - . ID=name"RXLR_789"

PHYCAScaffold_32 DSRXLR CDS 244593 245015 . + . ID=name"RXLR_790"

PHYCAScaffold_4 DSRXLR CDS 1003059 1005497 . + . ID=name"RXLR_791"

PHYCAScaffold_29 DSRXLR CDS 259530 260222 . + . ID=name"RXLR_792"

PHYCAScaffold_32 DSRXLR CDS 305082 306866 . - . ID=name"RXLR_793"

PHYCAScaffold_27 DSRXLR CDS 266719 267087 . + . ID=name"RXLR_794"

PHYCAScaffold_438 DSRXLR CDS 904 1398 . - . ID=name"RXLR_795"

PHYCAScaffold_32 DSRXLR CDS 489908 490210 . - . ID=name"RXLR_796"

PHYCAScaffold_29 DSRXLR CDS 539609 540103 . + . ID=name"RXLR_797"

PHYCAScaffold_11 DSRXLR CDS 871880 872260 . + . ID=name"RXLR_798"

PHYCAScaffold_39 DSRXLR CDS 485628 485849 . + . ID=name"RXLR_799"

PHYCAScaffold_1 DSRXLR CDS 504573 505334 . - . ID=name"RXLR_800"

PHYCAScaffold_2 DSRXLR CDS 425505 425978 . - . ID=name"RXLR_801"

PHYCAScaffold_98 DSRXLR CDS 689 1987 . + . ID=name"RXLR_802"

PHYCAScaffold_33 DSRXLR CDS 111557 112903 . - . ID=name"RXLR_803"

PHYCAScaffold_31 DSRXLR CDS 421565 422896 . + . ID=name"RXLR_804"

PHYCAScaffold_10 DSRXLR CDS 752474 752974 . + . ID=name"RXLR_805"

PHYCAScaffold_49 DSRXLR CDS 284587 285864 . + . ID=name"RXLR_806"

PHYCAScaffold_83 DSRXLR CDS 138006 138236 . + . ID=name"RXLR_807"

PHYCAScaffold_11 DSRXLR CDS 456141 456377 . + . ID=name"RXLR_808"

PHYCAScaffold_191 DSRXLR CDS 414 707 . - . ID=name"RXLR_809"

PHYCAScaffold_57 DSRXLR CDS 50035 51768 . + . ID=name"RXLR_810"

PHYCAScaffold_62 DSRXLR CDS 189951 198422 . + . ID=name"RXLR_811"

PHYCAScaffold_16 DSRXLR CDS 586868 587305 . - . ID=name"RXLR_812"

PHYCAScaffold_24 DSRXLR CDS 207467 207847 . + . ID=name"RXLR_813"

PHYCAScaffold_32 DSRXLR CDS 248391 249854 . - . ID=name"RXLR_814"

PHYCAScaffold_27 DSRXLR CDS 302431 302877 . + . ID=name"RXLR_815"

PHYCAScaffold_5 DSRXLR CDS 892132 892935 . - . ID=name"RXLR_816"

PHYCAScaffold_41 DSRXLR CDS 334650 337559 . - . ID=name"RXLR_817"

PHYCAScaffold_40 DSRXLR CDS 304009 307125 . - . ID=name"RXLR_818"

PHYCAScaffold_51 DSRXLR CDS 86964 87206 . + . ID=name"RXLR_819"

PHYCAScaffold_8 DSRXLR CDS 524299 524778 . + . ID=name"RXLR_820"

PHYCAScaffold_36 DSRXLR CDS 326614 326832 . - . ID=name"RXLR_821"

PHYCAScaffold_47 DSRXLR CDS 386544 386813 . - . ID=name"RXLR_822"

PHYCAScaffold_49 DSRXLR CDS 352440 352736 . - . ID=name"RXLR_823"

PHYCAScaffold_4 DSRXLR CDS 1495566 1499558 . - . ID=name"RXLR_824"

PHYCAScaffold_81 DSRXLR CDS 121896 123353 . - . ID=name"RXLR_825"

PHYCAScaffold_46 DSRXLR CDS 357612 359504 . - . ID=name"RXLR_826"

PHYCAScaffold_18 DSRXLR CDS 426007 428646 . + . ID=name"RXLR_827"

PHYCAScaffold_37 DSRXLR CDS 110618 110923 . + . ID=name"RXLR_828"

PHYCAScaffold_83 DSRXLR CDS 50154 50396 . - . ID=name"RXLR_829"

PHYCAScaffold_104 DSRXLR CDS 111228 111578 . - . ID=name"RXLR_830"

PHYCAScaffold_16 DSRXLR CDS 446246 448993 . + . ID=name"RXLR_831"

PHYCAScaffold_7 DSRXLR CDS 572430 572711 . - . ID=name"RXLR_832"

PHYCAScaffold_18 DSRXLR CDS 800464 800745 . + . ID=name"RXLR_833"

PHYCAScaffold_1 DSRXLR CDS 1417667 1418146 . - . ID=name"RXLR_834"

PHYCAScaffold_43 DSRXLR CDS 410852 411220 . + . ID=name"RXLR_835"

PHYCAScaffold_53 DSRXLR CDS 293624 293968 . - . ID=name"RXLR_836"

PHYCAScaffold_17 DSRXLR CDS 124154 124603 . - . ID=name"RXLR_837"

PHYCAScaffold_13 DSRXLR CDS 689150 690370 . - . ID=name"RXLR_838"

PHYCAScaffold_1 DSRXLR CDS 1919760 1921748 . - . ID=name"RXLR_839"

PHYCAScaffold_71 DSRXLR CDS 94224 94865 . - . ID=name"RXLR_840"

PHYCAScaffold_18 DSRXLR CDS 860804 861229 . - . ID=name"RXLR_841"

PHYCAScaffold_3 DSRXLR CDS 662698 663237 . + . ID=name"RXLR_842"

PHYCAScaffold_63 DSRXLR CDS 145590 145826 . - . ID=name"RXLR_843"

PHYCAScaffold_81 DSRXLR CDS 100602 101795 . - . ID=name"RXLR_844"

PHYCAScaffold_3 DSRXLR CDS 351635 351859 . + . ID=name"RXLR_845"

PHYCAScaffold_68 DSRXLR CDS 323426 323848 . - . ID=name"RXLR_846"

PHYCAScaffold_26 DSRXLR CDS 469290 471011 . - . ID=name"RXLR_847"

PHYCAScaffold_9 DSRXLR CDS 1010008 1010943 . - . ID=name"RXLR_848"

PHYCAScaffold_7 DSRXLR CDS 355223 355588 . - . ID=name"RXLR_849"

PHYCAScaffold_2 DSRXLR CDS 549735 551720 . + . ID=name"RXLR_850"

PHYCAScaffold_49 DSRXLR CDS 465996 467165 . - . ID=name"RXLR_851"

PHYCAScaffold_77 DSRXLR CDS 139392 139688 . - . ID=name"RXLR_852"

PHYCAScaffold_46 DSRXLR CDS 58557 59000 . - . ID=name"RXLR_853"

PHYCAScaffold_13 DSRXLR CDS 1027831 1028313 . - . ID=name"RXLR_854"

PHYCAScaffold_46 DSRXLR CDS 60926 61369 . - . ID=name"RXLR_855"

PHYCAScaffold_3 DSRXLR CDS 203980 204324 . - . ID=name"RXLR_856"

PHYCAScaffold_2 DSRXLR CDS 486007 486669 . - . ID=name"RXLR_857"

PHYCAScaffold_13 DSRXLR CDS 543477 545432 . - . ID=name"RXLR_858"

PHYCAScaffold_151 DSRXLR CDS 27527 27745 . - . ID=name"RXLR_859"

PHYCAScaffold_16 DSRXLR CDS 994058 994522 . + . ID=name"RXLR_860"

PHYCAScaffold_44 DSRXLR CDS 437982 439175 . - . ID=name"RXLR_861"

PHYCAScaffold_8 DSRXLR CDS 1009613 1012246 . - . ID=name"RXLR_862"

PHYCAScaffold_10 DSRXLR CDS 824233 825318 . + . ID=name"RXLR_863"

PHYCAScaffold_1 DSRXLR CDS 1207674 1209431 . + . ID=name"RXLR_864"

PHYCAScaffold_46 DSRXLR CDS 92165 93607 . + . ID=name"RXLR_865"

PHYCAScaffold_44 DSRXLR CDS 42801 43133 . + . ID=name"RXLR_866"

PHYCAScaffold_32 DSRXLR CDS 547753 549132 . + . ID=name"RXLR_867"

PHYCAScaffold_113 DSRXLR CDS 19206 21374 . + . ID=name"RXLR_868"

PHYCAScaffold_11 DSRXLR CDS 494458 494727 . + . ID=name"RXLR_869"

PHYCAScaffold_1 DSRXLR CDS 519904 520356 . - . ID=name"RXLR_870"

PHYCAScaffold_73 DSRXLR CDS 74975 75337 . + . ID=name"RXLR_871"

PHYCAScaffold_3 DSRXLR CDS 1343872 1344270 . - . ID=name"RXLR_872"

PHYCAScaffold_49 DSRXLR CDS 24582 25361 . + . ID=name"RXLR_873"

PHYCAScaffold_49 DSRXLR CDS 200051 201061 . - . ID=name"RXLR_874"

PHYCAScaffold_16 DSRXLR CDS 611290 611697 . + . ID=name"RXLR_875"

PHYCAScaffold_41 DSRXLR CDS 325128 326303 . + . ID=name"RXLR_876"

PHYCAScaffold_46 DSRXLR CDS 448800 449219 . + . ID=name"RXLR_877"

PHYCAScaffold_22 DSRXLR CDS 579791 580213 . + . ID=name"RXLR_878"

PHYCAScaffold_61 DSRXLR CDS 247267 249033 . + . ID=name"RXLR_879"

PHYCAScaffold_93 DSRXLR CDS 69864 71450 . - . ID=name"RXLR_880"

PHYCAScaffold_35 DSRXLR CDS 488619 499655 . - . ID=name"RXLR_881"

PHYCAScaffold_24 DSRXLR CDS 111767 112891 . + . ID=name"RXLR_882"

PHYCAScaffold_17 DSRXLR CDS 537411 537782 . + . ID=name"RXLR_883"

PHYCAScaffold_35 DSRXLR CDS 143322 143558 . - . ID=name"RXLR_884"

PHYCAScaffold_30 DSRXLR CDS 155538 156443 . - . ID=name"RXLR_885"

PHYCAScaffold_31 DSRXLR CDS 430631 430903 . - . ID=name"RXLR_886"

PHYCAScaffold_296 DSRXLR CDS 188 580 . + . ID=name"RXLR_887"

PHYCAScaffold_6 DSRXLR CDS 1022430 1023941 . - . ID=name"RXLR_888"

PHYCAScaffold_1 DSRXLR CDS 2005249 2006181 . - . ID=name"RXLR_889"

PHYCAScaffold_67 DSRXLR CDS 101730 102038 . - . ID=name"RXLR_890"

PHYCAScaffold_37 DSRXLR CDS 252222 253319 . - . ID=name"RXLR_891"

PHYCAScaffold_6 DSRXLR CDS 284229 284501 . + . ID=name"RXLR_892"

PHYCAScaffold_10 DSRXLR CDS 1065303 1065542 . - . ID=name"RXLR_893"

PHYCAScaffold_2 DSRXLR CDS 1175297 1177102 . - . ID=name"RXLR_894"

PHYCAScaffold_968 DSRXLR CDS 484 741 . + . ID=name"RXLR_895"

PHYCAScaffold_2 DSRXLR CDS 382264 383133 . + . ID=name"RXLR_896"

PHYCAScaffold_17 DSRXLR CDS 342000 342296 . - . ID=name"RXLR_897"

PHYCAScaffold_7 DSRXLR CDS 865395 866750 . + . ID=name"RXLR_898"

PHYCAScaffold_2 DSRXLR CDS 1294169 1294648 . + . ID=name"RXLR_899"

PHYCAScaffold_853 DSRXLR CDS 871 1251 . - . ID=name"RXLR_900"

PHYCAScaffold_47 DSRXLR CDS 34970 35890 . - . ID=name"RXLR_901"

PHYCAScaffold_50 DSRXLR CDS 105140 105541 . - . ID=name"RXLR_902"

PHYCAScaffold_13 DSRXLR CDS 679872 680624 . + . ID=name"RXLR_903"

PHYCAScaffold_8 DSRXLR CDS 1071364 1071600 . + . ID=name"RXLR_904"

PHYCAScaffold_104 DSRXLR CDS 57494 59236 . - . ID=name"RXLR_905"

PHYCAScaffold_11 DSRXLR CDS 235619 237274 . - . ID=name"RXLR_906"

PHYCAScaffold_21 DSRXLR CDS 663329 665083 . - . ID=name"RXLR_907"

PHYCAScaffold_11 DSRXLR CDS 112872 113345 . - . ID=name"RXLR_908"

PHYCAScaffold_19 DSRXLR CDS 624407 624691 . - . ID=name"RXLR_909"

PHYCAScaffold_10 DSRXLR CDS 1052370 1058066 . + . ID=name"RXLR_910"

PHYCAScaffold_28 DSRXLR CDS 363997 364839 . - . ID=name"RXLR_911"

PHYCAScaffold_14 DSRXLR CDS 854200 854583 . - . ID=name"RXLR_912"

PHYCAScaffold_33 DSRXLR CDS 114805 115179 . + . ID=name"RXLR_913"

PHYCAScaffold_28 DSRXLR CDS 333267 333818 . + . ID=name"RXLR_914"

PHYCAScaffold_15 DSRXLR CDS 493084 493365 . - . ID=name"RXLR_915"

PHYCAScaffold_2 DSRXLR CDS 1027828 1028061 . + . ID=name"RXLR_916"

PHYCAScaffold_35 DSRXLR CDS 563307 563564 . + . ID=name"RXLR_917"

PHYCAScaffold_24 DSRXLR CDS 136845 137114 . - . ID=name"RXLR_918"

PHYCAScaffold_44 DSRXLR CDS 487002 487553 . + . ID=name"RXLR_919"

PHYCAScaffold_15 DSRXLR CDS 751336 751674 . + . ID=name"RXLR_920"

PHYCAScaffold_63 DSRXLR CDS 92708 103078 . - . ID=name"RXLR_921"

PHYCAScaffold_5 DSRXLR CDS 800048 800458 . + . ID=name"RXLR_922"

PHYCAScaffold_44 DSRXLR CDS 397996 401847 . + . ID=name"RXLR_923"

PHYCAScaffold_3 DSRXLR CDS 887862 888080 . + . ID=name"RXLR_924"

PHYCAScaffold_81 DSRXLR CDS 45118 46083 . + . ID=name"RXLR_925"

PHYCAScaffold_27 DSRXLR CDS 345186 345422 . - . ID=name"RXLR_926"

PHYCAScaffold_8 DSRXLR CDS 717435 720053 . + . ID=name"RXLR_927"

PHYCAScaffold_63 DSRXLR CDS 23138 23461 . + . ID=name"RXLR_928"

PHYCAScaffold_5 DSRXLR CDS 1437534 1437887 . - . ID=name"RXLR_929"

PHYCAScaffold_2 DSRXLR CDS 521400 521684 . - . ID=name"RXLR_930"

PHYCAScaffold_52 DSRXLR CDS 417467 423493 . - . ID=name"RXLR_931"

PHYCAScaffold_15 DSRXLR CDS 450241 450456 . - . ID=name"RXLR_932"

PHYCAScaffold_5 DSRXLR CDS 209604 209861 . - . ID=name"RXLR_933"

PHYCAScaffold_47 DSRXLR CDS 260340 261614 . - . ID=name"RXLR_934"

PHYCAScaffold_81 DSRXLR CDS 72509 73942 . + . ID=name"RXLR_935"

PHYCAScaffold_50 DSRXLR CDS 16430 17887 . - . ID=name"RXLR_936"

PHYCAScaffold_7 DSRXLR CDS 1315959 1316414 . - . ID=name"RXLR_937"

PHYCAScaffold_5 DSRXLR CDS 716107 718254 . - . ID=name"RXLR_938"

PHYCAScaffold_614 DSRXLR CDS 865 1173 . + . ID=name"RXLR_939"

PHYCAScaffold_2 DSRXLR CDS 615498 616130 . + . ID=name"RXLR_940"

PHYCAScaffold_62 DSRXLR CDS 199515 204329 . + . ID=name"RXLR_941"

PHYCAScaffold_3 DSRXLR CDS 1300914 1303873 . + . ID=name"RXLR_942"

PHYCAScaffold_6 DSRXLR CDS 1024846 1026279 . - . ID=name"RXLR_943"

PHYCAScaffold_93 DSRXLR CDS 72031 79764 . - . ID=name"RXLR_944"

PHYCAScaffold_16 DSRXLR CDS 275266 276477 . + . ID=name"RXLR_945"

PHYCAScaffold_3 DSRXLR CDS 1139517 1139768 . + . ID=name"RXLR_946"

PHYCAScaffold_76 DSRXLR CDS 111278 111553 . + . ID=name"RXLR_947"

PHYCAScaffold_29 DSRXLR CDS 659702 660157 . - . ID=name"RXLR_948"

PHYCAScaffold_42 DSRXLR CDS 346250 349264 . - . ID=name"RXLR_949"

PHYCAScaffold_2 DSRXLR CDS 269480 271204 . + . ID=name"RXLR_950"

PHYCAScaffold_51 DSRXLR CDS 282640 283641 . - . ID=name"RXLR_951"

PHYCAScaffold_36 DSRXLR CDS 578126 578401 . - . ID=name"RXLR_952"

PHYCAScaffold_6 DSRXLR CDS 1203183 1203482 . + . ID=name"RXLR_953"

PHYCAScaffold_11 DSRXLR CDS 968875 969144 . - . ID=name"RXLR_954"

PHYCAScaffold_15 DSRXLR CDS 81971 84916 . - . ID=name"RXLR_955"

PHYCAScaffold_6 DSRXLR CDS 1301592 1307225 . - . ID=name"RXLR_956"

PHYCAScaffold_71 DSRXLR CDS 168204 171374 . - . ID=name"RXLR_957"

PHYCAScaffold_81 DSRXLR CDS 105924 106193 . - . ID=name"RXLR_958"

PHYCAScaffold_21 DSRXLR CDS 328942 333372 . - . ID=name"RXLR_959"

PHYCAScaffold_29 DSRXLR CDS 318752 319168 . + . ID=name"RXLR_960"

PHYCAScaffold_44 DSRXLR CDS 382109 384604 . + . ID=name"RXLR_961"

PHYCAScaffold_11 DSRXLR CDS 742959 744575 . - . ID=name"RXLR_962"

PHYCAScaffold_2 DSRXLR CDS 1780639 1780920 . + . ID=name"RXLR_963"

PHYCAScaffold_22 DSRXLR CDS 75295 75891 . - . ID=name"RXLR_964"

PHYCAScaffold_49 DSRXLR CDS 25487 25798 . - . ID=name"RXLR_965"

PHYCAScaffold_3 DSRXLR CDS 380713 380958 . - . ID=name"RXLR_966"

PHYCAScaffold_52 DSRXLR CDS 136758 138599 . + . ID=name"RXLR_967"

PHYCAScaffold_31 DSRXLR CDS 5650 6465 . + . ID=name"RXLR_968"

PHYCAScaffold_52 DSRXLR CDS 143961 144326 . - . ID=name"RXLR_969"

PHYCAScaffold_104 DSRXLR CDS 66860 67468 . + . ID=name"RXLR_970"

PHYCAScaffold_1 DSRXLR CDS 931242 931868 . + . ID=name"RXLR_971"

PHYCAScaffold_11 DSRXLR CDS 564036 564470 . - . ID=name"RXLR_972"

PHYCAScaffold_10 DSRXLR CDS 688931 689269 . - . ID=name"RXLR_973"

PHYCAScaffold_5 DSRXLR CDS 1476415 1476723 . - . ID=name"RXLR_974"

PHYCAScaffold_2 DSRXLR CDS 674068 674478 . - . ID=name"RXLR_975"

PHYCAScaffold_4 DSRXLR CDS 94149 94379 . + . ID=name"RXLR_976"

PHYCAScaffold_47 DSRXLR CDS 102868 105789 . + . ID=name"RXLR_977"

PHYCAScaffold_6 DSRXLR CDS 1104601 1106184 . + . ID=name"RXLR_978"

PHYCAScaffold_39 DSRXLR CDS 44530 44946 . + . ID=name"RXLR_979"

PHYCAScaffold_1 DSRXLR CDS 1455875 1456456 . - . ID=name"RXLR_980"

PHYCAScaffold_51 DSRXLR CDS 122947 123981 . + . ID=name"RXLR_981"

PHYCAScaffold_2 DSRXLR CDS 958450 959196 . - . ID=name"RXLR_982"

PHYCAScaffold_58 DSRXLR CDS 79137 80780 . + . ID=name"RXLR_983"

PHYCAScaffold_37 DSRXLR CDS 109409 110335 . - . ID=name"RXLR_984"

PHYCAScaffold_25 DSRXLR CDS 316455 316919 . - . ID=name"RXLR_985"

PHYCAScaffold_1 DSRXLR CDS 1267469 1267681 . - . ID=name"RXLR_986"

PHYCAScaffold_72 DSRXLR CDS 46643 46990 . - . ID=name"RXLR_987"

PHYCAScaffold_1 DSRXLR CDS 2008650 2008877 . + . ID=name"RXLR_988"

PHYCAScaffold_17 DSRXLR CDS 236509 238197 . - . ID=name"RXLR_989"

PHYCAScaffold_22 DSRXLR CDS 828410 828955 . - . ID=name"RXLR_990"

PHYCAScaffold_78 DSRXLR CDS 157990 159486 . - . ID=name"RXLR_991"

PHYCAScaffold_87 DSRXLR CDS 54445 54792 . + . ID=name"RXLR_992"

PHYCAScaffold_24 DSRXLR CDS 506798 507097 . + . ID=name"RXLR_993"

PHYCAScaffold_41 DSRXLR CDS 471851 472135 . + . ID=name"RXLR_994"

PHYCAScaffold_2 DSRXLR CDS 289800 290132 . - . ID=name"RXLR_995"

PHYCAScaffold_72 DSRXLR CDS 171049 171288 . + . ID=name"RXLR_996"

PHYCAScaffold_60 DSRXLR CDS 261046 261270 . + . ID=name"RXLR_997"

PHYCAScaffold_3 DSRXLR CDS 509629 513564 . - . ID=name"RXLR_998"

PHYCAScaffold_7 DSRXLR CDS 563912 564364 . + . ID=name"RXLR_999"

PHYCAScaffold_48 DSRXLR CDS 296659 304083 . - . ID=name"RXLR_1000"

PHYCAScaffold_38 DSRXLR CDS 299016 299327 . + . ID=name"RXLR_1001"

PHYCAScaffold_96 DSRXLR CDS 137119 137749 . + . ID=name"RXLR_1002"

PHYCAScaffold_37 DSRXLR CDS 226057 226899 . - . ID=name"RXLR_1003"

PHYCAScaffold_78 DSRXLR CDS 171168 171401 . + . ID=name"RXLR_1004"

PHYCAScaffold_96 DSRXLR CDS 80507 80746 . - . ID=name"RXLR_1005"

PHYCAScaffold_81 DSRXLR CDS 44120 44689 . + . ID=name"RXLR_1006"

PHYCAScaffold_11 DSRXLR CDS 99466 99747 . + . ID=name"RXLR_1007"

PHYCAScaffold_49 DSRXLR CDS 98264 100132 . - . ID=name"RXLR_1008"

PHYCAScaffold_98 DSRXLR CDS 3926 4306 . - . ID=name"RXLR_1009"

PHYCAScaffold_25 DSRXLR CDS 524607 525011 . - . ID=name"RXLR_1010"

PHYCAScaffold_2 DSRXLR CDS 854153 854449 . + . ID=name"RXLR_1011"

PHYCAScaffold_184 DSRXLR CDS 10199 10726 . - . ID=name"RXLR_1012"

PHYCAScaffold_25 DSRXLR CDS 230650 230997 . + . ID=name"RXLR_1013"

PHYCAScaffold_12 DSRXLR CDS 307439 309022 . - . ID=name"RXLR_1014"

PHYCAScaffold_3 DSRXLR CDS 1170492 1170887 . - . ID=name"RXLR_1015"

PHYCAScaffold_38 DSRXLR CDS 453671 454222 . + . ID=name"RXLR_1016"

PHYCAScaffold_95 DSRXLR CDS 88443 89705 . + . ID=name"RXLR_1017"

PHYCAScaffold_77 DSRXLR CDS 107711 108052 . - . ID=name"RXLR_1018"

PHYCAScaffold_2 DSRXLR CDS 1796093 1796770 . + . ID=name"RXLR_1019"

PHYCAScaffold_25 DSRXLR CDS 556556 556954 . + . ID=name"RXLR_1020"

PHYCAScaffold_44 DSRXLR CDS 339704 340381 . + . ID=name"RXLR_1021"

PHYCAScaffold_4 DSRXLR CDS 463963 465624 . - . ID=name"RXLR_1022"

PHYCAScaffold_50 DSRXLR CDS 75104 75439 . - . ID=name"RXLR_1023"

PHYCAScaffold_335 DSRXLR CDS 5757 6074 . + . ID=name"RXLR_1024"

PHYCAScaffold_35 DSRXLR CDS 542903 543199 . - . ID=name"RXLR_1025"

PHYCAScaffold_49 DSRXLR CDS 426088 427068 . - . ID=name"RXLR_1026"

PHYCAScaffold_42 DSRXLR CDS 279826 280128 . - . ID=name"RXLR_1027"

PHYCAScaffold_25 DSRXLR CDS 87545 88864 . - . ID=name"RXLR_1028"

PHYCAScaffold_97 DSRXLR CDS 91291 91980 . - . ID=name"RXLR_1029"

PHYCAScaffold_41 DSRXLR CDS 247229 247612 . + . ID=name"RXLR_1030"

PHYCAScaffold_710 DSRXLR CDS 1126 1734 . + . ID=name"RXLR_1031"

PHYCAScaffold_103 DSRXLR CDS 19456 20064 . + . ID=name"RXLR_1032"

PHYCAScaffold_13 DSRXLR CDS 792473 795268 . - . ID=name"RXLR_1033"

PHYCAScaffold_86 DSRXLR CDS 31504 38790 . - . ID=name"RXLR_1034"

PHYCAScaffold_3 DSRXLR CDS 1412248 1412757 . + . ID=name"RXLR_1035"

PHYCAScaffold_5 DSRXLR CDS 1217837 1218700 . - . ID=name"RXLR_1036"

PHYCAScaffold_16 DSRXLR CDS 478192 479040 . - . ID=name"RXLR_1037"

PHYCAScaffold_3 DSRXLR CDS 269364 270860 . + . ID=name"RXLR_1038"

PHYCAScaffold_8 DSRXLR CDS 222643 228027 . - . ID=name"RXLR_1039"

PHYCAScaffold_28 DSRXLR CDS 637423 637644 . - . ID=name"RXLR_1040"

PHYCAScaffold_70 DSRXLR CDS 242303 242695 . - . ID=name"RXLR_1041"

PHYCAScaffold_71 DSRXLR CDS 95694 96353 . - . ID=name"RXLR_1042"

PHYCAScaffold_85 DSRXLR CDS 89806 93492 . - . ID=name"RXLR_1043"

PHYCAScaffold_30 DSRXLR CDS 139444 141627 . - . ID=name"RXLR_1044"

PHYCAScaffold_81 DSRXLR CDS 149221 150687 . + . ID=name"RXLR_1045"

PHYCAScaffold_2 DSRXLR CDS 286623 287969 . + . ID=name"RXLR_1046"

PHYCAScaffold_10 DSRXLR CDS 439948 440256 . + . ID=name"RXLR_1047"

PHYCAScaffold_636 DSRXLR CDS 1562 1942 . - . ID=name"RXLR_1048"

PHYCAScaffold_71 DSRXLR CDS 193102 193893 . - . ID=name"RXLR_1049"

PHYCAScaffold_20 DSRXLR CDS 432586 433107 . - . ID=name"RXLR_1050"

PHYCAScaffold_38 DSRXLR CDS 352463 353323 . - . ID=name"RXLR_1051"

PHYCAScaffold_35 DSRXLR CDS 443757 444098 . + . ID=name"RXLR_1052"

PHYCAScaffold_18 DSRXLR CDS 542710 543063 . - . ID=name"RXLR_1053"

PHYCAScaffold_1 DSRXLR CDS 1924386 1925672 . - . ID=name"RXLR_1054"

PHYCAScaffold_2 DSRXLR CDS 1020050 1020370 . + . ID=name"RXLR_1055"

PHYCAScaffold_44 DSRXLR CDS 241210 241590 . + . ID=name"RXLR_1056"

PHYCAScaffold_47 DSRXLR CDS 526950 527249 . - . ID=name"RXLR_1057"

PHYCAScaffold_2 DSRXLR CDS 329467 329871 . - . ID=name"RXLR_1058"

PHYCAScaffold_10 DSRXLR CDS 45241 45555 . + . ID=name"RXLR_1059"

PHYCAScaffold_44 DSRXLR CDS 447467 447802 . + . ID=name"RXLR_1060"

PHYCAScaffold_143 DSRXLR CDS 5896 6138 . - . ID=name"RXLR_1061"

PHYCAScaffold_21 DSRXLR CDS 319104 319454 . + . ID=name"RXLR_1062"

PHYCAScaffold_9 DSRXLR CDS 626254 626478 . + . ID=name"RXLR_1063"

PHYCAScaffold_4 DSRXLR CDS 1035146 1035364 . - . ID=name"RXLR_1064"

PHYCAScaffold_44 DSRXLR CDS 243687 244067 . - . ID=name"RXLR_1065"

PHYCAScaffold_31 DSRXLR CDS 110907 111629 . - . ID=name"RXLR_1066"

PHYCAScaffold_2 DSRXLR CDS 592438 592650 . + . ID=name"RXLR_1067"

PHYCAScaffold_6 DSRXLR CDS 1420586 1421032 . - . ID=name"RXLR_1068"

PHYCAScaffold_2 DSRXLR CDS 779335 779568 . + . ID=name"RXLR_1069"

PHYCAScaffold_94 DSRXLR CDS 114157 115503 . + . ID=name"RXLR_1070"

PHYCAScaffold_86 DSRXLR CDS 123016 124227 . - . ID=name"RXLR_1071"

PHYCAScaffold_22 DSRXLR CDS 400935 402659 . - . ID=name"RXLR_1072"

PHYCAScaffold_3 DSRXLR CDS 1485775 1488750 . + . ID=name"RXLR_1073"

PHYCAScaffold_10 DSRXLR CDS 1169151 1169453 . - . ID=name"RXLR_1074"

PHYCAScaffold_54 DSRXLR CDS 68446 68826 . + . ID=name"RXLR_1075"

PHYCAScaffold_4 DSRXLR CDS 125862 126134 . - . ID=name"RXLR_1076"

PHYCAScaffold_9 DSRXLR CDS 218170 218553 . + . ID=name"RXLR_1077"

PHYCAScaffold_153 DSRXLR CDS 16000 16245 . + . ID=name"RXLR_1078"

PHYCAScaffold_11 DSRXLR CDS 1019254 1020036 . - . ID=name"RXLR_1079"

PHYCAScaffold_94 DSRXLR CDS 182681 183256 . + . ID=name"RXLR_1080"

PHYCAScaffold_3 DSRXLR CDS 894078 894299 . - . ID=name"RXLR_1081"

PHYCAScaffold_79 DSRXLR CDS 92569 92814 . + . ID=name"RXLR_1082"

PHYCAScaffold_42 DSRXLR CDS 479232 479456 . + . ID=name"RXLR_1083"

PHYCAScaffold_71 DSRXLR CDS 97428 98075 . + . ID=name"RXLR_1084"

PHYCAScaffold_85 DSRXLR CDS 100722 101459 . - . ID=name"RXLR_1085"

PHYCAScaffold_104 DSRXLR CDS 77235 77927 . + . ID=name"RXLR_1086"

PHYCAScaffold_51 DSRXLR CDS 119061 119924 . - . ID=name"RXLR_1087"

PHYCAScaffold_6 DSRXLR CDS 574411 575112 . - . ID=name"RXLR_1088"

PHYCAScaffold_175 DSRXLR CDS 44938 45261 . + . ID=name"RXLR_1089"

PHYCAScaffold_29 DSRXLR CDS 522768 528287 . + . ID=name"RXLR_1090"

PHYCAScaffold_50 DSRXLR CDS 192379 192801 . - . ID=name"RXLR_1091"

PHYCAScaffold_29 DSRXLR CDS 244659 246365 . - . ID=name"RXLR_1092"

PHYCAScaffold_16 DSRXLR CDS 620562 620846 . - . ID=name"RXLR_1093"

PHYCAScaffold_7 DSRXLR CDS 672110 672391 . + . ID=name"RXLR_1094"

PHYCAScaffold_54 DSRXLR CDS 251342 251671 . + . ID=name"RXLR_1095"

PHYCAScaffold_60 DSRXLR CDS 198150 198482 . + . ID=name"RXLR_1096"

PHYCAScaffold_23 DSRXLR CDS 394728 395180 . + . ID=name"RXLR_1097"

PHYCAScaffold_22 DSRXLR CDS 427887 429266 . - . ID=name"RXLR_1098"

PHYCAScaffold_3 DSRXLR CDS 203880 204515 . + . ID=name"RXLR_1099"

PHYCAScaffold_11 DSRXLR CDS 336939 337175 . - . ID=name"RXLR_1100"

PHYCAScaffold_42 DSRXLR CDS 219990 220430 . - . ID=name"RXLR_1101"

PHYCAScaffold_3 DSRXLR CDS 1376013 1378904 . + . ID=name"RXLR_1102"

PHYCAScaffold_19 DSRXLR CDS 525339 525620 . - . ID=name"RXLR_1103"

PHYCAScaffold_80 DSRXLR CDS 45589 46047 . - . ID=name"RXLR_1104"

PHYCAScaffold_77 DSRXLR CDS 68076 68390 . - . ID=name"RXLR_1105"

PHYCAScaffold_33 DSRXLR CDS 510439 510753 . + . ID=name"RXLR_1106"

PHYCAScaffold_75 DSRXLR CDS 161426 161650 . + . ID=name"RXLR_1107"

PHYCAScaffold_61 DSRXLR CDS 33871 37341 . - . ID=name"RXLR_1108"

PHYCAScaffold_58 DSRXLR CDS 206411 206638 . + . ID=name"RXLR_1109"

PHYCAScaffold_2 DSRXLR CDS 1835404 1835910 . - . ID=name"RXLR_1110"

PHYCAScaffold_60 DSRXLR CDS 102409 103224 . - . ID=name"RXLR_1111"

PHYCAScaffold_18 DSRXLR CDS 810682 810906 . - . ID=name"RXLR_1112"

PHYCAScaffold_1 DSRXLR CDS 795282 795974 . - . ID=name"RXLR_1113"

PHYCAScaffold_32 DSRXLR CDS 3975 4229 . - . ID=name"RXLR_1114"

PHYCAScaffold_5 DSRXLR CDS 669334 669942 . + . ID=name"RXLR_1115"

PHYCAScaffold_46 DSRXLR CDS 400944 401279 . - . ID=name"RXLR_1116"

PHYCAScaffold_13 DSRXLR CDS 982115 985396 . - . ID=name"RXLR_1117"

PHYCAScaffold_24 DSRXLR CDS 158316 158690 . + . ID=name"RXLR_1118"

PHYCAScaffold_80 DSRXLR CDS 22475 22864 . - . ID=name"RXLR_1119"

PHYCAScaffold_46 DSRXLR CDS 402844 403119 . + . ID=name"RXLR_1120"

PHYCAScaffold_47 DSRXLR CDS 232264 232479 . + . ID=name"RXLR_1121"

PHYCAScaffold_7 DSRXLR CDS 569249 569530 . + . ID=name"RXLR_1122"

PHYCAScaffold_25 DSRXLR CDS 459945 460388 . - . ID=name"RXLR_1123"

PHYCAScaffold_55 DSRXLR CDS 58774 59382 . - . ID=name"RXLR_1124"

PHYCAScaffold_47 DSRXLR CDS 43038 44210 . + . ID=name"RXLR_1125"

PHYCAScaffold_12 DSRXLR CDS 1093672 1095585 . - . ID=name"RXLR_1126"

PHYCAScaffold_47 DSRXLR CDS 398527 401088 . - . ID=name"RXLR_1127"

PHYCAScaffold_24 DSRXLR CDS 761670 766400 . - . ID=name"RXLR_1128"

PHYCAScaffold_129 DSRXLR CDS 25815 26162 . - . ID=name"RXLR_1129"

PHYCAScaffold_6 DSRXLR CDS 410370 410873 . + . ID=name"RXLR_1130"

PHYCAScaffold_57 DSRXLR CDS 8325 8654 . - . ID=name"RXLR_1131"

PHYCAScaffold_81 DSRXLR CDS 76609 77481 . + . ID=name"RXLR_1132"

PHYCAScaffold_24 DSRXLR CDS 627009 627587 . - . ID=name"RXLR_1133"

PHYCAScaffold_20 DSRXLR CDS 338320 341118 . + . ID=name"RXLR_1134"

PHYCAScaffold_67 DSRXLR CDS 232580 237610 . - . ID=name"RXLR_1135"

PHYCAScaffold_64 DSRXLR CDS 26717 27610 . - . ID=name"RXLR_1136"

PHYCAScaffold_26 DSRXLR CDS 728333 728956 . - . ID=name"RXLR_1137"

PHYCAScaffold_29 DSRXLR CDS 150553 151962 . - . ID=name"RXLR_1138"

PHYCAScaffold_25 DSRXLR CDS 687391 687729 . - . ID=name"RXLR_1139"

PHYCAScaffold_6 DSRXLR CDS 1310556 1315202 . + . ID=name"RXLR_1140"

PHYCAScaffold_29 DSRXLR CDS 164999 165355 . + . ID=name"RXLR_1141"

PHYCAScaffold_4 DSRXLR CDS 36539 39190 . - . ID=name"RXLR_1142"

PHYCAScaffold_28 DSRXLR CDS 125421 125744 . - . ID=name"RXLR_1143"

PHYCAScaffold_86 DSRXLR CDS 156986 157333 . + . ID=name"RXLR_1144"

PHYCAScaffold_77 DSRXLR CDS 121977 122273 . + . ID=name"RXLR_1145"

PHYCAScaffold_10 DSRXLR CDS 603882 605429 . + . ID=name"RXLR_1146"

PHYCAScaffold_30 DSRXLR CDS 487604 489778 . + . ID=name"RXLR_1147"

PHYCAScaffold_15 DSRXLR CDS 576084 576536 . - . ID=name"RXLR_1148"

PHYCAScaffold_15 DSRXLR CDS 392005 393702 . - . ID=name"RXLR_1149"

PHYCAScaffold_111 DSRXLR CDS 25254 25841 . - . ID=name"RXLR_1150"

PHYCAScaffold_46 DSRXLR CDS 520896 521141 . - . ID=name"RXLR_1151"

PHYCAScaffold_19 DSRXLR CDS 175068 175466 . + . ID=name"RXLR_1152"

PHYCAScaffold_11 DSRXLR CDS 421616 422014 . + . ID=name"RXLR_1153"

PHYCAScaffold_42 DSRXLR CDS 141260 141985 . + . ID=name"RXLR_1154"

PHYCAScaffold_6 DSRXLR CDS 82678 82992 . - . ID=name"RXLR_1155"

PHYCAScaffold_11 DSRXLR CDS 307766 308056 . - . ID=name"RXLR_1156"

PHYCAScaffold_4 DSRXLR CDS 777667 777960 . - . ID=name"RXLR_1157"

PHYCAScaffold_29 DSRXLR CDS 602093 602542 . - . ID=name"RXLR_1158"

PHYCAScaffold_6 DSRXLR CDS 222423 223112 . - . ID=name"RXLR_1159"

PHYCAScaffold_4 DSRXLR CDS 455477 456871 . + . ID=name"RXLR_1160"

PHYCAScaffold_16 DSRXLR CDS 355615 356106 . + . ID=name"RXLR_1161"

PHYCAScaffold_15 DSRXLR CDS 335443 335724 . + . ID=name"RXLR_1162"

PHYCAScaffold_9 DSRXLR CDS 213694 214200 . - . ID=name"RXLR_1163"

PHYCAScaffold_9 DSRXLR CDS 241885 242148 . - . ID=name"RXLR_1164"

PHYCAScaffold_35 DSRXLR CDS 482279 484687 . + . ID=name"RXLR_1165"

PHYCAScaffold_11 DSRXLR CDS 676667 678328 . + . ID=name"RXLR_1166"

PHYCAScaffold_6 DSRXLR CDS 599206 601446 . + . ID=name"RXLR_1167"

PHYCAScaffold_46 DSRXLR CDS 256905 257810 . + . ID=name"RXLR_1168"

PHYCAScaffold_29 DSRXLR CDS 638127 638417 . - . ID=name"RXLR_1169"

PHYCAScaffold_5 DSRXLR CDS 171504 172301 . - . ID=name"RXLR_1170"

PHYCAScaffold_8 DSRXLR CDS 5929 6804 . + . ID=name"RXLR_1171"

PHYCAScaffold_30 DSRXLR CDS 546447 546701 . - . ID=name"RXLR_1172"

PHYCAScaffold_2 DSRXLR CDS 353401 354267 . + . ID=name"RXLR_1173"

PHYCAScaffold_22 DSRXLR CDS 56245 56457 . + . ID=name"RXLR_1174"

PHYCAScaffold_6 DSRXLR CDS 133609 133833 . - . ID=name"RXLR_1175"

PHYCAScaffold_28 DSRXLR CDS 387432 388652 . - . ID=name"RXLR_1176"

PHYCAScaffold_48 DSRXLR CDS 187283 188161 . - . ID=name"RXLR_1177"

PHYCAScaffold_5 DSRXLR CDS 688240 688665 . - . ID=name"RXLR_1178"

PHYCAScaffold_4 DSRXLR CDS 1478023 1478826 . - . ID=name"RXLR_1179"

PHYCAScaffold_22 DSRXLR CDS 189866 191233 . - . ID=name"RXLR_1180"

PHYCAScaffold_22 DSRXLR CDS 511259 511507 . - . ID=name"RXLR_1181"

PHYCAScaffold_11 DSRXLR CDS 762580 762801 . - . ID=name"RXLR_1182"

PHYCAScaffold_13 DSRXLR CDS 536085 538082 . - . ID=name"RXLR_1183"

PHYCAScaffold_360 DSRXLR CDS 1917 2261 . - . ID=name"RXLR_1184"

PHYCAScaffold_443 DSRXLR CDS 3325 3831 . + . ID=name"RXLR_1185"

PHYCAScaffold_61 DSRXLR CDS 227609 227977 . - . ID=name"RXLR_1186"

PHYCAScaffold_7 DSRXLR CDS 856840 859101 . - . ID=name"RXLR_1187"

PHYCAScaffold_25 DSRXLR CDS 577741 578130 . + . ID=name"RXLR_1188"

PHYCAScaffold_12 DSRXLR CDS 350946 351764 . - . ID=name"RXLR_1189"

PHYCAScaffold_12 DSRXLR CDS 868181 868678 . + . ID=name"RXLR_1190"

PHYCAScaffold_50 DSRXLR CDS 138059 138391 . + . ID=name"RXLR_1191"

PHYCAScaffold_10 DSRXLR CDS 838302 838808 . - . ID=name"RXLR_1192"

PHYCAScaffold_47 DSRXLR CDS 486903 487325 . + . ID=name"RXLR_1193"

PHYCAScaffold_2 DSRXLR CDS 91107 91394 . + . ID=name"RXLR_1194"

PHYCAScaffold_3 DSRXLR CDS 212284 212649 . + . ID=name"RXLR_1195"

PHYCAScaffold_10 DSRXLR CDS 339903 341219 . - . ID=name"RXLR_1196"

PHYCAScaffold_48 DSRXLR CDS 260199 260915 . + . ID=name"RXLR_1197"

PHYCAScaffold_49 DSRXLR CDS 120723 121133 . - . ID=name"RXLR_1198"

PHYCAScaffold_47 DSRXLR CDS 434721 434933 . + . ID=name"RXLR_1199"

PHYCAScaffold_41 DSRXLR CDS 508181 508741 . + . ID=name"RXLR_1200"

PHYCAScaffold_18 DSRXLR CDS 801800 802237 . + . ID=name"RXLR_1201"

PHYCAScaffold_35 DSRXLR CDS 165225 165587 . - . ID=name"RXLR_1202"

PHYCAScaffold_25 DSRXLR CDS 448216 448584 . + . ID=name"RXLR_1203"

PHYCAScaffold_9 DSRXLR CDS 843133 843501 . + . ID=name"RXLR_1204"

PHYCAScaffold_18 DSRXLR CDS 847938 848318 . + . ID=name"RXLR_1205"

PHYCAScaffold_35 DSRXLR CDS 549293 549508 . - . ID=name"RXLR_1206"

PHYCAScaffold_27 DSRXLR CDS 260360 260668 . + . ID=name"RXLR_1207"

PHYCAScaffold_13 DSRXLR CDS 290717 291127 . - . ID=name"RXLR_1208"

PHYCAScaffold_17 DSRXLR CDS 568393 568932 . + . ID=name"RXLR_1209"

PHYCAScaffold_228 DSRXLR CDS 6691 7203 . + . ID=name"RXLR_1210"

PHYCAScaffold_47 DSRXLR CDS 328592 329002 . - . ID=name"RXLR_1211"

PHYCAScaffold_18 DSRXLR CDS 625164 625490 . - . ID=name"RXLR_1212"

PHYCAScaffold_3 DSRXLR CDS 1163792 1164310 . + . ID=name"RXLR_1213"

PHYCAScaffold_29 DSRXLR CDS 636357 636893 . + . ID=name"RXLR_1214"

PHYCAScaffold_21 DSRXLR CDS 854938 856191 . + . ID=name"RXLR_1215"

PHYCAScaffold_14 DSRXLR CDS 653961 654353 . - . ID=name"RXLR_1216"

PHYCAScaffold_5 DSRXLR CDS 1358400 1359233 . - . ID=name"RXLR_1217"

PHYCAScaffold_38 DSRXLR CDS 510351 510611 . - . ID=name"RXLR_1218"

PHYCAScaffold_16 DSRXLR CDS 68137 69948 . - . ID=name"RXLR_1219"

PHYCAScaffold_4 DSRXLR CDS 107996 110347 . + . ID=name"RXLR_1220"

PHYCAScaffold_21 DSRXLR CDS 274492 274716 . + . ID=name"RXLR_1221"

PHYCAScaffold_17 DSRXLR CDS 743670 744077 . - . ID=name"RXLR_1222"

PHYCAScaffold_8 DSRXLR CDS 14251 15237 . - . ID=name"RXLR_1223"

PHYCAScaffold_11 DSRXLR CDS 82398 82697 . - . ID=name"RXLR_1224"

PHYCAScaffold_7 DSRXLR CDS 567125 567595 . - . ID=name"RXLR_1225"

PHYCAScaffold_57 DSRXLR CDS 199945 200250 . - . ID=name"RXLR_1226"

PHYCAScaffold_40 DSRXLR CDS 192378 192635 . - . ID=name"RXLR_1227"

PHYCAScaffold_58 DSRXLR CDS 67017 67364 . - . ID=name"RXLR_1228"

PHYCAScaffold_93 DSRXLR CDS 115378 116028 . + . ID=name"RXLR_1229"

PHYCAScaffold_61 DSRXLR CDS 198259 201159 . + . ID=name"RXLR_1230"

PHYCAScaffold_143 DSRXLR CDS 3914 5920 . + . ID=name"RXLR_1231"

PHYCAScaffold_7 DSRXLR CDS 176015 176527 . + . ID=name"RXLR_1232"

PHYCAScaffold_137 DSRXLR CDS 37864 38148 . + . ID=name"RXLR_1233"

PHYCAScaffold_18 DSRXLR CDS 805541 806935 . - . ID=name"RXLR_1234"

PHYCAScaffold_16 DSRXLR CDS 949018 949479 . + . ID=name"RXLR_1235"

PHYCAScaffold_2 DSRXLR CDS 1470268 1470615 . - . ID=name"RXLR_1236"

PHYCAScaffold_33 DSRXLR CDS 490666 491217 . + . ID=name"RXLR_1237"

PHYCAScaffold_3 DSRXLR CDS 1585681 1586028 . - . ID=name"RXLR_1238"

PHYCAScaffold_20 DSRXLR CDS 748052 749260 . - . ID=name"RXLR_1239"

PHYCAScaffold_40 DSRXLR CDS 469143 469508 . - . ID=name"RXLR_1240"

PHYCAScaffold_19 DSRXLR CDS 343005 344756 . + . ID=name"RXLR_1241"

PHYCAScaffold_38 DSRXLR CDS 367447 367740 . - . ID=name"RXLR_1242"

PHYCAScaffold_13 DSRXLR CDS 452756 455830 . - . ID=name"RXLR_1243"

PHYCAScaffold_6 DSRXLR CDS 1188845 1189165 . - . ID=name"RXLR_1244"

PHYCAScaffold_17 DSRXLR CDS 572949 573221 . + . ID=name"RXLR_1245"

PHYCAScaffold_38 DSRXLR CDS 79869 84617 . - . ID=name"RXLR_1246"

PHYCAScaffold_10 DSRXLR CDS 852102 852434 . - . ID=name"RXLR_1247"

PHYCAScaffold_12 DSRXLR CDS 382504 387399 . + . ID=name"RXLR_1248"

PHYCAScaffold_23 DSRXLR CDS 137110 137673 . + . ID=name"RXLR_1249"

PHYCAScaffold_17 DSRXLR CDS 191820 192170 . + . ID=name"RXLR_1250"

PHYCAScaffold_37 DSRXLR CDS 97116 97625 . + . ID=name"RXLR_1251"

PHYCAScaffold_27 DSRXLR CDS 624931 625143 . - . ID=name"RXLR_1252"

PHYCAScaffold_574 DSRXLR CDS 658 990 . - . ID=name"RXLR_1253"

PHYCAScaffold_33 DSRXLR CDS 490759 490995 . - . ID=name"RXLR_1254"

PHYCAScaffold_47 DSRXLR CDS 32319 33491 . - . ID=name"RXLR_1255"

PHYCAScaffold_25 DSRXLR CDS 389012 390313 . - . ID=name"RXLR_1256"

PHYCAScaffold_237 DSRXLR CDS 678 1058 . - . ID=name"RXLR_1257"

PHYCAScaffold_36 DSRXLR CDS 239282 240904 . - . ID=name"RXLR_1258"

PHYCAScaffold_2 DSRXLR CDS 334289 334666 . - . ID=name"RXLR_1259"

PHYCAScaffold_40 DSRXLR CDS 252573 252881 . - . ID=name"RXLR_1260"

PHYCAScaffold_1 DSRXLR CDS 695995 696213 . + . ID=name"RXLR_1261"

PHYCAScaffold_53 DSRXLR CDS 300941 302506 . + . ID=name"RXLR_1262"

PHYCAScaffold_27 DSRXLR CDS 492845 500449 . + . ID=name"RXLR_1263"

PHYCAScaffold_2 DSRXLR CDS 355209 355649 . + . ID=name"RXLR_1264"

PHYCAScaffold_76 DSRXLR CDS 72434 73891 . + . ID=name"RXLR_1265"

PHYCAScaffold_81 DSRXLR CDS 116241 117638 . + . ID=name"RXLR_1266"

PHYCAScaffold_6 DSRXLR CDS 130366 132063 . - . ID=name"RXLR_1267"

PHYCAScaffold_29 DSRXLR CDS 240323 240637 . + . ID=name"RXLR_1268"

PHYCAScaffold_16 DSRXLR CDS 188371 190479 . + . ID=name"RXLR_1269"

PHYCAScaffold_8 DSRXLR CDS 1127986 1128318 . + . ID=name"RXLR_1270"

PHYCAScaffold_57 DSRXLR CDS 130423 131106 . - . ID=name"RXLR_1271"

PHYCAScaffold_86 DSRXLR CDS 30292 30588 . - . ID=name"RXLR_1272"

PHYCAScaffold_44 DSRXLR CDS 249911 250405 . + . ID=name"RXLR_1273"

PHYCAScaffold_29 DSRXLR CDS 676642 679875 . + . ID=name"RXLR_1274"

PHYCAScaffold_93 DSRXLR CDS 45450 46289 . + . ID=name"RXLR_1275"

PHYCAScaffold_92 DSRXLR CDS 40172 41473 . + . ID=name"RXLR_1276"

PHYCAScaffold_58 DSRXLR CDS 113087 113701 . - . ID=name"RXLR_1277"

PHYCAScaffold_41 DSRXLR CDS 307646 307906 . + . ID=name"RXLR_1278"

PHYCAScaffold_60 DSRXLR CDS 70730 71137 . - . ID=name"RXLR_1279"

PHYCAScaffold_9 DSRXLR CDS 1075088 1075330 . + . ID=name"RXLR_1280"

PHYCAScaffold_42 DSRXLR CDS 349378 352032 . - . ID=name"RXLR_1281"

PHYCAScaffold_40 DSRXLR CDS 171857 172390 . - . ID=name"RXLR_1282"

PHYCAScaffold_13 DSRXLR CDS 903222 903623 . - . ID=name"RXLR_1283"

PHYCAScaffold_79 DSRXLR CDS 18060 18554 . - . ID=name"RXLR_1284"

PHYCAScaffold_25 DSRXLR CDS 406574 406837 . + . ID=name"RXLR_1285"

PHYCAScaffold_23 DSRXLR CDS 63574 65586 . - . ID=name"RXLR_1286"

PHYCAScaffold_5 DSRXLR CDS 480457 481200 . - . ID=name"RXLR_1287"

PHYCAScaffold_66 DSRXLR CDS 269867 270487 . + . ID=name"RXLR_1288"

PHYCAScaffold_2 DSRXLR CDS 627391 627606 . + . ID=name"RXLR_1289"

PHYCAScaffold_16 DSRXLR CDS 861507 861743 . - . ID=name"RXLR_1290"

PHYCAScaffold_116 DSRXLR CDS 84709 85488 . + . ID=name"RXLR_1291"

PHYCAScaffold_14 DSRXLR CDS 612475 612960 . - . ID=name"RXLR_1292"

PHYCAScaffold_20 DSRXLR CDS 108931 109383 . + . ID=name"RXLR_1293"

PHYCAScaffold_1 DSRXLR CDS 1737035 1737262 . - . ID=name"RXLR_1294"

PHYCAScaffold_13 DSRXLR CDS 914080 914451 . + . ID=name"RXLR_1295"

PHYCAScaffold_24 DSRXLR CDS 281451 281741 . + . ID=name"RXLR_1296"

PHYCAScaffold_53 DSRXLR CDS 97352 97657 . + . ID=name"RXLR_1297"

PHYCAScaffold_89 DSRXLR CDS 79407 79856 . + . ID=name"RXLR_1298"

PHYCAScaffold_107 DSRXLR CDS 56377 57189 . + . ID=name"RXLR_1299"

PHYCAScaffold_142 DSRXLR CDS 2427 2708 . - . ID=name"RXLR_1300"

PHYCAScaffold_54 DSRXLR CDS 7127 7363 . - . ID=name"RXLR_1301"

PHYCAScaffold_46 DSRXLR CDS 518515 518754 . - . ID=name"RXLR_1302"

PHYCAScaffold_14 DSRXLR CDS 1020015 1021322 . - . ID=name"RXLR_1303"

PHYCAScaffold_1 DSRXLR CDS 1363689 1363916 . + . ID=name"RXLR_1304"

PHYCAScaffold_67 DSRXLR CDS 230645 230917 . + . ID=name"RXLR_1305"

PHYCAScaffold_325 DSRXLR CDS 2058 2351 . + . ID=name"RXLR_1306"

PHYCAScaffold_18 DSRXLR CDS 356564 356779 . + . ID=name"RXLR_1307"

PHYCAScaffold_5 DSRXLR CDS 1540177 1540488 . + . ID=name"RXLR_1308"

PHYCAScaffold_104 DSRXLR CDS 81501 82217 . + . ID=name"RXLR_1309"

PHYCAScaffold_8 DSRXLR CDS 325877 326851 . - . ID=name"RXLR_1310"

PHYCAScaffold_16 DSRXLR CDS 588275 588514 . + . ID=name"RXLR_1311"

PHYCAScaffold_29 DSRXLR CDS 547987 552303 . - . ID=name"RXLR_1312"

PHYCAScaffold_405 DSRXLR CDS 1114 1545 . + . ID=name"RXLR_1313"

PHYCAScaffold_117 DSRXLR CDS 44039 44320 . + . ID=name"RXLR_1314"

PHYCAScaffold_49 DSRXLR CDS 205259 205489 . + . ID=name"RXLR_1315"

PHYCAScaffold_24 DSRXLR CDS 754199 754450 . - . ID=name"RXLR_1316"

PHYCAScaffold_51 DSRXLR CDS 412795 413199 . - . ID=name"RXLR_1317"

PHYCAScaffold_118 DSRXLR CDS 46687 47208 . + . ID=name"RXLR_1318"

PHYCAScaffold_7 DSRXLR CDS 1012698 1014245 . - . ID=name"RXLR_1319"

PHYCAScaffold_6 DSRXLR CDS 1101811 1103256 . + . ID=name"RXLR_1320"

PHYCAScaffold_11 DSRXLR CDS 92822 93136 . - . ID=name"RXLR_1321"

PHYCAScaffold_7 DSRXLR CDS 1199778 1200041 . + . ID=name"RXLR_1322"

PHYCAScaffold_1 DSRXLR CDS 771928 772677 . - . ID=name"RXLR_1323"

PHYCAScaffold_3 DSRXLR CDS 824013 824288 . - . ID=name"RXLR_1324"

PHYCAScaffold_326 DSRXLR CDS 8106 8525 . + . ID=name"RXLR_1325"

PHYCAScaffold_686 DSRXLR CDS 1 755 . - . ID=name"RXLR_1326"

PHYCAScaffold_32 DSRXLR CDS 393625 393870 . + . ID=name"RXLR_1327"

PHYCAScaffold_30 DSRXLR CDS 635624 635899 . - . ID=name"RXLR_1328"

PHYCAScaffold_54 DSRXLR CDS 53190 53495 . - . ID=name"RXLR_1329"

PHYCAScaffold_43 DSRXLR CDS 56581 57582 . + . ID=name"RXLR_1330"

PHYCAScaffold_13 DSRXLR CDS 399908 400468 . + . ID=name"RXLR_1331"

PHYCAScaffold_9 DSRXLR CDS 960513 963197 . + . ID=name"RXLR_1332"

PHYCAScaffold_33 DSRXLR CDS 311693 312625 . + . ID=name"RXLR_1333"

PHYCAScaffold_11 DSRXLR CDS 105930 106256 . - . ID=name"RXLR_1334"

PHYCAScaffold_53 DSRXLR CDS 281793 282050 . - . ID=name"RXLR_1335"

PHYCAScaffold_50 DSRXLR CDS 21816 23822 . + . ID=name"RXLR_1336"

PHYCAScaffold_78 DSRXLR CDS 32737 33099 . + . ID=name"RXLR_1337"

PHYCAScaffold_2 DSRXLR CDS 1461558 1461905 . - . ID=name"RXLR_1338"

PHYCAScaffold_97 DSRXLR CDS 100933 101193 . - . ID=name"RXLR_1339"

PHYCAScaffold_12 DSRXLR CDS 1029334 1029573 . + . ID=name"RXLR_1340"

PHYCAScaffold_27 DSRXLR CDS 239182 245970 . + . ID=name"RXLR_1341"

PHYCAScaffold_42 DSRXLR CDS 56231 57184 . - . ID=name"RXLR_1342"

PHYCAScaffold_6 DSRXLR CDS 1377688 1377924 . - . ID=name"RXLR_1343"

PHYCAScaffold_10 DSRXLR CDS 701633 702136 . - . ID=name"RXLR_1344"

PHYCAScaffold_24 DSRXLR CDS 103644 107426 . - . ID=name"RXLR_1345"

PHYCAScaffold_30 DSRXLR CDS 72955 74037 . + . ID=name"RXLR_1346"

PHYCAScaffold_31 DSRXLR CDS 264353 264817 . + . ID=name"RXLR_1347"

PHYCAScaffold_29 DSRXLR CDS 493530 493787 . + . ID=name"RXLR_1348"

PHYCAScaffold_13 DSRXLR CDS 489695 492583 . + . ID=name"RXLR_1349"

PHYCAScaffold_10 DSRXLR CDS 1095725 1097626 . + . ID=name"RXLR_1350"

PHYCAScaffold_28 DSRXLR CDS 313522 314814 . + . ID=name"RXLR_1351"

PHYCAScaffold_118 DSRXLR CDS 42160 42483 . + . ID=name"RXLR_1352"

PHYCAScaffold_7 DSRXLR CDS 1334650 1335105 . - . ID=name"RXLR_1353"

PHYCAScaffold_34 DSRXLR CDS 615670 615999 . - . ID=name"RXLR_1354"

PHYCAScaffold_7 DSRXLR CDS 430797 431207 . + . ID=name"RXLR_1355"

PHYCAScaffold_31 DSRXLR CDS 615963 616187 . + . ID=name"RXLR_1356"

PHYCAScaffold_16 DSRXLR CDS 937511 937906 . + . ID=name"RXLR_1357"

PHYCAScaffold_67 DSRXLR CDS 128571 130565 . + . ID=name"RXLR_1358"

PHYCAScaffold_117 DSRXLR CDS 28155 28775 . + . ID=name"RXLR_1359"

PHYCAScaffold_3 DSRXLR CDS 1589611 1589958 . + . ID=name"RXLR_1360"

PHYCAScaffold_7 DSRXLR CDS 1367395 1367763 . - . ID=name"RXLR_1361"

PHYCAScaffold_36 DSRXLR CDS 149330 149566 . - . ID=name"RXLR_1362"

PHYCAScaffold_3 DSRXLR CDS 271054 271413 . + . ID=name"RXLR_1363"

PHYCAScaffold_7 DSRXLR CDS 175343 175645 . + . ID=name"RXLR_1364"

PHYCAScaffold_440 DSRXLR CDS 4092 4340 . + . ID=name"RXLR_1365"

PHYCAScaffold_26 DSRXLR CDS 304295 304558 . - . ID=name"RXLR_1366"

PHYCAScaffold_50 DSRXLR CDS 443486 443755 . - . ID=name"RXLR_1367"

PHYCAScaffold_604 DSRXLR CDS 956 1282 . + . ID=name"RXLR_1368"

PHYCAScaffold_33 DSRXLR CDS 517688 517969 . - . ID=name"RXLR_1369"

PHYCAScaffold_18 DSRXLR CDS 804195 804716 . + . ID=name"RXLR_1370"

PHYCAScaffold_24 DSRXLR CDS 255872 256126 . + . ID=name"RXLR_1371"

PHYCAScaffold_12 DSRXLR CDS 355479 356018 . + . ID=name"RXLR_1372"

PHYCAScaffold_2 DSRXLR CDS 1229449 1229919 . - . ID=name"RXLR_1373"

PHYCAScaffold_375 DSRXLR CDS 4259 4843 . - . ID=name"RXLR_1374"

PHYCAScaffold_12 DSRXLR CDS 645908 646435 . - . ID=name"RXLR_1375"

PHYCAScaffold_104 DSRXLR CDS 74277 75014 . - . ID=name"RXLR_1376"

PHYCAScaffold_50 DSRXLR CDS 188669 189022 . - . ID=name"RXLR_1377"

PHYCAScaffold_143 DSRXLR CDS 17747 18172 . - . ID=name"RXLR_1378"

PHYCAScaffold_19 DSRXLR CDS 769575 770075 . - . ID=name"RXLR_1379"

PHYCAScaffold_42 DSRXLR CDS 331001 331216 . + . ID=name"RXLR_1380"

PHYCAScaffold_47 DSRXLR CDS 93561 96044 . - . ID=name"RXLR_1381"

PHYCAScaffold_90 DSRXLR CDS 105965 106444 . + . ID=name"RXLR_1382"

PHYCAScaffold_30 DSRXLR CDS 147269 147496 . + . ID=name"RXLR_1383"

PHYCAScaffold_3 DSRXLR CDS 467379 468401 . - . ID=name"RXLR_1384"

PHYCAScaffold_27 DSRXLR CDS 34076 34912 . + . ID=name"RXLR_1385"

PHYCAScaffold_77 DSRXLR CDS 79448 81505 . - . ID=name"RXLR_1386"

PHYCAScaffold_55 DSRXLR CDS 151363 152856 . - . ID=name"RXLR_1387"

PHYCAScaffold_1 DSRXLR CDS 765315 767981 . - . ID=name"RXLR_1388"

PHYCAScaffold_3 DSRXLR CDS 620563 620775 . - . ID=name"RXLR_1389"

PHYCAScaffold_568 DSRXLR CDS 1566 1967 . - . ID=name"RXLR_1390"

PHYCAScaffold_50 DSRXLR CDS 157076 159088 . - . ID=name"RXLR_1391"

PHYCAScaffold_104 DSRXLR CDS 78501 79283 . - . ID=name"RXLR_1392"

PHYCAScaffold_6 DSRXLR CDS 598688 598957 . + . ID=name"RXLR_1393"

PHYCAScaffold_11 DSRXLR CDS 1069818 1070279 . - . ID=name"RXLR_1394"

PHYCAScaffold_16 DSRXLR CDS 991473 991931 . + . ID=name"RXLR_1395"

PHYCAScaffold_269 DSRXLR CDS 5054 5290 . - . ID=name"RXLR_1396"

PHYCAScaffold_27 DSRXLR CDS 279091 279444 . - . ID=name"RXLR_1397"

PHYCAScaffold_6 DSRXLR CDS 1335436 1337289 . - . ID=name"RXLR_1398"

PHYCAScaffold_100 DSRXLR CDS 86398 86766 . - . ID=name"RXLR_1399"

PHYCAScaffold_63 DSRXLR CDS 155664 156368 . + . ID=name"RXLR_1400"

PHYCAScaffold_125 DSRXLR CDS 10083 11117 . - . ID=name"RXLR_1401"

PHYCAScaffold_11 DSRXLR CDS 39683 40162 . + . ID=name"RXLR_1402"

PHYCAScaffold_138 DSRXLR CDS 15417 15878 . - . ID=name"RXLR_1403"

PHYCAScaffold_43 DSRXLR CDS 297060 297989 . - . ID=name"RXLR_1404"

PHYCAScaffold_66 DSRXLR CDS 268601 269221 . - . ID=name"RXLR_1405"

PHYCAScaffold_8 DSRXLR CDS 1088237 1088740 . + . ID=name"RXLR_1406"

PHYCAScaffold_5 DSRXLR CDS 1415526 1416431 . + . ID=name"RXLR_1407"

PHYCAScaffold_462 DSRXLR CDS 2064 2483 . + . ID=name"RXLR_1408"

PHYCAScaffold_13 DSRXLR CDS 1009245 1011677 . + . ID=name"RXLR_1409"

PHYCAScaffold_4 DSRXLR CDS 513051 515162 . + . ID=name"RXLR_1410"

PHYCAScaffold_8 DSRXLR CDS 330523 330747 . + . ID=name"RXLR_1411"

PHYCAScaffold_9 DSRXLR CDS 952865 953701 . - . ID=name"RXLR_1412"

PHYCAScaffold_51 DSRXLR CDS 51396 51836 . + . ID=name"RXLR_1413"

PHYCAScaffold_35 DSRXLR CDS 108550 108999 . - . ID=name"RXLR_1414"

PHYCAScaffold_42 DSRXLR CDS 164154 165233 . + . ID=name"RXLR_1415"

PHYCAScaffold_15 DSRXLR CDS 350966 351373 . + . ID=name"RXLR_1416"

PHYCAScaffold_19 DSRXLR CDS 804574 805071 . - . ID=name"RXLR_1417"

PHYCAScaffold_20 DSRXLR CDS 781901 782362 . + . ID=name"RXLR_1418"

PHYCAScaffold_9 DSRXLR CDS 330893 331126 . + . ID=name"RXLR_1419"

PHYCAScaffold_16 DSRXLR CDS 358140 358418 . + . ID=name"RXLR_1420"

PHYCAScaffold_3 DSRXLR CDS 704701 705171 . + . ID=name"RXLR_1421"

PHYCAScaffold_2 DSRXLR CDS 60783 61232 . - . ID=name"RXLR_1422"

PHYCAScaffold_2 DSRXLR CDS 1444749 1445129 . + . ID=name"RXLR_1423"

PHYCAScaffold_85 DSRXLR CDS 12550 12801 . - . ID=name"RXLR_1424"

PHYCAScaffold_12 DSRXLR CDS 736218 736472 . + . ID=name"RXLR_1425"

PHYCAScaffold_1 DSRXLR CDS 132400 133014 . - . ID=name"RXLR_1426"

PHYCAScaffold_7 DSRXLR CDS 353286 354224 . - . ID=name"RXLR_1427"

PHYCAScaffold_8 DSRXLR CDS 1165328 1165552 . + . ID=name"RXLR_1428"

PHYCAScaffold_748 DSRXLR CDS 494 943 . - . ID=name"RXLR_1429"

PHYCAScaffold_882 DSRXLR CDS 549 1298 . - . ID=name"RXLR_1430"

PHYCAScaffold_29 DSRXLR CDS 177687 178817 . + . ID=name"RXLR_1431"

PHYCAScaffold_19 DSRXLR CDS 901813 902025 . - . ID=name"RXLR_1432"

PHYCAScaffold_60 DSRXLR CDS 128053 128331 . + . ID=name"RXLR_1433"

PHYCAScaffold_29 DSRXLR CDS 300620 300919 . + . ID=name"RXLR_1434"

F.2 CRN Node Descriptions

PHYCAScaffold_121 DSCRN CDS 61069 62028 . + . ID=name"CRN_0"

PHYCAScaffold_67 DSCRN CDS 201540 202004 . + . ID=name"CRN_1"

PHYCAScaffold_42 DSCRN CDS 449122 450342 . - . ID=name"CRN_2"

PHYCAScaffold_1 DSCRN CDS 748948 751227 . - . ID=name"CRN_3"

PHYCAScaffold_83 DSCRN CDS 174383 174634 . + . ID=name"CRN_4"

PHYCAScaffold_12 DSCRN CDS 74554 76539 . - . ID=name"CRN_5"

PHYCAScaffold_2 DSCRN CDS 482347 483000 . - . ID=name"CRN_6"

PHYCAScaffold_42 DSCRN CDS 414938 415381 . + . ID=name"CRN_7"

PHYCAScaffold_83 DSCRN CDS 129731 131011 . - . ID=name"CRN_8"

PHYCAScaffold_5 DSCRN CDS 1061823 1063514 . + . ID=name"CRN_9"

PHYCAScaffold_12 DSCRN CDS 703039 703707 . - . ID=name"CRN_10"

PHYCAScaffold_2 DSCRN CDS 1135174 1136916 . - . ID=name"CRN_11"

PHYCAScaffold_105 DSCRN CDS 45500 45784 . + . ID=name"CRN_12"

PHYCAScaffold_15 DSCRN CDS 605846 606310 . - . ID=name"CRN_13"

PHYCAScaffold_91 DSCRN CDS 64129 66108 . + . ID=name"CRN_14"

PHYCAScaffold_83 DSCRN CDS 2355 2744 . - . ID=name"CRN_15"

PHYCAScaffold_16 DSCRN CDS 625387 626859 . - . ID=name"CRN_16"

PHYCAScaffold_839 DSCRN CDS 767 1258 . - . ID=name"CRN_17"

PHYCAScaffold_12 DSCRN CDS 359118 360497 . - . ID=name"CRN_18"

PHYCAScaffold_42 DSCRN CDS 118395 119666 . - . ID=name"CRN_19"

PHYCAScaffold_77 DSCRN CDS 82122 84200 . + . ID=name"CRN_20"

PHYCAScaffold_75 DSCRN CDS 99989 101980 . + . ID=name"CRN_21"

PHYCAScaffold_16 DSCRN CDS 11235 11717 . + . ID=name"CRN_22"

PHYCAScaffold_10 DSCRN CDS 34310 34648 . - . ID=name"CRN_23"

PHYCAScaffold_5 DSCRN CDS 1311080 1312153 . - . ID=name"CRN_24"

PHYCAScaffold_125 DSCRN CDS 34250 35722 . - . ID=name"CRN_25"

PHYCAScaffold_12 DSCRN CDS 786448 787647 . - . ID=name"CRN_26"

PHYCAScaffold_16 DSCRN CDS 64426 65673 . + . ID=name"CRN_27"

PHYCAScaffold_86 DSCRN CDS 51082 53370 . - . ID=name"CRN_28"

PHYCAScaffold_12 DSCRN CDS 569514 570017 . + . ID=name"CRN_29"

PHYCAScaffold_32 DSCRN CDS 557601 560564 . + . ID=name"CRN_30"

PHYCAScaffold_1 DSCRN CDS 1360189 1361955 . + . ID=name"CRN_31"

PHYCAScaffold_75 DSCRN CDS 52868 53095 . + . ID=name"CRN_32"

PHYCAScaffold_2 DSCRN CDS 1645183 1646427 . - . ID=name"CRN_33"

PHYCAScaffold_12 DSCRN CDS 538203 538886 . - . ID=name"CRN_34"

PHYCAScaffold_94 DSCRN CDS 94279 95415 . + . ID=name"CRN_35"

PHYCAScaffold_16 DSCRN CDS 791517 793370 . + . ID=name"CRN_36"

PHYCAScaffold_75 DSCRN CDS 126078 126593 . - . ID=name"CRN_37"

PHYCAScaffold_15 DSCRN CDS 530323 531720 . - . ID=name"CRN_38"

PHYCAScaffold_31 DSCRN CDS 234587 235492 . - . ID=name"CRN_39"

PHYCAScaffold_1 DSCRN CDS 762947 763318 . + . ID=name"CRN_40"

PHYCAScaffold_47 DSCRN CDS 322665 324545 . - . ID=name"CRN_41"

PHYCAScaffold_12 DSCRN CDS 394791 395468 . + . ID=name"CRN_42"

PHYCAScaffold_10 DSCRN CDS 1145326 1147503 . + . ID=name"CRN_43"

PHYCAScaffold_22 DSCRN CDS 468272 469138 . + . ID=name"CRN_44"

PHYCAScaffold_83 DSCRN CDS 82055 82537 . - . ID=name"CRN_45"

PHYCAScaffold_12 DSCRN CDS 498623 498997 . + . ID=name"CRN_46"

PHYCAScaffold_51 DSCRN CDS 133443 135695 . - . ID=name"CRN_47"

PHYCAScaffold_18 DSCRN CDS 552282 552983 . - . ID=name"CRN_48"

PHYCAScaffold_68 DSCRN CDS 271737 272189 . - . ID=name"CRN_49"

PHYCAScaffold_83 DSCRN CDS 4684 4926 . + . ID=name"CRN_50"

PHYCAScaffold_16 DSCRN CDS 484746 484958 . + . ID=name"CRN_51"

PHYCAScaffold_24 DSCRN CDS 600681 600959 . + . ID=name"CRN_52"

PHYCAScaffold_83 DSCRN CDS 131580 131807 . + . ID=name"CRN_53"

PHYCAScaffold_5 DSCRN CDS 1520879 1521334 . + . ID=name"CRN_54"

PHYCAScaffold_10 DSCRN CDS 93544 94815 . - . ID=name"CRN_55"

PHYCAScaffold_55 DSCRN CDS 398199 398921 . - . ID=name"CRN_56"

PHYCAScaffold_18 DSCRN CDS 916649 917479 . + . ID=name"CRN_57"

PHYCAScaffold_26 DSCRN CDS 424794 427664 . + . ID=name"CRN_58"

PHYCAScaffold_6 DSCRN CDS 1199823 1200515 . + . ID=name"CRN_59"

PHYCAScaffold_125 DSCRN CDS 24873 26246 . + . ID=name"CRN_60"

PHYCAScaffold_12 DSCRN CDS 399564 400955 . - . ID=name"CRN_61"

PHYCAScaffold_36 DSCRN CDS 553791 555779 . + . ID=name"CRN_62"

PHYCAScaffold_36 DSCRN CDS 74960 77266 . + . ID=name"CRN_63"

PHYCAScaffold_10 DSCRN CDS 39005 39859 . + . ID=name"CRN_64"

PHYCAScaffold_12 DSCRN CDS 211306 213930 . - . ID=name"CRN_65"

PHYCAScaffold_83 DSCRN CDS 12377 12670 . + . ID=name"CRN_66"

PHYCAScaffold_25 DSCRN CDS 531595 532683 . - . ID=name"CRN_67"

PHYCAScaffold_37 DSCRN CDS 204234 205379 . - . ID=name"CRN_68"

PHYCAScaffold_36 DSCRN CDS 558420 559001 . + . ID=name"CRN_69"

PHYCAScaffold_60 DSCRN CDS 150071 151795 . - . ID=name"CRN_70"

PHYCAScaffold_79 DSCRN CDS 52802 54622 . - . ID=name"CRN_71"

PHYCAScaffold_10 DSCRN CDS 82847 83830 . + . ID=name"CRN_72"

PHYCAScaffold_74 DSCRN CDS 19852 20253 . + . ID=name"CRN_73"

PHYCAScaffold_33 DSCRN CDS 36190 37362 . + . ID=name"CRN_74"

PHYCAScaffold_108 DSCRN CDS 66053 66559 . + . ID=name"CRN_75"

PHYCAScaffold_12 DSCRN CDS 274831 275325 . - . ID=name"CRN_76"

PHYCAScaffold_15 DSCRN CDS 846304 846963 . + . ID=name"CRN_77"

PHYCAScaffold_36 DSCRN CDS 557647 558168 . - . ID=name"CRN_78"

PHYCAScaffold_21 DSCRN CDS 181939 183717 . + . ID=name"CRN_79"

PHYCAScaffold_47 DSCRN CDS 281583 283142 . + . ID=name"CRN_80"

PHYCAScaffold_27 DSCRN CDS 363334 365391 . - . ID=name"CRN_81"

PHYCAScaffold_34 DSCRN CDS 64595 65047 . - . ID=name"CRN_82"

PHYCAScaffold_75 DSCRN CDS 242079 242378 . - . ID=name"CRN_83"

PHYCAScaffold_10 DSCRN CDS 129874 130308 . - . ID=name"CRN_84"

PHYCAScaffold_90 DSCRN CDS 137061 138023 . - . ID=name"CRN_85"

PHYCAScaffold_13 DSCRN CDS 821926 823296 . - . ID=name"CRN_86"

PHYCAScaffold_77 DSCRN CDS 73080 75248 . - . ID=name"CRN_87"

PHYCAScaffold_15 DSCRN CDS 884570 885082 . - . ID=name"CRN_88"

PHYCAScaffold_33 DSCRN CDS 56775 58310 . + . ID=name"CRN_89"

PHYCAScaffold_73 DSCRN CDS 170556 172319 . - . ID=name"CRN_90"

PHYCAScaffold_10 DSCRN CDS 1136157 1136465 . - . ID=name"CRN_91"

PHYCAScaffold_1 DSCRN CDS 1307174 1308307 . - . ID=name"CRN_92"

PHYCAScaffold_42 DSCRN CDS 393695 394789 . + . ID=name"CRN_93"

PHYCAScaffold_29 DSCRN CDS 683843 684088 . + . ID=name"CRN_94"

PHYCAScaffold_74 DSCRN CDS 89521 91335 . + . ID=name"CRN_95"

PHYCAScaffold_77 DSCRN CDS 79448 81505 . - . ID=name"CRN_96"

PHYCAScaffold_108 DSCRN CDS 48279 48575 . + . ID=name"CRN_97"

PHYCAScaffold_1 DSCRN CDS 2135056 2136027 . - . ID=name"CRN_98"

PHYCAScaffold_75 DSCRN CDS 231853 232284 . - . ID=name"CRN_99"

PHYCAScaffold_55 DSCRN CDS 183083 185641 . - . ID=name"CRN_100"

PHYCAScaffold_83 DSCRN CDS 84487 84729 . - . ID=name"CRN_101"

PHYCAScaffold_52 DSCRN CDS 4646 6550 . + . ID=name"CRN_102"

PHYCAScaffold_12 DSCRN CDS 445357 447297 . + . ID=name"CRN_103"

PHYCAScaffold_47 DSCRN CDS 258842 259204 . + . ID=name"CRN_104"

PHYCAScaffold_25 DSCRN CDS 570415 571497 . - . ID=name"CRN_105"

PHYCAScaffold_10 DSCRN CDS 38138 38785 . - . ID=name"CRN_106"

PHYCAScaffold_9 DSCRN CDS 412048 412743 . - . ID=name"CRN_107"

PHYCAScaffold_10 DSCRN CDS 86239 86586 . - . ID=name"CRN_108"

PHYCAScaffold_20 DSCRN CDS 748052 749260 . - . ID=name"CRN_109"

PHYCAScaffold_83 DSCRN CDS 48308 50026 . - . ID=name"CRN_110"

PHYCAScaffold_22 DSCRN CDS 454620 455585 . + . ID=name"CRN_111"

PHYCAScaffold_11 DSCRN CDS 686529 687809 . - . ID=name"CRN_112"

PHYCAScaffold_83 DSCRN CDS 8678 9115 . - . ID=name"CRN_113"

PHYCAScaffold_278 DSCRN CDS 372 662 . + . ID=name"CRN_114"

PHYCAScaffold_111 DSCRN CDS 83428 85671 . - . ID=name"CRN_115"

PHYCAScaffold_5 DSCRN CDS 1027742 1028233 . + . ID=name"CRN_116"

PHYCAScaffold_5 DSCRN CDS 1112294 1114069 . - . ID=name"CRN_117"

PHYCAScaffold_51 DSCRN CDS 116003 117376 . + . ID=name"CRN_118"

PHYCAScaffold_15 DSCRN CDS 47618 48634 . - . ID=name"CRN_119"

PHYCAScaffold_474 DSCRN CDS 381 647 . + . ID=name"CRN_120"

PHYCAScaffold_10 DSCRN CDS 140301 140525 . + . ID=name"CRN_121"

PHYCAScaffold_75 DSCRN CDS 110966 111535 . - . ID=name"CRN_122"

PHYCAScaffold_67 DSCRN CDS 164450 164827 . + . ID=name"CRN_123"

PHYCAScaffold_10 DSCRN CDS 34858 35673 . + . ID=name"CRN_124"

PHYCAScaffold_10 DSCRN CDS 123803 124162 . - . ID=name"CRN_125"

PHYCAScaffold_67 DSCRN CDS 213035 213529 . + . ID=name"CRN_126"

PHYCAScaffold_21 DSCRN CDS 823078 824340 . + . ID=name"CRN_127"

PHYCAScaffold_10 DSCRN CDS 47436 48005 . - . ID=name"CRN_128"

PHYCAScaffold_85 DSCRN CDS 41262 43313 . - . ID=name"CRN_129"

PHYCAScaffold_121 DSCRN CDS 48112 50733 . + . ID=name"CRN_130"

PHYCAScaffold_116 DSCRN CDS 83498 83725 . + . ID=name"CRN_131"

PHYCAScaffold_12 DSCRN CDS 153366 155837 . + . ID=name"CRN_132"

PHYCAScaffold_21 DSCRN CDS 669946 670422 . - . ID=name"CRN_133"

PHYCAScaffold_42 DSCRN CDS 416887 417126 . + . ID=name"CRN_134"

PHYCAScaffold_942 DSCRN CDS 42 920 . + . ID=name"CRN_135"

PHYCAScaffold_12 DSCRN CDS 166924 167418 . + . ID=name"CRN_136"

PHYCAScaffold_10 DSCRN CDS 124322 124552 . + . ID=name"CRN_137"

PHYCAScaffold_86 DSCRN CDS 87338 87718 . + . ID=name"CRN_138"

PHYCAScaffold_12 DSCRN CDS 128787 129242 . + . ID=name"CRN_139"

Appendix G

RxLR Paralagous Groups

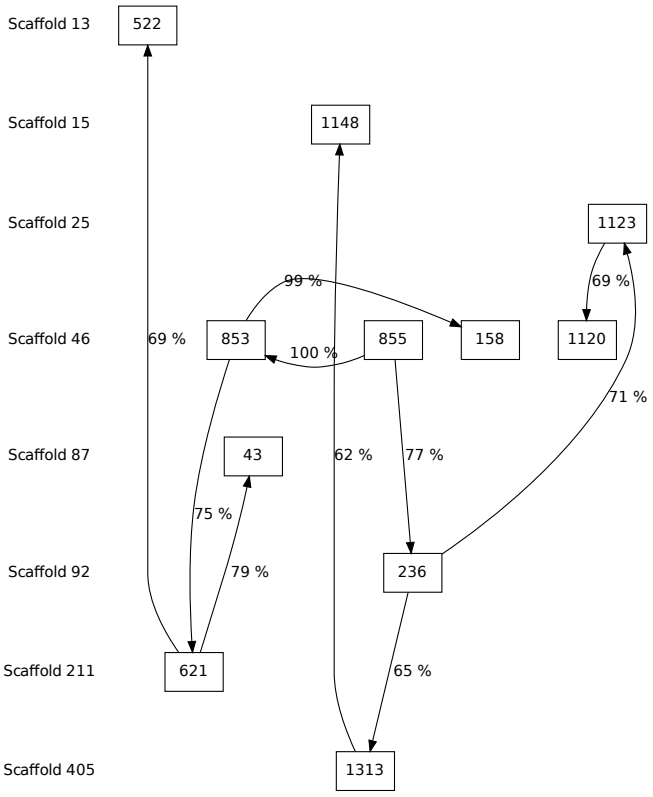

Figure G.1: Paralagous group 37 of the RxLR effector family.

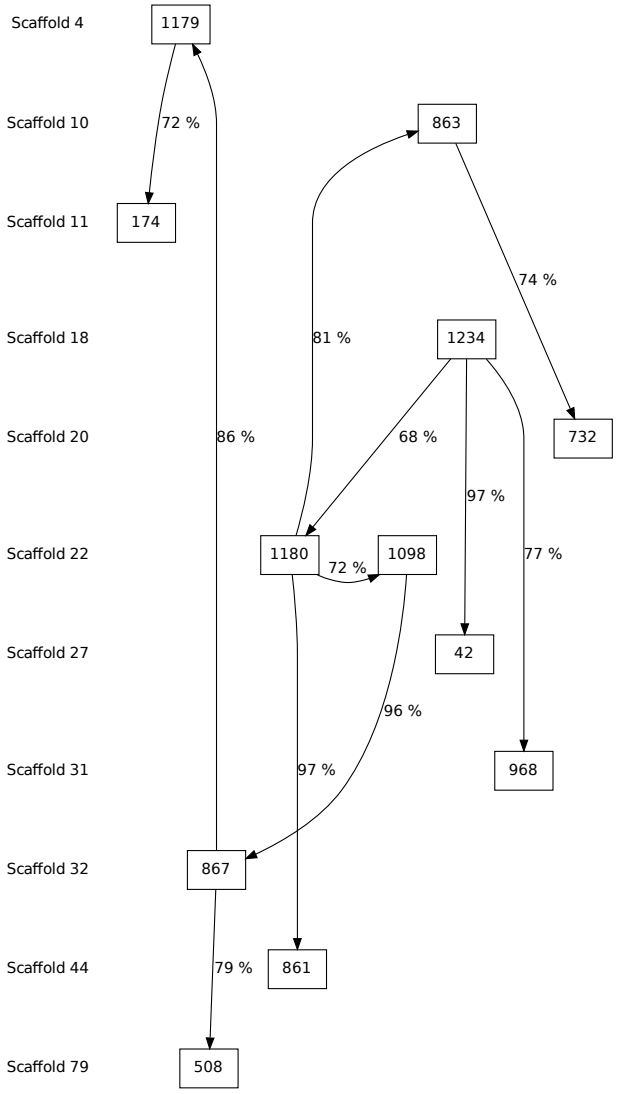

Figure G.2: Paralagous group 43 of the RxLR effector family.

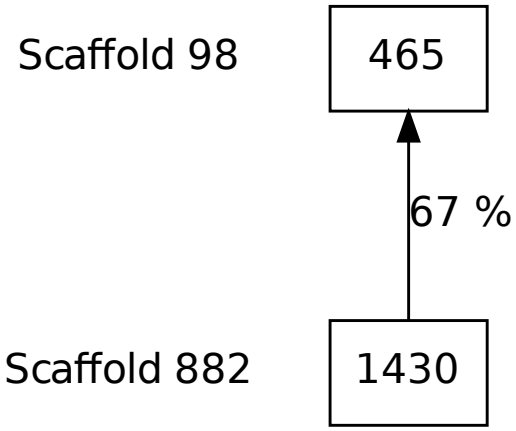

Figure G.3: Paralagous group 0 of the RxLR effector family.

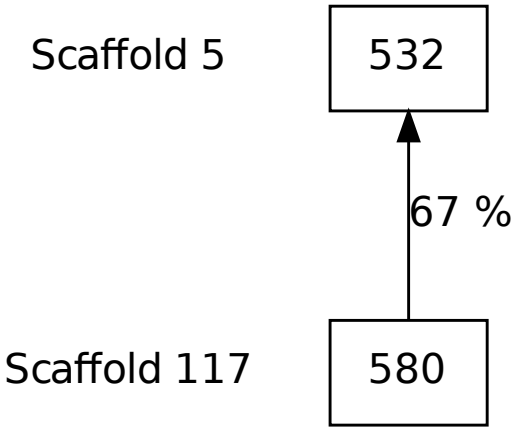

Figure G.4: Paralagous group 100 of the RxLR effector family.

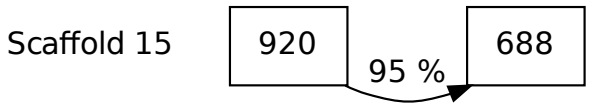

Figure G.5: Paralagous group 101 of the RxLR effector family.

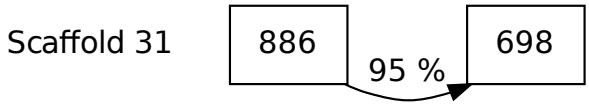

Figure G.6: Paralagous group 103 of the RxLR effector family.

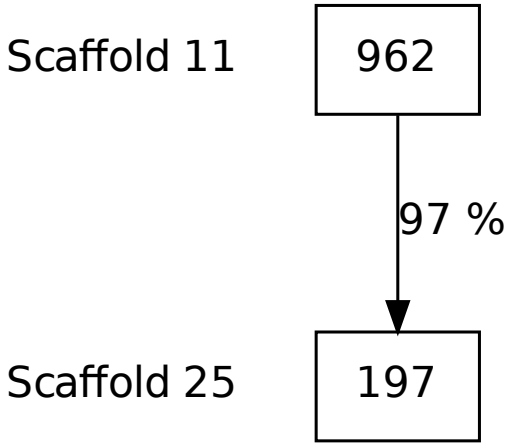

Figure G.7: Paralagous group 104 of the RxLR effector family.

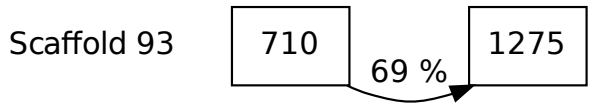

Figure G.8: Paralagous group 105 of the RxLR effector family.

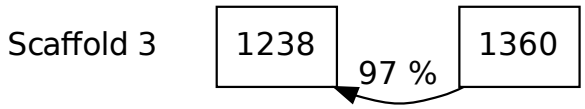

Figure G.9: Paralagous group 106 of the RxLR effector family.

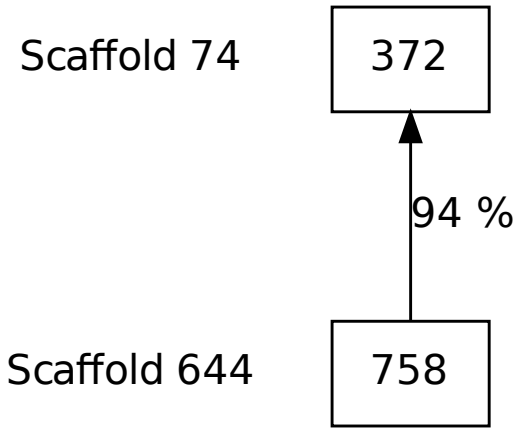

Figure G.10: Paralagous group 107 of the RxLR effector family.

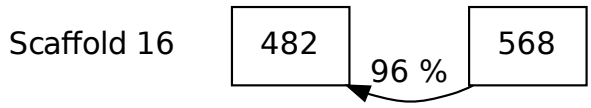

Figure G.11: Paralagous group 10 of the RxLR effector family.

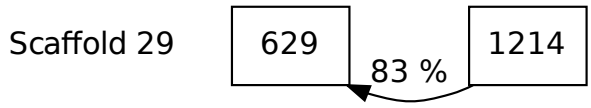

Figure G.12: Paralagous group 110 of the RxLR effector family.

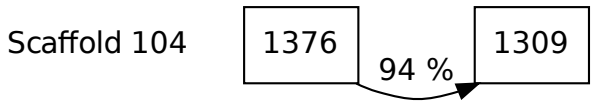

Figure G.13: Paralagous group 111 of the RxLR effector family.

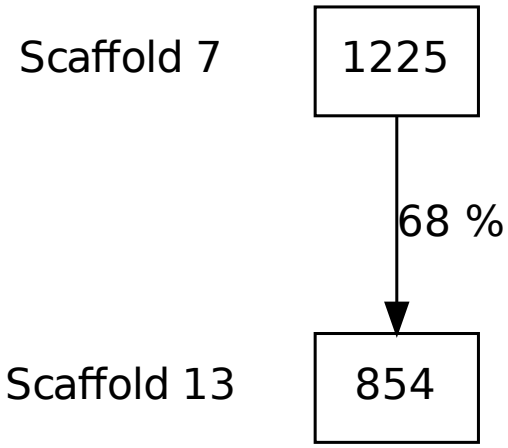

Figure G.14: Paralagous group 115 of the RxLR effector family.

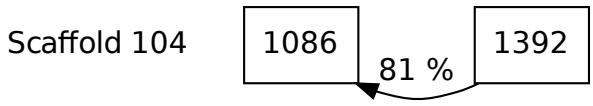

Figure G.15: Paralagous group 116 of the RxLR effector family.

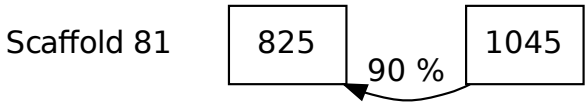

Figure G.16: Paralagous group 117 of the RxLR effector family.

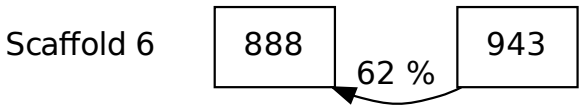

Figure G.17: Paralagous group 12 of the RxLR effector family.

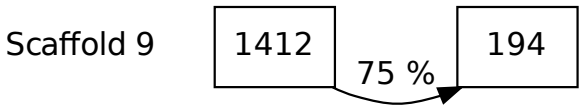

Figure G.18: Paralagous group 13 of the RxLR effector family.

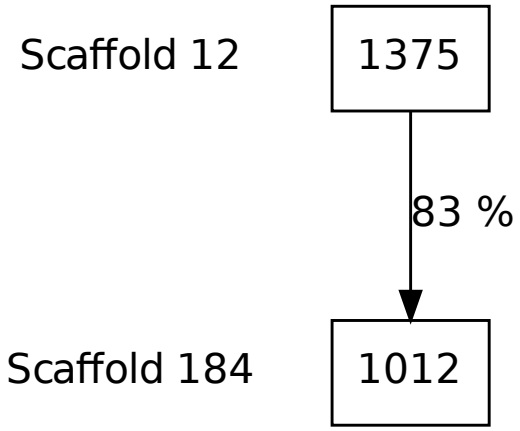

Figure G.19: Paralagous group 17 of the RxLR effector family.

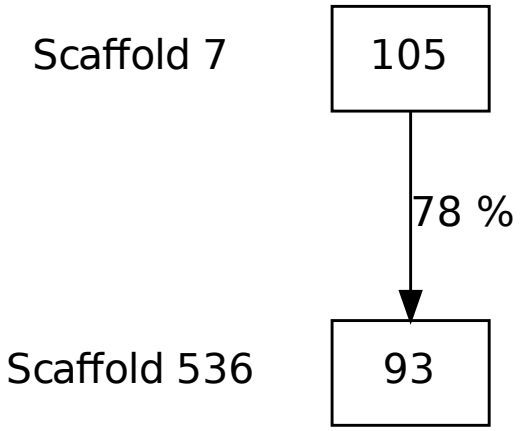

Figure G.20: Paralagous group 18 of the RxLR effector family.

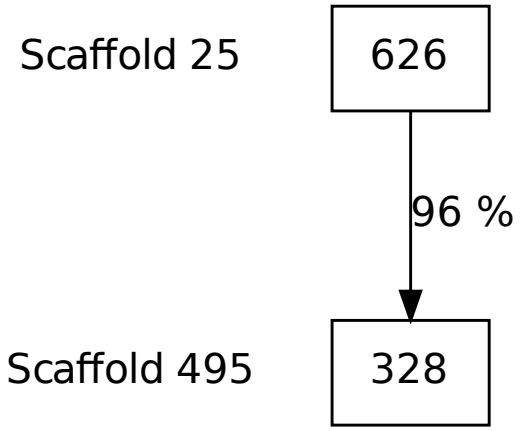

Figure G.21: Paralagous group 19 of the RxLR effector family.

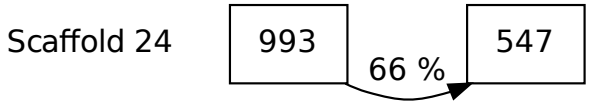

Figure G.22: Paralagous group 20 of the RxLR effector family.

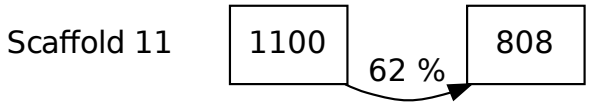

Figure G.23: Paralagous group 22 of the RxLR effector family.

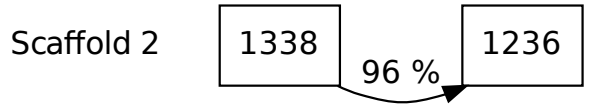

Figure G.24: Paralagous group 23 of the RxLR effector family.

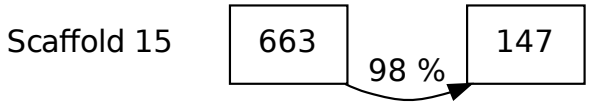

Figure G.25: Paralagous group 25 of the RxLR effector family.

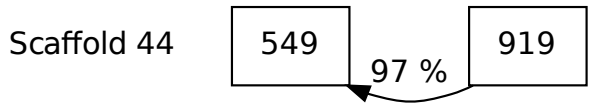

Figure G.26: Paralagous group 27 of the RxLR effector family.

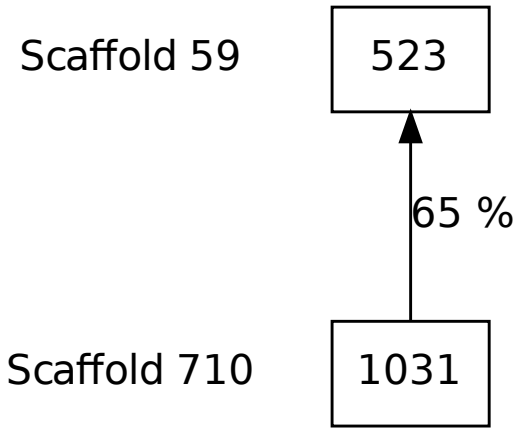

Figure G.27: Paralagous group 29 of the RxLR effector family.

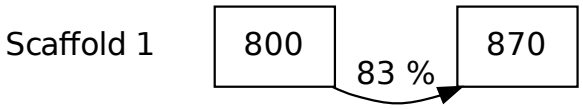

Figure G.28: Paralagous group 2 of the RxLR effector family.

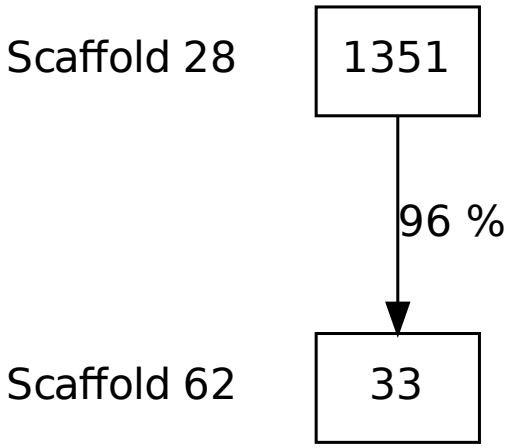

Figure G.29: Paralagous group 31 of the RxLR effector family.

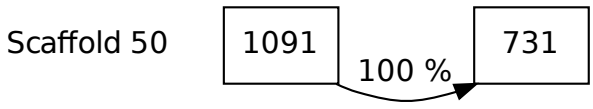

Figure G.30: Paralagous group 32 of the RxLR effector family.

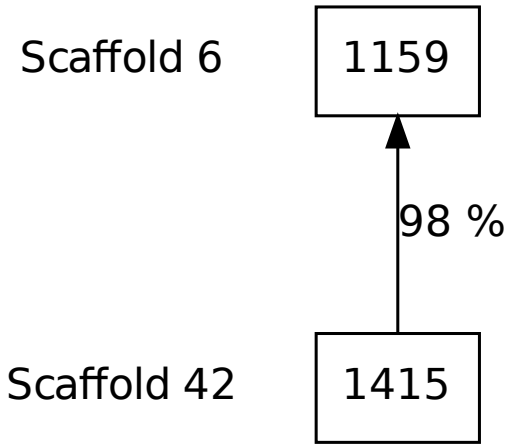

Figure G.31: Paralagous group 34 of the RxLR effector family.

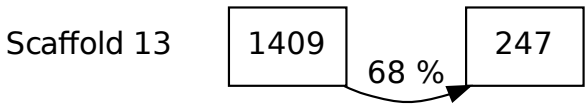

Figure G.32: Paralagous group 36 of the RxLR effector family.

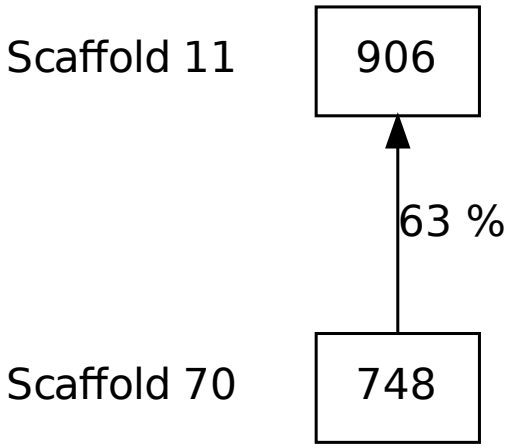

Figure G.33: Paralagous group 39 of the RxLR effector family.

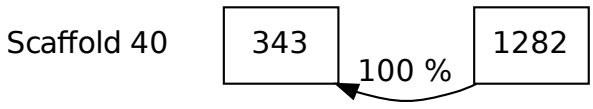

Figure G.34: Paralagous group 40 of the RxLR effector family.

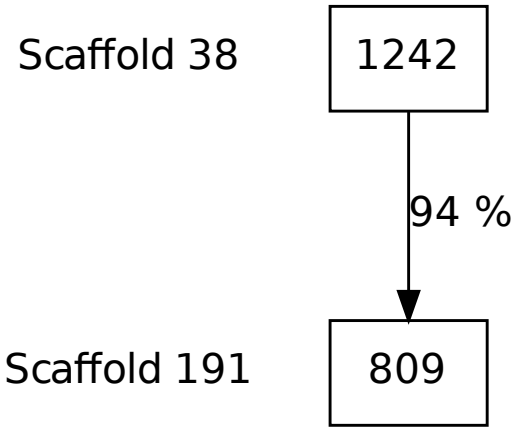

Figure G.35: Paralagous group 41 of the RxLR effector family.

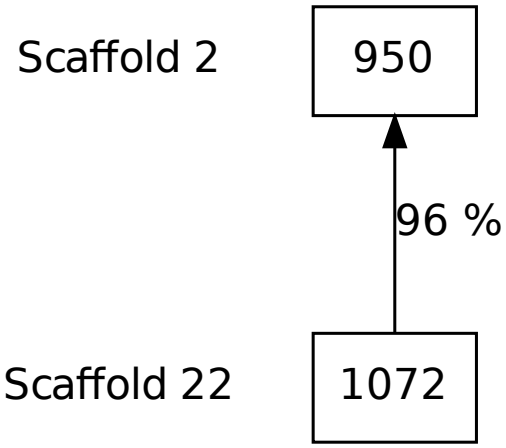

Figure G.36: Paralagous group 42 of the RxLR effector family.

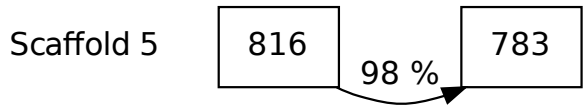

Figure G.37: Paralagous group 44 of the RxLR effector family.

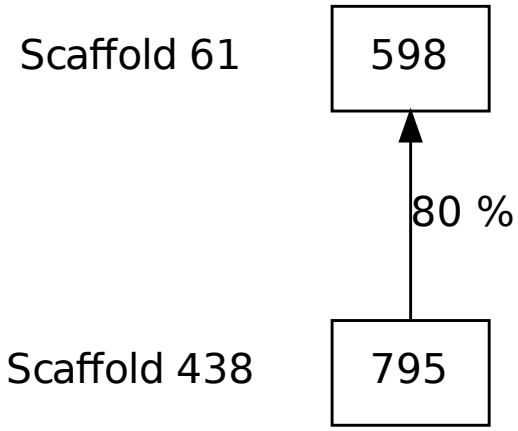

Figure G.38: Paralagous group 45 of the RxLR effector family.

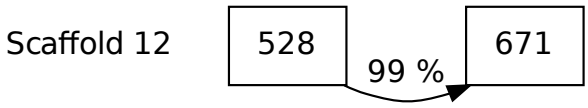

Figure G.39: Paralagous group 48 of the RxLR effector family.

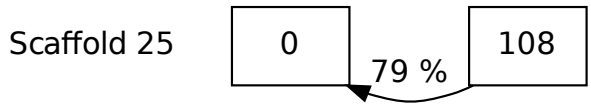

Figure G.40: Paralagous group 49 of the RxLR effector family.

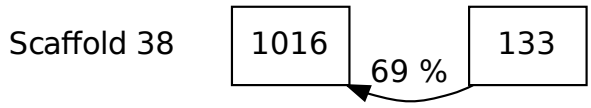

Figure G.41: Paralagous group 4 of the RxLR effector family.

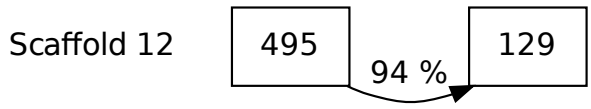

Figure G.42: Paralagous group 50 of the RxLR effector family.

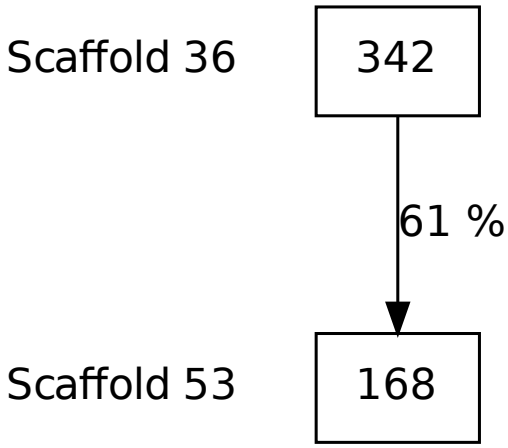

Figure G.43: Paralagous group 54 of the RxLR effector family.

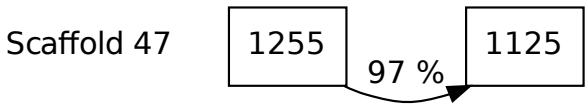

Figure G.44: Paralagous group 57 of the RxLR effector family.

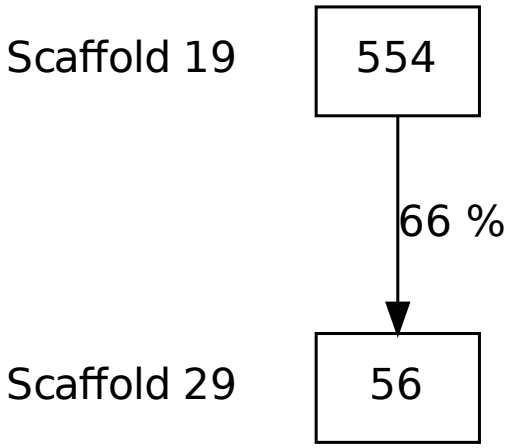

Figure G.45: Paralagous group 5 of the RxLR effector family.

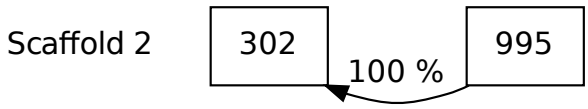

Figure G.46: Paralagous group 61 of the RxLR effector family.

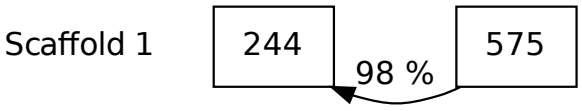

Figure G.47: Paralagous group 62 of the RxLR effector family.

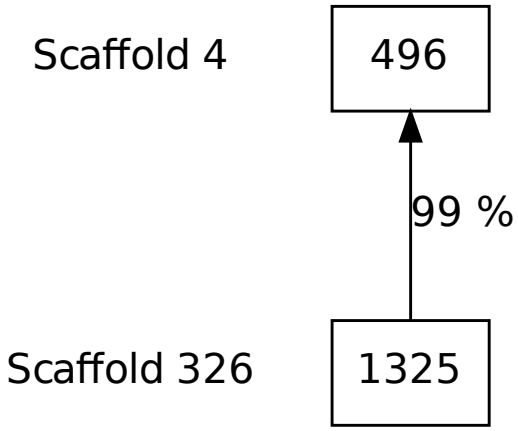

Figure G.48: Paralagous group 65 of the RxLR effector family.

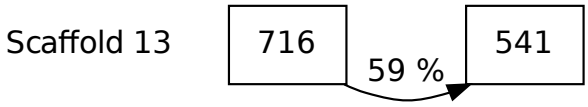

Figure G.49: Paralagous group 68 of the RxLR effector family.

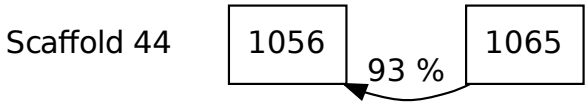

Figure G.50: Paralagous group 69 of the RxLR effector family.

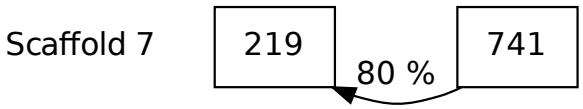

Figure G.51: Paralagous group 6 of the RxLR effector family.

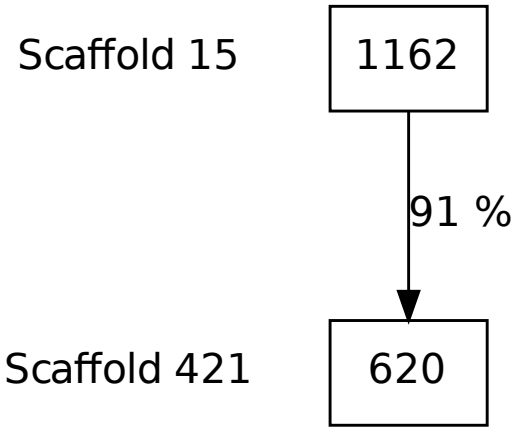

Figure G.52: Paralagous group 71 of the RxLR effector family.

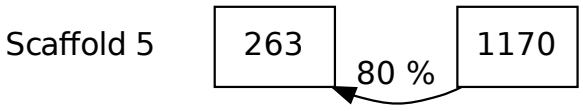

Figure G.53: Paralagous group 72 of the RxLR effector family.

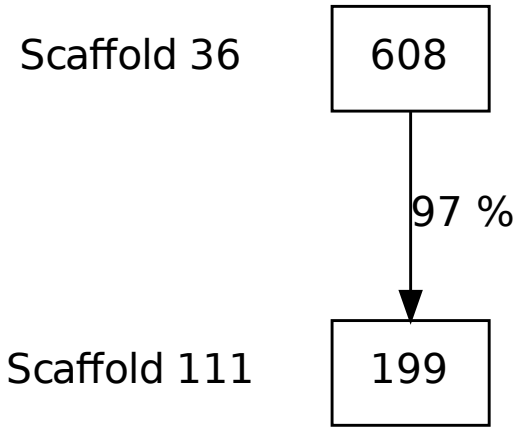

Figure G.54: Paralagous group 74 of the RxLR effector family.

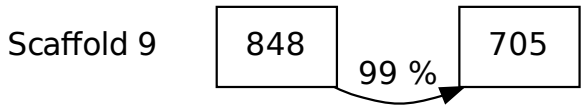

Figure G.55: Paralagous group 75 of the RxLR effector family.

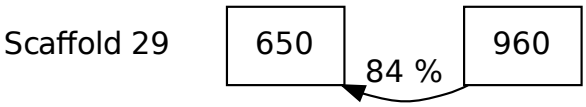

Figure G.56: Paralagous group 76 of the RxLR effector family.

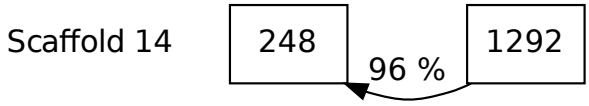

Figure G.57: Paralagous group 77 of the RxLR effector family.

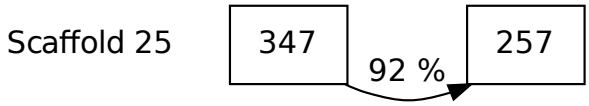

Figure G.58: Paralagous group 78 of the RxLR effector family.

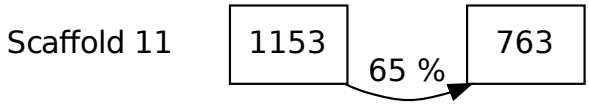

Figure G.59: Paralagous group 80 of the RxLR effector family.

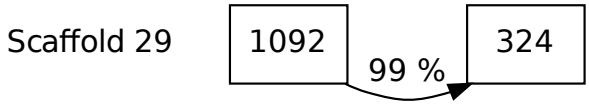

Figure G.60: Paralagous group 81 of the RxLR effector family.

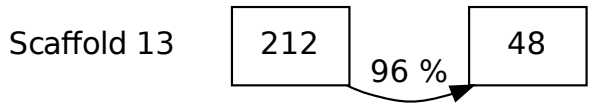

Figure G.61: Paralagous group 84 of the RxLR effector family.

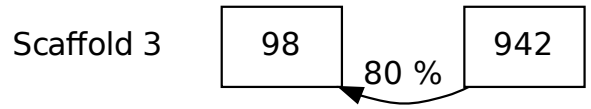

Figure G.62: Paralagous group 85 of the RxLR effector family.

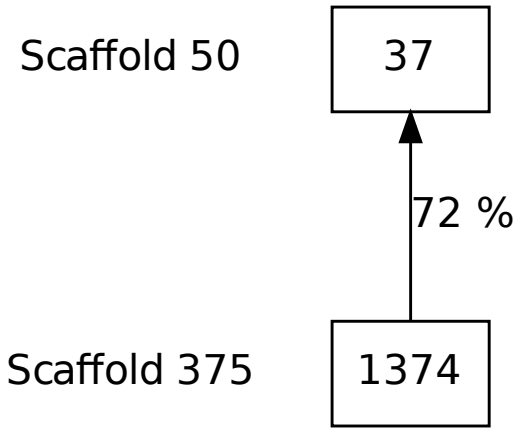

Figure G.63: Paralagous group 86 of the RxLR effector family.

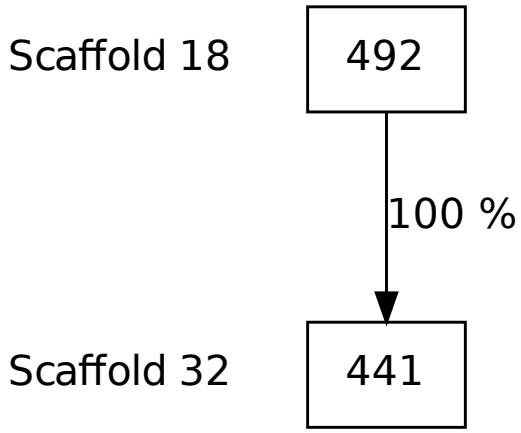

Figure G.64: Paralagous group 88 of the RxLR effector family.

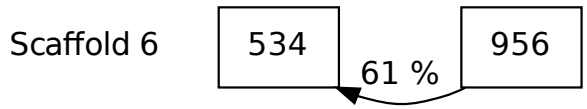

Figure G.65: Paralagous group 89 of the RxLR effector family.

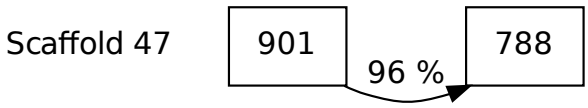

Figure G.66: Paralagous group 8 of the RxLR effector family.

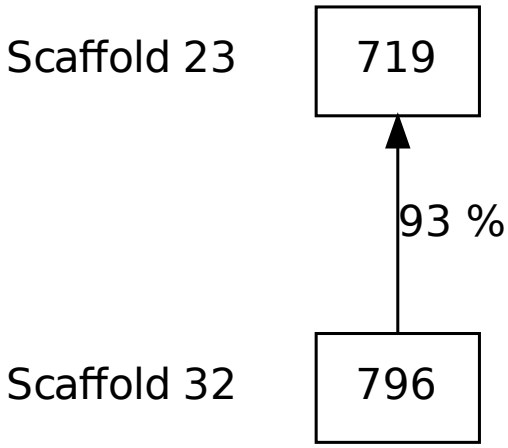

Figure G.67: Paralagous group 91 of the RxLR effector family.

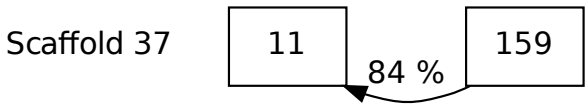

Figure G.68: Paralagous group 92 of the RxLR effector family.

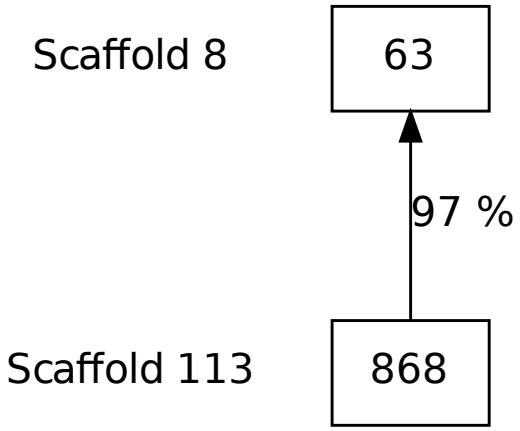

Figure G.69: Paralagous group 98 of the RxLR effector family.

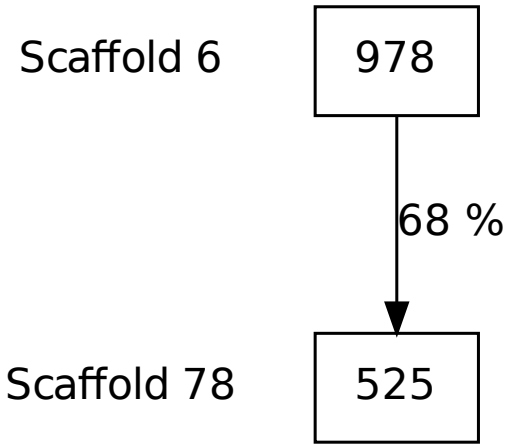

Figure G.70: Paralagous group 9 of the RxLR effector family.

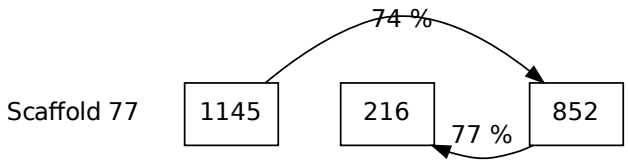

Figure G.71: Paralagous group 113 of the RxLR effector family.

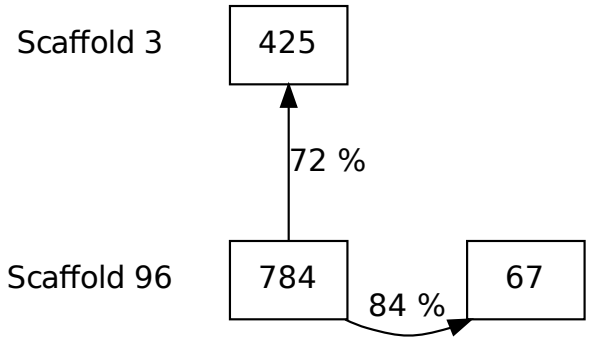

Figure G.72: Paralagous group 114 of the RxLR effector family.

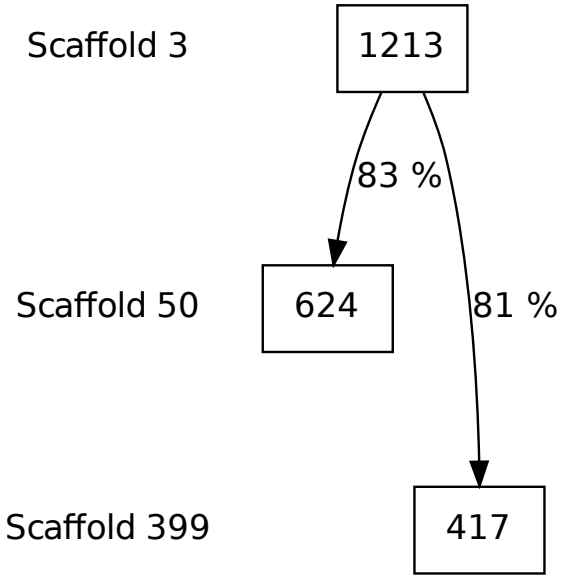

Figure G.73: Paralagous group 16 of the RxLR effector family.

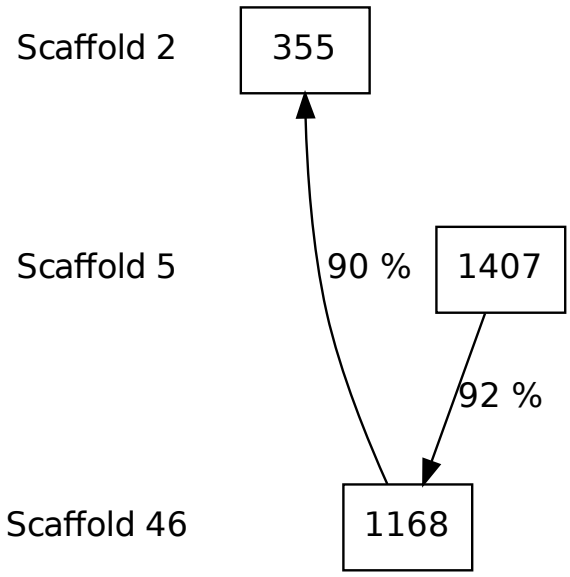

Figure G.74: Paralagous group 21 of the RxLR effector family.

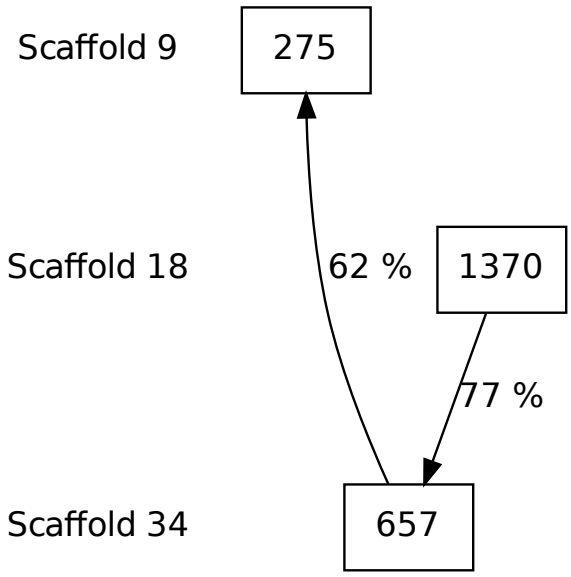

Figure G.75: Paralagous group 24 of the RxLR effector family.

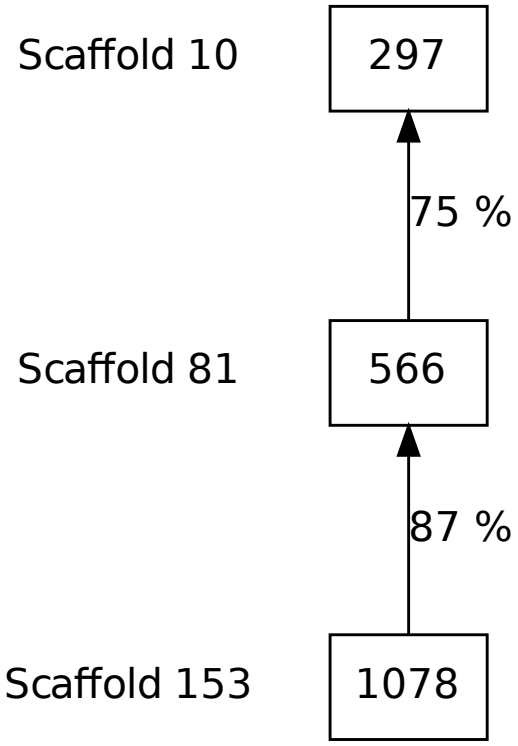

Figure G.76: Paralagous group 26 of the RxLR effector family.

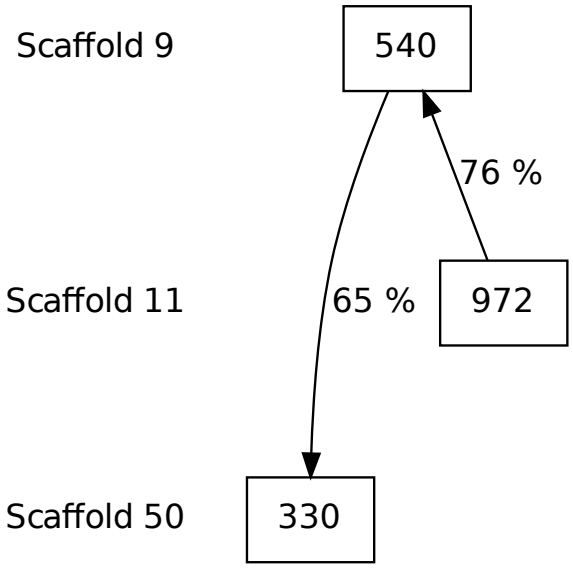

Figure G.77: Paralagous group 30 of the RxLR effector family.

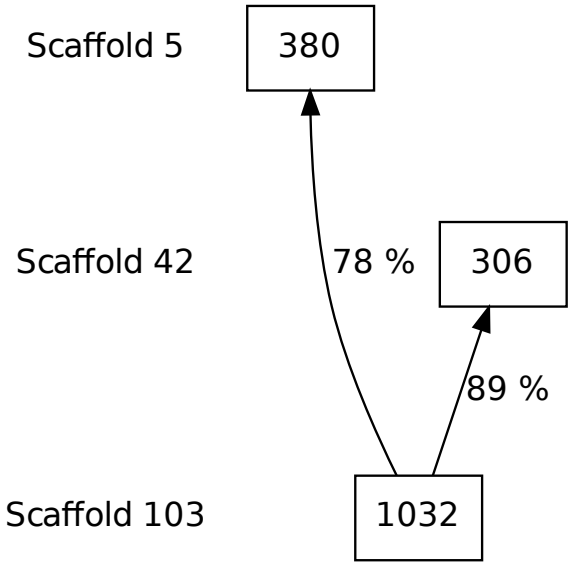

Figure G.78: Paralagous group 35 of the RxLR effector family.

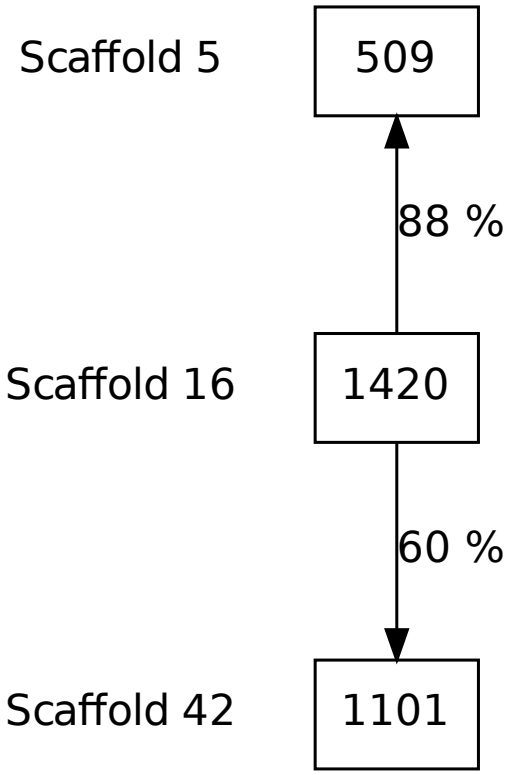

Figure G.79: Paralagous group 46 of the RxLR effector family.

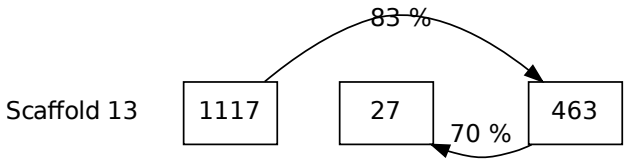

Figure G.80: Paralagous group 52 of the RxLR effector family.

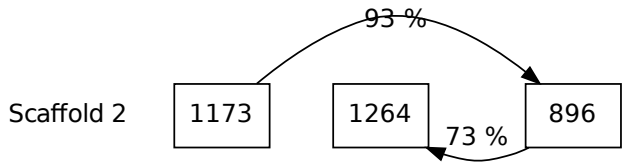

Figure G.81: Paralagous group 55 of the RxLR effector family.

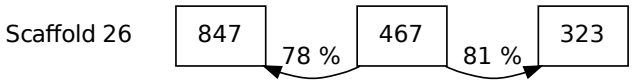

Figure G.82: Paralagous group 64 of the RxLR effector family.

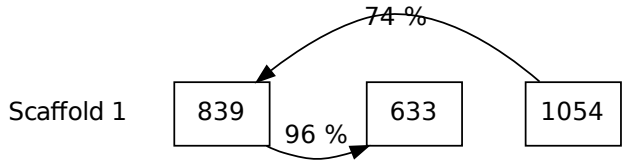

Figure G.83: Paralagous group 66 of the RxLR effector family.

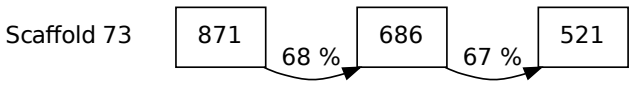

Figure G.84: Paralagous group 67 of the RxLR effector family.

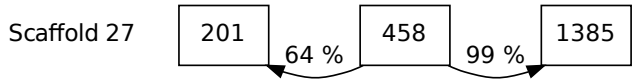

Figure G.85: Paralagous group 70 of the RxLR effector family.

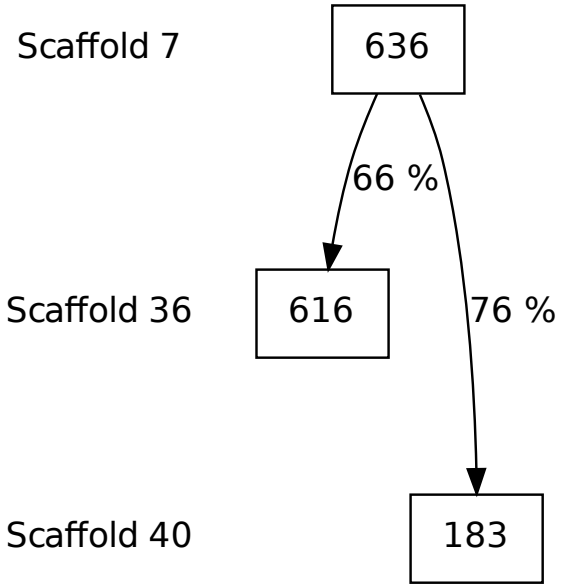

Figure G.86: Paralagous group 73 of the RxLR effector family.

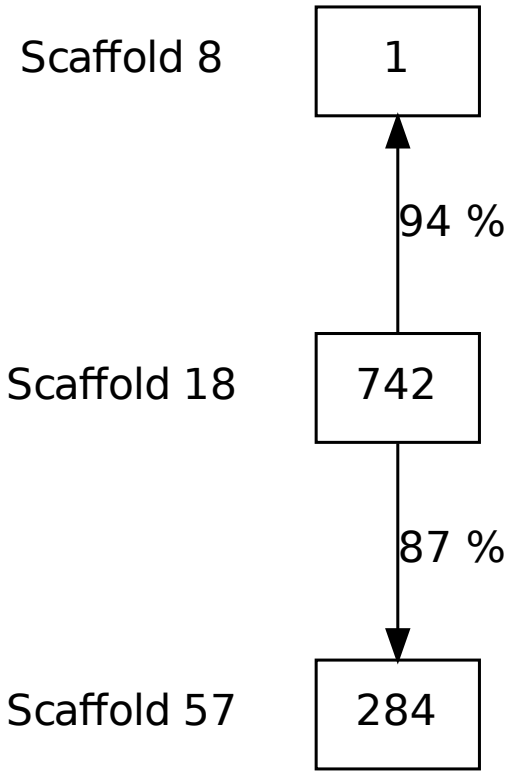

Figure G.87: Paralagous group 79 of the RxLR effector family.

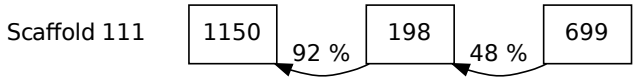

Figure G.88: Paralagous group 82 of the RxLR effector family.

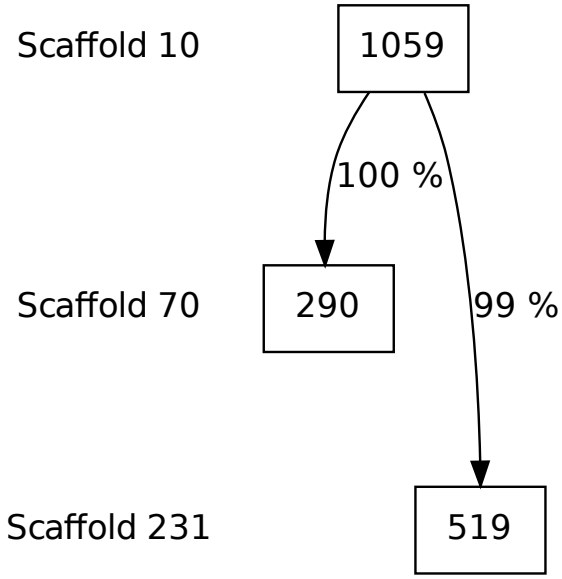

Figure G.89: Paralagous group 93 of the RxLR effector family.

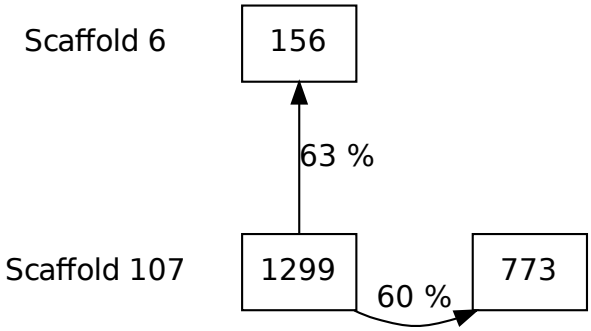

Figure G.90: Paralagous group 99 of the RxLR effector family.

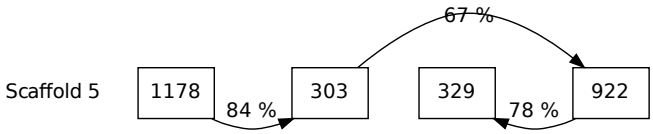

Figure G.91: Paralagous group 102 of the RxLR effector family.

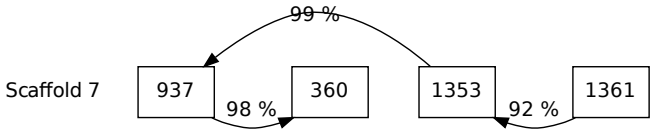

Figure G.92: Paralagous group 112 of the RxLR effector family.

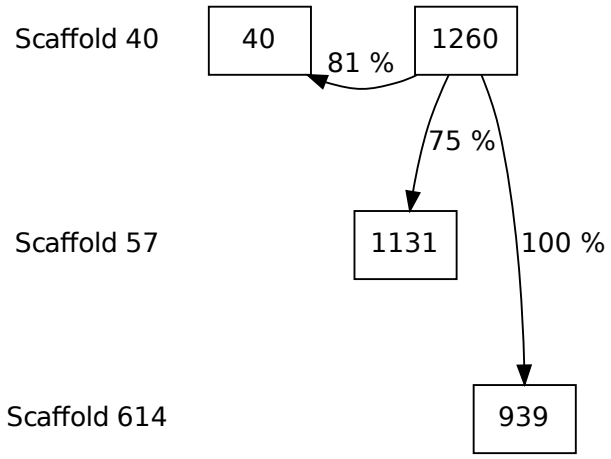

Figure G.93: Paralagous group 14 of the RxLR effector family.

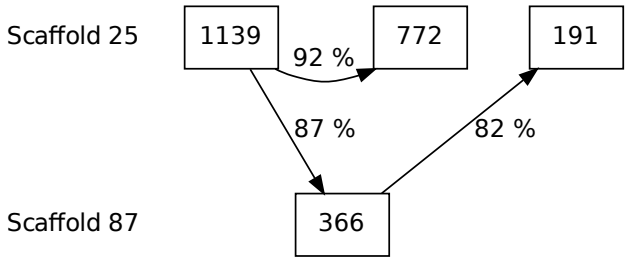

Figure G.94: Paralagous group 15 of the RxLR effector family.

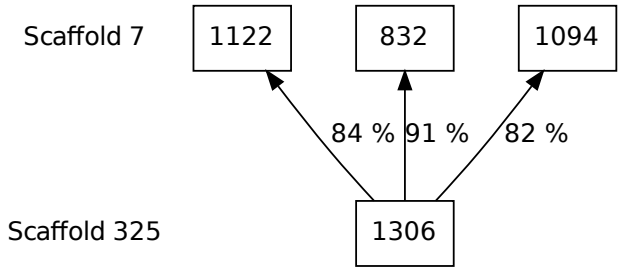

Figure G.95: Paralagous group 1 of the RxLR effector family.

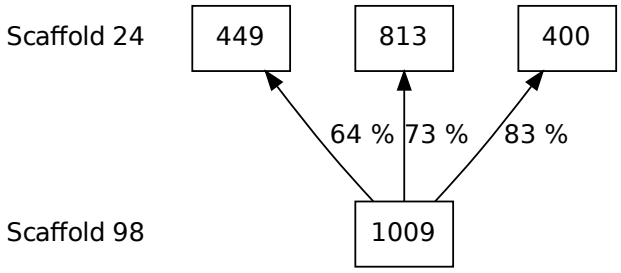

Figure G.96: Paralagous group 47 of the RxLR effector family.

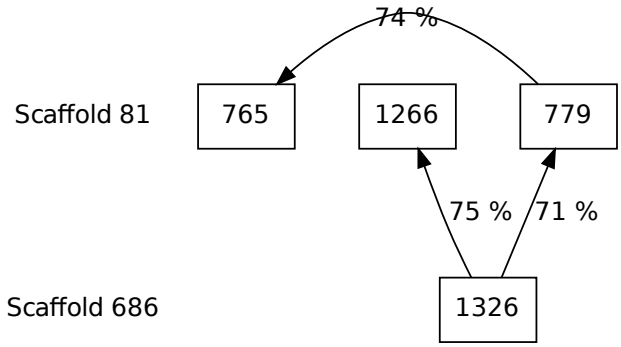

Figure G.97: Paralagous group 53 of the RxLR effector family.

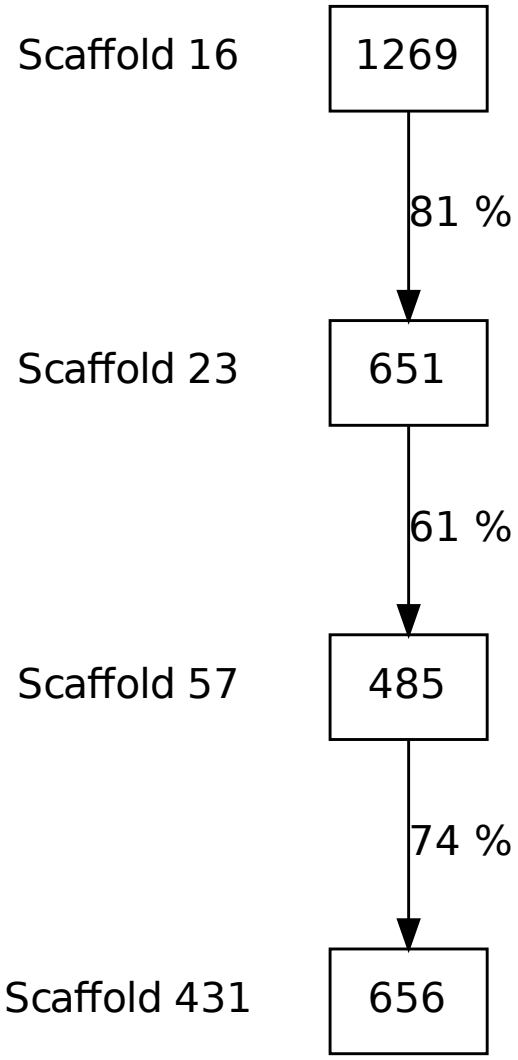

Figure G.98: Paralagous group 56 of the RxLR effector family.

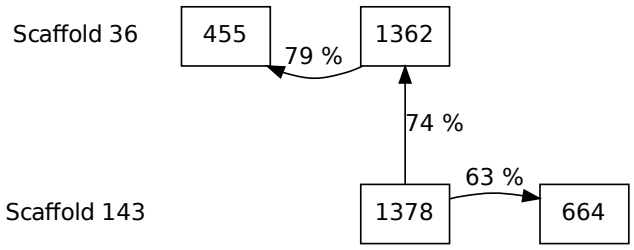

Figure G.99: Paralagous group 59 of the RxLR effector family.

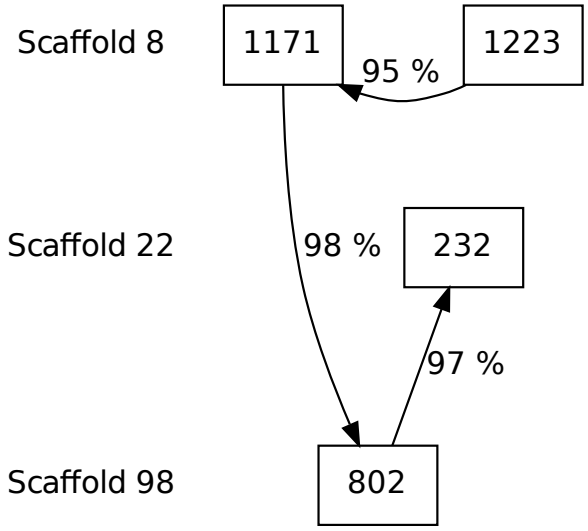

Figure G.100: Paralagous group 60 of the RxLR effector family.

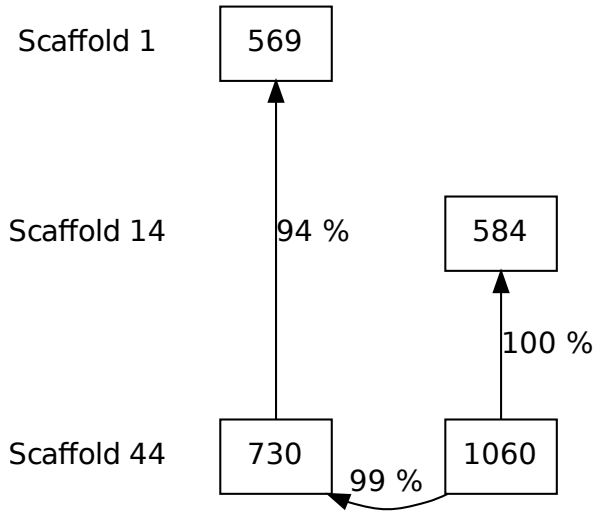

Figure G.101: Paralagous group 7 of the RxLR effector family.

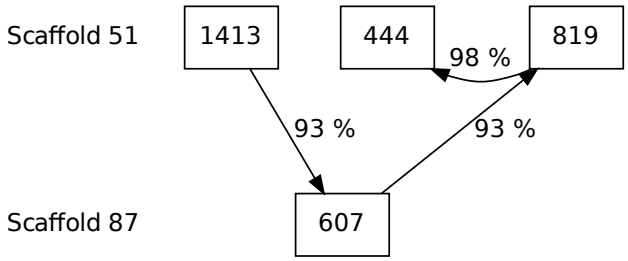

Figure G.102: Paralagous group 90 of the RxLR effector family.

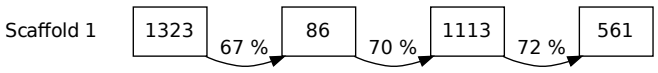

Figure G.103: Paralagous group 95 of the RxLR effector family.

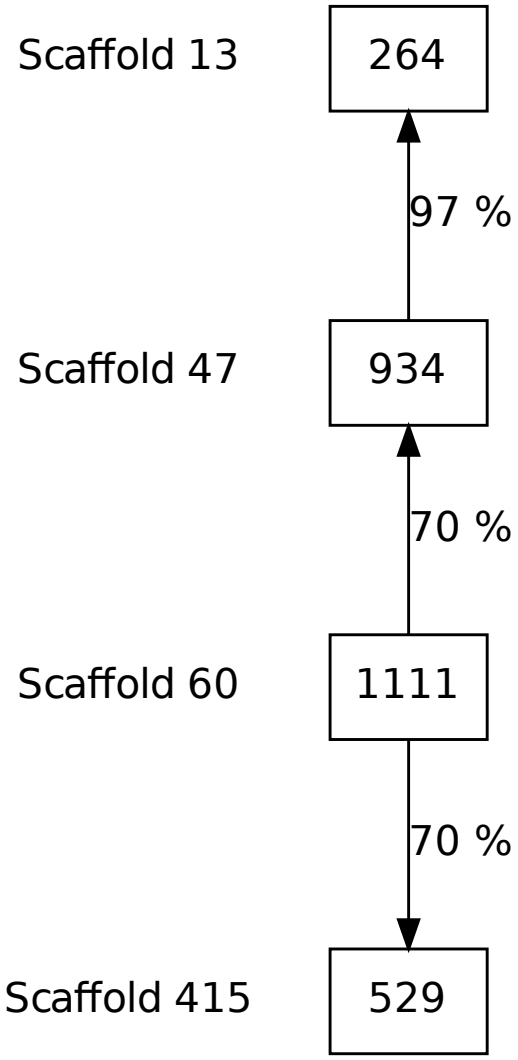

Figure G.104: Paralagous group 96 of the RxLR effector family.

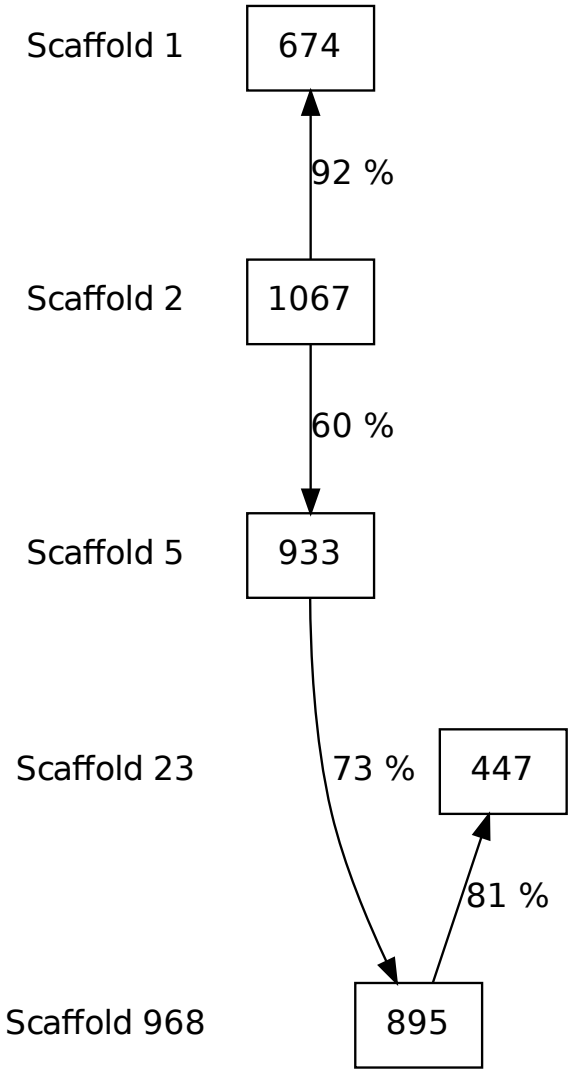

Figure G.105: Paralagous group 108 of the RxLR effector family.

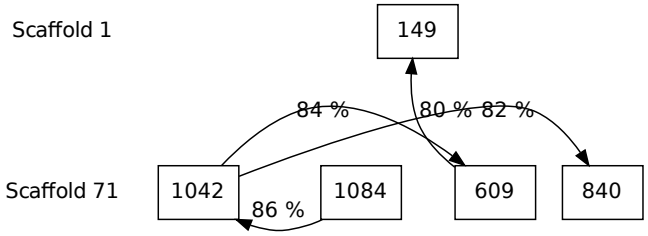

Figure G.106: Paralagous group 38 of the RxLR effector family.

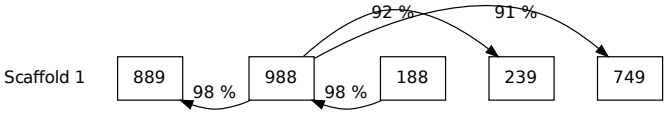

Figure G.107: Paralagous group 3 of the RxLR effector family.

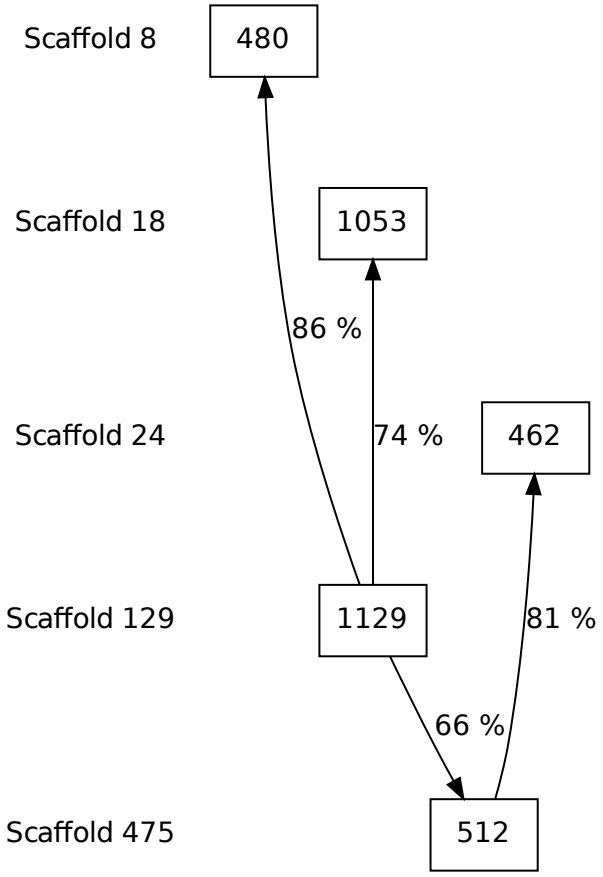

Figure G.108: Paralagous group 97 of the RxLR effector family.

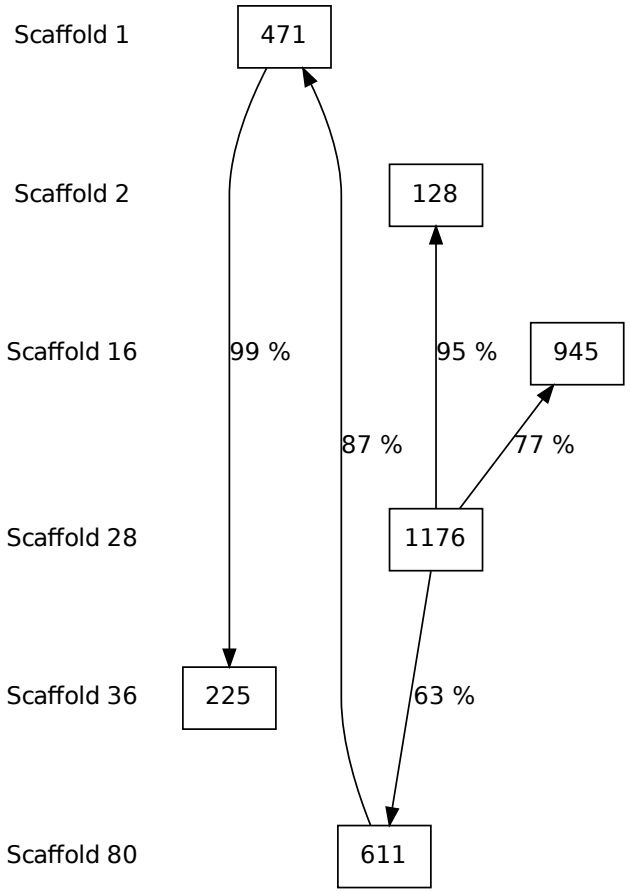

Figure G.109: Paralagous group 63 of the RxLR effector family.

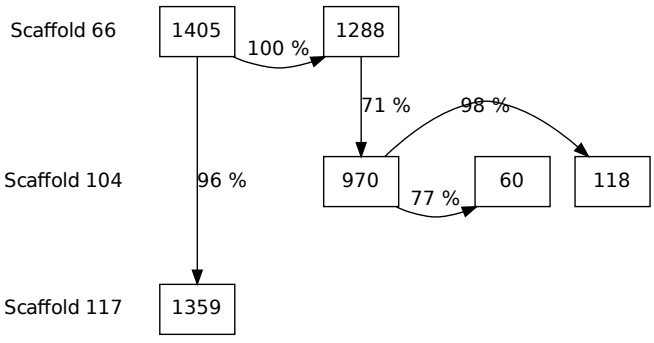

Figure G.110: Paralagous group 94 of the RxLR effector family.

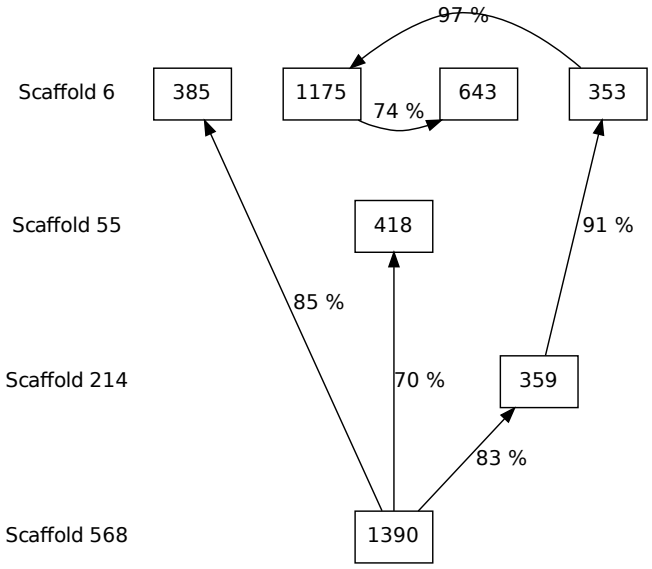

Figure G.111: Paralagous group 87 of the RxLR effector family.

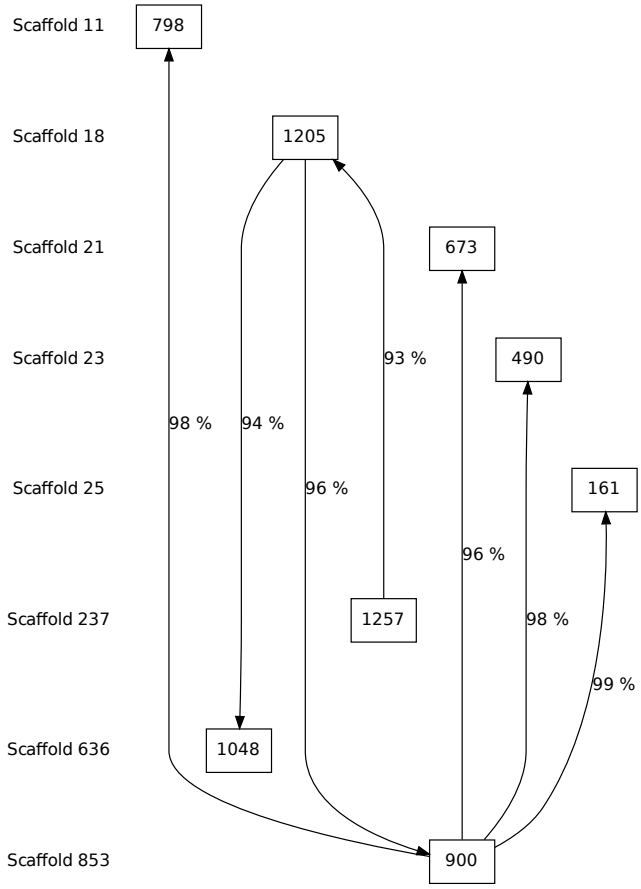

Figure G.112: Paralagous group 109 of the RxLR effector family.

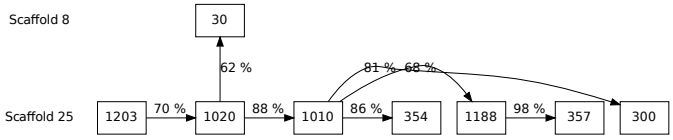

Figure G.113: Paralagous group 51 of the RxLR effector family.

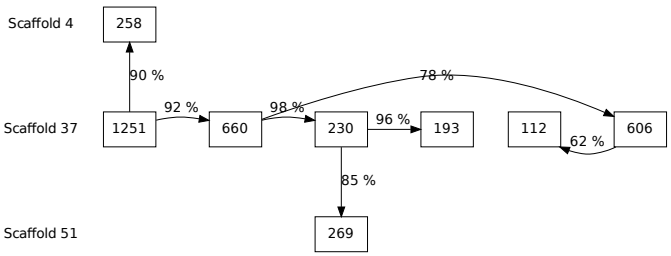

Figure G.114: Paralagous group 58 of the RxLR effector family.

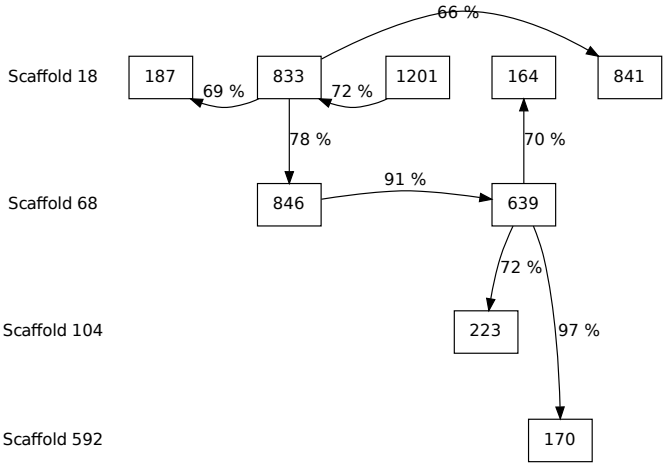

Figure G.115: Paralagous group 11 of the RxLR effector family.

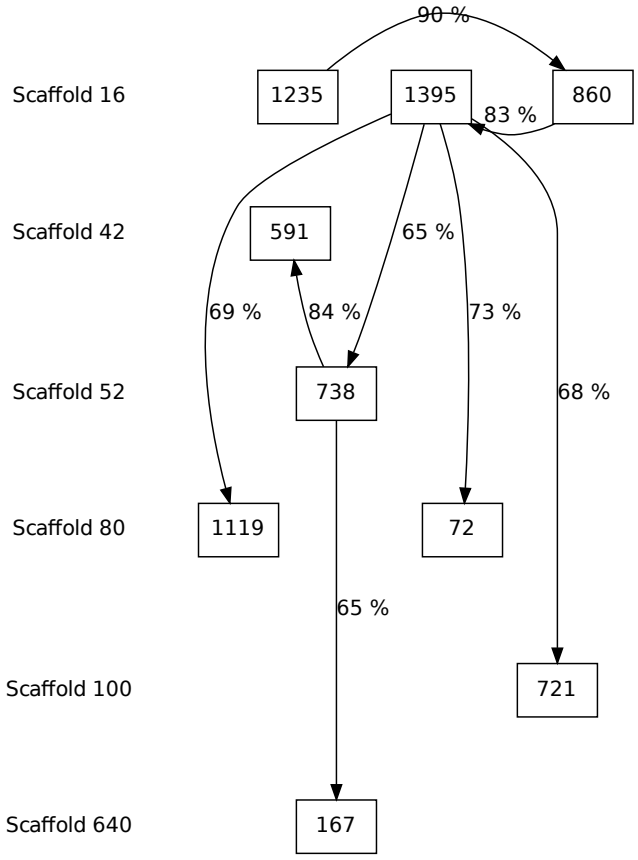

Figure G.116: Paralagous group 28 of the RxLR effector family.

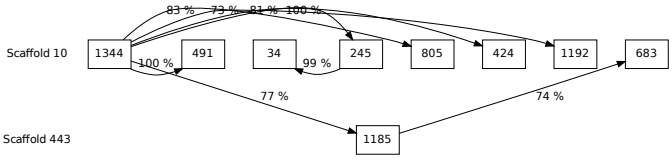

Figure G.117: Paralagous group 33 of the RxLR effector family.

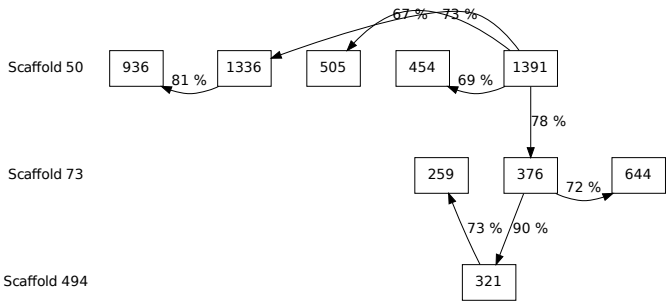

Figure G.118: Paralagous group 83 of the RxLR effector family.

Appendix H

CRN Paralagous Groups

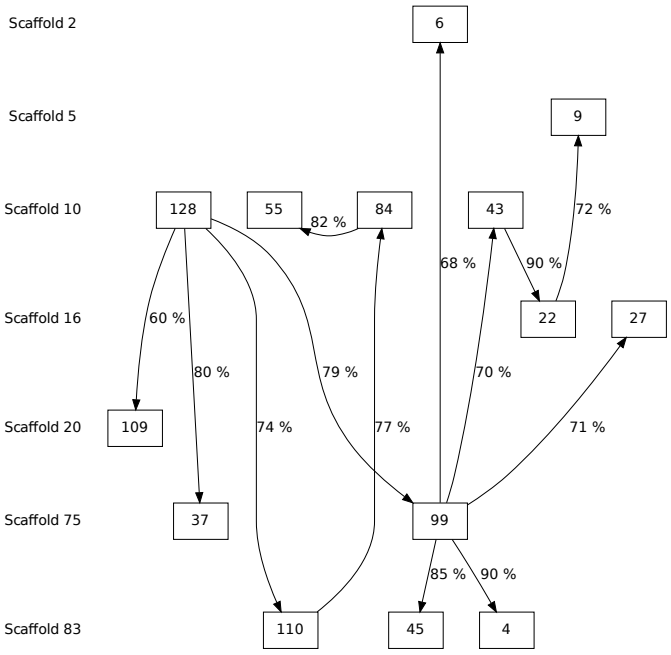

Figure H.1: Paralagous group 15 of the CRN effector family.

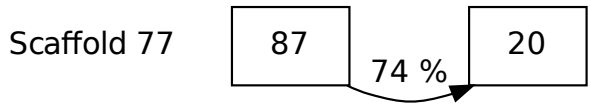

Figure H.2: Paralagous group 10 of the CRN effector family.

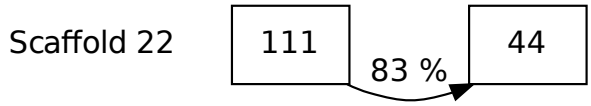

Figure H.3: Paralagous group 11 of the CRN effector family.

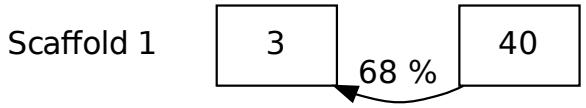

Figure H.4: Paralagous group 12 of the CRN effector family.

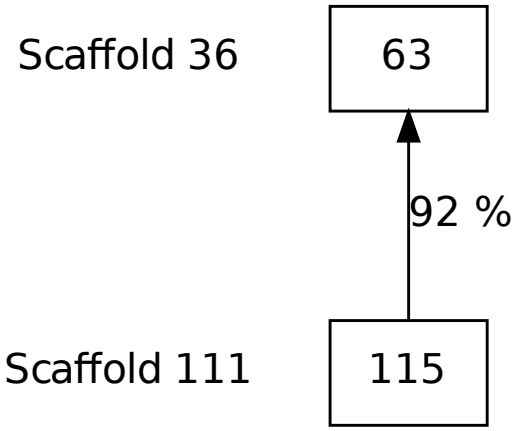

Figure H.5: Paralagous group 14 of the CRN effector family.

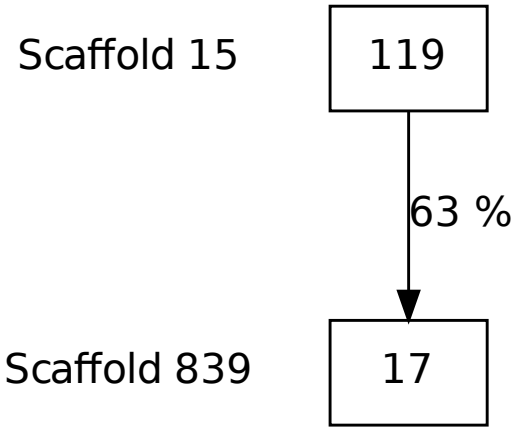

Figure H.6: Paralagous group 19 of the CRN effector family.

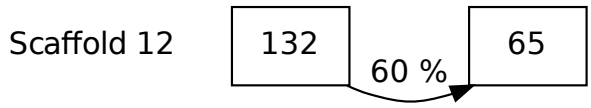

Figure H.7: Paralagous group 1 of the CRN effector family.

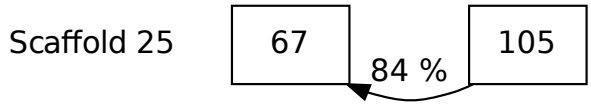

Figure H.8: Paralagous group 3 of the CRN effector family.

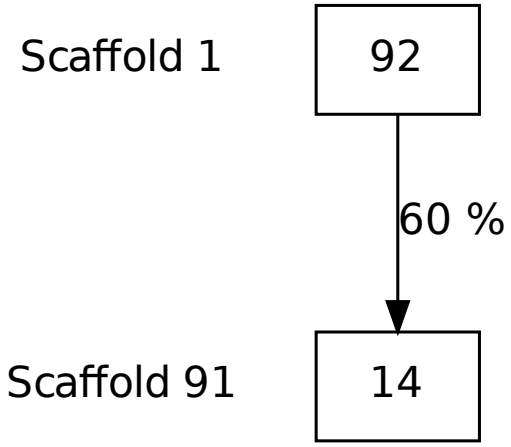

Figure H.9: Paralagous group 4 of the CRN effector family.

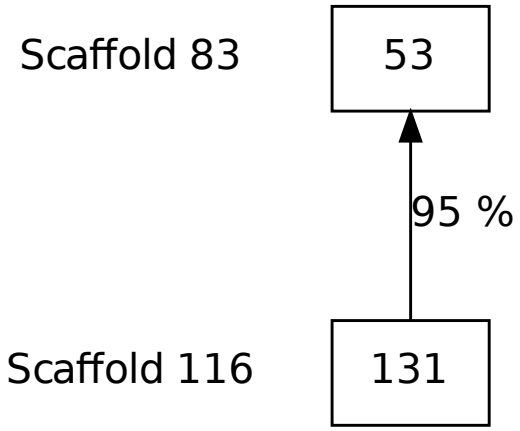

Figure H.10: Paralagous group 8 of the CRN effector family.

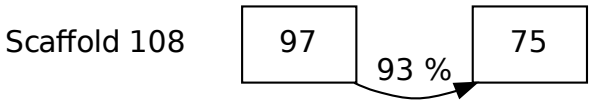

Figure H.11: Paralagous group 9 of the CRN effector family.

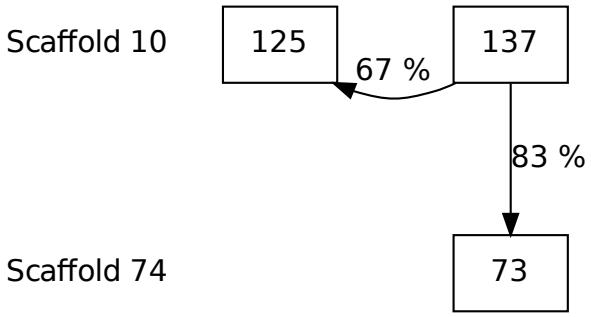

Figure H.12: Paralagous group 0 of the CRN effector family.

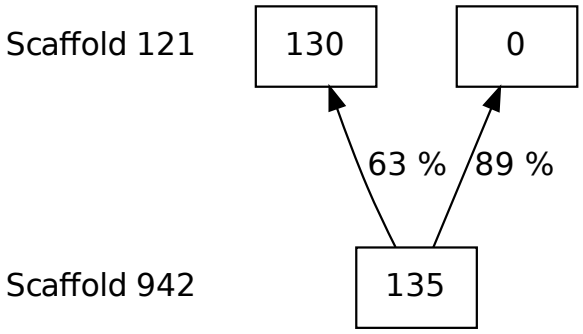

Figure H.13: Paralagous group 13 of the CRN effector family.

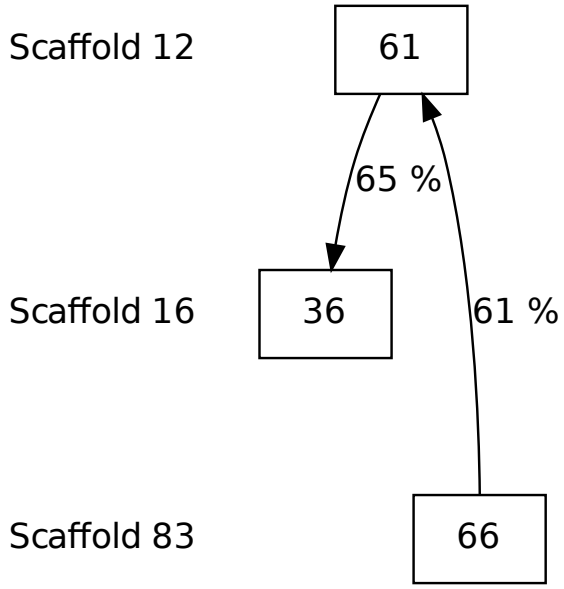

Figure H.14: Paralagous group 17 of the CRN effector family.

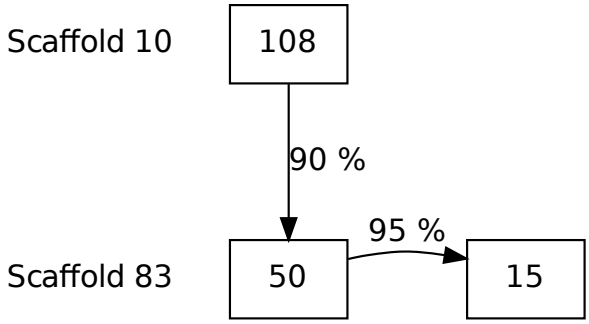

Figure H.15: Paralagous group 18 of the CRN effector family.

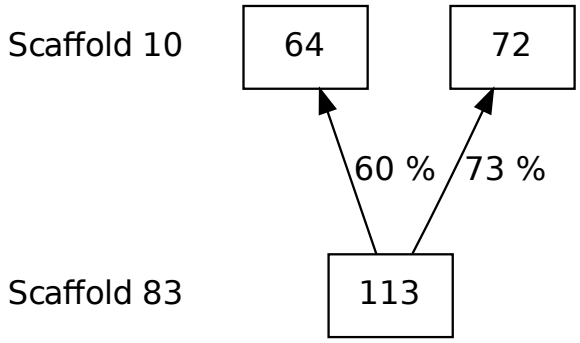

Figure H.16: Paralagous group 22 of the CRN effector family.

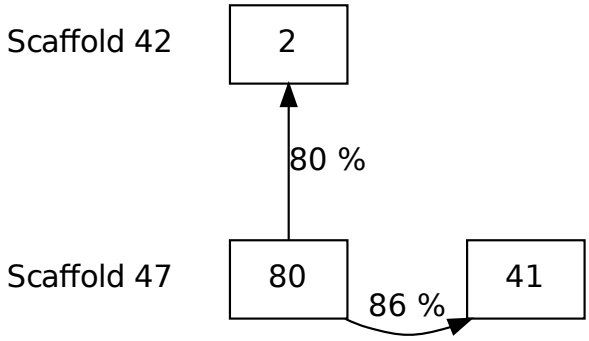

Figure H.17: Paralagous group 2 of the CRN effector family.

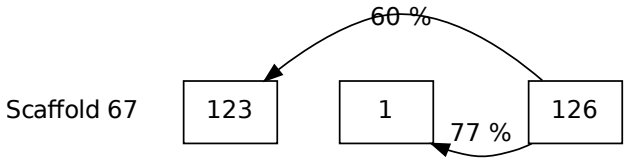

Figure H.18: Paralagous group 5 of the CRN effector family.

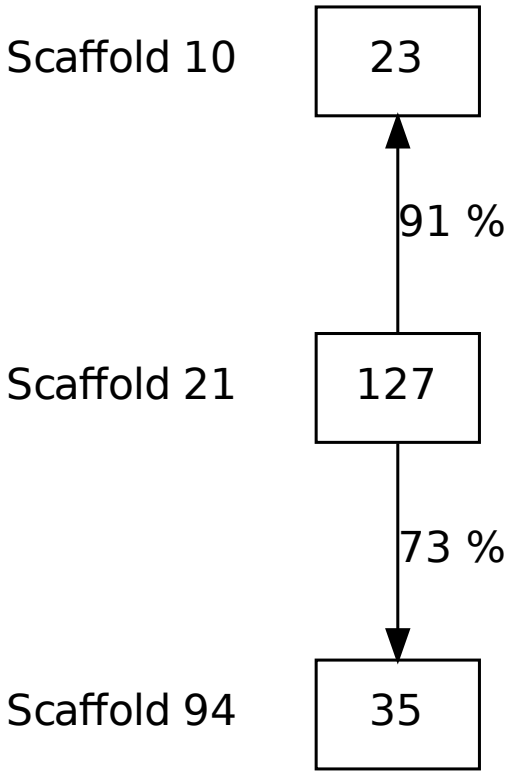

Figure H.19: Paralagous group 6 of the CRN effector family.

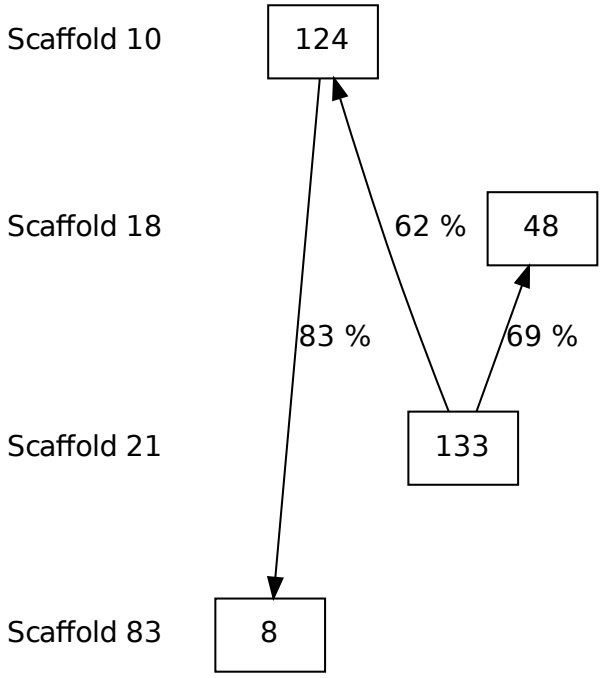

Figure H.20: Paralagous group 21 of the CRN effector family.

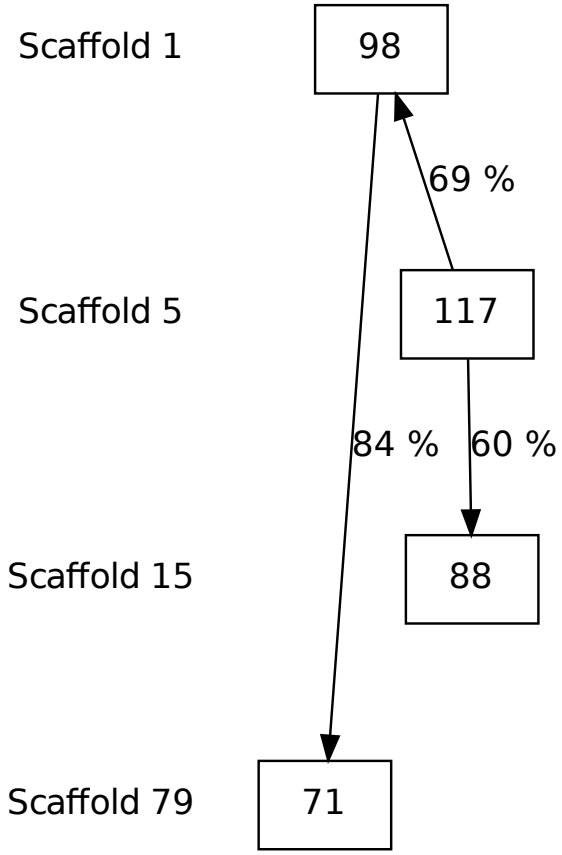

Figure H.21: Paralagous group 23 of the CRN effector family.

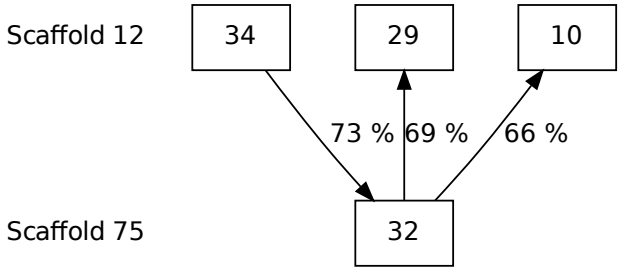

Figure H.22: Paralagous group 7 of the CRN effector family.

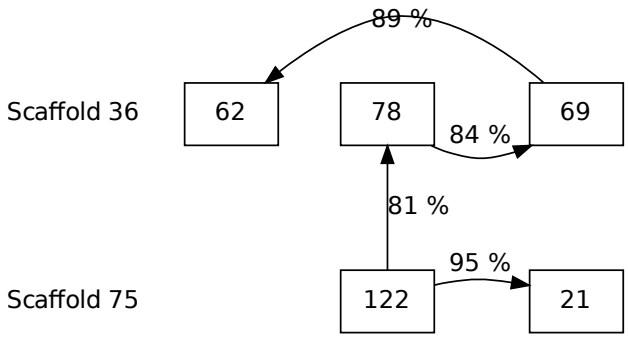

Figure H.23: Paralagous group 20 of the CRN effector family.

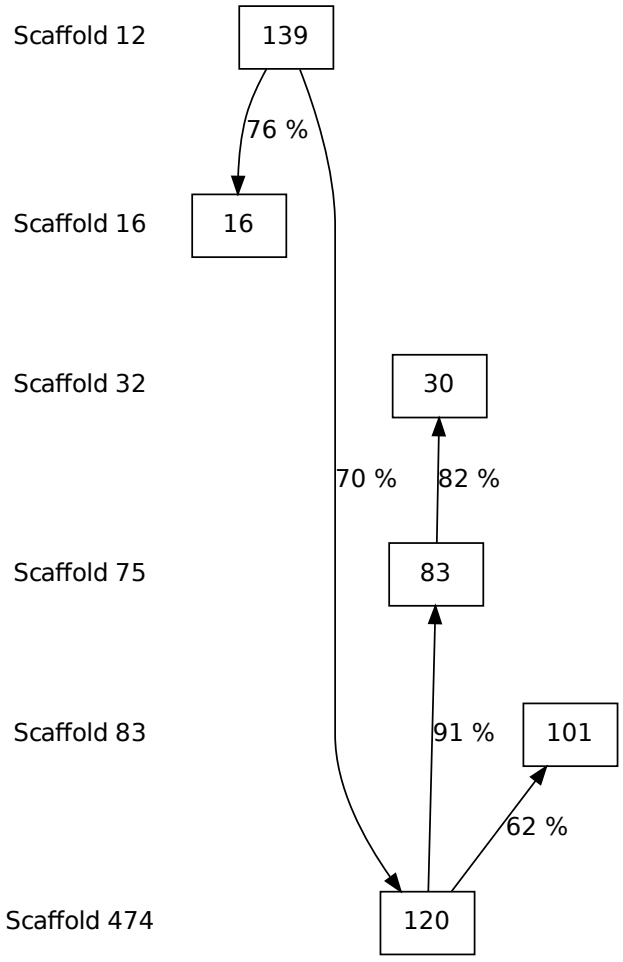

Figure H.24: Paralagous group 16 of the CRN effector family.

Appendix I

Calculated Selection Pressures on Paralagous RxLR Groups

Figure I.1: Calculated codon level selection pressure on paralagous group 0. Levels above 0 are correspondent to positive selection pressure and levels below 0 are negative selection pressures. Anything over a selection pressure of ±0.9 is considered significant.

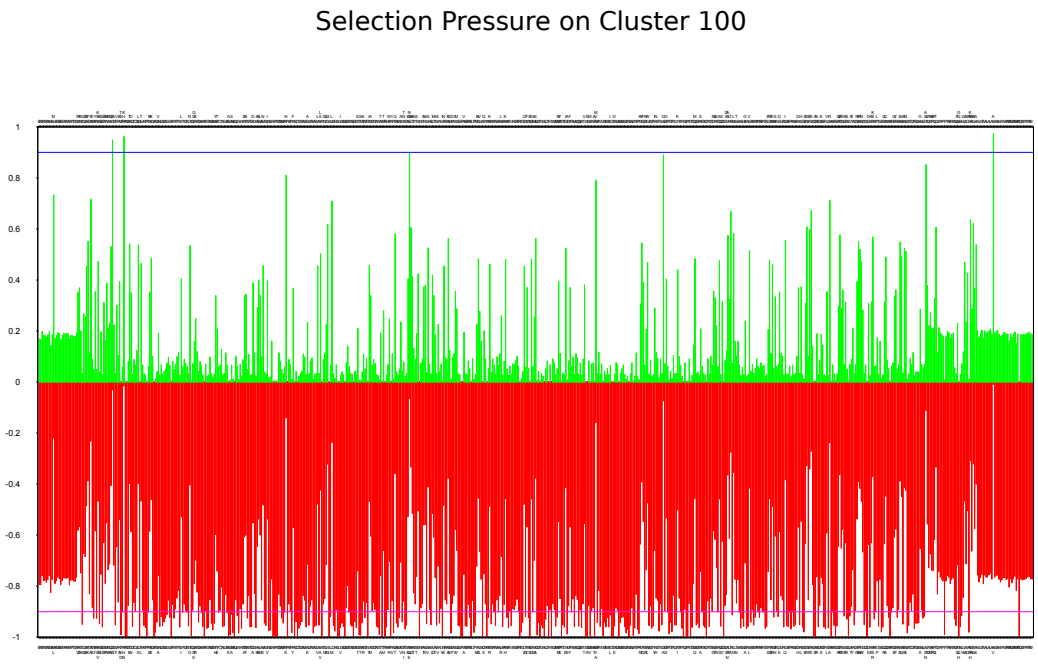

Figure I.2: Calculated codon level selection pressure on paralagous group 100. Levels above 0 are correspondent to positive selection pressure and levels below 0 are negative selection pressures. Anything over a selection pressure of ± 0.9 is considered significant.

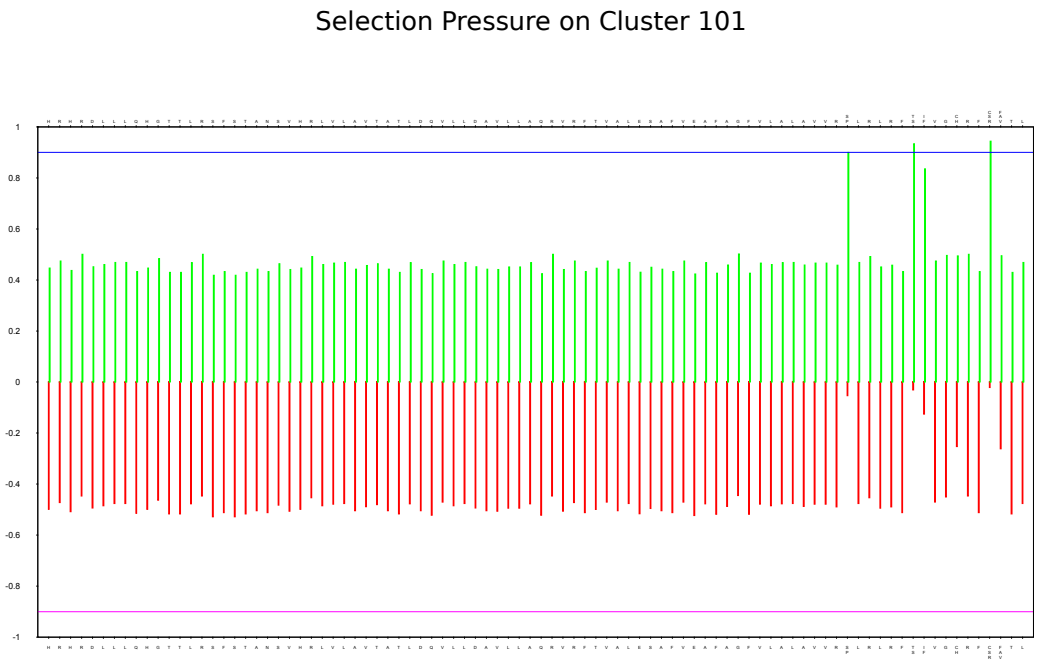

Figure I.3: Calculated codon level selection pressure on paralagous group 101. Levels above 0 are correspondent to positive selection pressure and levels below 0 are negative selection pressures. Anything over a selection pressure of ± 0.9 is considered significant.

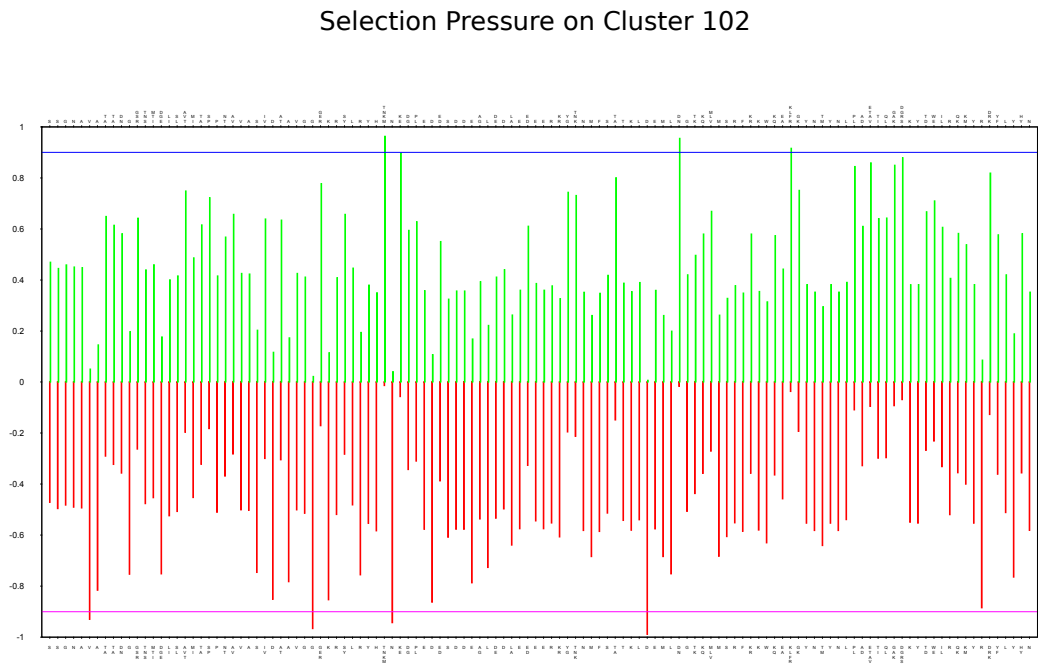

Figure I.4: Calculated codon level selection pressure on paralagous group 102. Levels above 0 are correspondent to positive selection pressure and levels below 0 are negative selection pressures. Anything over a selection pressure of ± 0.9 is considered significant.

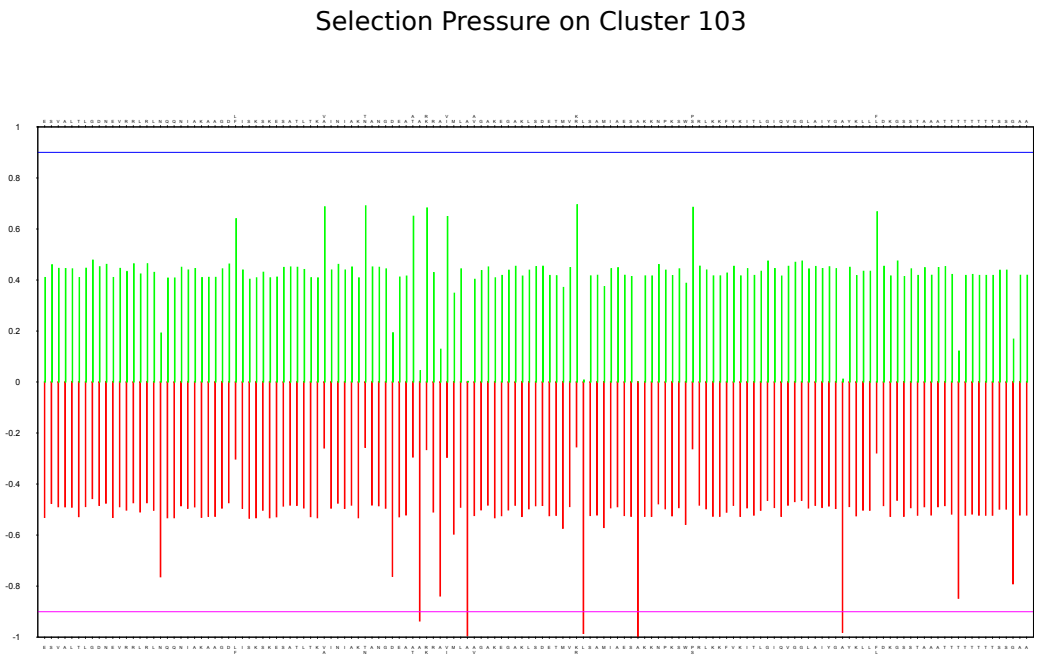

Figure I.5: Calculated codon level selection pressure on paralagous group 103. Levels above 0 are correspondent to positive selection pressure and levels below 0 are negative selection pressures. Anything over a selection pressure of ± 0.9 is considered significant.

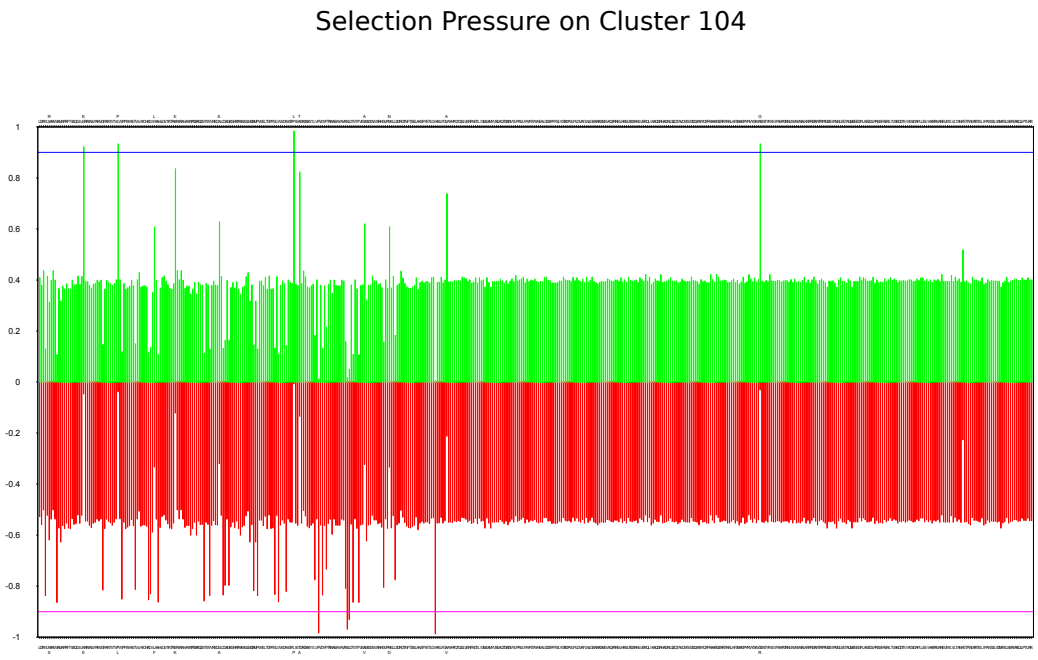

Figure I.6: Calculated codon level selection pressure on paralagous group 104. Levels above 0 are correspondent to positive selection pressure and levels below 0 are negative selection pressures. Anything over a selection pressure of ± 0.9 is considered significant.

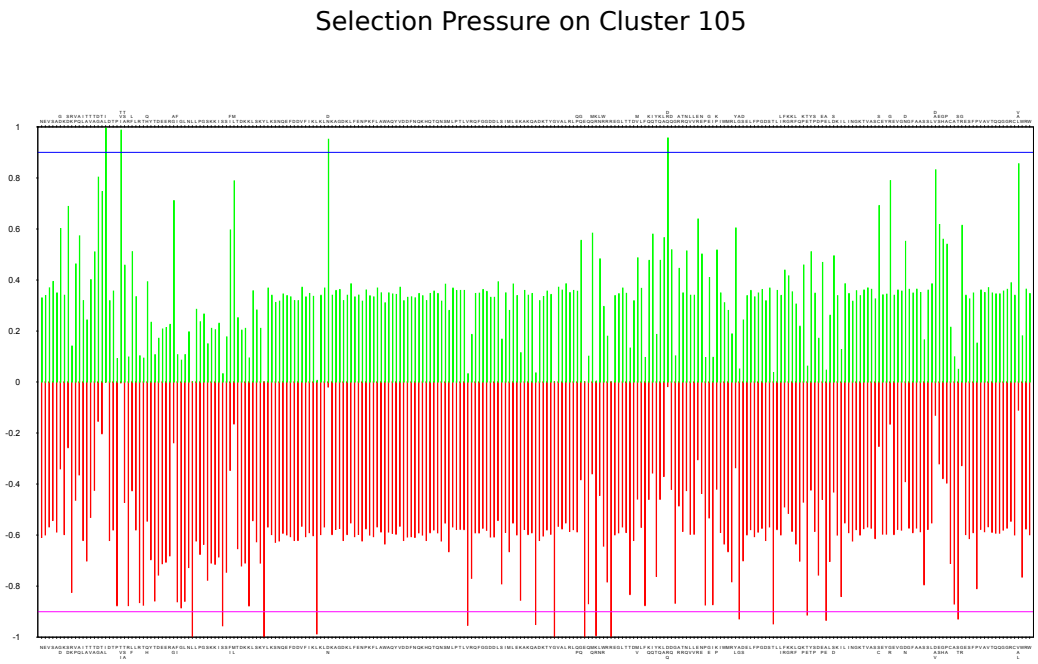

Figure I.7: Calculated codon level selection pressure on paralagous group 105. Levels above 0 are correspondent to positive selection pressure and levels below 0 are negative selection pressures. Anything over a selection pressure of ± 0.9 is considered significant.

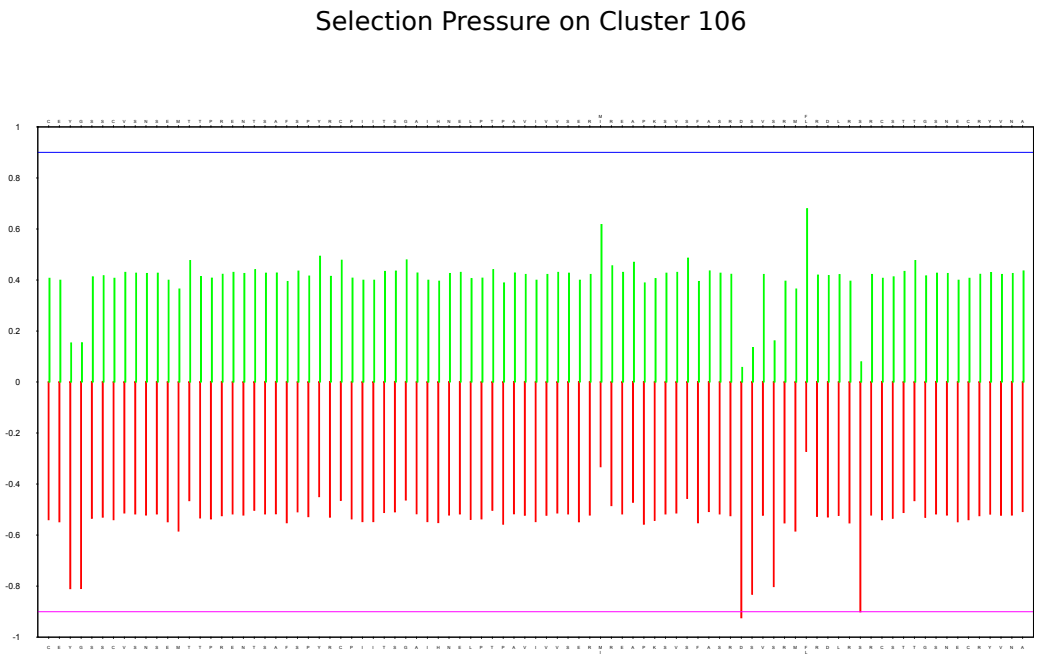

Figure I.8: Calculated codon level selection pressure on paralagous group 106. Levels above 0 are correspondent to positive selection pressure and levels below 0 are negative selection pressures. Anything over a selection pressure of ± 0.9 is considered significant.

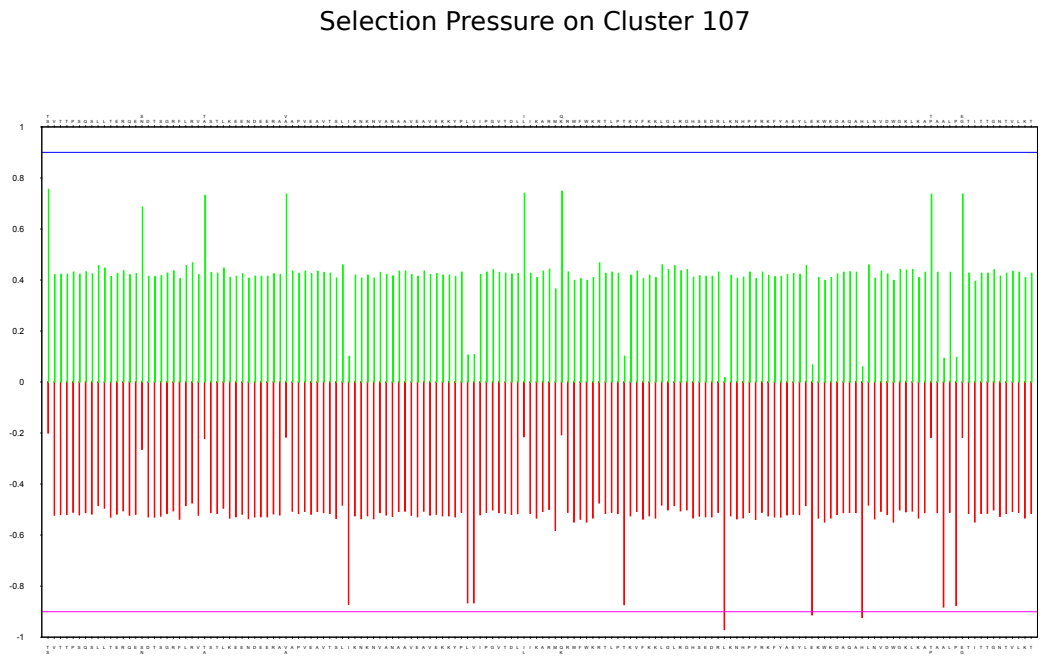

Figure I.9: Calculated codon level selection pressure on paralagous group 107. Levels above 0 are correspondent to positive selection pressure and levels below 0 are negative selection pressures. Anything over a selection pressure of ± 0.9 is considered significant.

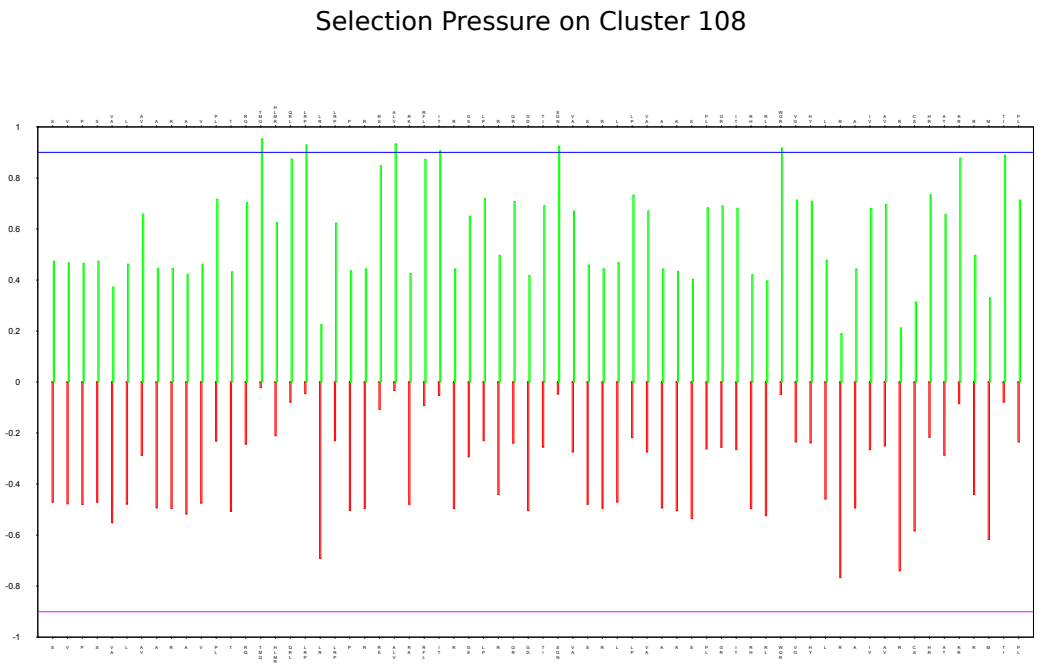

Figure I.10: Calculated codon level selection pressure on paralagous group 108. Levels above 0 are correspondent to positive selection pressure and levels below 0 are negative selection pressures. Anything over a selection pressure of ± 0.9 is considered significant.

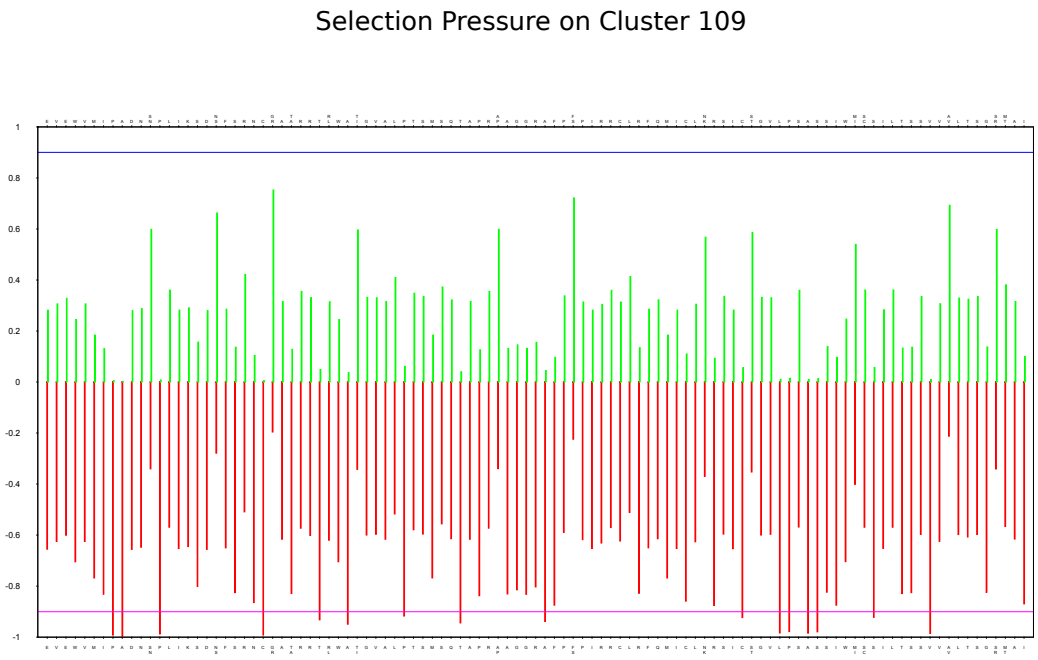

Figure I.11: Calculated codon level selection pressure on paralagous group 109. Levels above 0 are correspondent to positive selection pressure and levels below 0 are negative selection pressures. Anything over a selection pressure of ± 0.9 is considered significant.

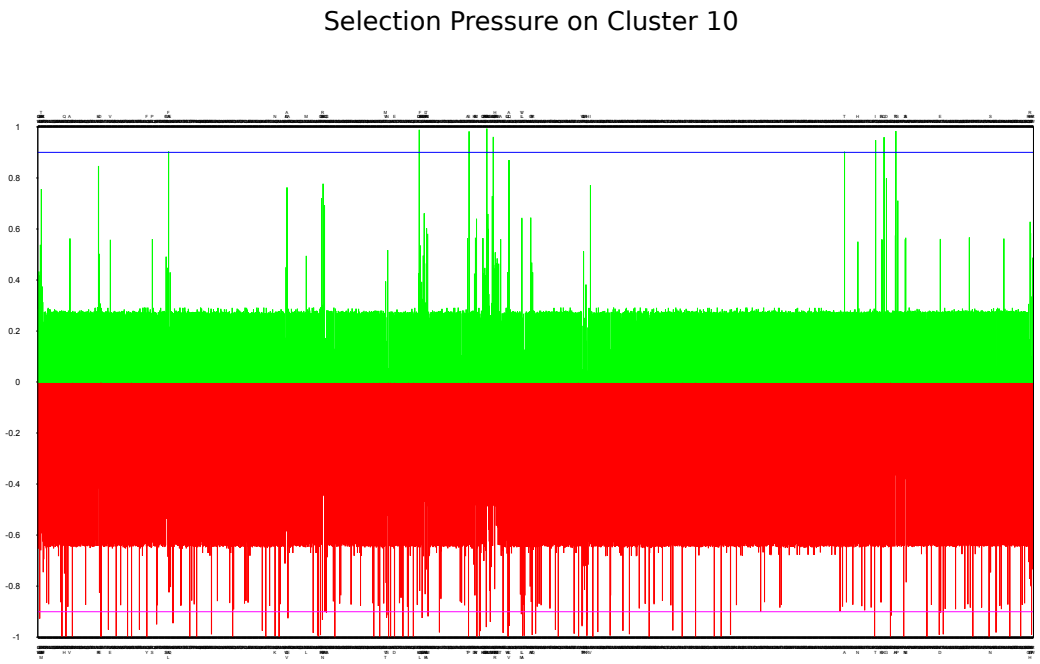

Figure I.12: Calculated codon level selection pressure on paralagous group 10. Levels above 0 are correspondent to positive selection pressure and levels below 0 are negative selection pressures. Anything over a selection pressure of ± 0.9 is considered significant.

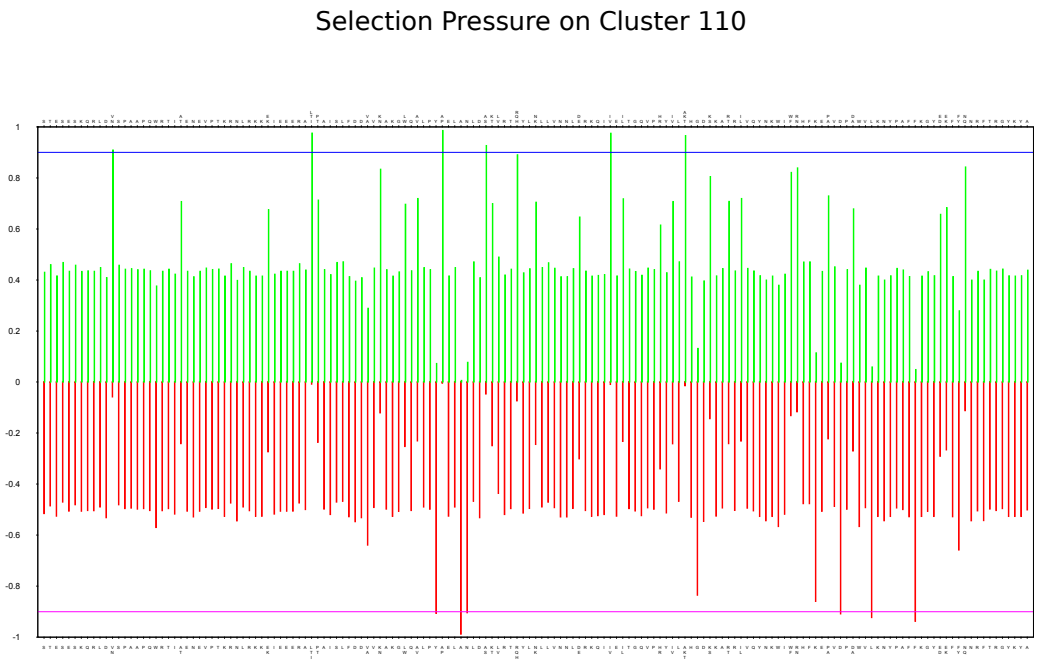

Figure I.13: Calculated codon level selection pressure on paralagous group 110. Levels above 0 are correspondent to positive selection pressure and levels below 0 are negative selection pressures. Anything over a selection pressure of ± 0.9 is considered significant.

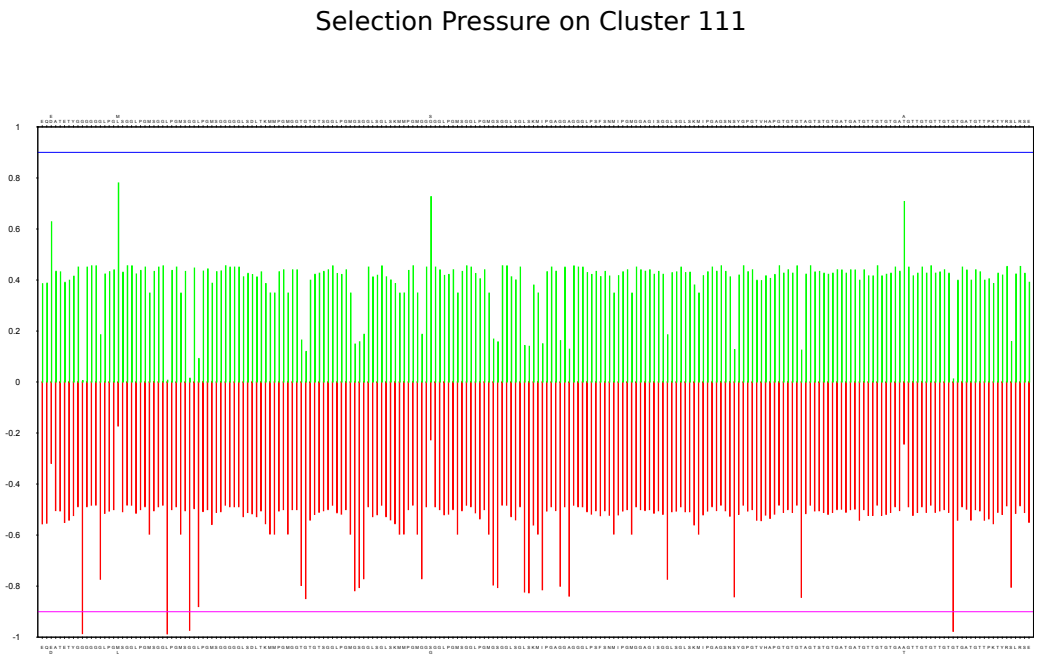

Figure I.14: Calculated codon level selection pressure on paralagous group 111. Levels above 0 are correspondent to positive selection pressure and levels below 0 are negative selection pressures. Anything over a selection pressure of ± 0.9 is considered significant.

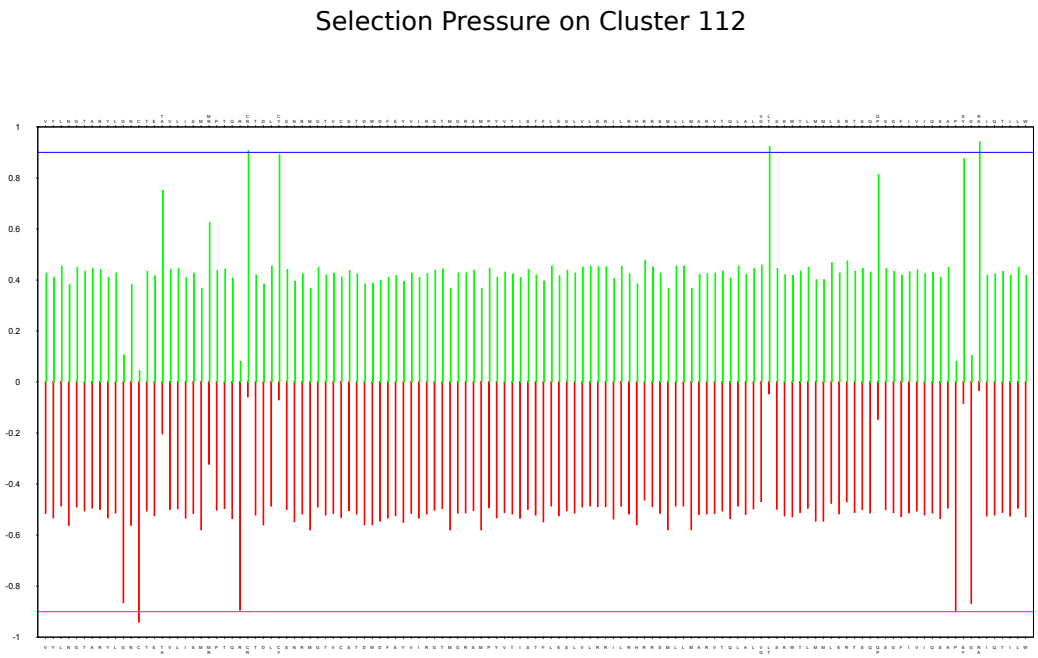

Figure I.15: Calculated codon level selection pressure on paralagous group 112. Levels above 0 are correspondent to positive selection pressure and levels below 0 are negative selection pressures. Anything over a selection pressure of ± 0.9 is considered significant.

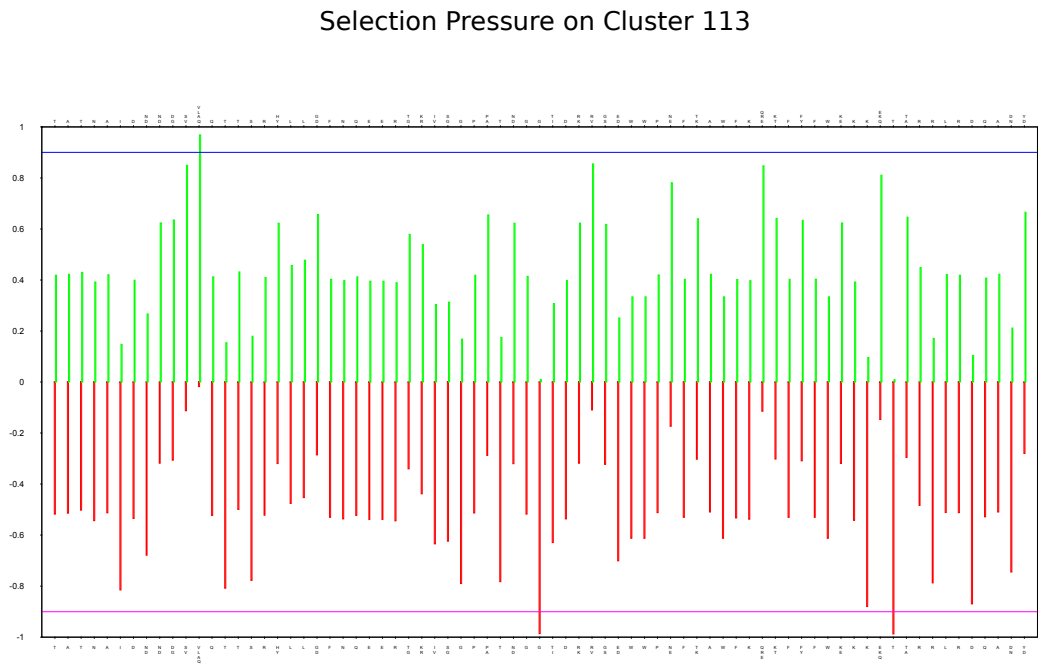

Figure I.16: Calculated codon level selection pressure on paralagous group 113. Levels above 0 are correspondent to positive selection pressure and levels below 0 are negative selection pressures. Anything over a selection pressure of ± 0.9 is considered significant.

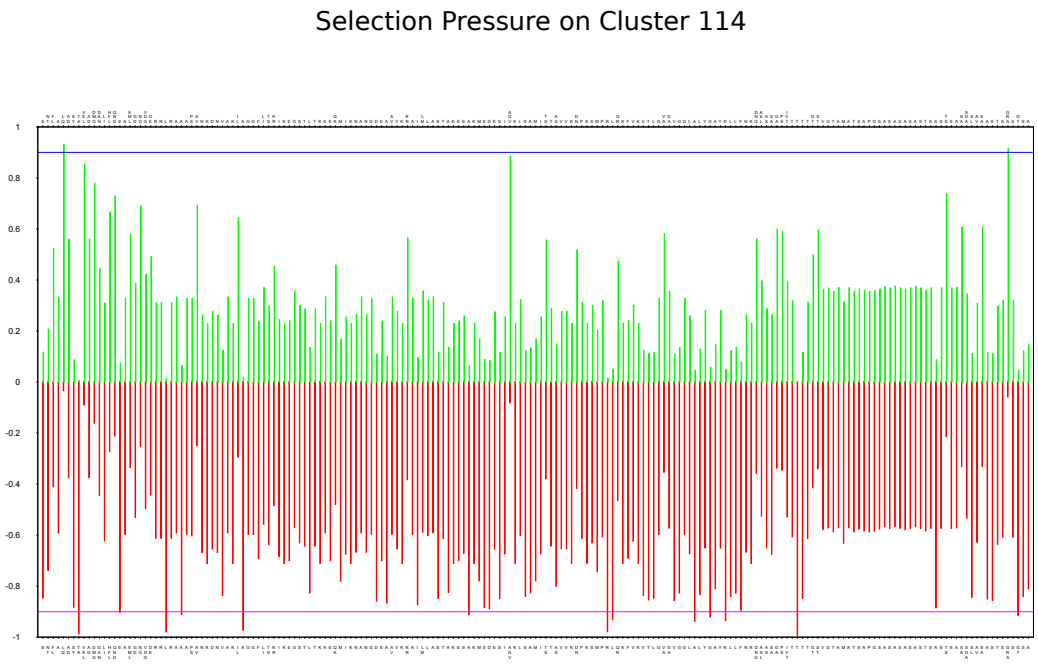

Figure I.17: Calculated codon level selection pressure on paralagous group 114. Levels above 0 are correspondent to positive selection pressure and levels below 0 are negative selection pressures. Anything over a selection pressure of ± 0.9 is considered significant.

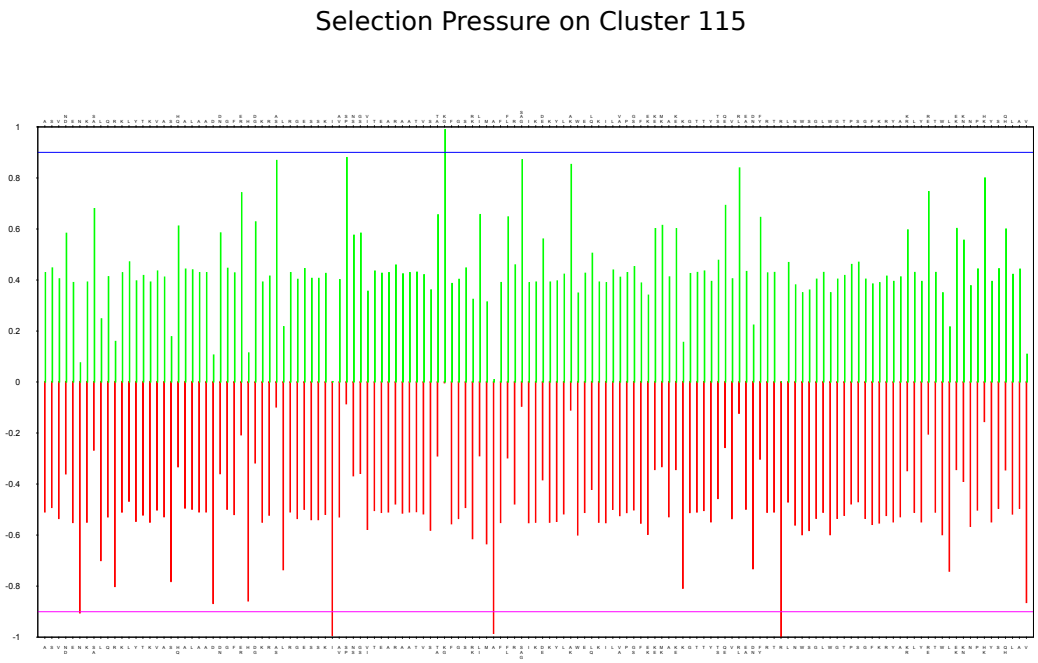

Figure I.18: Calculated codon level selection pressure on paralagous group 115. Levels above 0 are correspondent to positive selection pressure and levels below 0 are negative selection pressures. Anything over a selection pressure of ± 0.9 is considered significant.

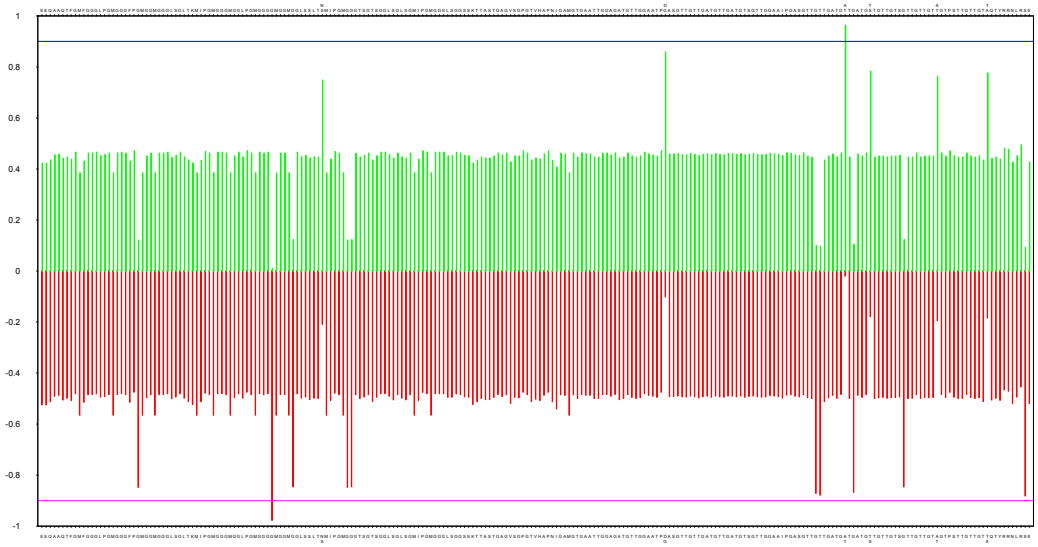

Figure I.19: Calculated codon level selection pressure on paralagous group 116. Levels above 0 are correspondent to positive selection pressure and levels below 0 are negative selection pressures. Anything over a selection pressure of ± 0.9 is considered significant.

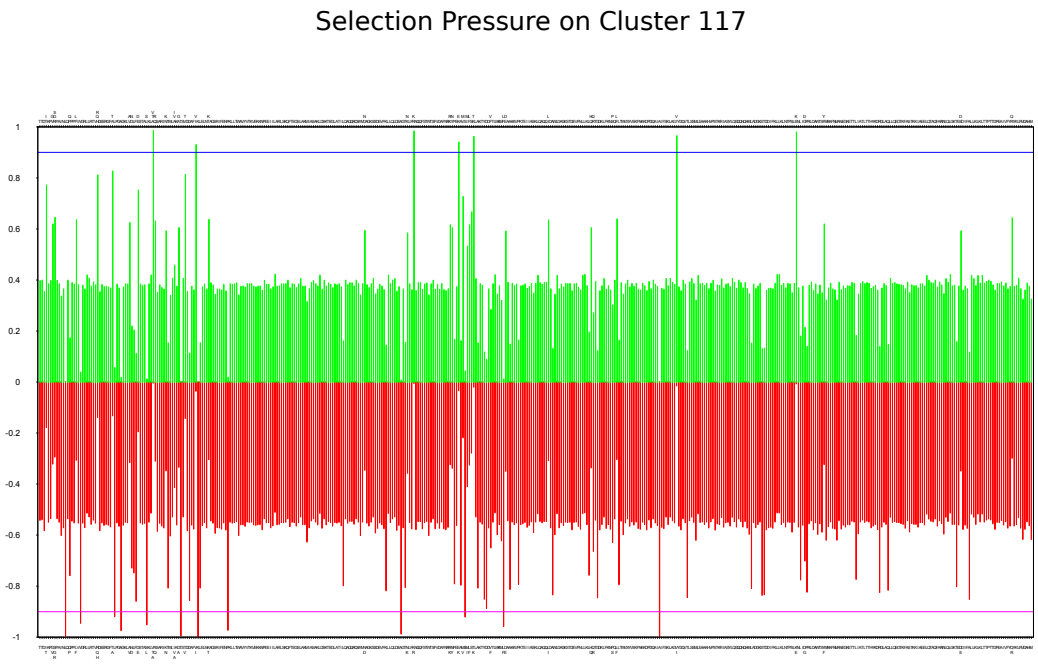

Figure I.20: Calculated codon level selection pressure on paralagous group 117. Levels above 0 are correspondent to positive selection pressure and levels below 0 are negative selection pressures. Anything over a selection pressure of ± 0.9 is considered significant.

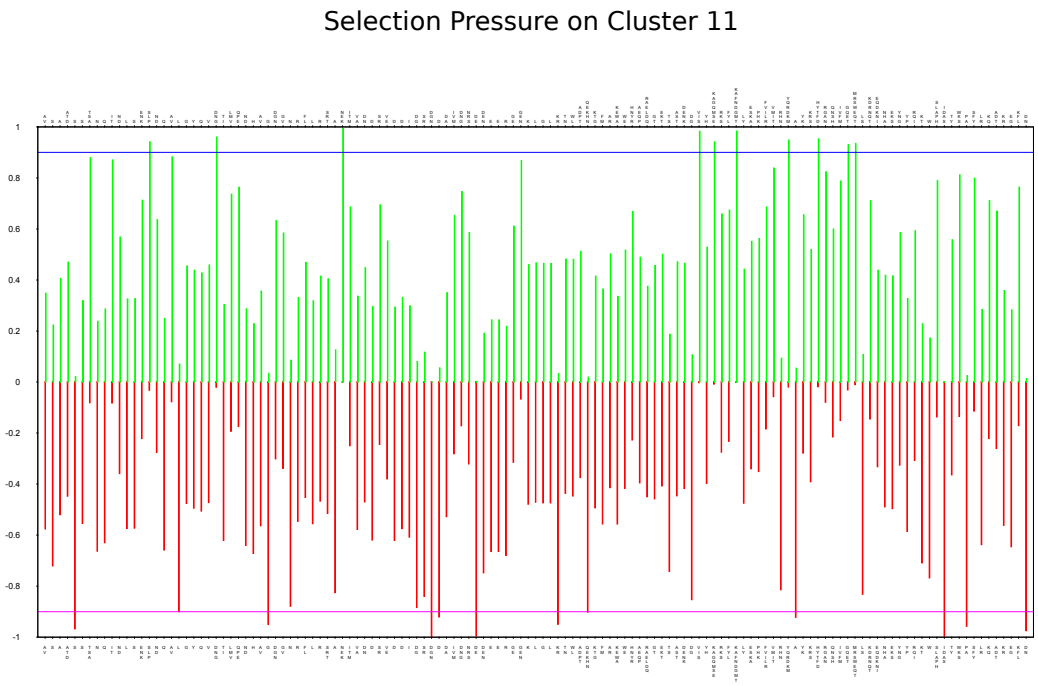

Figure I.21: Calculated codon level selection pressure on paralagous group 11. Levels above 0 are correspondent to positive selection pressure and levels below 0 are negative selection pressures. Anything over a selection pressure of ± 0.9 is considered significant.

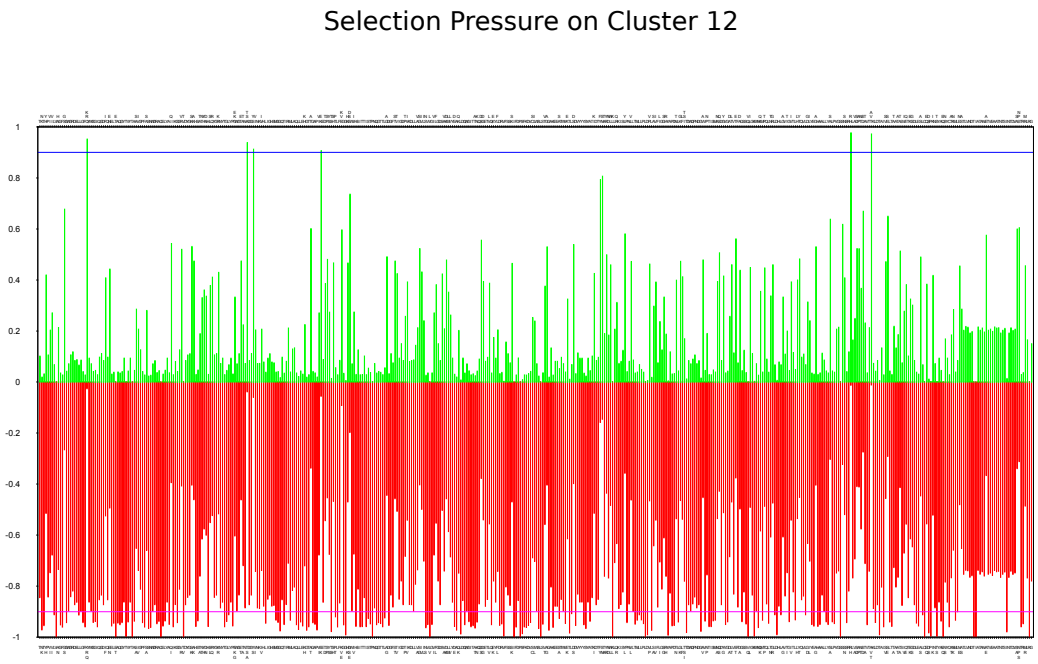

Figure I.22: Calculated codon level selection pressure on paralagous group 12. Levels above 0 are correspondent to positive selection pressure and levels below 0 are negative selection pressures. Anything over a selection pressure of ± 0.9 is considered significant.

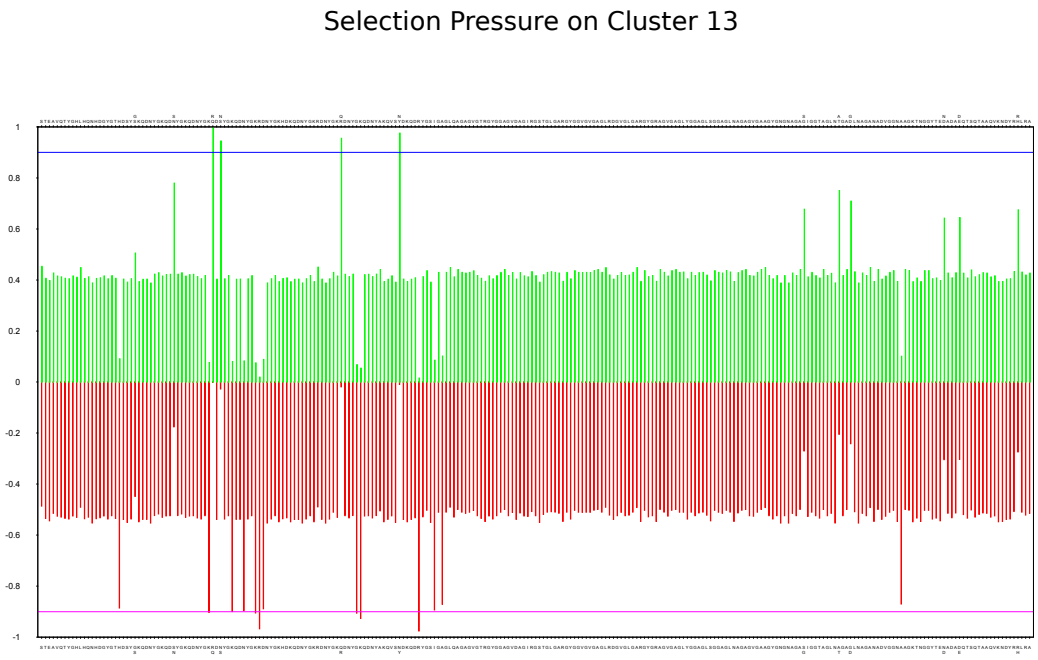

Figure I.23: Calculated codon level selection pressure on paralagous group 13. Levels above 0 are correspondent to positive selection pressure and levels below 0 are negative selection pressures. Anything over a selection pressure of ± 0.9 is considered significant.

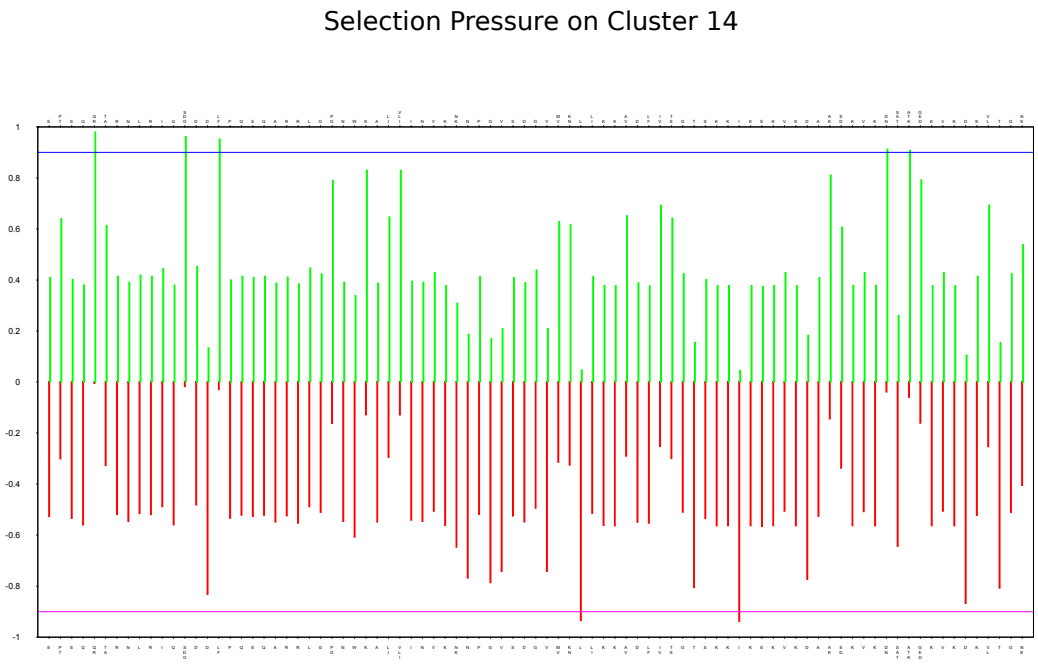

Figure I.24: Calculated codon level selection pressure on paralagous group 14. Levels above 0 are correspondent to positive selection pressure and levels below 0 are negative selection pressures. Anything over a selection pressure of ± 0.9 is considered significant.

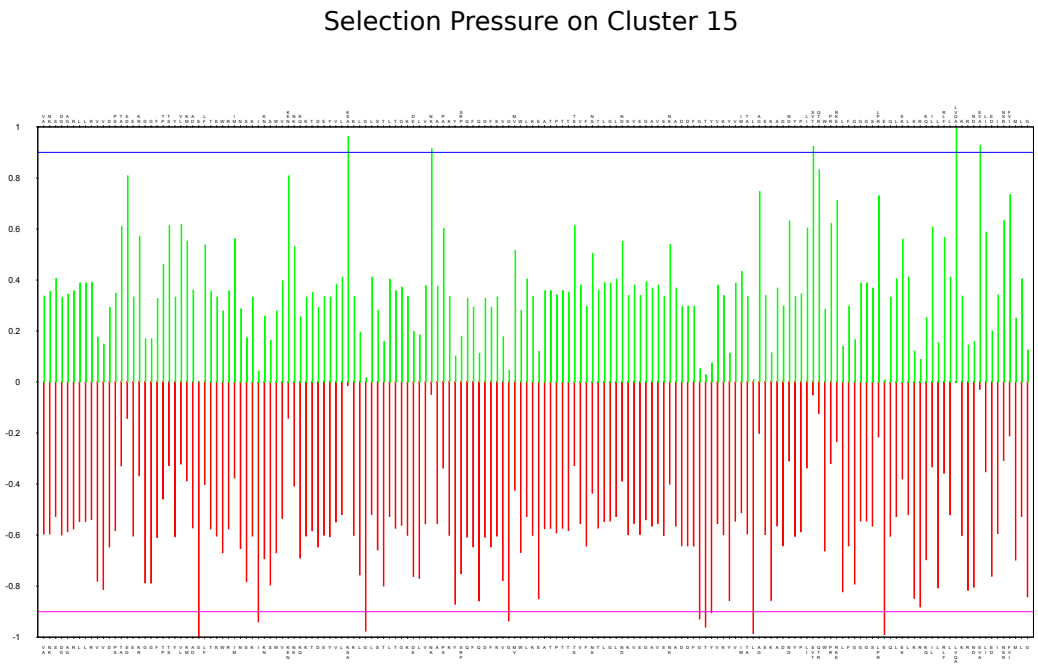

Figure I.25: Calculated codon level selection pressure on paralagous group 15. Levels above 0 are correspondent to positive selection pressure and levels below 0 are negative selection pressures. Anything over a selection pressure of ± 0.9 is considered significant.

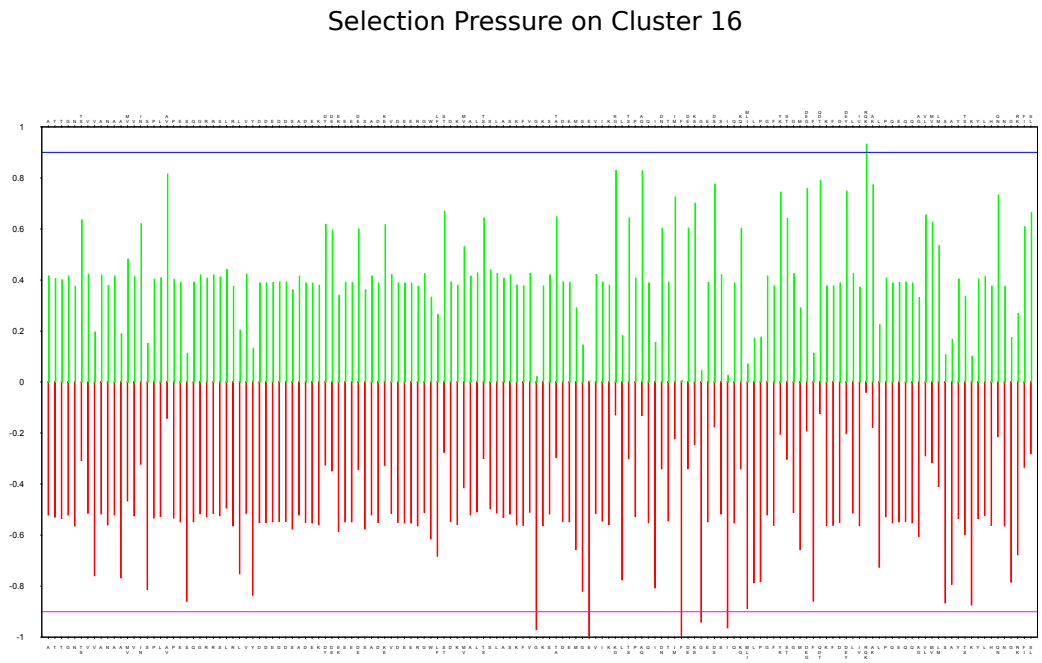

Figure I.26: Calculated codon level selection pressure on paralagous group 16. Levels above 0 are correspondent to positive selection pressure and levels below 0 are negative selection pressures. Anything over a selection pressure of ± 0.9 is considered significant.

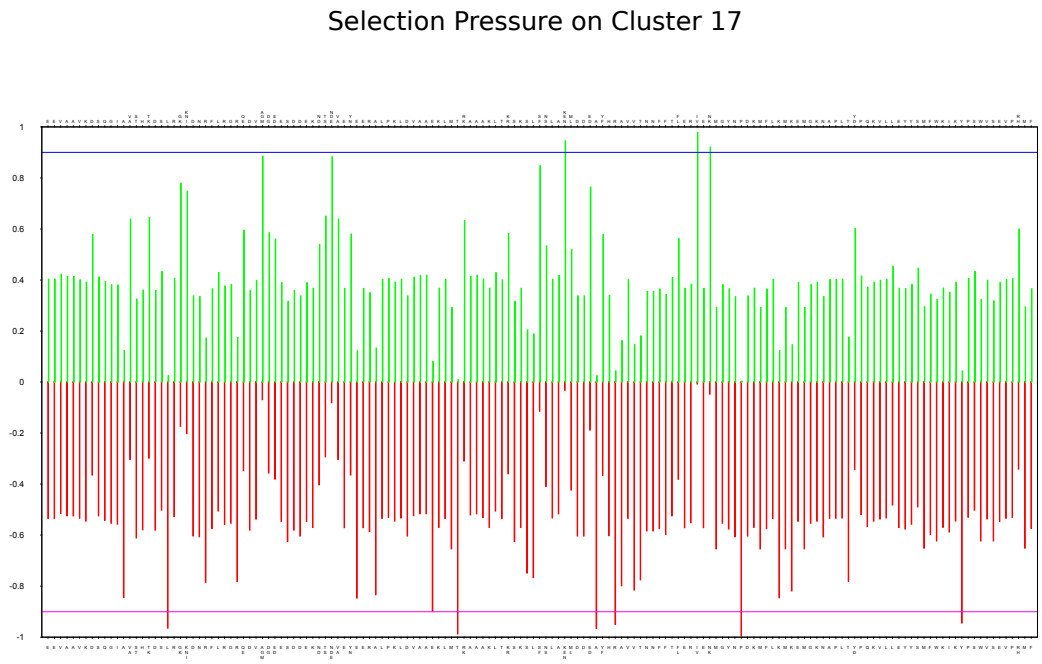

Figure I.27: Calculated codon level selection pressure on paralagous group 17. Levels above 0 are correspondent to positive selection pressure and levels below 0 are negative selection pressures. Anything over a selection pressure of ± 0.9 is considered significant.

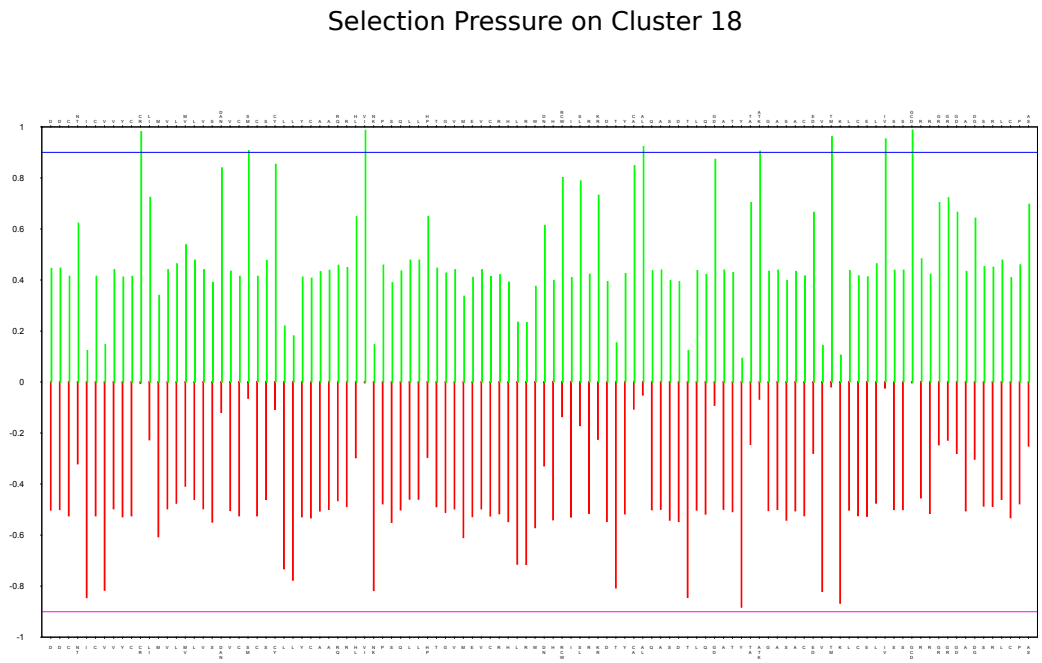

Figure I.28: Calculated codon level selection pressure on paralagous group 18. Levels above 0 are correspondent to positive selection pressure and levels below 0 are negative selection pressures. Anything over a selection pressure of ± 0.9 is considered significant.

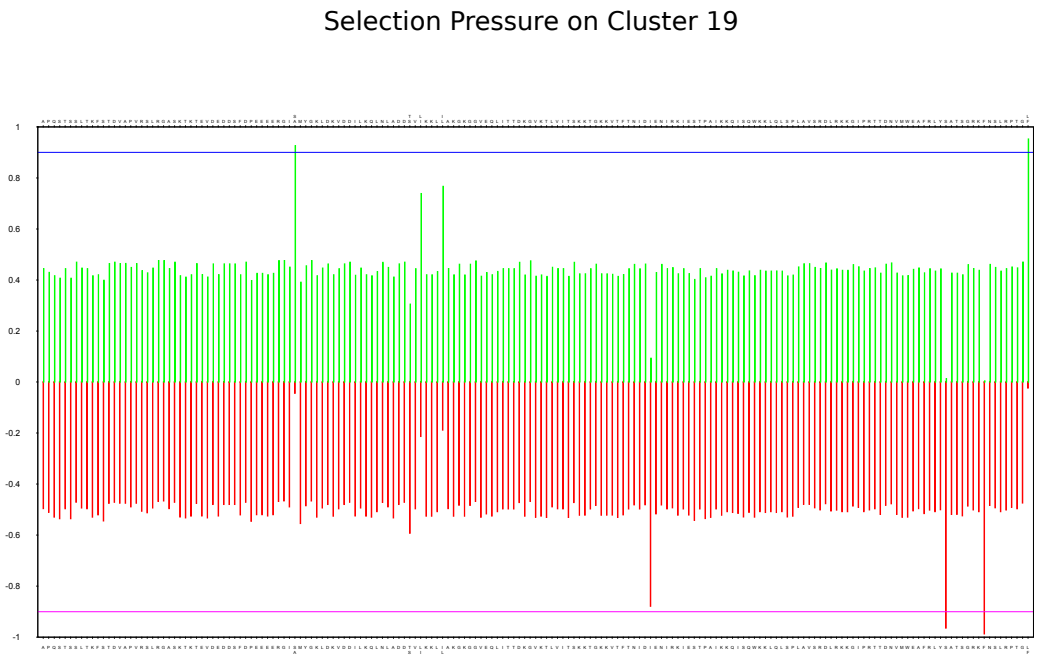

Figure I.29: Calculated codon level selection pressure on paralagous group 19. Levels above 0 are correspondent to positive selection pressure and levels below 0 are negative selection pressures. Anything over a selection pressure of ± 0.9 is considered significant.

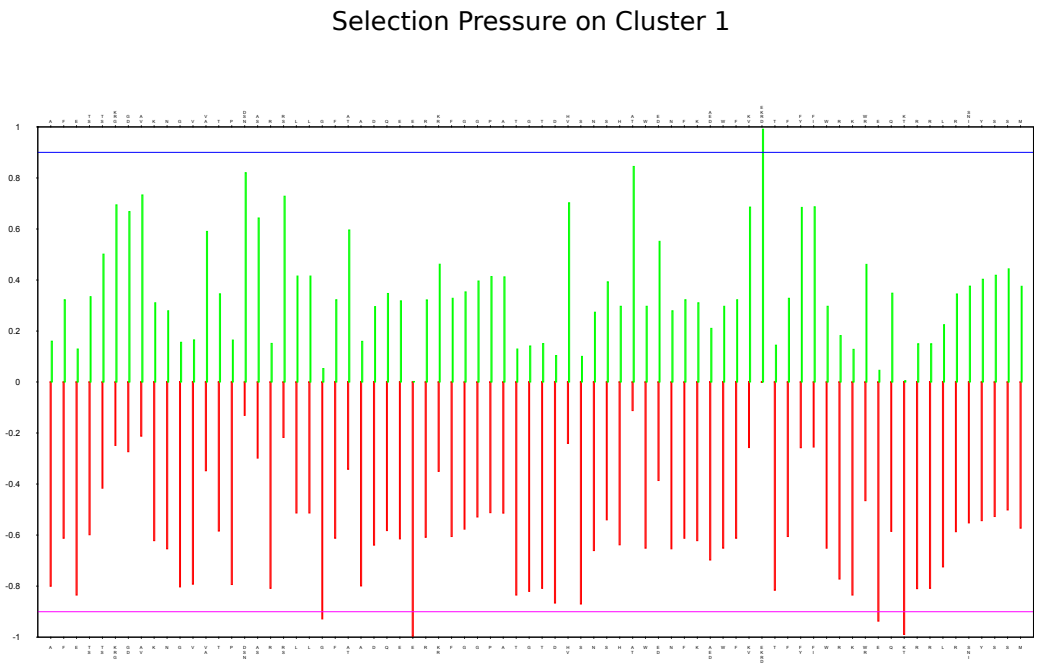

Figure I.30: Calculated codon level selection pressure on paralagous group 1. Levels above 0 are correspondent to positive selection pressure and levels below 0 are negative selection pressures. Anything over a selection pressure of ± 0.9 is considered significant.

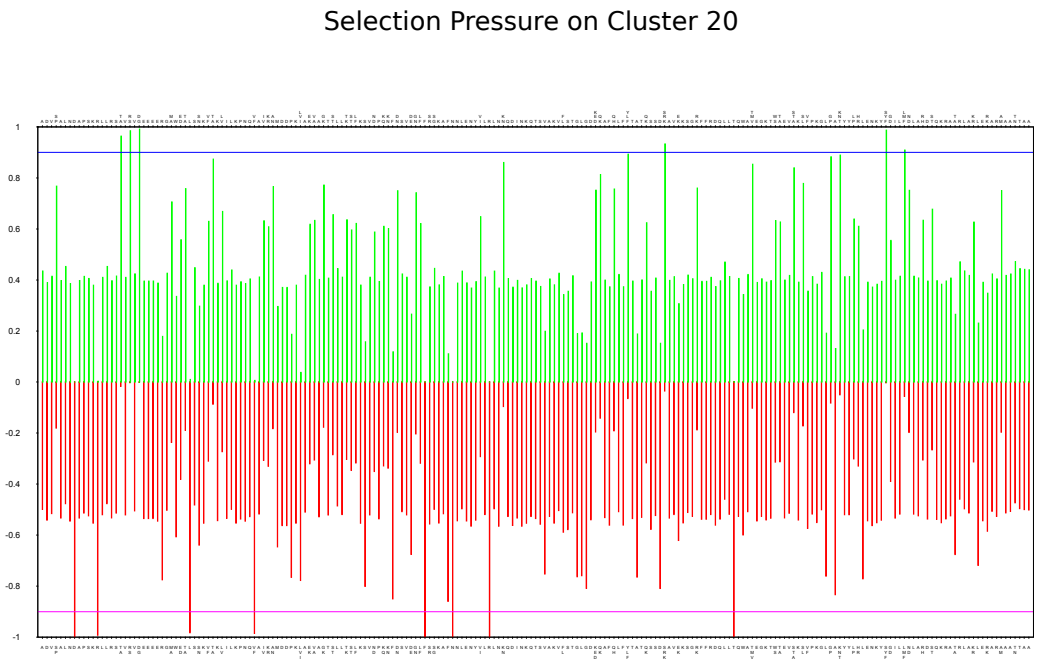

Figure I.31: Calculated codon level selection pressure on paralagous group 20. Levels above 0 are correspondent to positive selection pressure and levels below 0 are negative selection pressures. Anything over a selection pressure of ± 0.9 is considered significant.

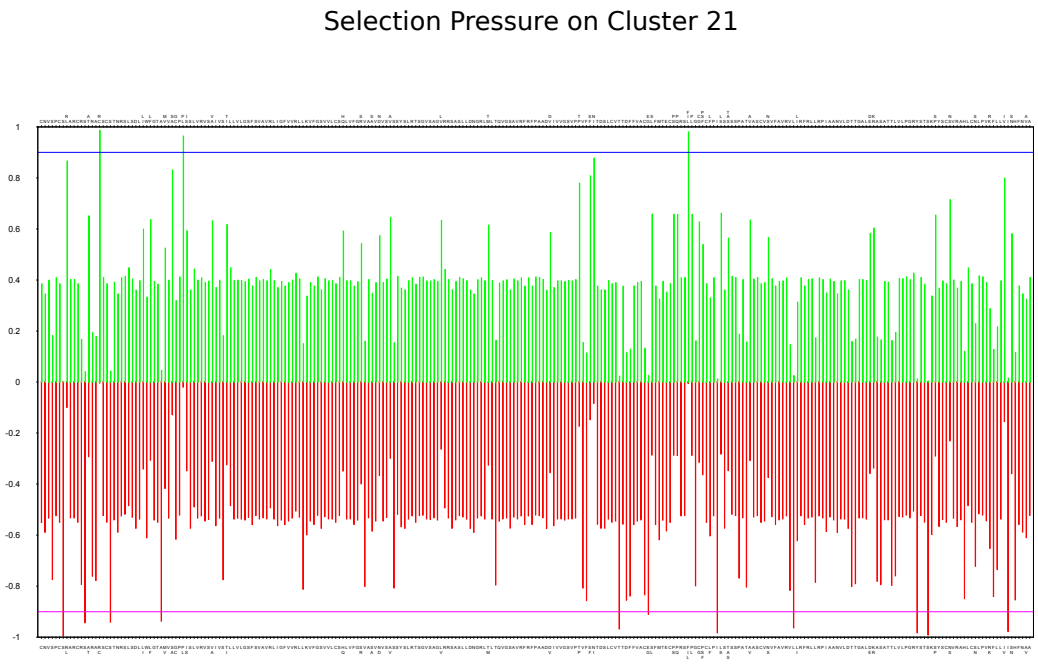

Figure I.32: Calculated codon level selection pressure on paralagous group 21. Levels above 0 are correspondent to positive selection pressure and levels below 0 are negative selection pressures. Anything over a selection pressure of ± 0.9 is considered significant.

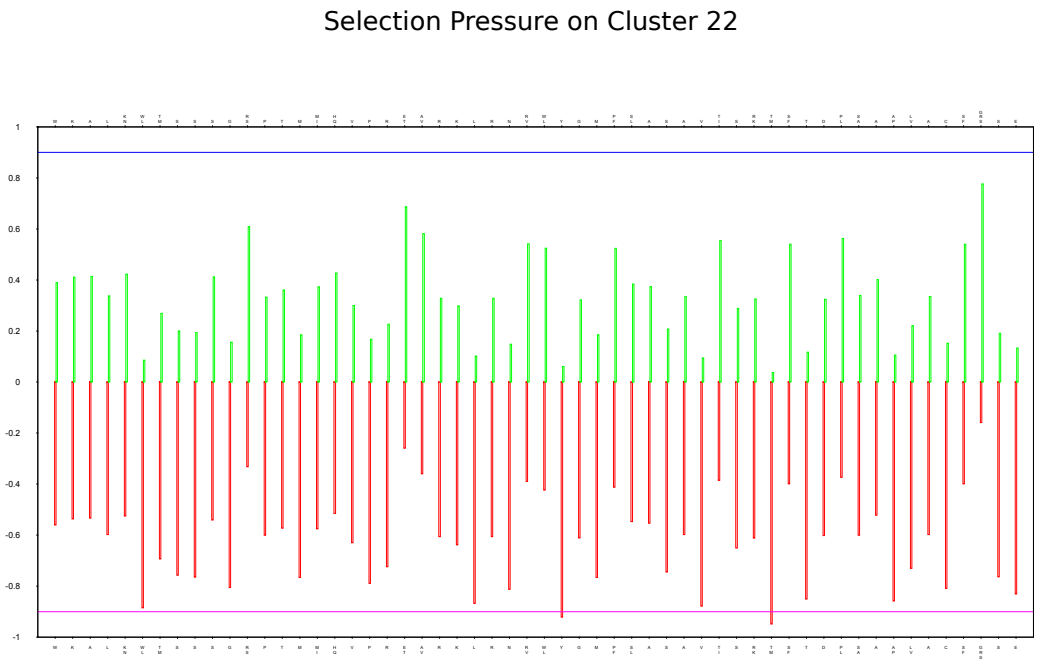

Figure I.33: Calculated codon level selection pressure on paralagous group 22. Levels above 0 are correspondent to positive selection pressure and levels below 0 are negative selection pressures. Anything over a selection pressure of ± 0.9 is considered significant.

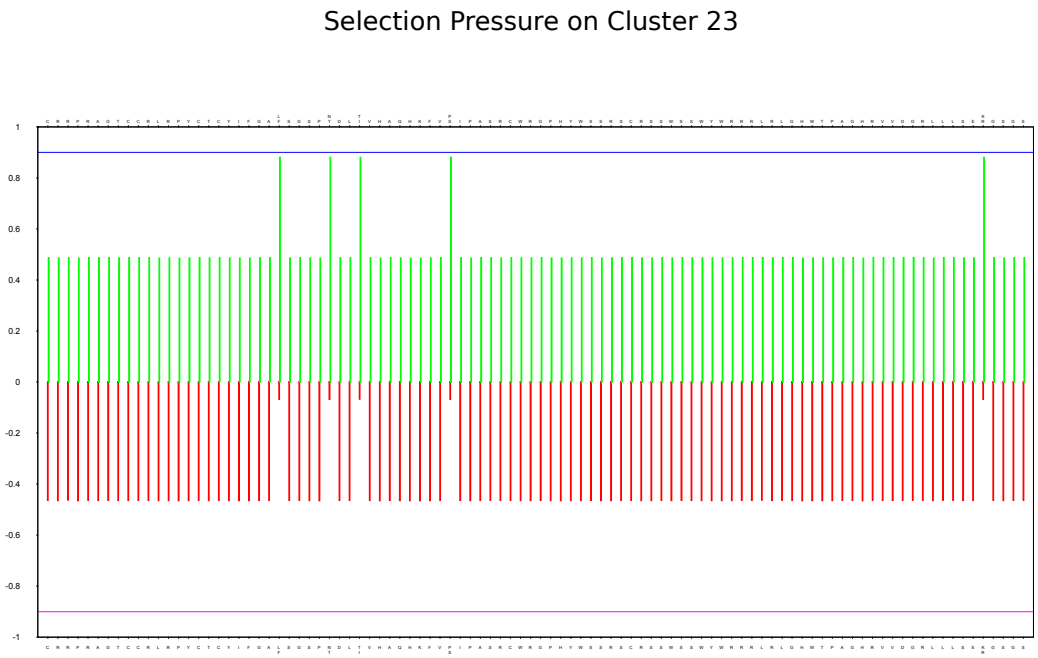

Figure I.34: Calculated codon level selection pressure on paralagous group 23. Levels above 0 are correspondent to positive selection pressure and levels below 0 are negative selection pressures. Anything over a selection pressure of ± 0.9 is considered significant.

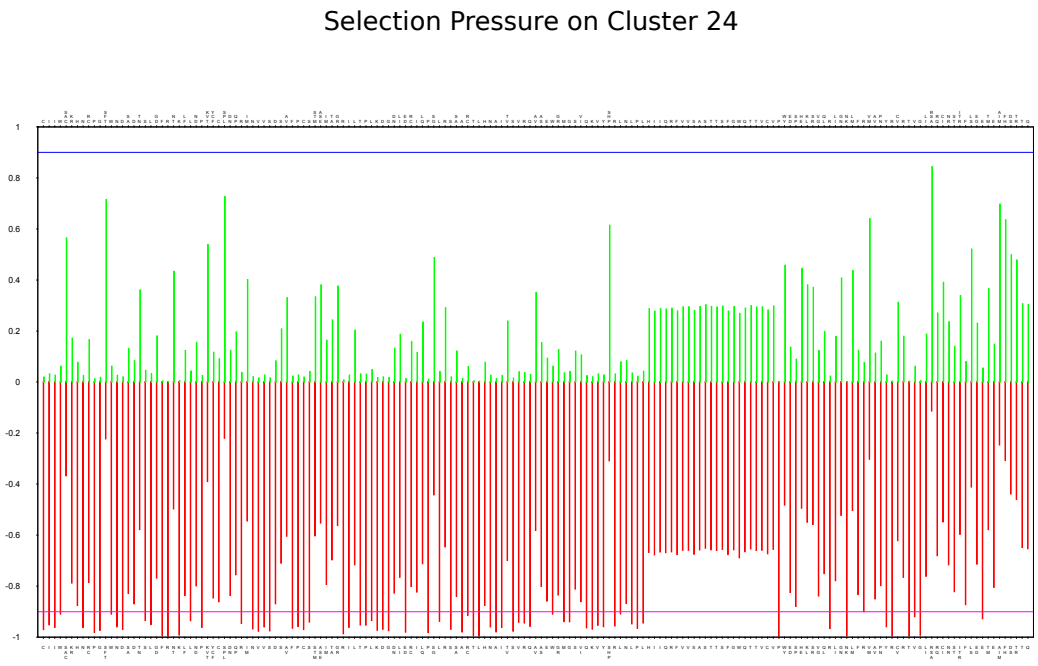

Figure I.35: Calculated codon level selection pressure on paralagous group 24. Levels above 0 are correspondent to positive selection pressure and levels below 0 are negative selection pressures. Anything over a selection pressure of ± 0.9 is considered significant.

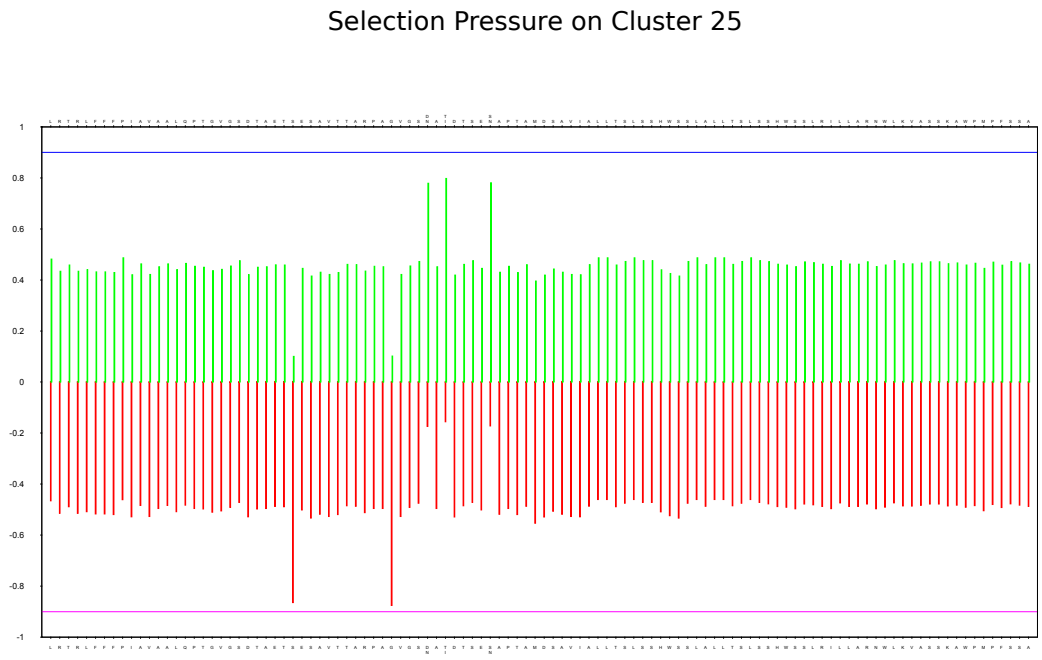

Figure I.36: Calculated codon level selection pressure on paralagous group 25. Levels above 0 are correspondent to positive selection pressure and levels below 0 are negative selection pressures. Anything over a selection pressure of ± 0.9 is considered significant.

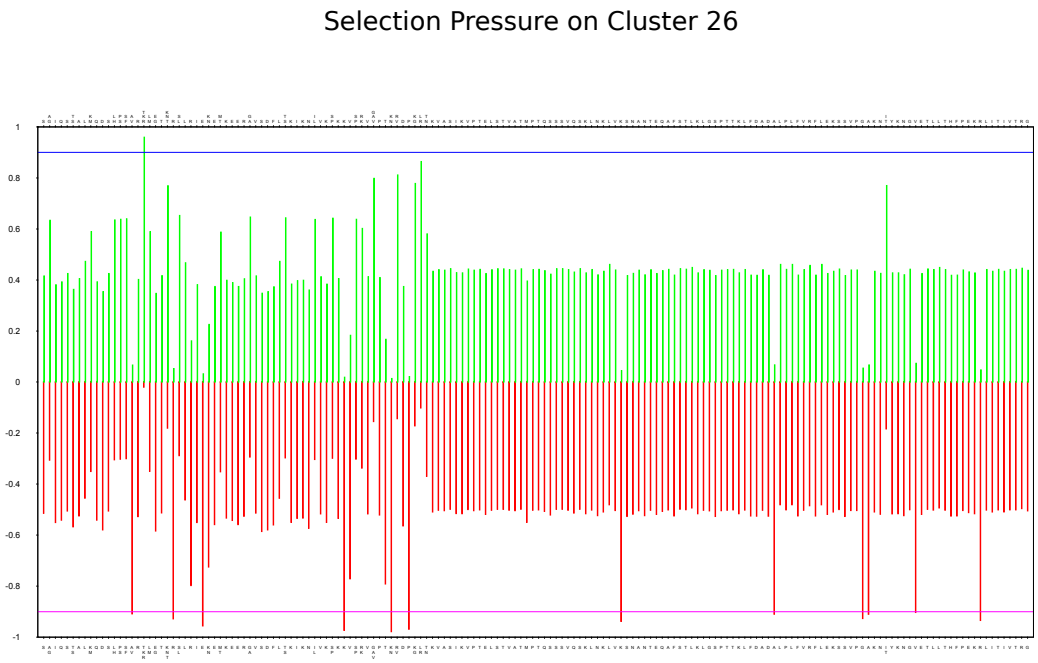

Figure I.37: Calculated codon level selection pressure on paralagous group 26. Levels above 0 are correspondent to positive selection pressure and levels below 0 are negative selection pressures. Anything over a selection pressure of ± 0.9 is considered significant.

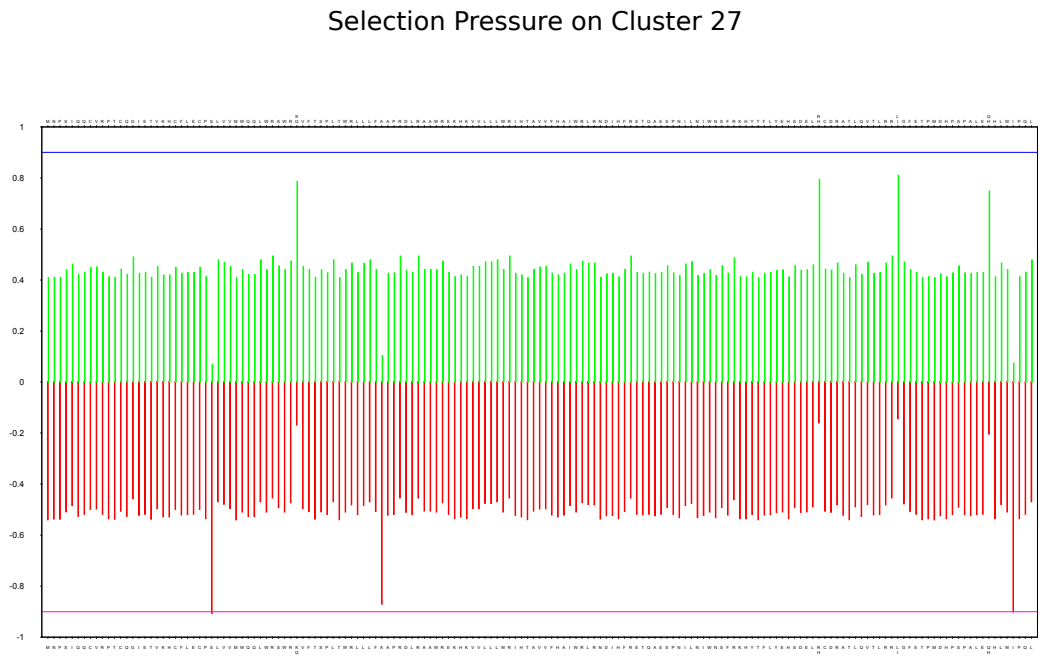

Figure I.38: Calculated codon level selection pressure on paralagous group 27. Levels above 0 are correspondent to positive selection pressure and levels below 0 are negative selection pressures. Anything over a selection pressure of ± 0.9 is considered significant.

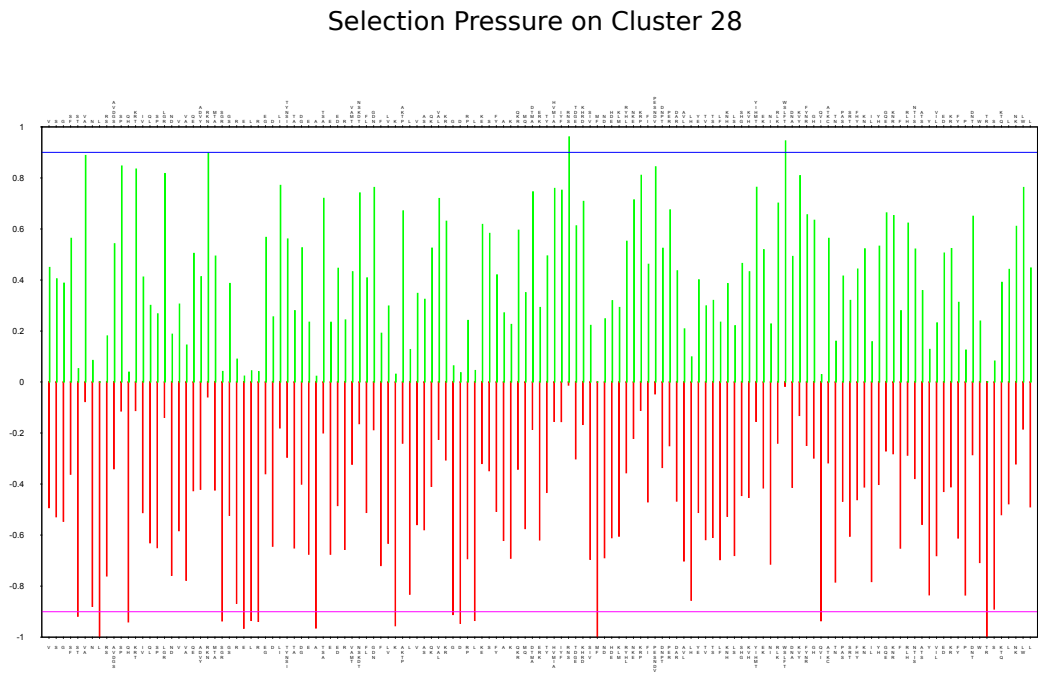

Figure I.39: Calculated codon level selection pressure on paralagous group 28. Levels above 0 are correspondent to positive selection pressure and levels below 0 are negative selection pressures. Anything over a selection pressure of ± 0.9 is considered significant.

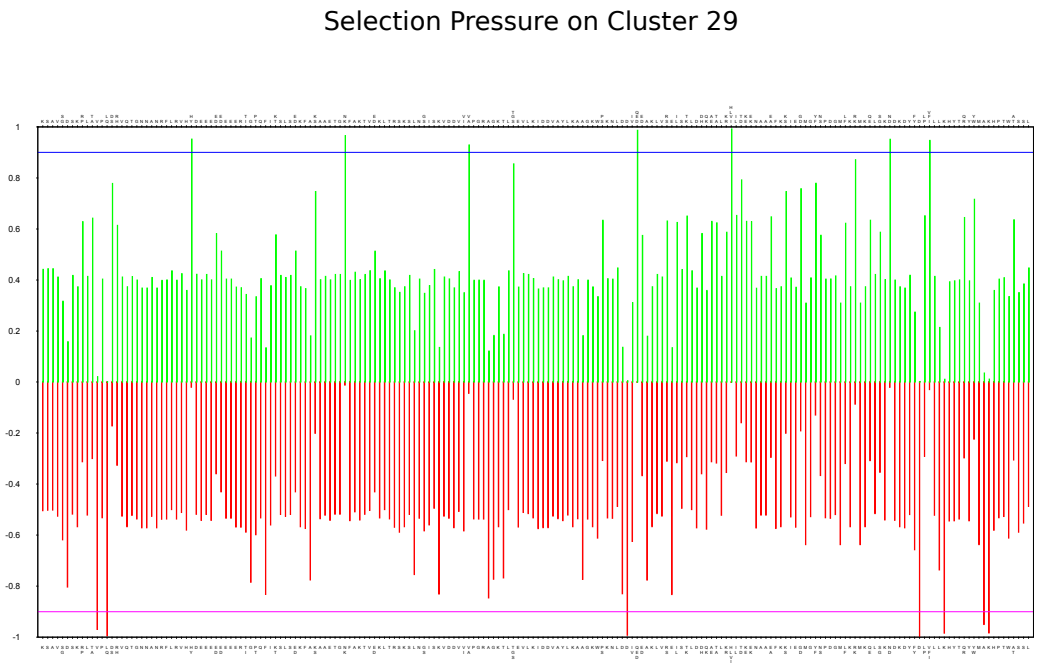

Figure I.40: Calculated codon level selection pressure on paralagous group 29. Levels above 0 are correspondent to positive selection pressure and levels below 0 are negative selection pressures. Anything over a selection pressure of ± 0.9 is considered significant.

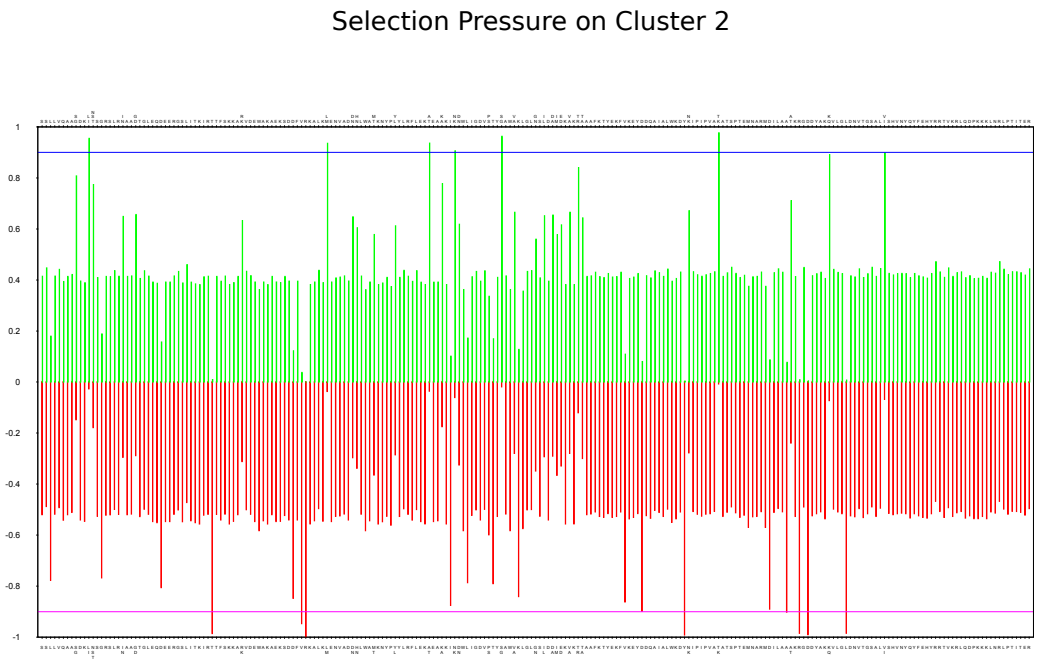

Figure I.41: Calculated codon level selection pressure on paralagous group 2. Levels above 0 are correspondent to positive selection pressure and levels below 0 are negative selection pressures. Anything over a selection pressure of ± 0.9 is considered significant.

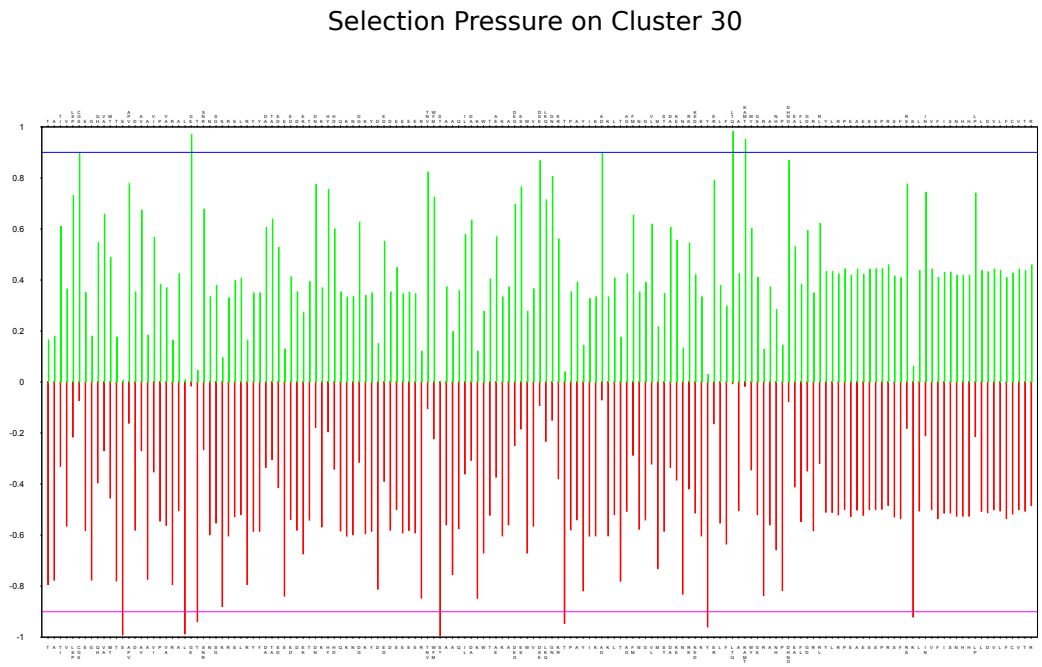

Figure I.42: Calculated codon level selection pressure on paralagous group 30. Levels above 0 are correspondent to positive selection pressure and levels below 0 are negative selection pressures. Anything over a selection pressure of ± 0.9 is considered significant.

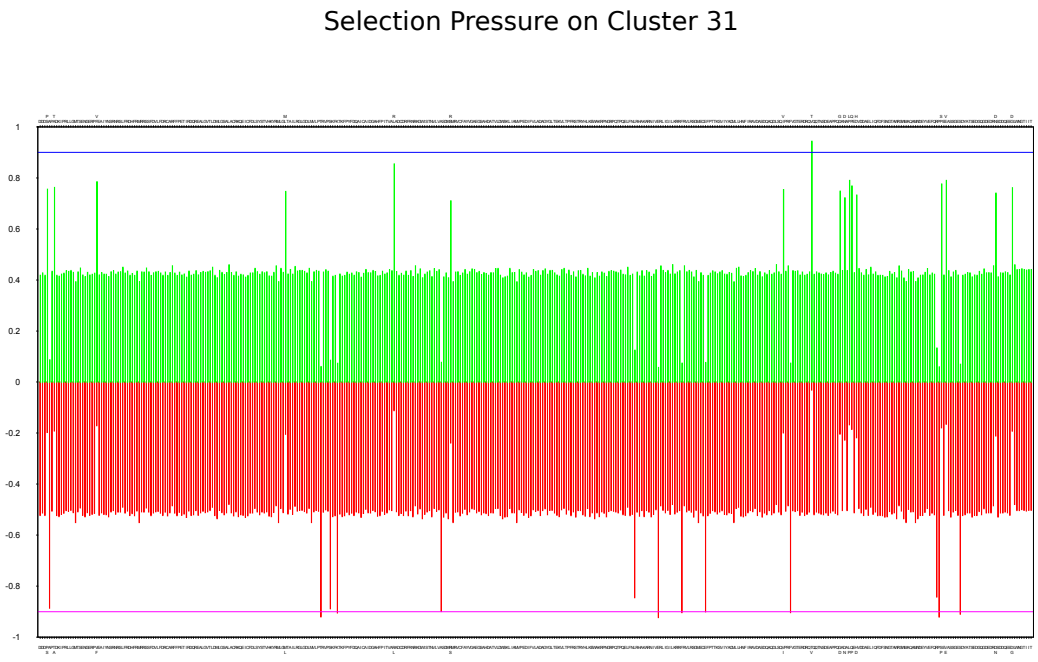

Figure I.43: Calculated codon level selection pressure on paralagous group 31. Levels above 0 are correspondent to positive selection pressure and levels below 0 are negative selection pressures. Anything over a selection pressure of ± 0.9 is considered significant.

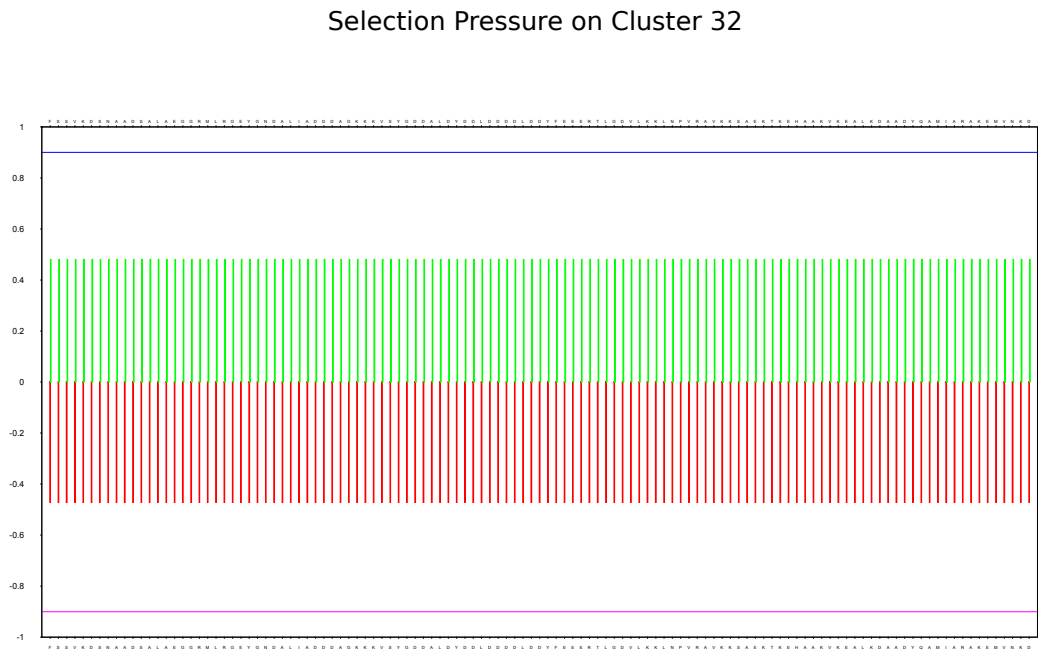

Figure I.44: Calculated codon level selection pressure on paralagous group 32. Levels above 0 are correspondent to positive selection pressure and levels below 0 are negative selection pressures. Anything over a selection pressure of ± 0.9 is considered significant.

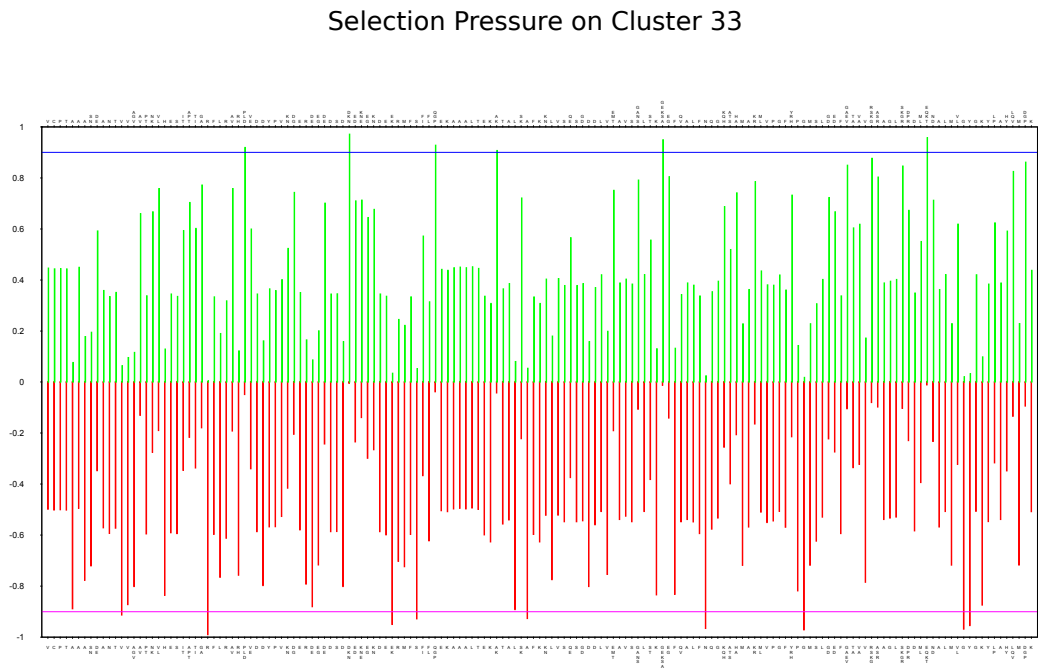

Figure I.45: Calculated codon level selection pressure on paralagous group 33. Levels above 0 are correspondent to positive selection pressure and levels below 0 are negative selection pressures. Anything over a selection pressure of ± 0.9 is considered significant.

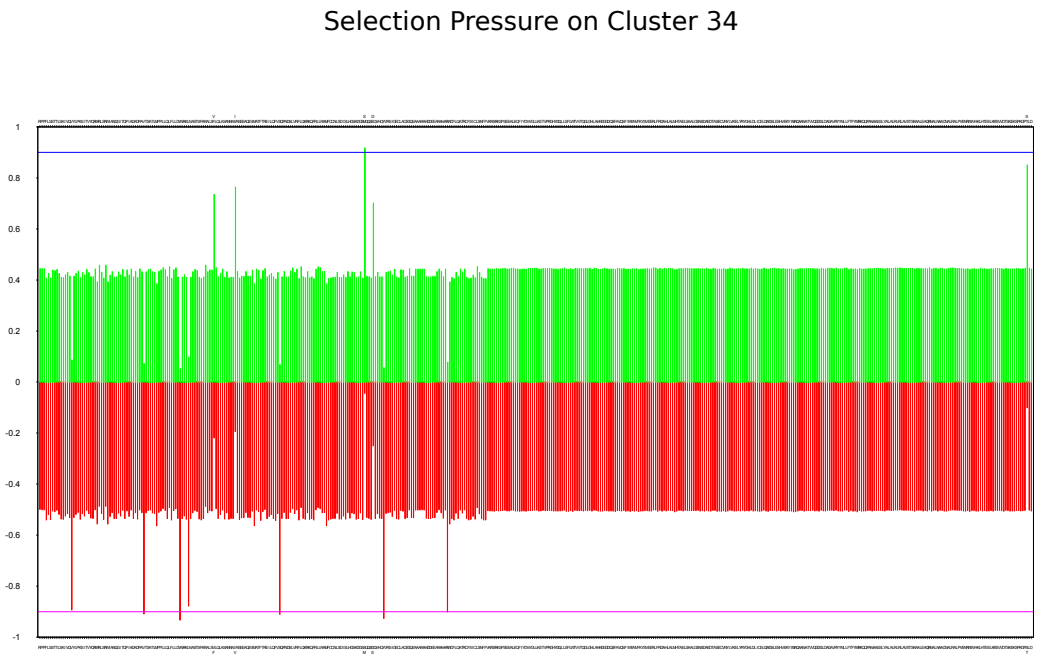

Figure I.46: Calculated codon level selection pressure on paralagous group 34. Levels above 0 are correspondent to positive selection pressure and levels below 0 are negative selection pressures. Anything over a selection pressure of ± 0.9 is considered significant.

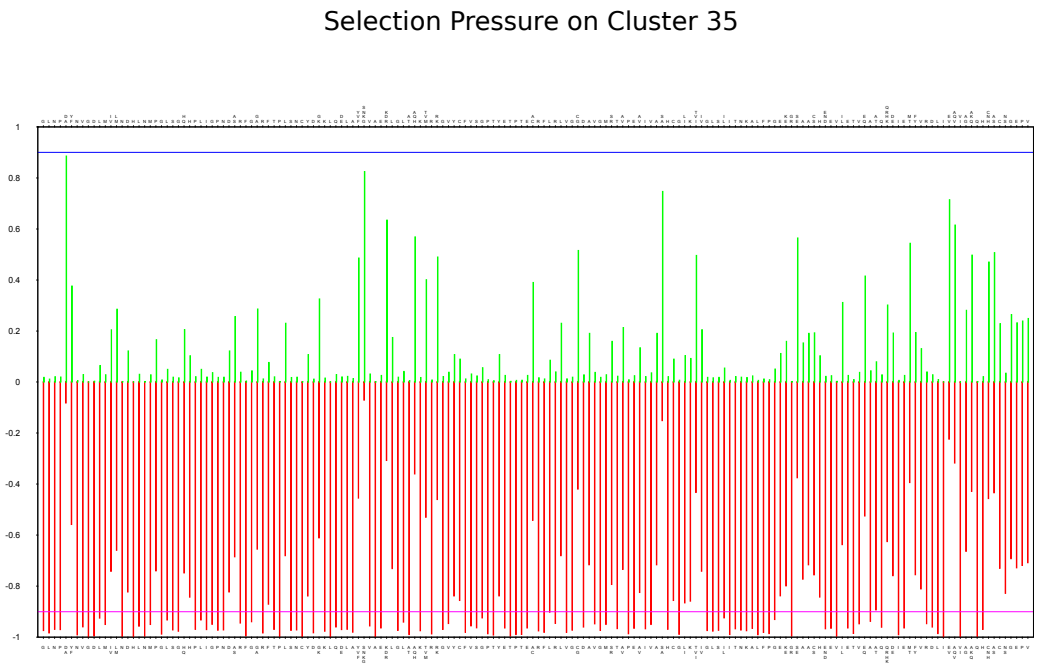

Figure I.47: Calculated codon level selection pressure on paralagous group 35. Levels above 0 are correspondent to positive selection pressure and levels below 0 are negative selection pressures. Anything over a selection pressure of ± 0.9 is considered significant.

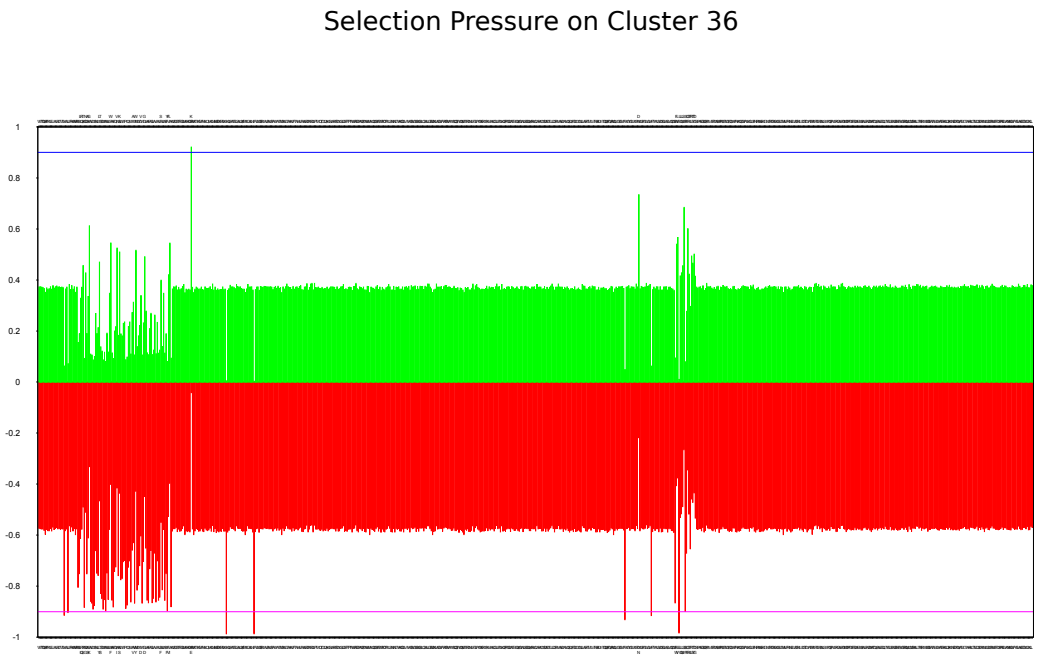

Figure I.48: Calculated codon level selection pressure on paralagous group 36. Levels above 0 are correspondent to positive selection pressure and levels below 0 are negative selection pressures. Anything over a selection pressure of ± 0.9 is considered significant.

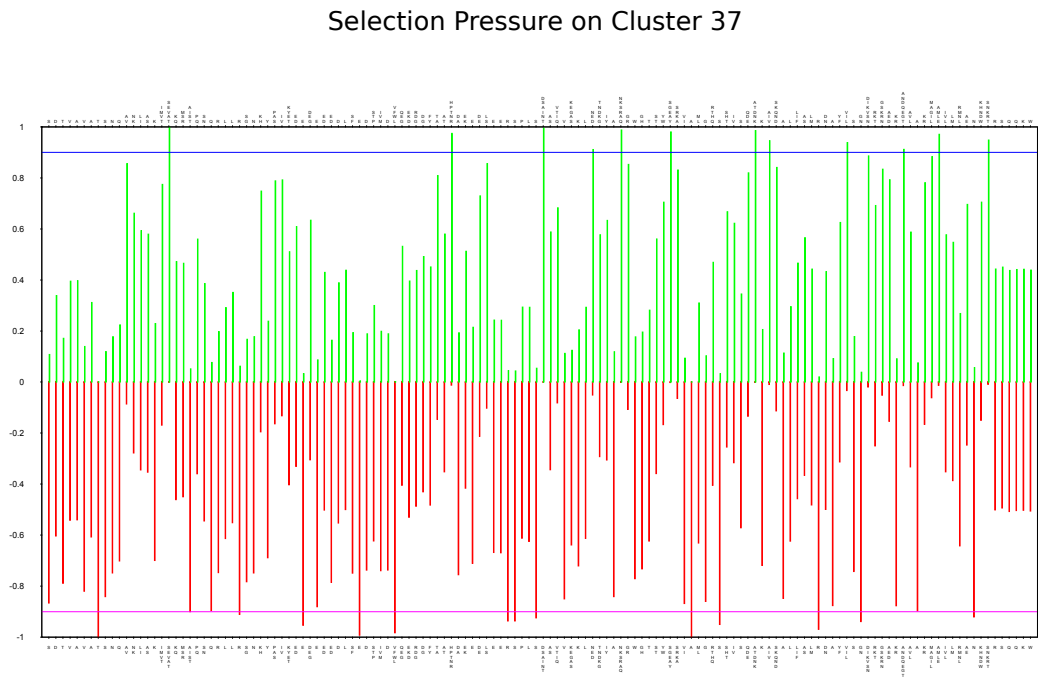

Figure I.49: Calculated codon level selection pressure on paralagous group 37. Levels above 0 are correspondent to positive selection pressure and levels below 0 are negative selection pressures. Anything over a selection pressure of ± 0.9 is considered significant.

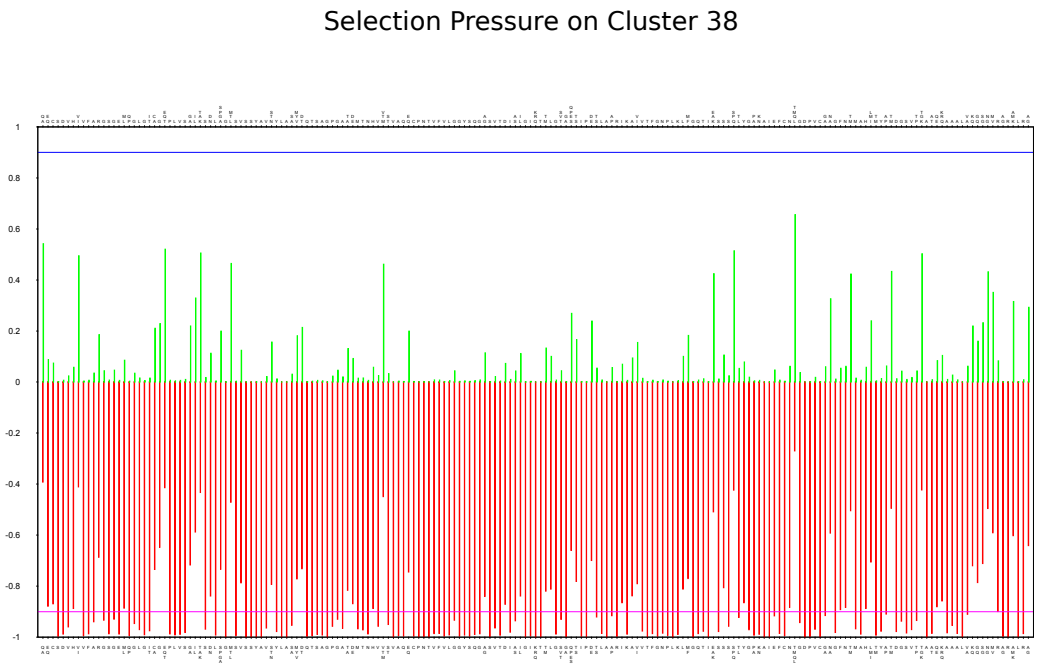

Figure I.50: Calculated codon level selection pressure on paralagous group 38. Levels above 0 are correspondent to positive selection pressure and levels below 0 are negative selection pressures. Anything over a selection pressure of ± 0.9 is considered significant.

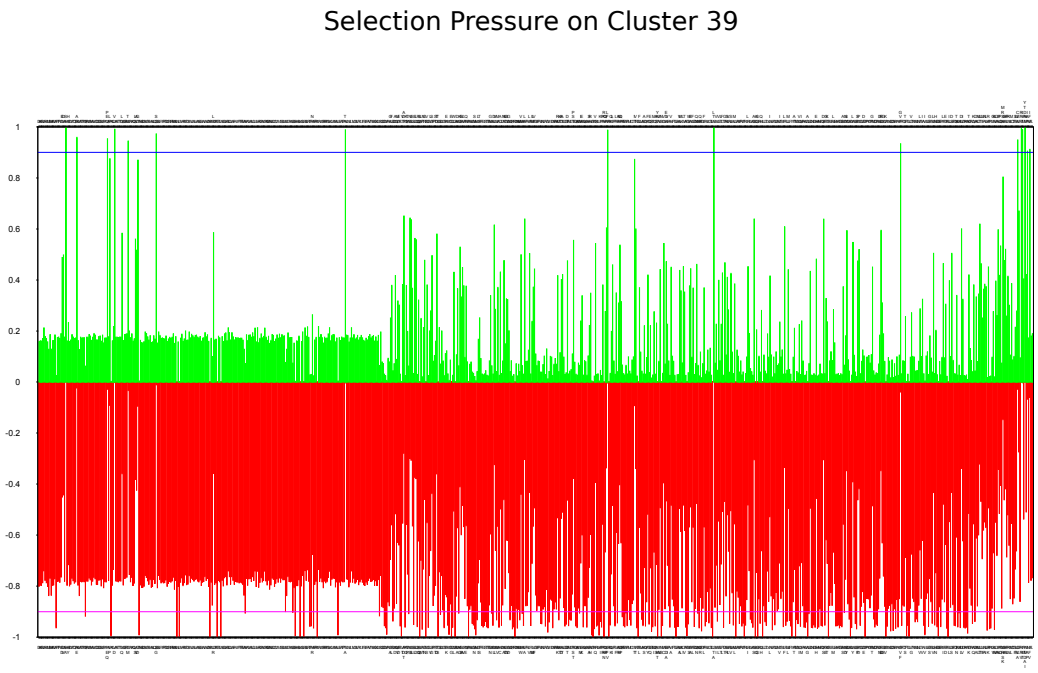

Figure I.51: Calculated codon level selection pressure on paralagous group 39. Levels above 0 are correspondent to positive selection pressure and levels below 0 are negative selection pressures. Anything over a selection pressure of ± 0.9 is considered significant.

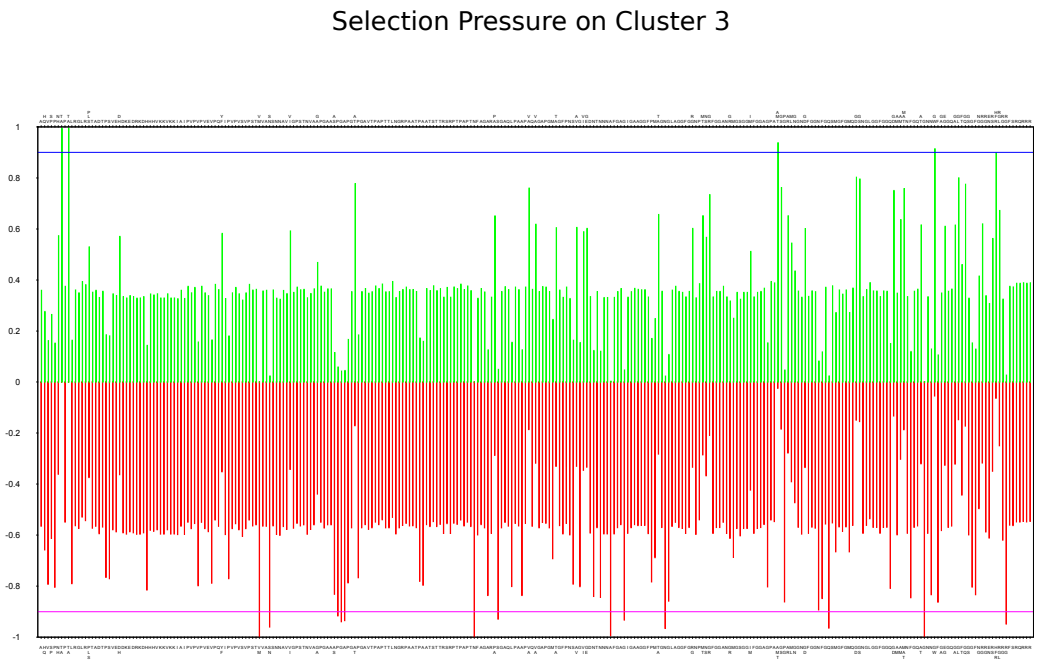

Figure I.52: Calculated codon level selection pressure on paralagous group 3. Levels above 0 are correspondent to positive selection pressure and levels below 0 are negative selection pressures. Anything over a selection pressure of ± 0.9 is considered significant.

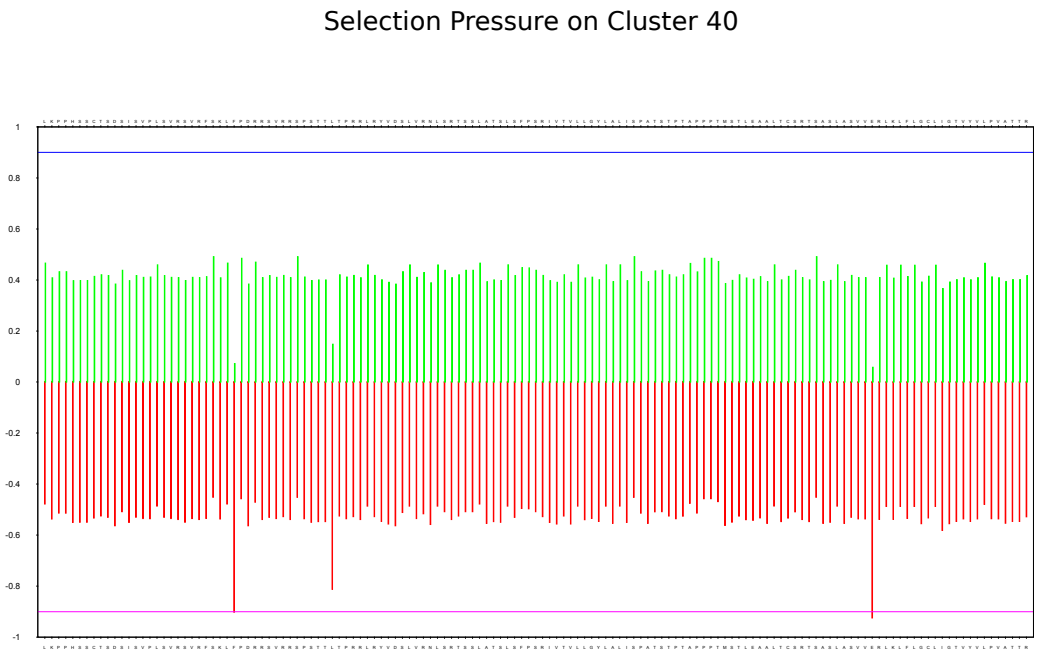

Figure I.53: Calculated codon level selection pressure on paralagous group 40. Levels above 0 are correspondent to positive selection pressure and levels below 0 are negative selection pressures. Anything over a selection pressure of ± 0.9 is considered significant.

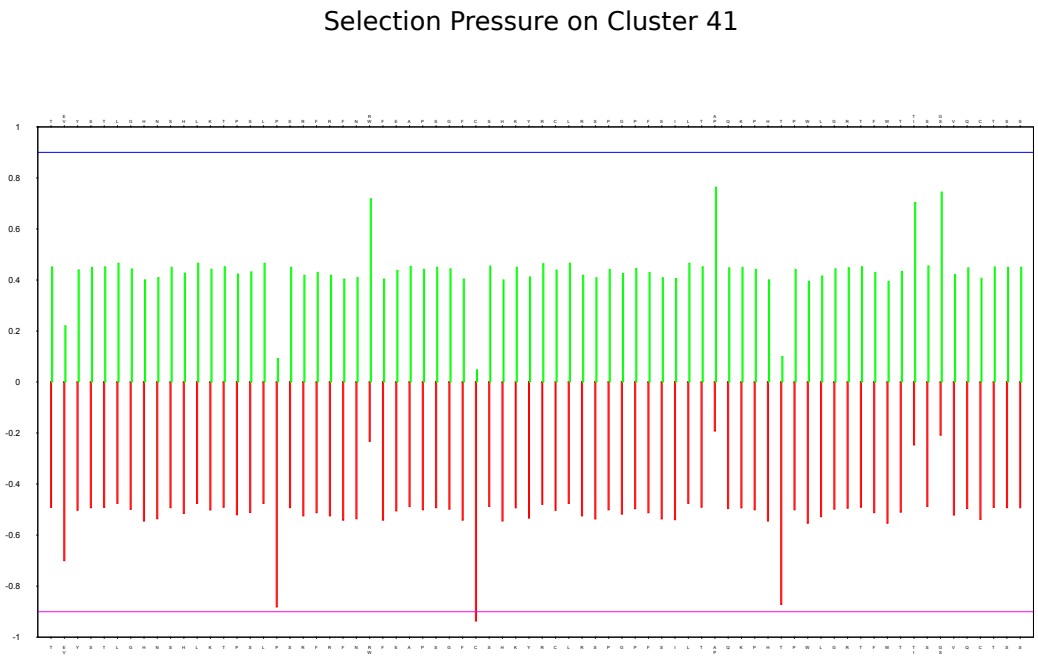

Figure I.54: Calculated codon level selection pressure on paralagous group 41. Levels above 0 are correspondent to positive selection pressure and levels below 0 are negative selection pressures. Anything over a selection pressure of ± 0.9 is considered significant.

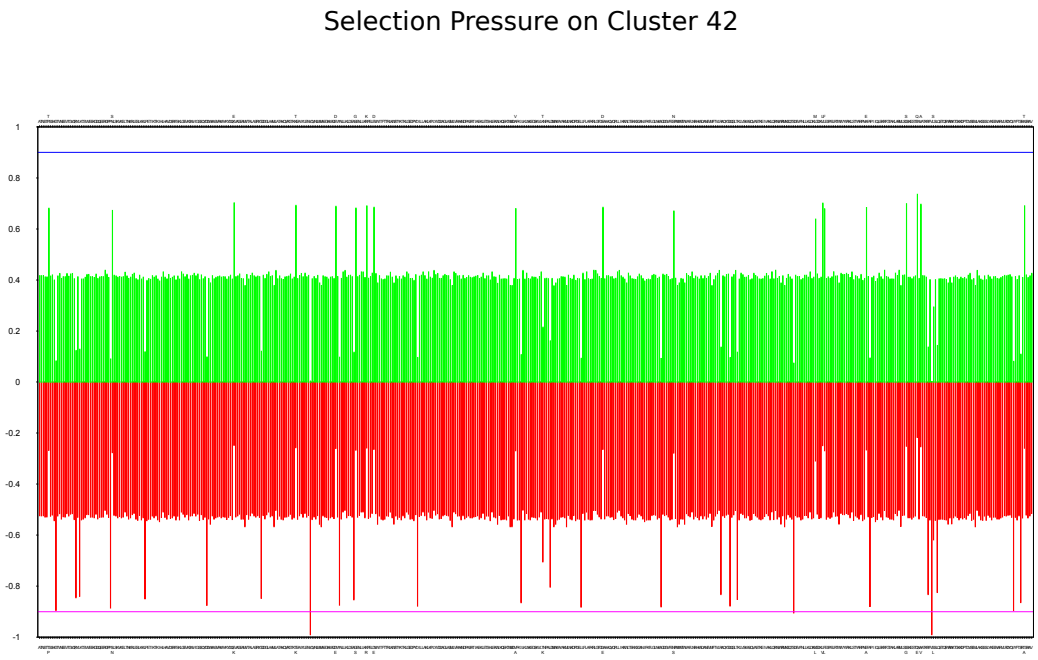

Figure I.55: Calculated codon level selection pressure on paralagous group 42. Levels above 0 are correspondent to positive selection pressure and levels below 0 are negative selection pressures. Anything over a selection pressure of ± 0.9 is considered significant.

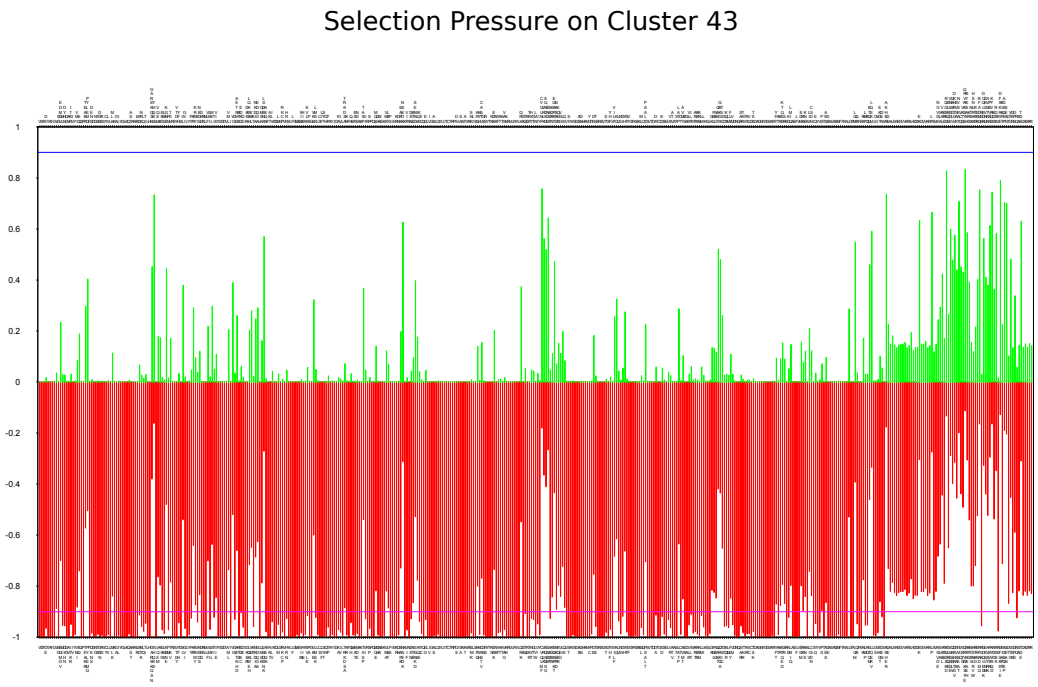

Figure I.56: Calculated codon level selection pressure on paralagous group 43. Levels above 0 are correspondent to positive selection pressure and levels below 0 are negative selection pressures. Anything over a selection pressure of ± 0.9 is considered significant.

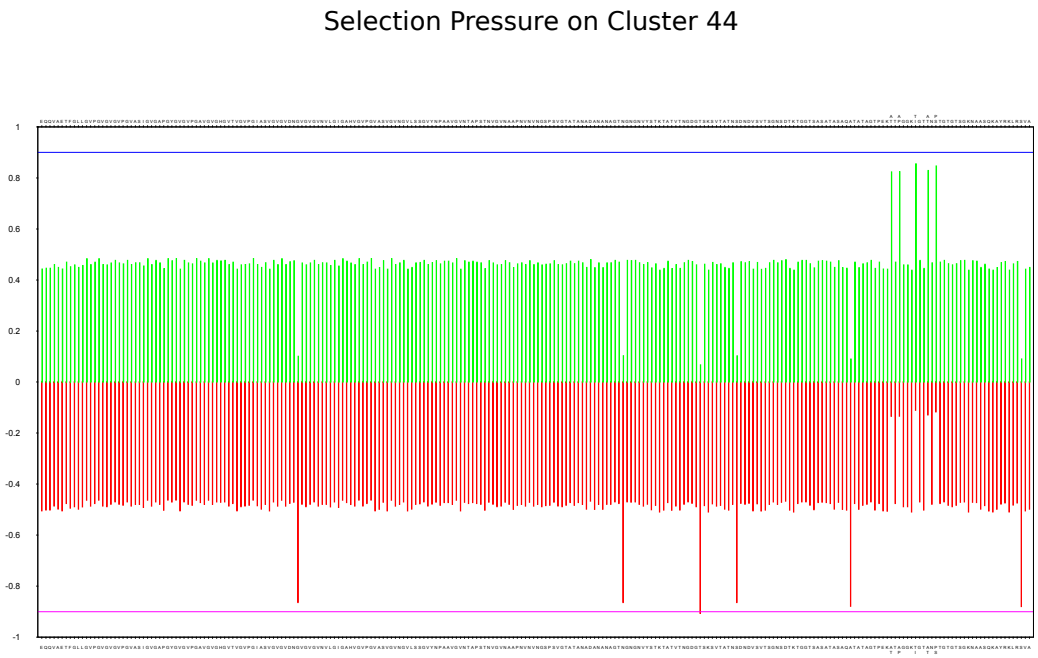

Figure I.57: Calculated codon level selection pressure on paralagous group 44. Levels above 0 are correspondent to positive selection pressure and levels below 0 are negative selection pressures. Anything over a selection pressure of ± 0.9 is considered significant.

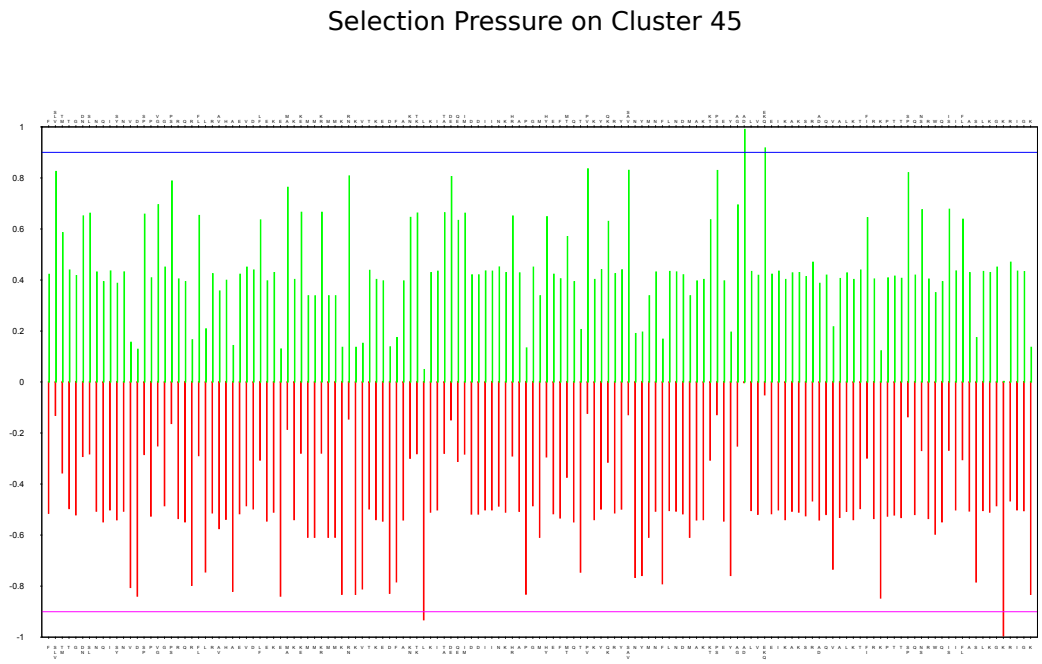

Figure I.58: Calculated codon level selection pressure on paralagous group 45. Levels above 0 are correspondent to positive selection pressure and levels below 0 are negative selection pressures. Anything over a selection pressure of ± 0.9 is considered significant.

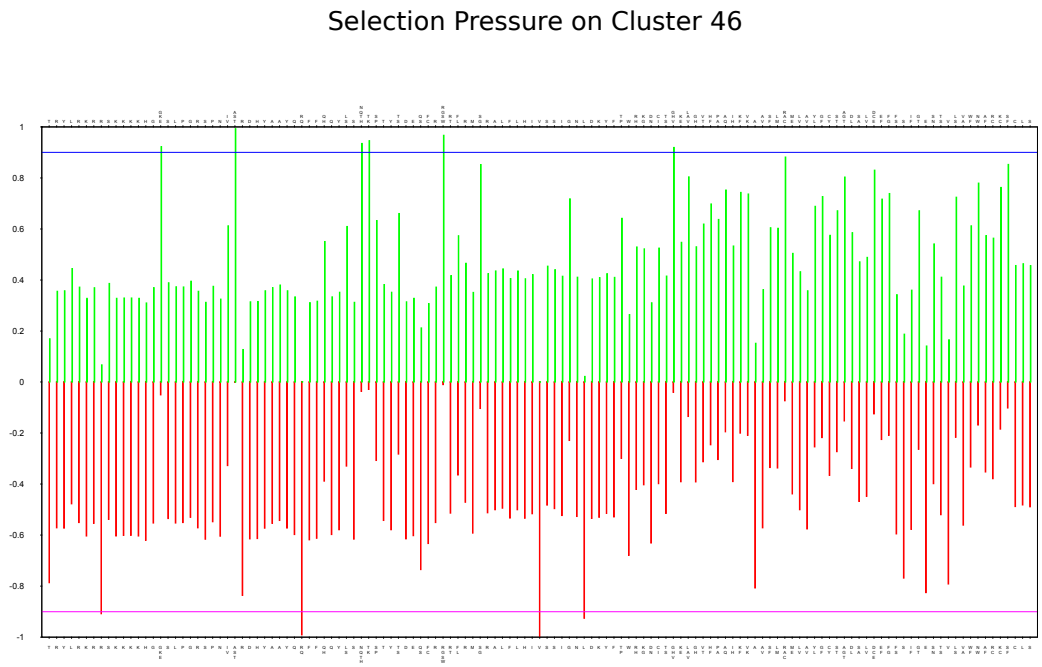

Figure I.59: Calculated codon level selection pressure on paralagous group 46. Levels above 0 are correspondent to positive selection pressure and levels below 0 are negative selection pressures. Anything over a selection pressure of ± 0.9 is considered significant.

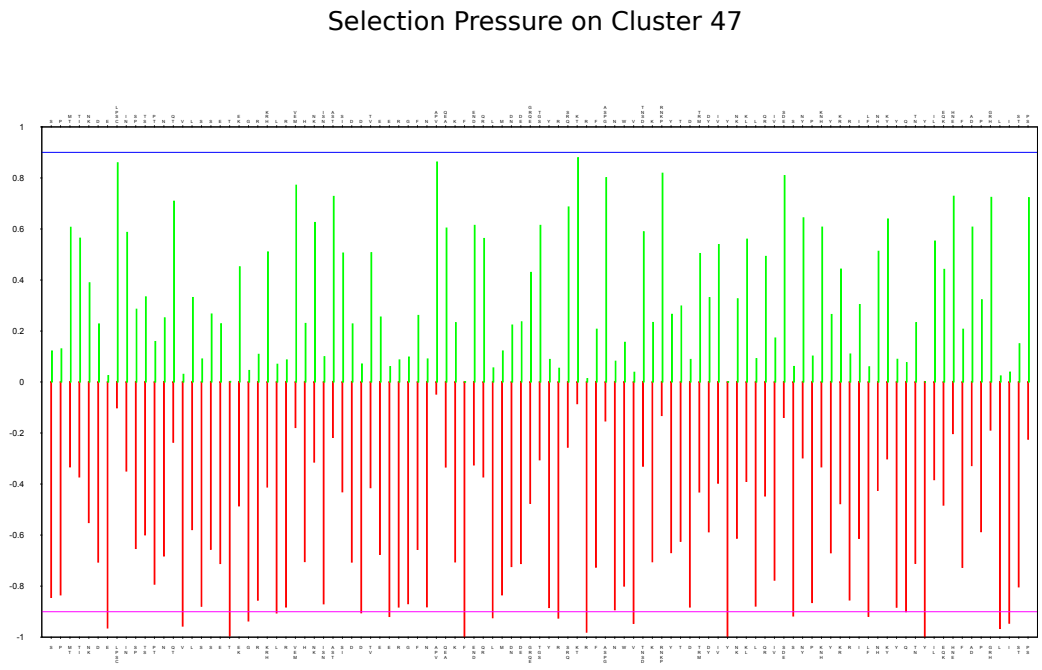

Figure I.60: Calculated codon level selection pressure on paralagous group 47. Levels above 0 are correspondent to positive selection pressure and levels below 0 are negative selection pressures. Anything over a selection pressure of ± 0.9 is considered significant.

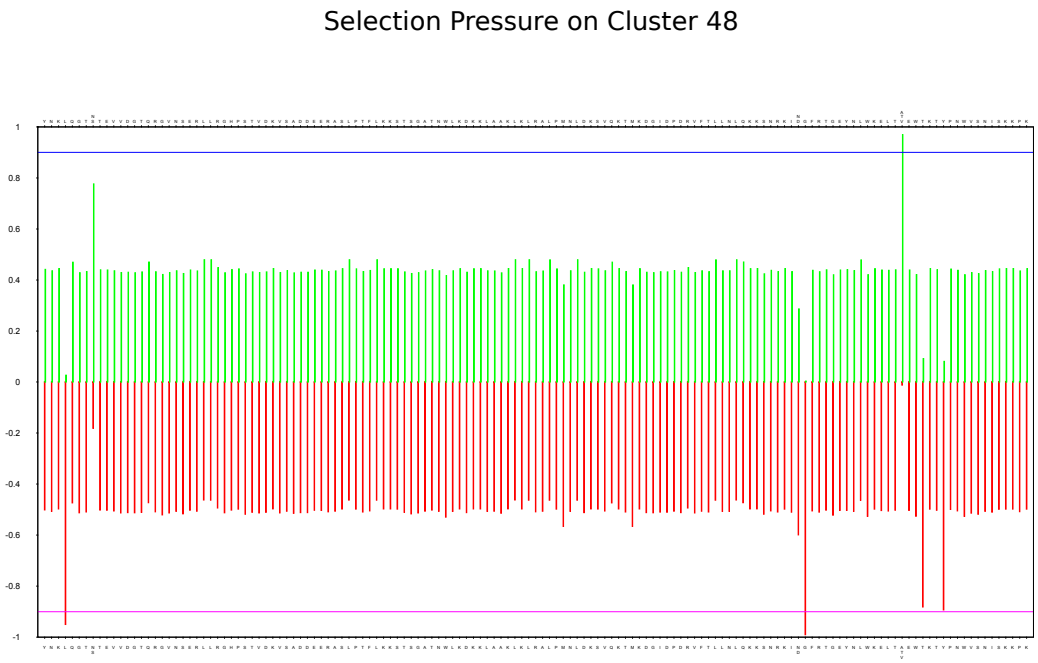

Figure I.61: Calculated codon level selection pressure on paralagous group 48. Levels above 0 are correspondent to positive selection pressure and levels below 0 are negative selection pressures. Anything over a selection pressure of ± 0.9 is considered significant.

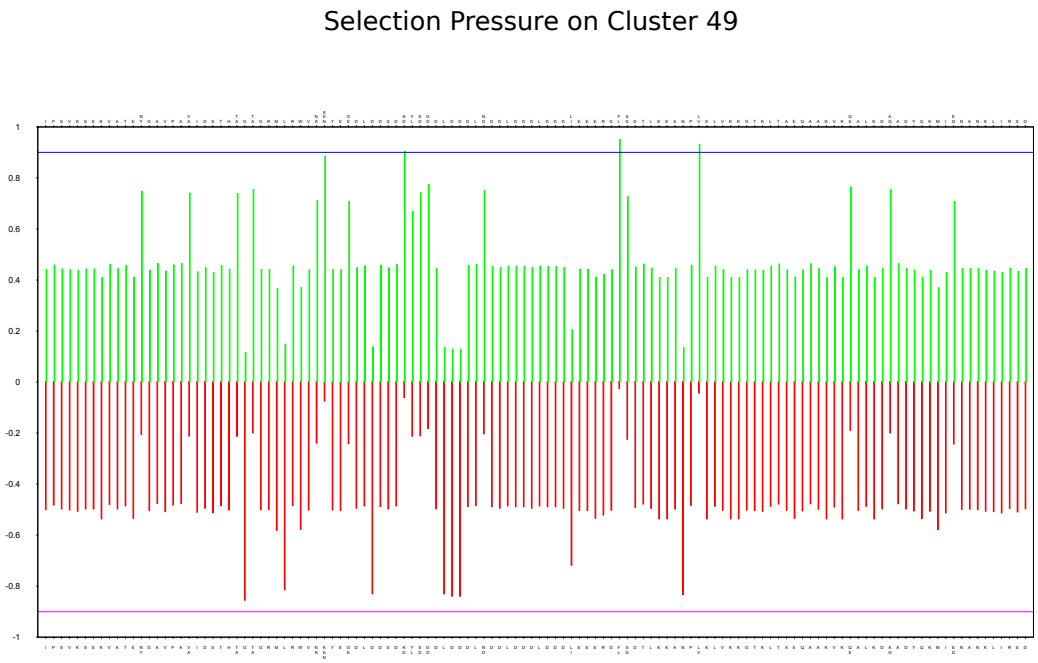

Figure I.62: Calculated codon level selection pressure on paralagous group 49. Levels above 0 are correspondent to positive selection pressure and levels below 0 are negative selection pressures. Anything over a selection pressure of ± 0.9 is considered significant.

Figure I.63: Calculated codon level selection pressure on paralagous group 4. Levels above 0 are correspondent to positive selection pressure and levels below 0 are negative selection pressures. Anything over a selection pressure of ± 0.9 is considered significant.

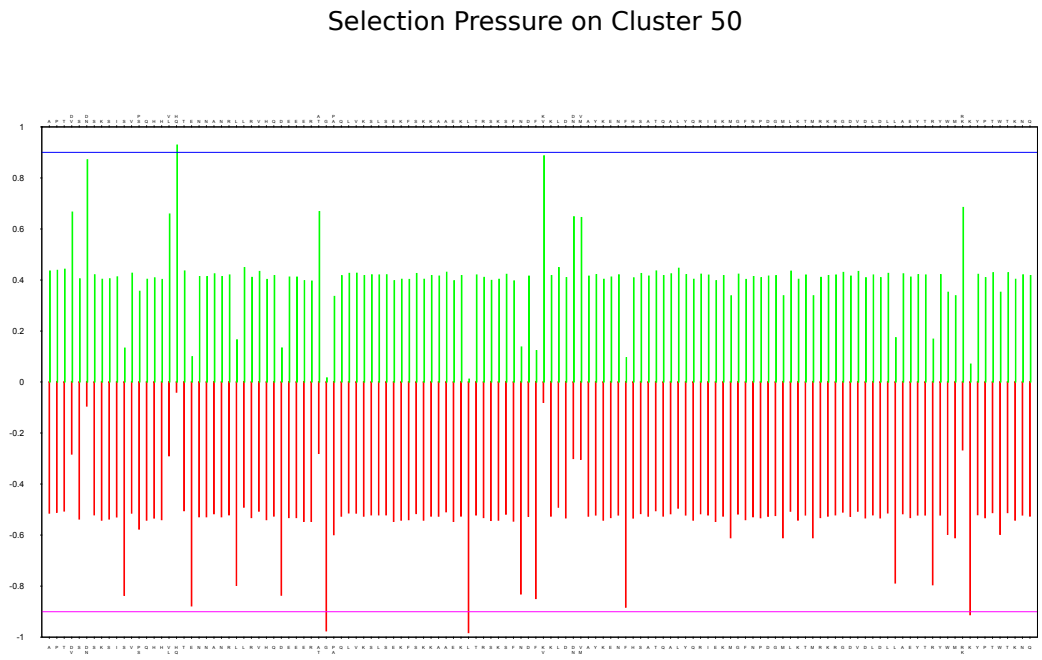

Figure I.64: Calculated codon level selection pressure on paralagous group 50. Levels above 0 are correspondent to positive selection pressure and levels below 0 are negative selection pressures. Anything over a selection pressure of ± 0.9 is considered significant.

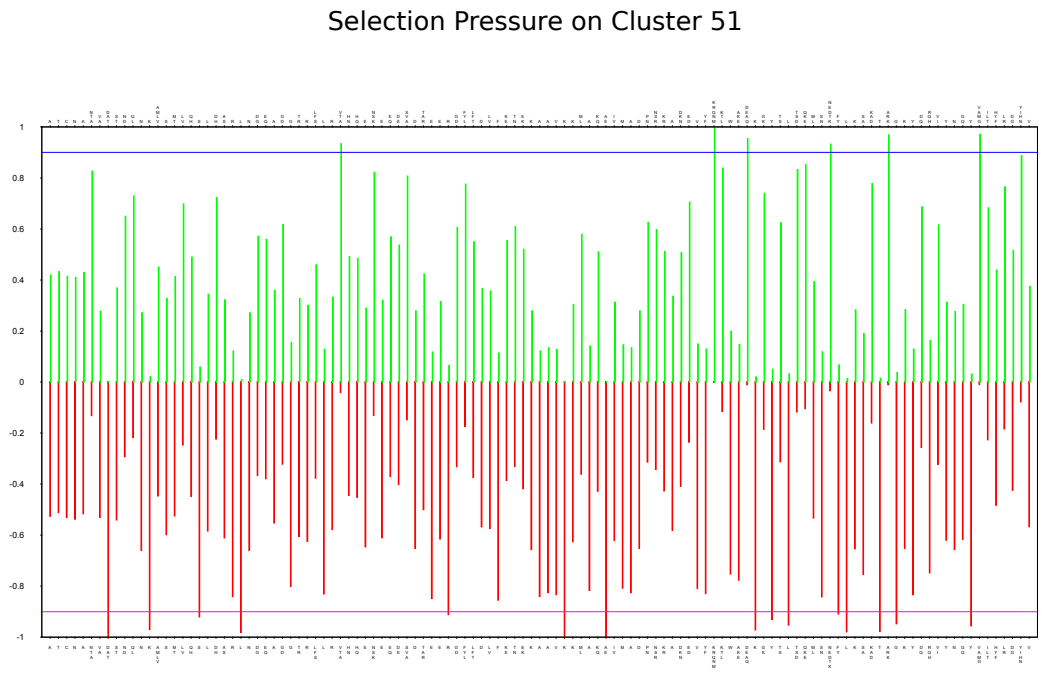

Figure I.65: Calculated codon level selection pressure on paralagous group 51. Levels above 0 are correspondent to positive selection pressure and levels below 0 are negative selection pressures. Anything over a selection pressure of ± 0.9 is considered significant.

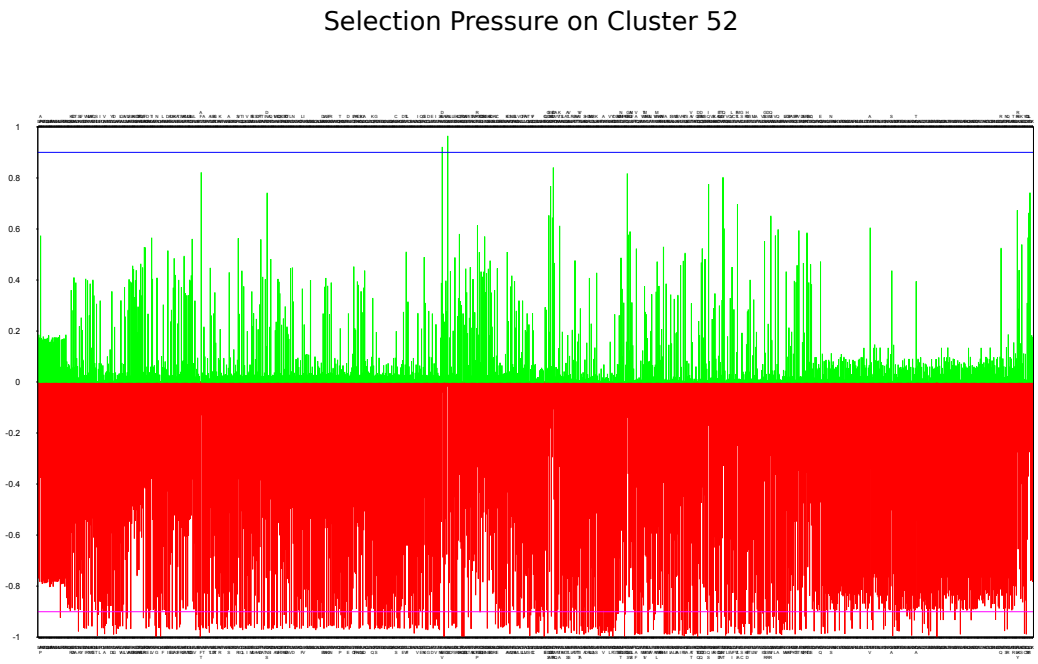

Figure I.66: Calculated codon level selection pressure on paralagous group 52. Levels above 0 are correspondent to positive selection pressure and levels below 0 are negative selection pressures. Anything over a selection pressure of ± 0.9 is considered significant.

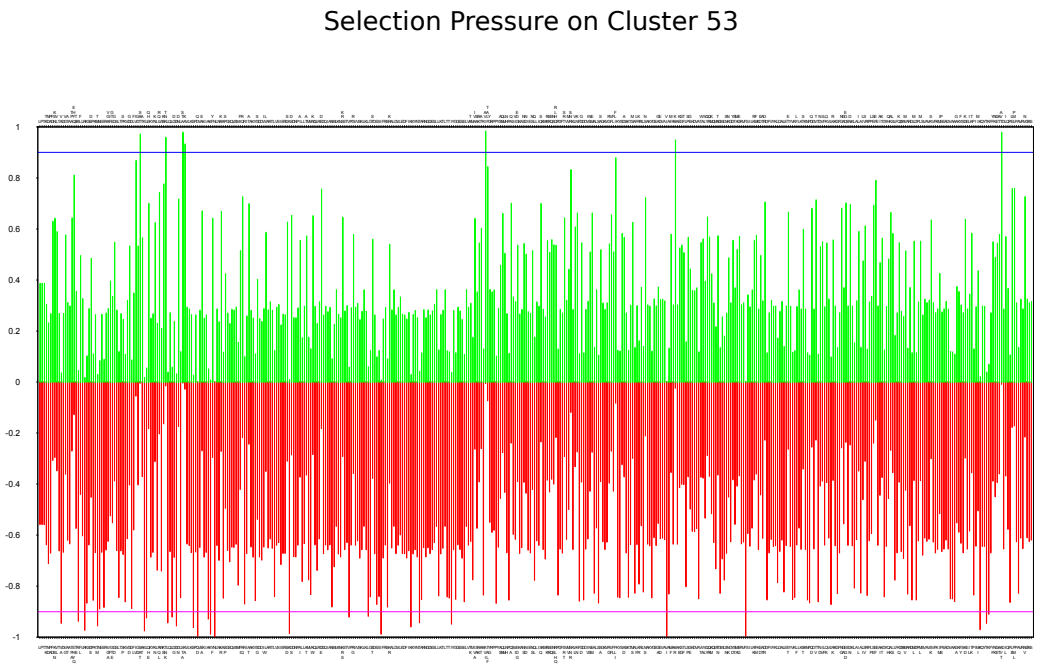

Figure I.67: Calculated codon level selection pressure on paralagous group 53. Levels above 0 are correspondent to positive selection pressure and levels below 0 are negative selection pressures. Anything over a selection pressure of ± 0.9 is considered significant.

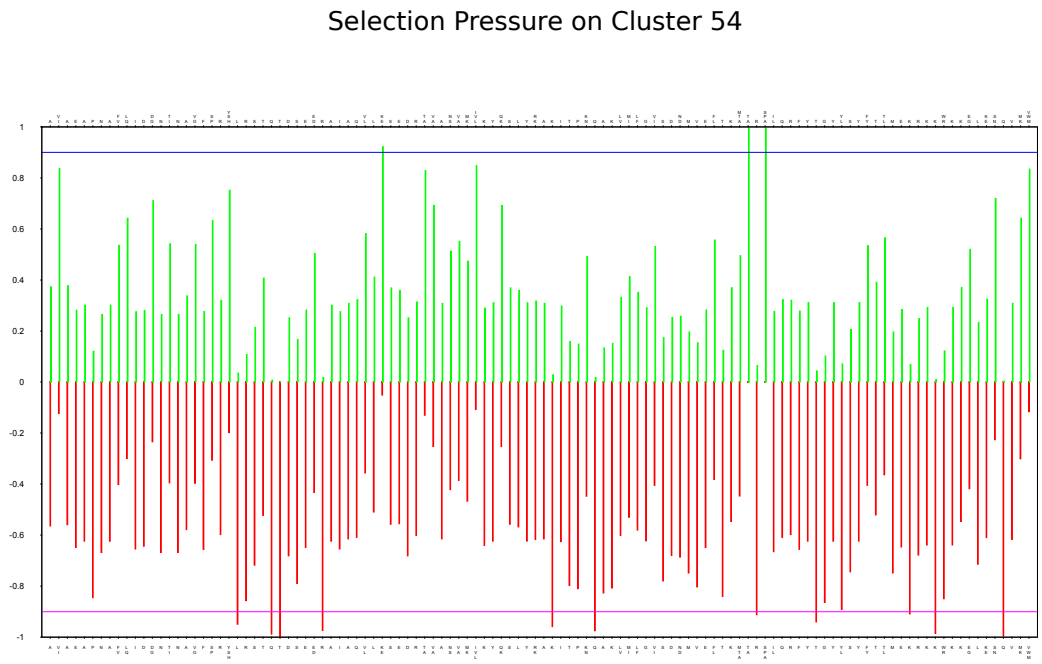

Figure I.68: Calculated codon level selection pressure on paralagous group 54. Levels above 0 are correspondent to positive selection pressure and levels below 0 are negative selection pressures. Anything over a selection pressure of ± 0.9 is considered significant.

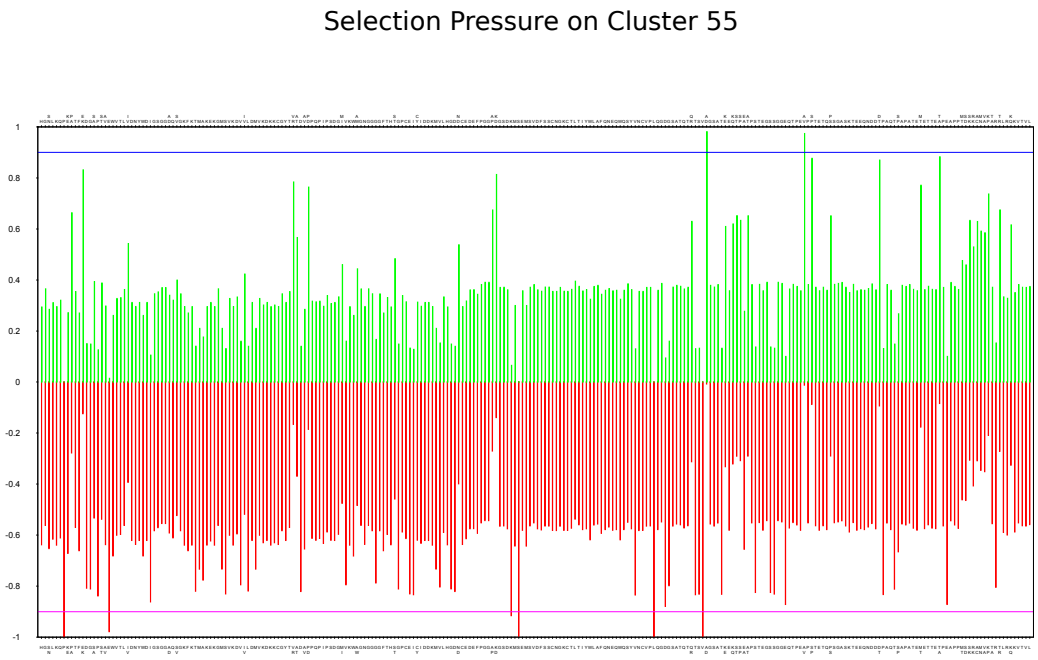

Figure I.69: Calculated codon level selection pressure on paralagous group 55. Levels above 0 are correspondent to positive selection pressure and levels below 0 are negative selection pressures. Anything over a selection pressure of ± 0.9 is considered significant.

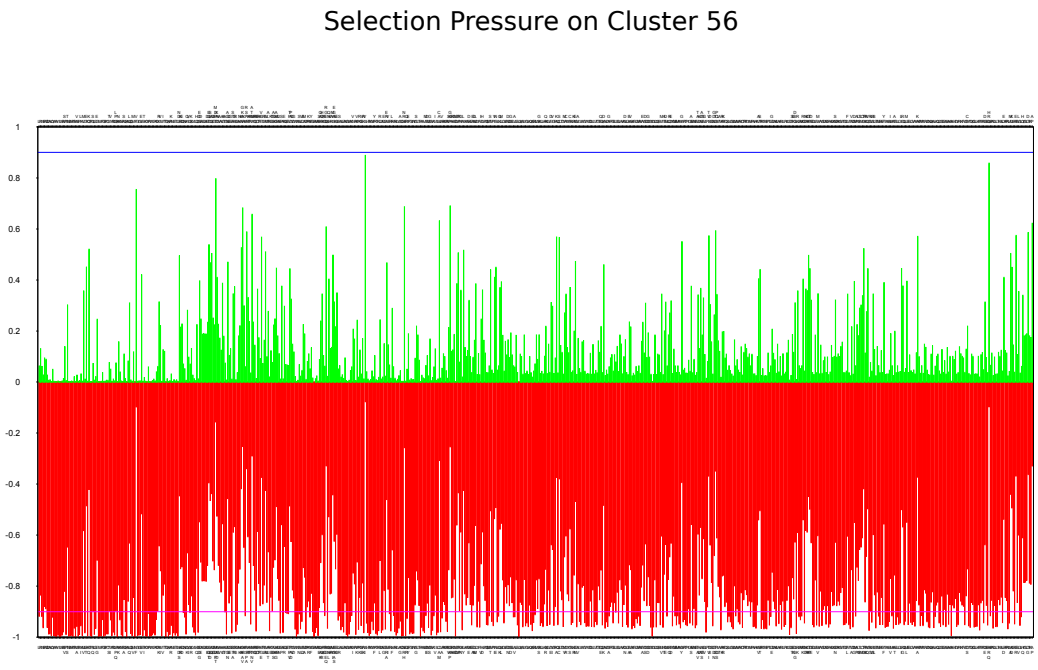

Figure I.70: Calculated codon level selection pressure on paralagous group 56. Levels above 0 are correspondent to positive selection pressure and levels below 0 are negative selection pressures. Anything over a selection pressure of ± 0.9 is considered significant.

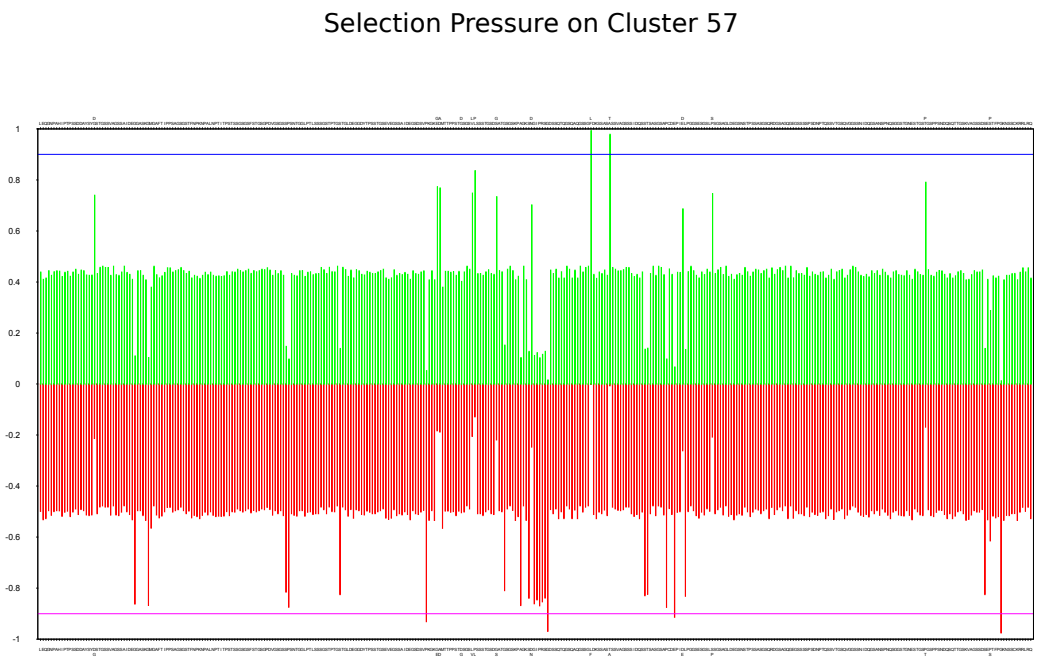

Figure I.71: Calculated codon level selection pressure on paralagous group 57. Levels above 0 are correspondent to positive selection pressure and levels below 0 are negative selection pressures. Anything over a selection pressure of ± 0.9 is considered significant.

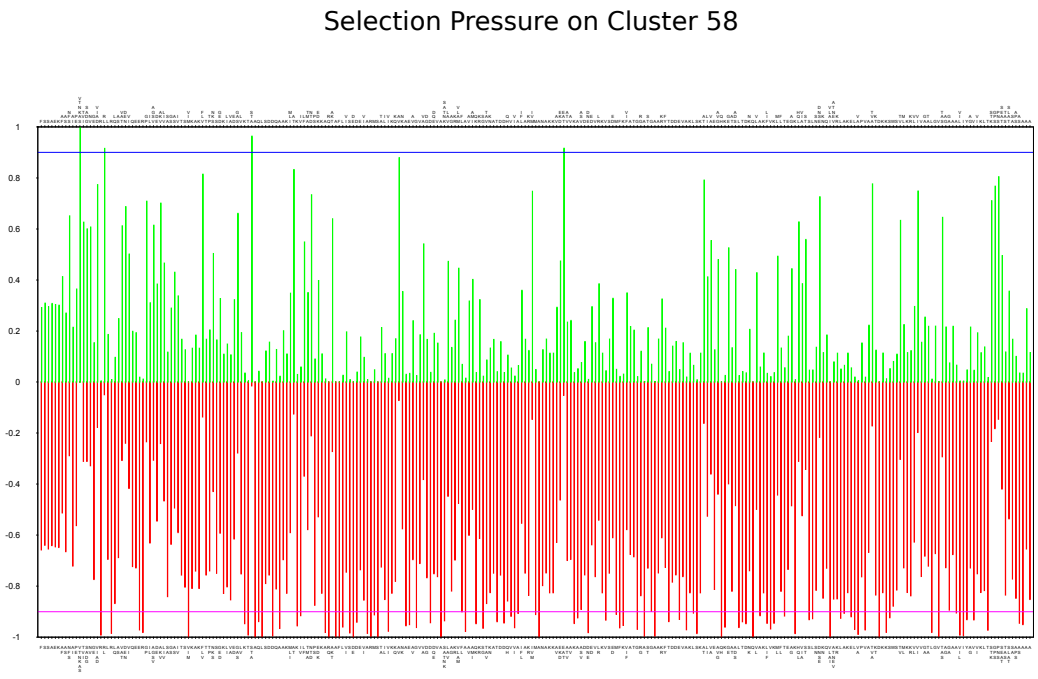

Figure I.72: Calculated codon level selection pressure on paralagous group 58. Levels above 0 are correspondent to positive selection pressure and levels below 0 are negative selection pressures. Anything over a selection pressure of ± 0.9 is considered significant.

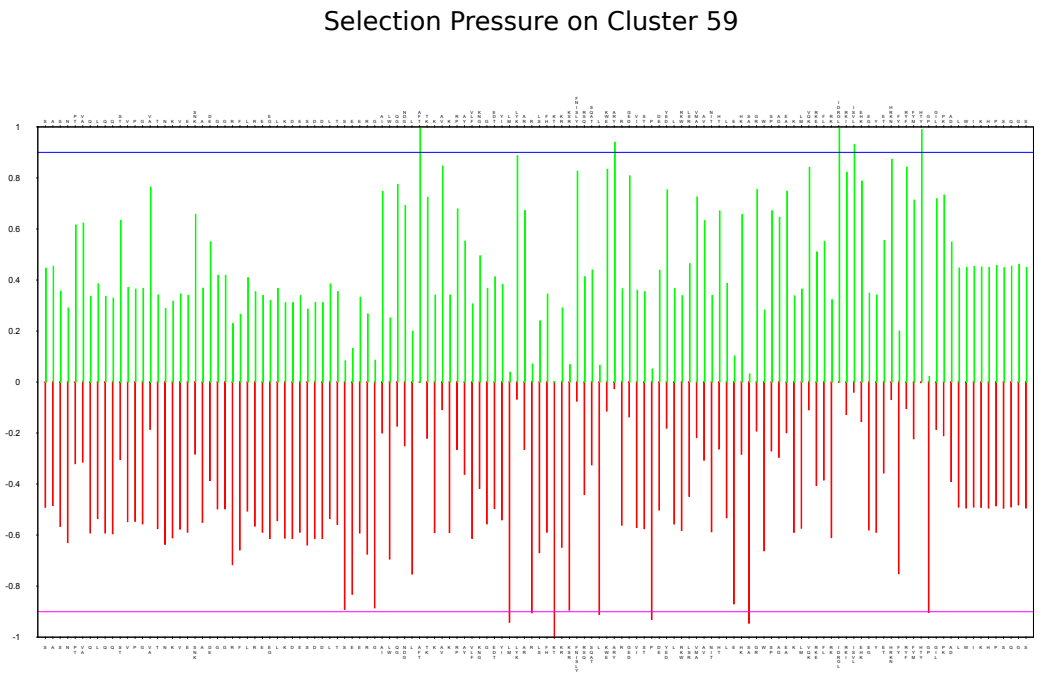

Figure I.73: Calculated codon level selection pressure on paralagous group 59. Levels above 0 are correspondent to positive selection pressure and levels below 0 are negative selection pressures. Anything over a selection pressure of ± 0.9 is considered significant.

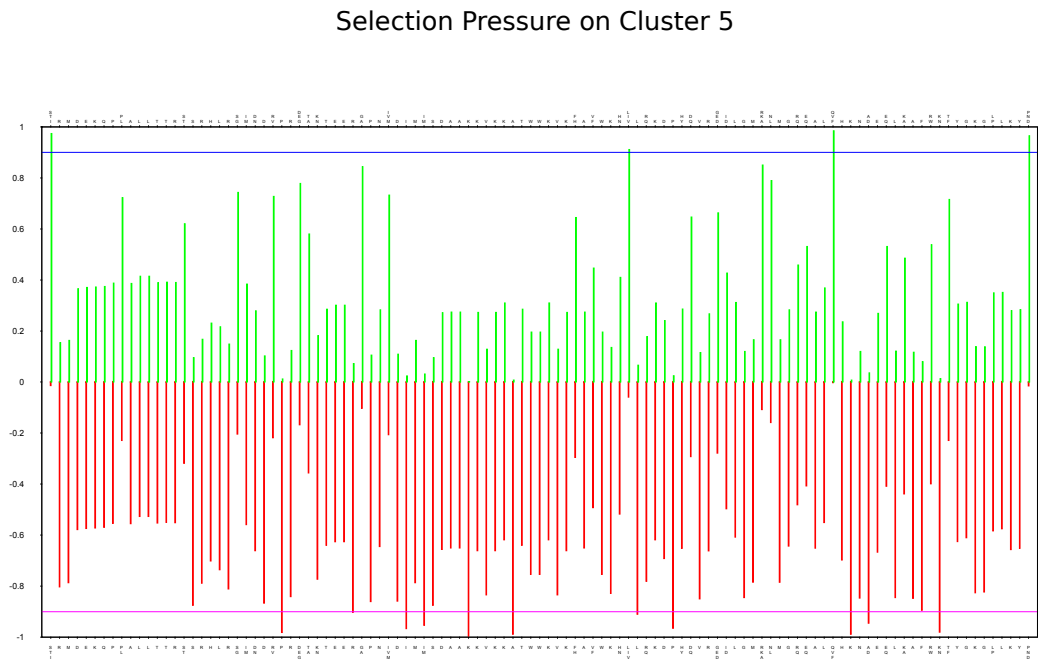

Figure I.74: Calculated codon level selection pressure on paralagous group 5. Levels above 0 are correspondent to positive selection pressure and levels below 0 are negative selection pressures. Anything over a selection pressure of ± 0.9 is considered significant.

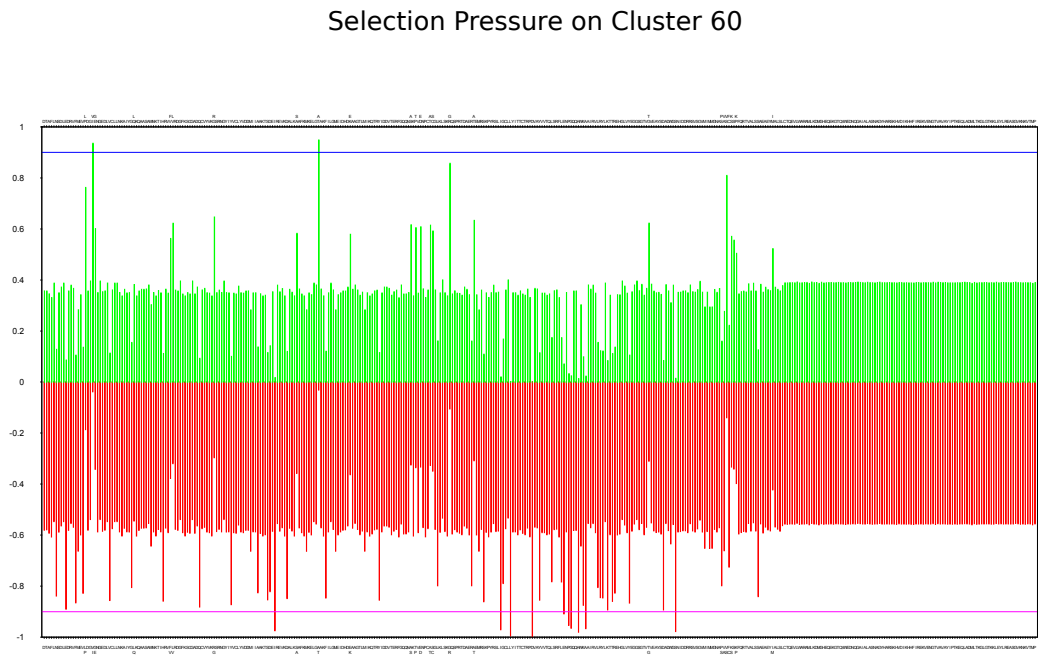

Figure I.75: Calculated codon level selection pressure on paralagous group 60. Levels above 0 are correspondent to positive selection pressure and levels below 0 are negative selection pressures. Anything over a selection pressure of ± 0.9 is considered significant.

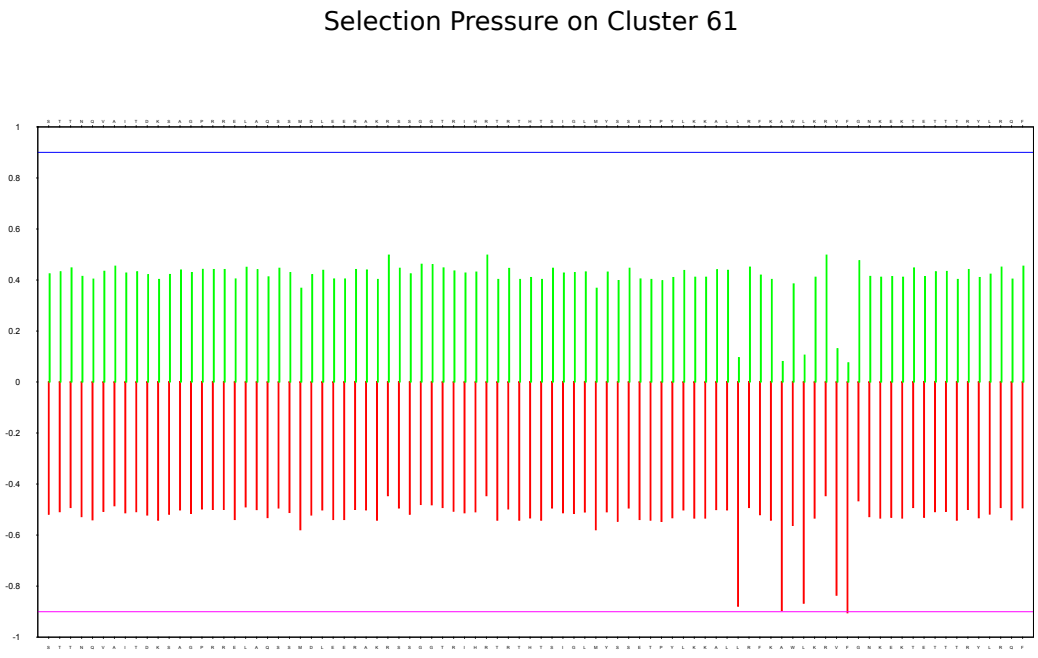

Figure I.76: Calculated codon level selection pressure on paralagous group 61. Levels above 0 are correspondent to positive selection pressure and levels below 0 are negative selection pressures. Anything over a selection pressure of ± 0.9 is considered significant.

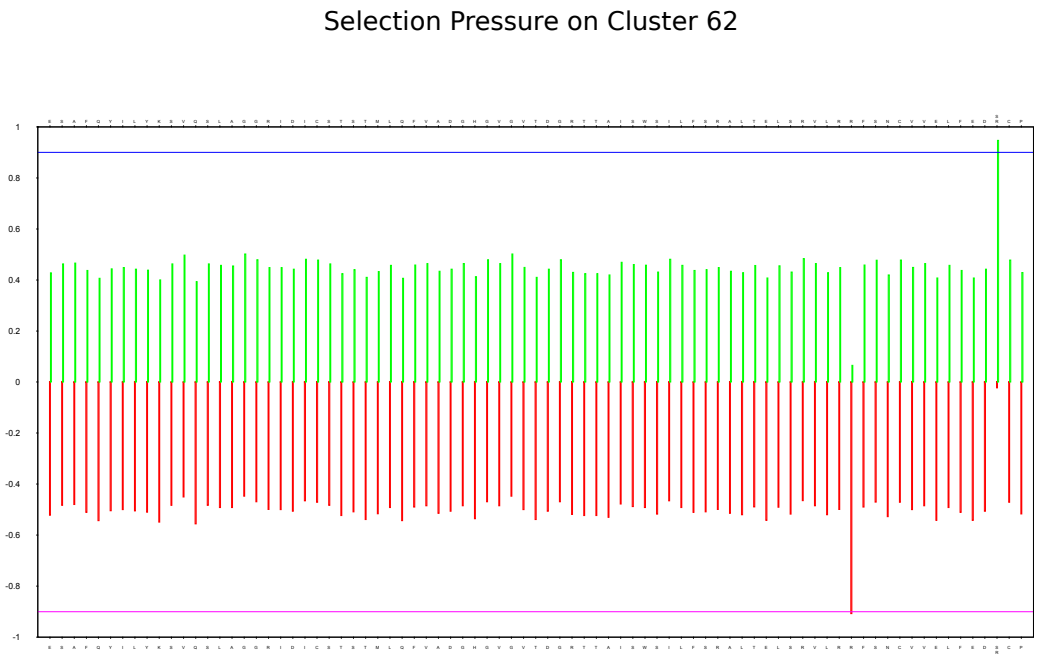

Figure I.77: Calculated codon level selection pressure on paralagous group 62. Levels above 0 are correspondent to positive selection pressure and levels below 0 are negative selection pressures. Anything over a selection pressure of ± 0.9 is considered significant.

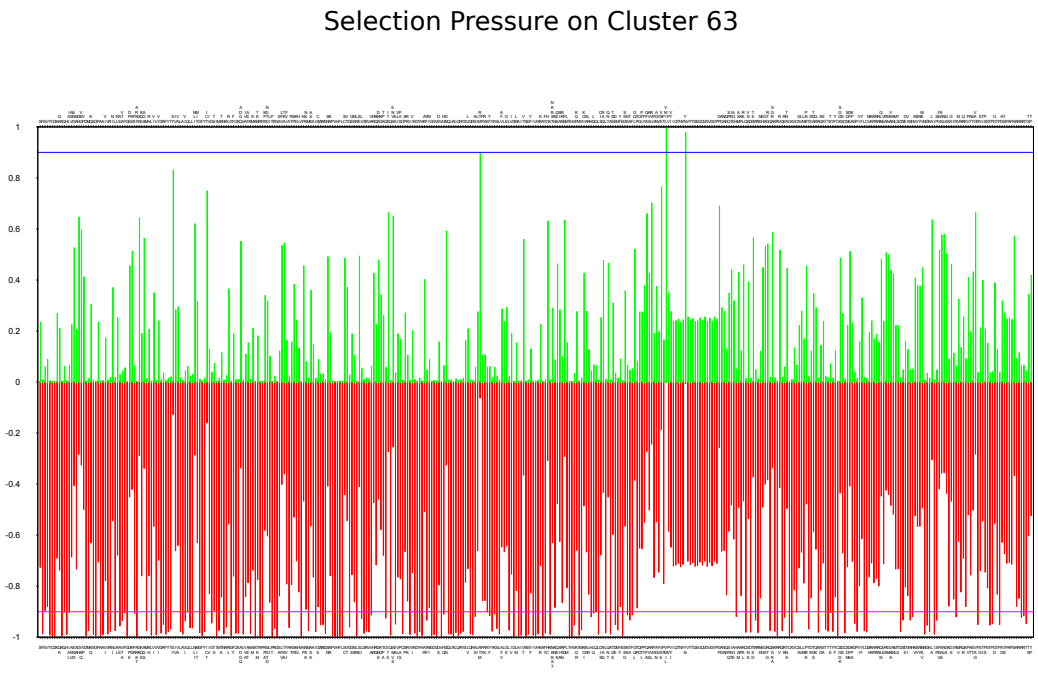

Figure I.78: Calculated codon level selection pressure on paralagous group 63. Levels above 0 are correspondent to positive selection pressure and levels below 0 are negative selection pressures. Anything over a selection pressure of ± 0.9 is considered significant.

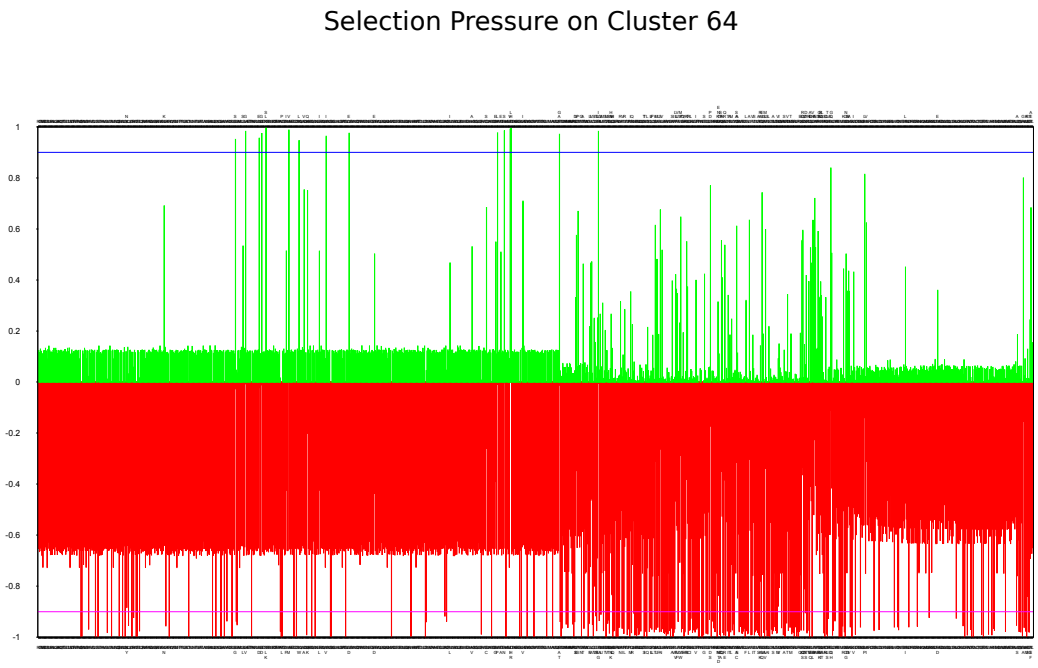

Figure I.79: Calculated codon level selection pressure on paralagous group 64. Levels above 0 are correspondent to positive selection pressure and levels below 0 are negative selection pressures. Anything over a selection pressure of ± 0.9 is considered significant.

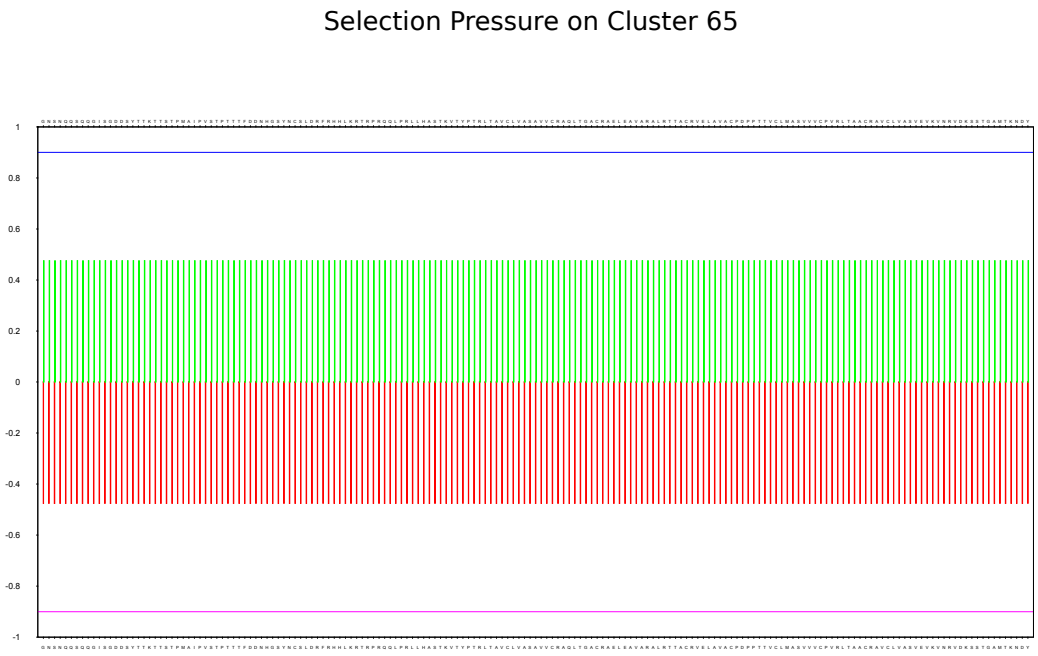

Figure I.80: Calculated codon level selection pressure on paralagous group 65. Levels above 0 are correspondent to positive selection pressure and levels below 0 are negative selection pressures. Anything over a selection pressure of ± 0.9 is considered significant.

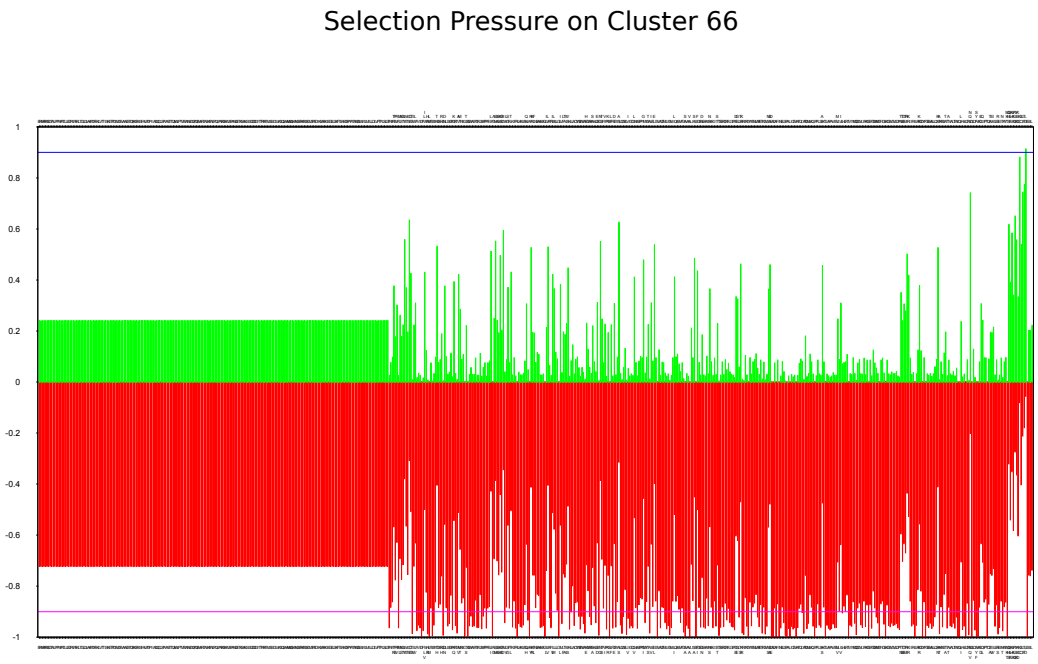

Figure I.81: Calculated codon level selection pressure on paralagous group 66. Levels above 0 are correspondent to positive selection pressure and levels below 0 are negative selection pressures. Anything over a selection pressure of ± 0.9 is considered significant.

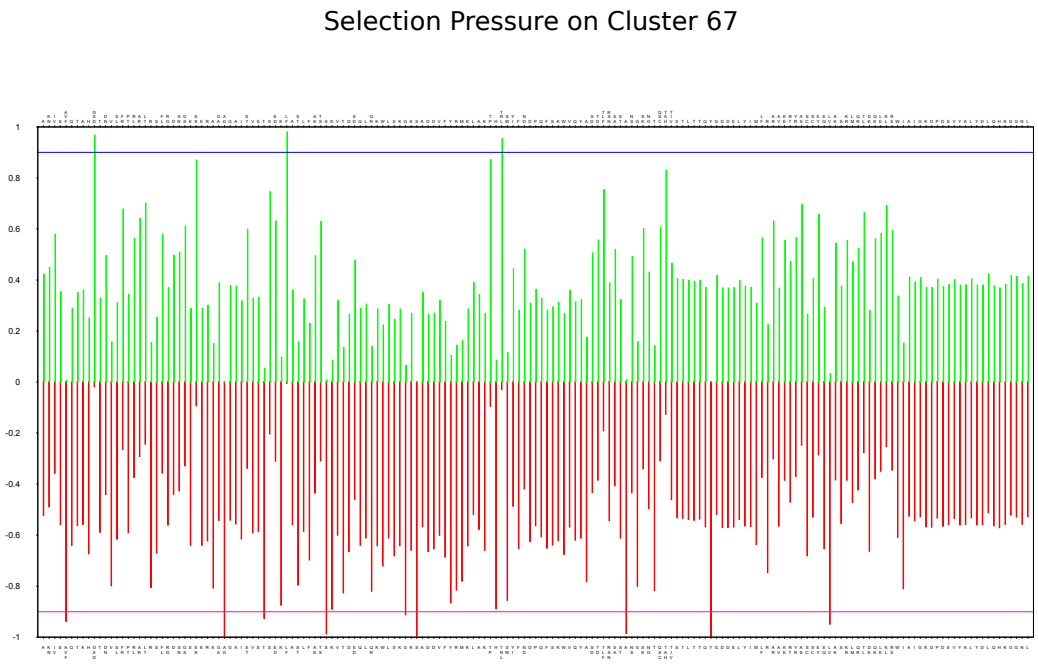

Figure I.82: Calculated codon level selection pressure on paralagous group 67. Levels above 0 are correspondent to positive selection pressure and levels below 0 are negative selection pressures. Anything over a selection pressure of ± 0.9 is considered significant.

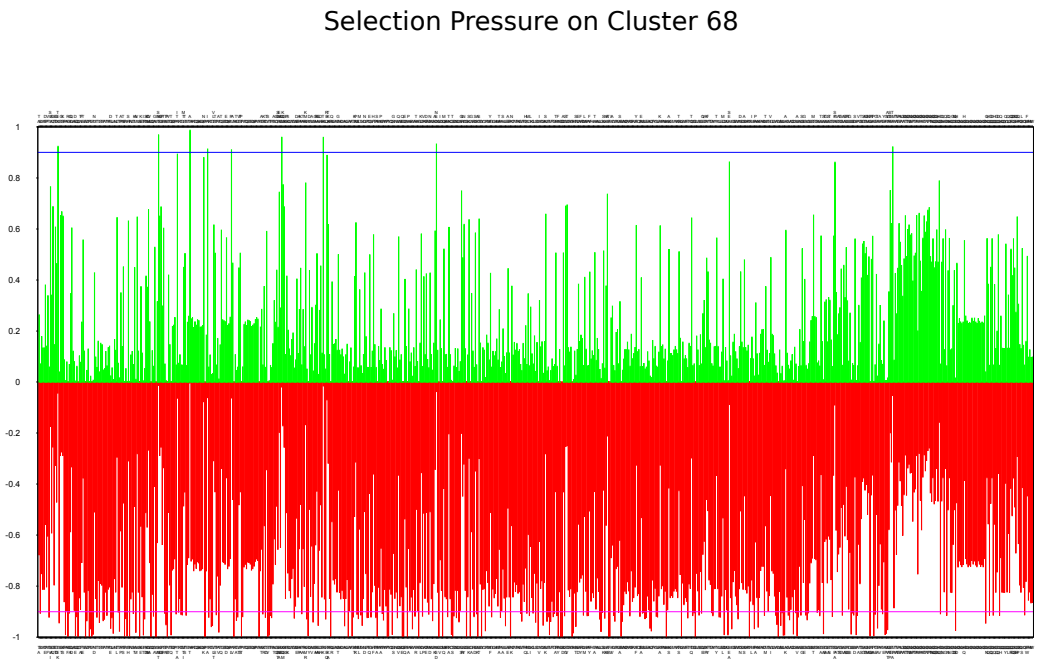

Figure I.83: Calculated codon level selection pressure on paralagous group 68. Levels above 0 are correspondent to positive selection pressure and levels below 0 are negative selection pressures. Anything over a selection pressure of ± 0.9 is considered significant.

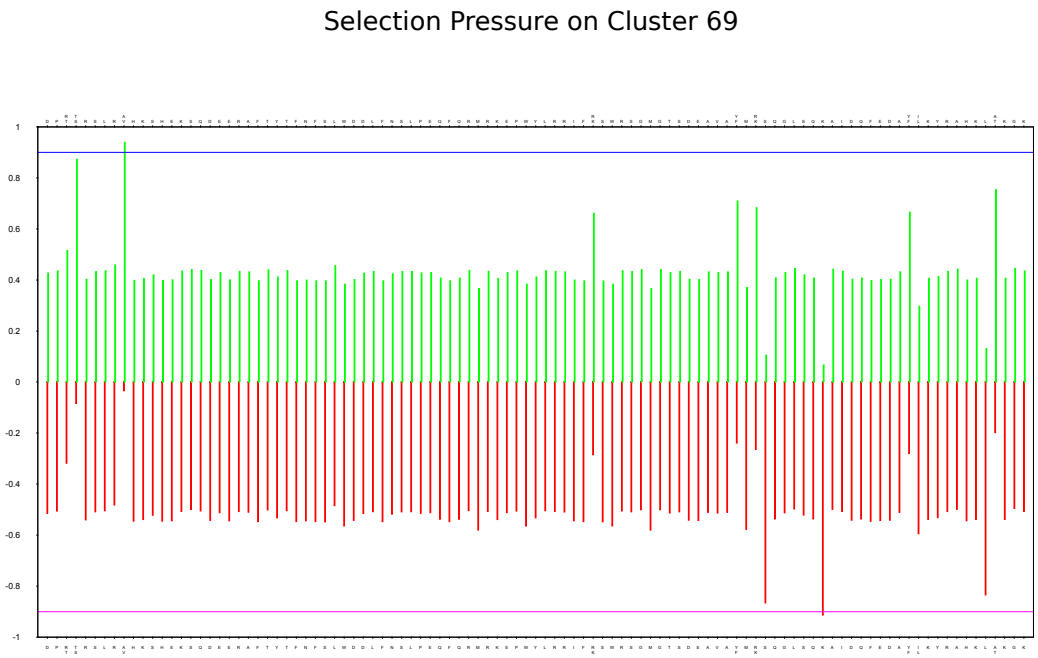

Figure I.84: Calculated codon level selection pressure on paralagous group 69. Levels above 0 are correspondent to positive selection pressure and levels below 0 are negative selection pressures. Anything over a selection pressure of ± 0.9 is considered significant.

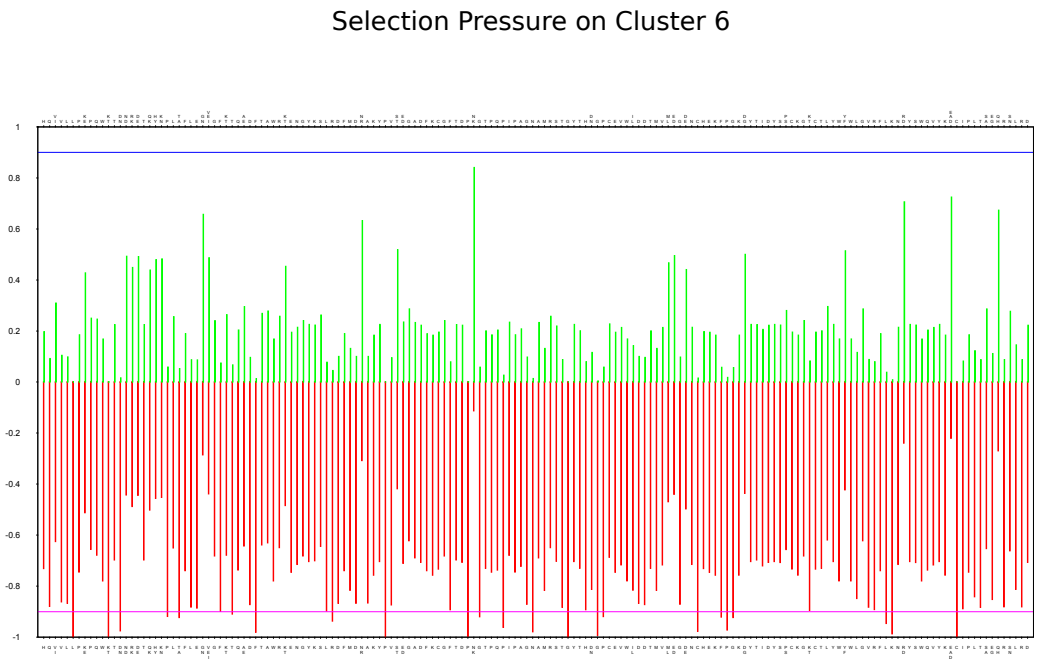

Figure I.85: Calculated codon level selection pressure on paralagous group 6. Levels above 0 are correspondent to positive selection pressure and levels below 0 are negative selection pressures. Anything over a selection pressure of ± 0.9 is considered significant.

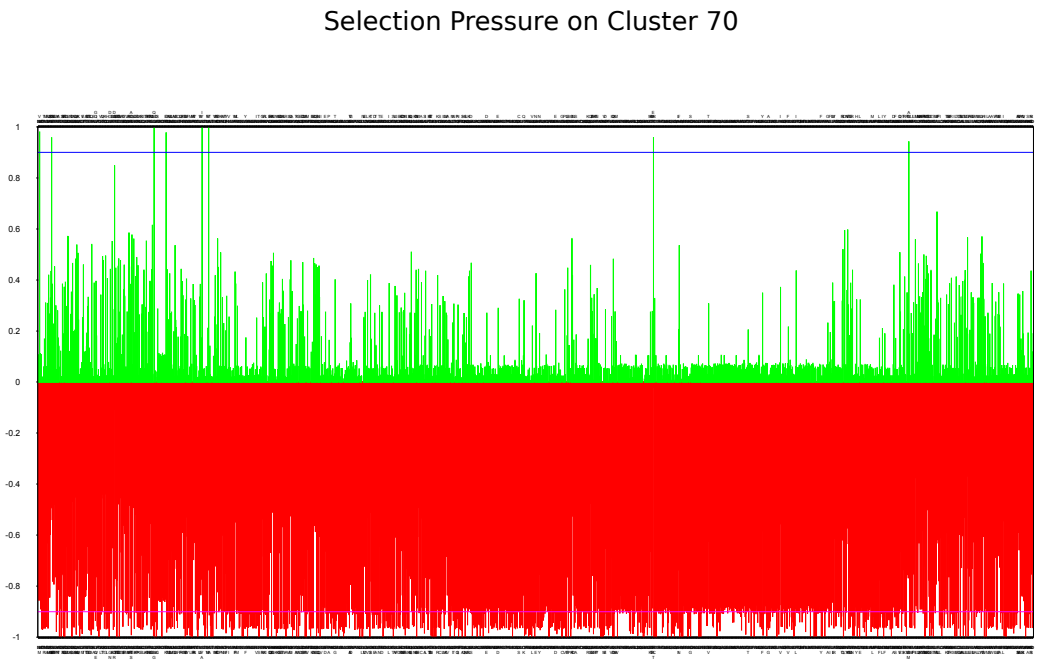

Figure I.86: Calculated codon level selection pressure on paralagous group 70. Levels above 0 are correspondent to positive selection pressure and levels below 0 are negative selection pressures. Anything over a selection pressure of ± 0.9 is considered significant.

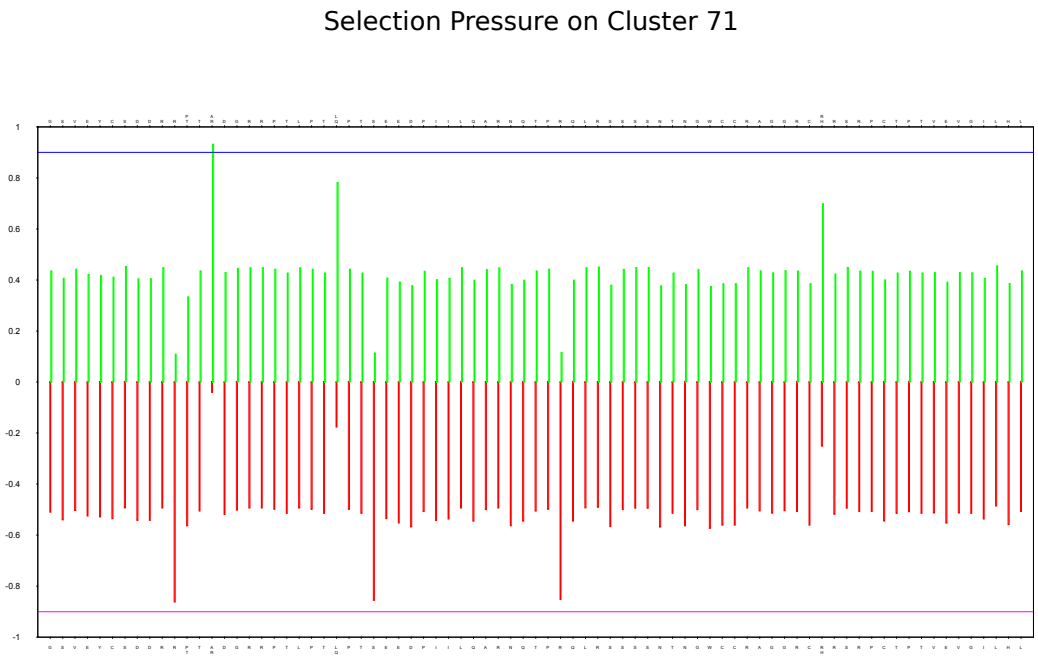

Figure I.87: Calculated codon level selection pressure on paralagous group 71. Levels above 0 are correspondent to positive selection pressure and levels below 0 are negative selection pressures. Anything over a selection pressure of ± 0.9 is considered significant.

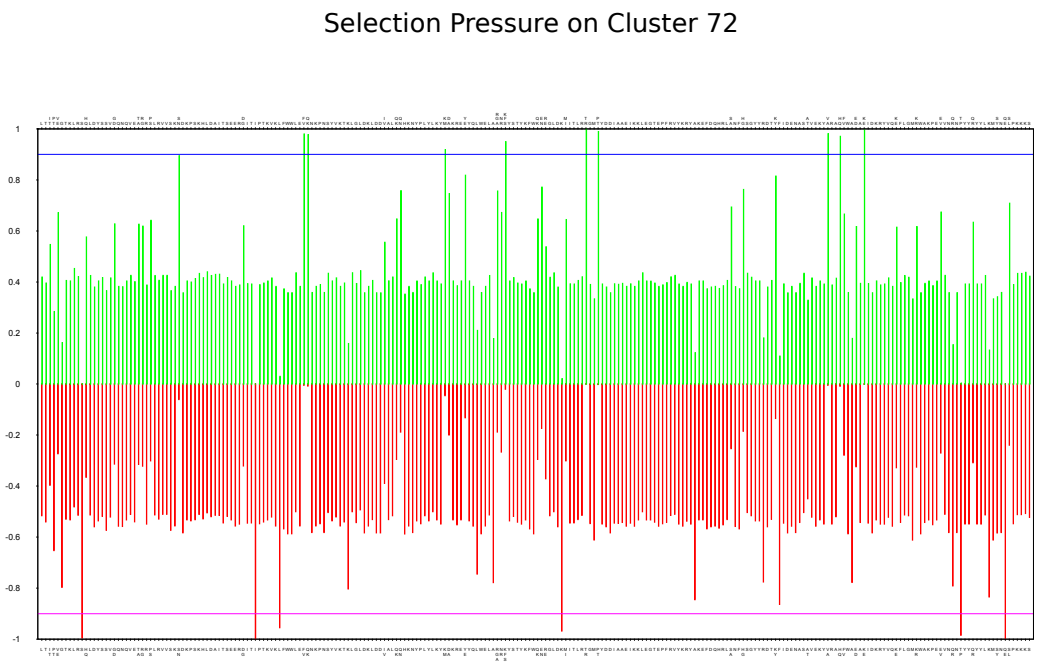

Figure I.88: Calculated codon level selection pressure on paralagous group 72. Levels above 0 are correspondent to positive selection pressure and levels below 0 are negative selection pressures. Anything over a selection pressure of ± 0.9 is considered significant.

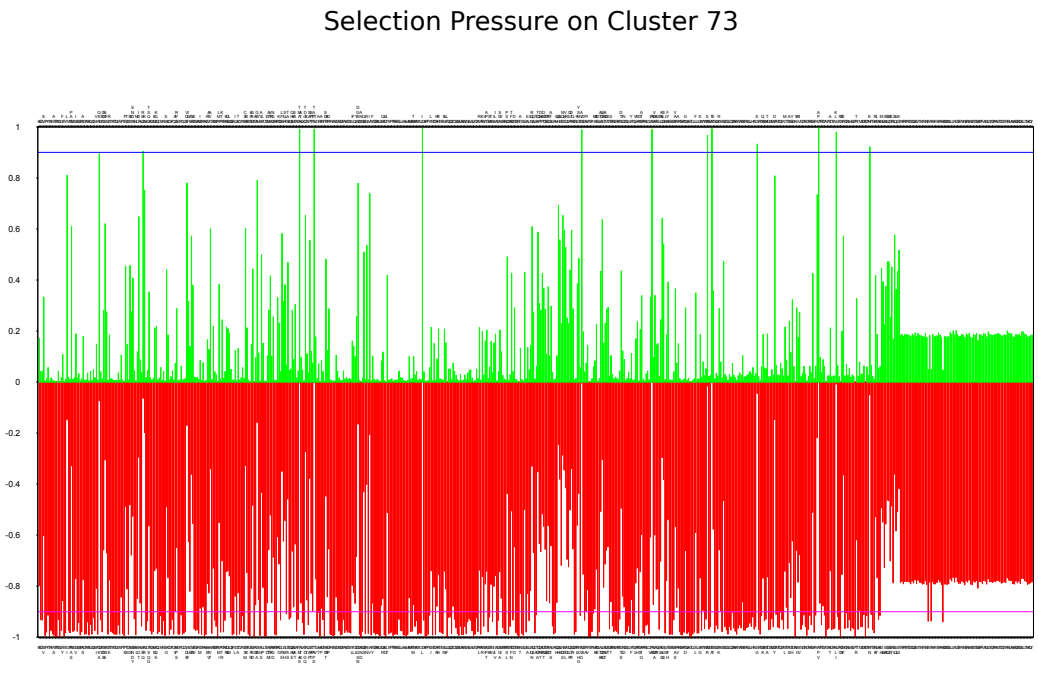

Figure I.89: Calculated codon level selection pressure on paralagous group 73. Levels above 0 are correspondent to positive selection pressure and levels below 0 are negative selection pressures. Anything over a selection pressure of ± 0.9 is considered significant.

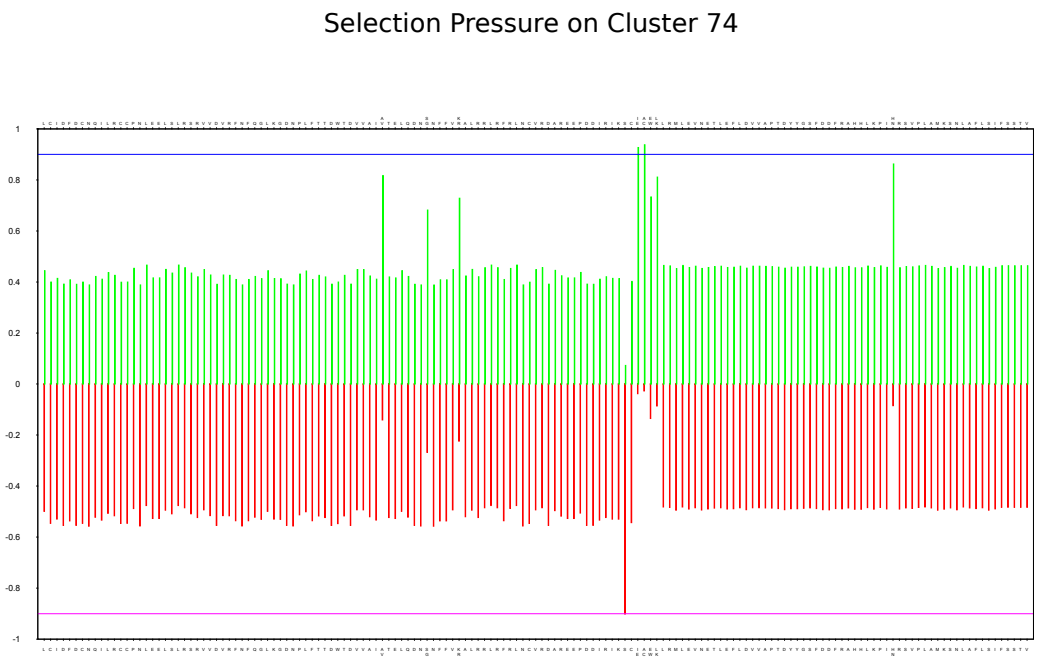

Figure I.90: Calculated codon level selection pressure on paralagous group 74. Levels above 0 are correspondent to positive selection pressure and levels below 0 are negative selection pressures. Anything over a selection pressure of ± 0.9 is considered significant.

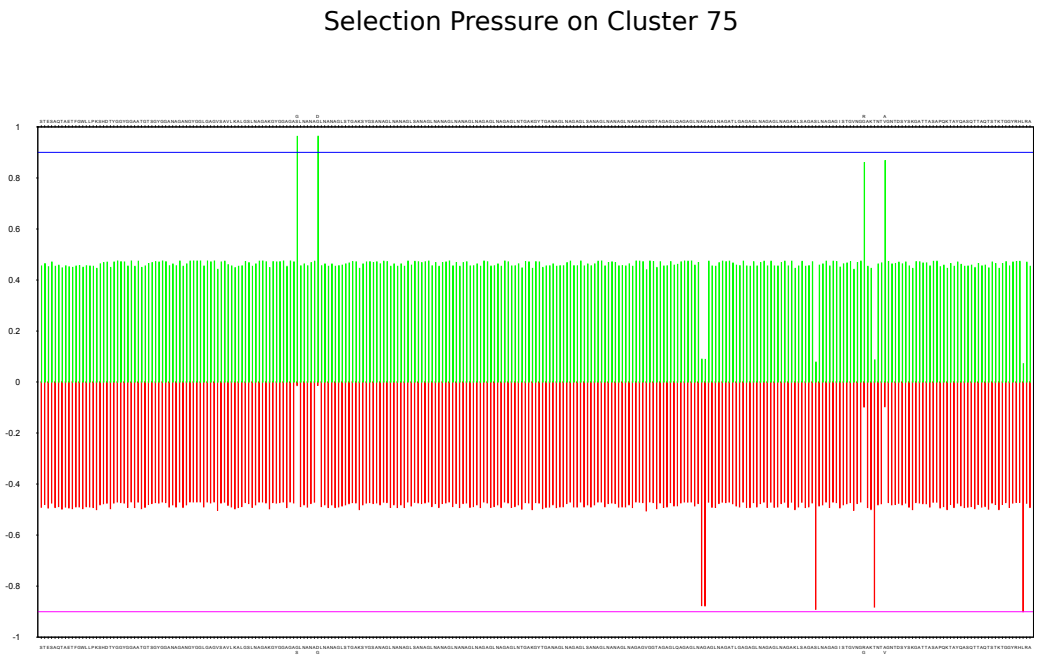

Figure I.91: Calculated codon level selection pressure on paralagous group 75. Levels above 0 are correspondent to positive selection pressure and levels below 0 are negative selection pressures. Anything over a selection pressure of ± 0.9 is considered significant.

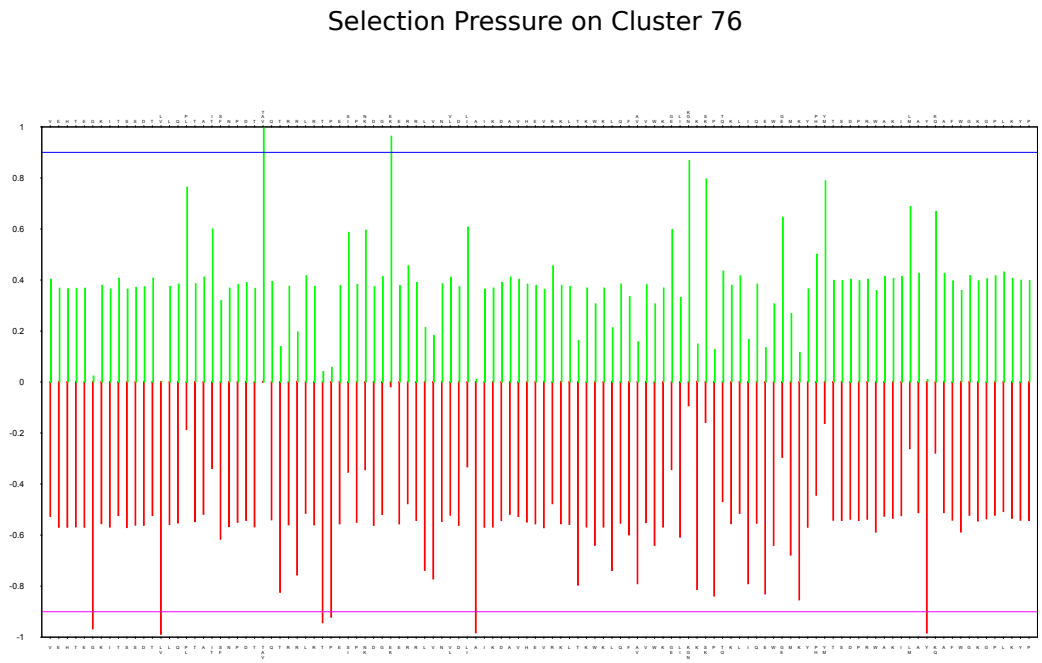

Figure I.92: Calculated codon level selection pressure on paralagous group 76. Levels above 0 are correspondent to positive selection pressure and levels below 0 are negative selection pressures. Anything over a selection pressure of ± 0.9 is considered significant.

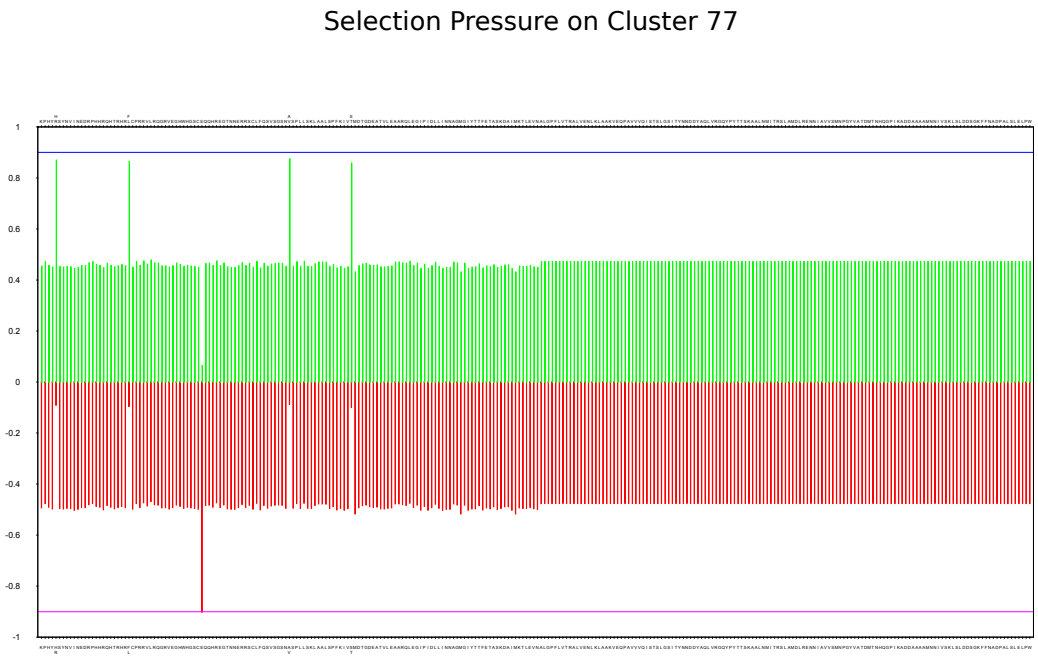

Figure I.93: Calculated codon level selection pressure on paralagous group 77. Levels above 0 are correspondent to positive selection pressure and levels below 0 are negative selection pressures. Anything over a selection pressure of ± 0.9 is considered significant.

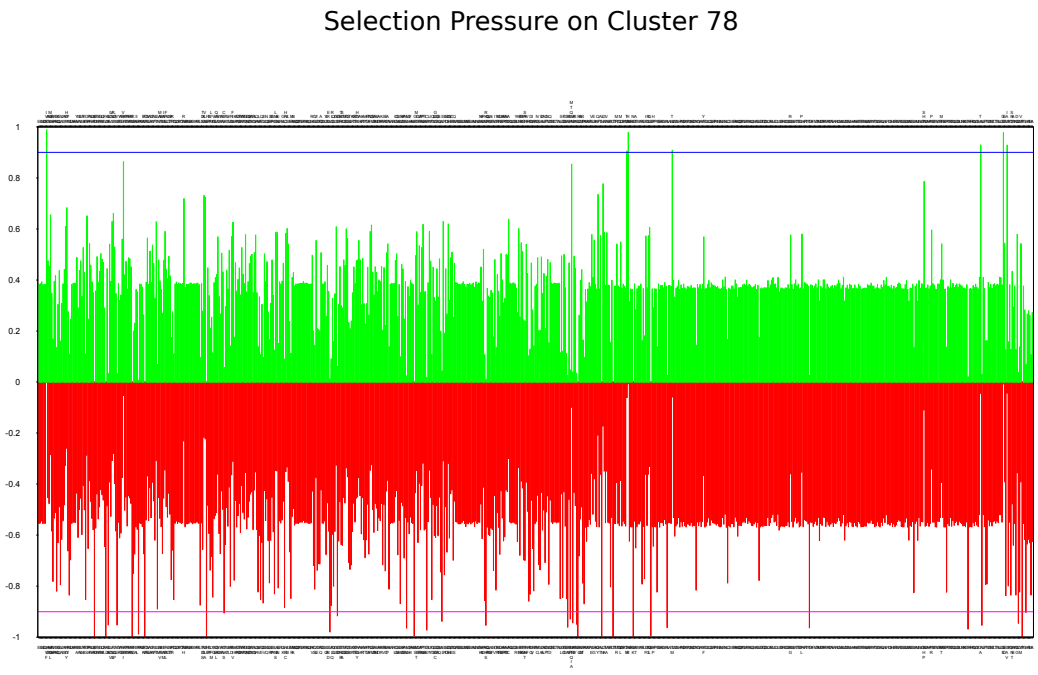

Figure I.94: Calculated codon level selection pressure on paralagous group 78. Levels above 0 are correspondent to positive selection pressure and levels below 0 are negative selection pressures. Anything over a selection pressure of ± 0.9 is considered significant.

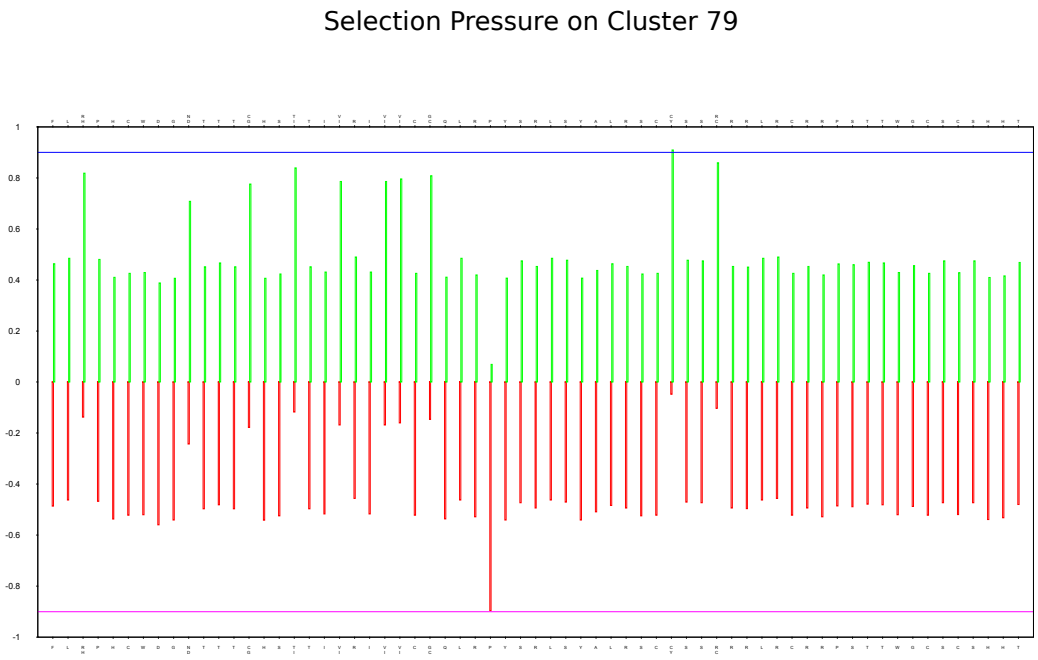

Figure I.95: Calculated codon level selection pressure on paralagous group 79. Levels above 0 are correspondent to positive selection pressure and levels below 0 are negative selection pressures. Anything over a selection pressure of ± 0.9 is considered significant.

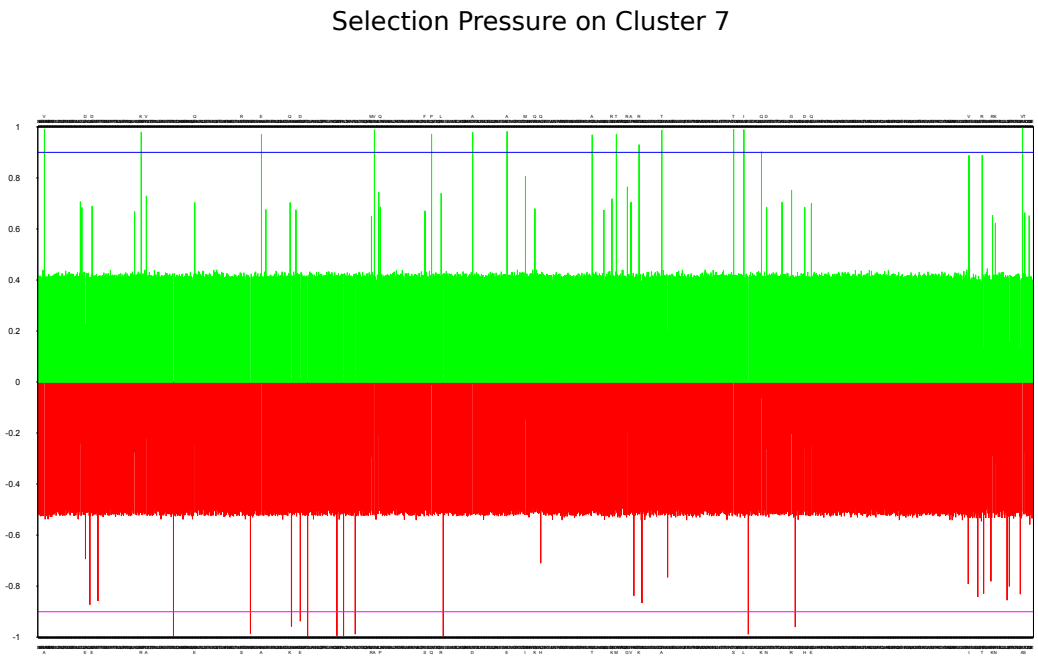

Figure I.96: Calculated codon level selection pressure on paralagous group 7. Levels above 0 are correspondent to positive selection pressure and levels below 0 are negative selection pressures. Anything over a selection pressure of ± 0.9 is considered significant.

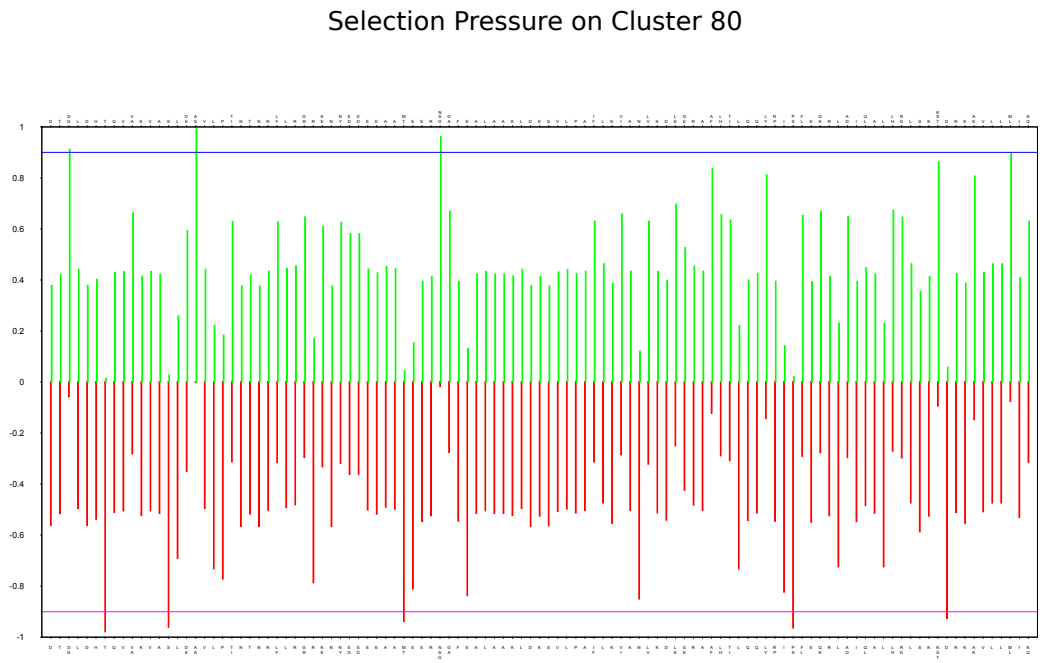

Figure I.97: Calculated codon level selection pressure on paralagous group 80. Levels above 0 are correspondent to positive selection pressure and levels below 0 are negative selection pressures. Anything over a selection pressure of ± 0.9 is considered significant.

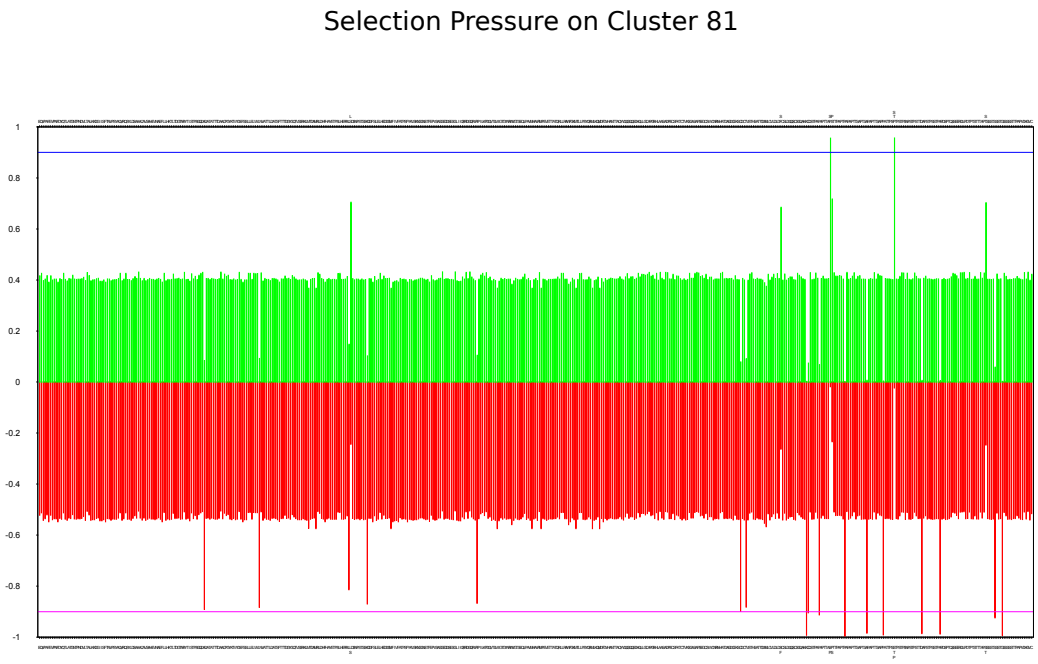

Figure I.98: Calculated codon level selection pressure on paralagous group 81. Levels above 0 are correspondent to positive selection pressure and levels below 0 are negative selection pressures. Anything over a selection pressure of ± 0.9 is considered significant.

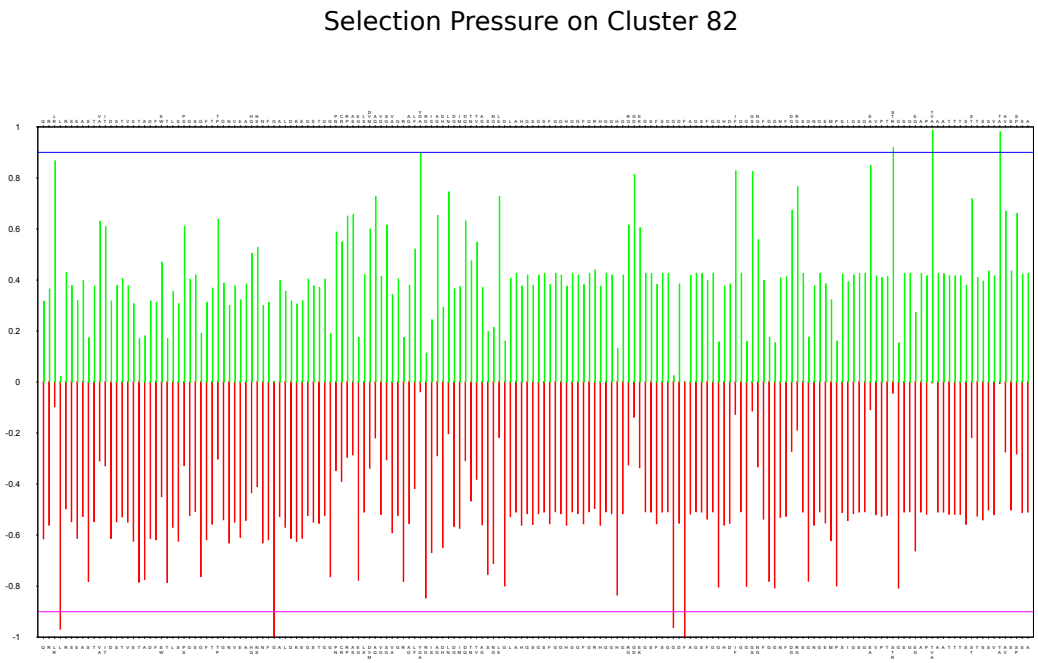

Figure I.99: Calculated codon level selection pressure on paralagous group 82. Levels above 0 are correspondent to positive selection pressure and levels below 0 are negative selection pressures. Anything over a selection pressure of ± 0.9 is considered significant.

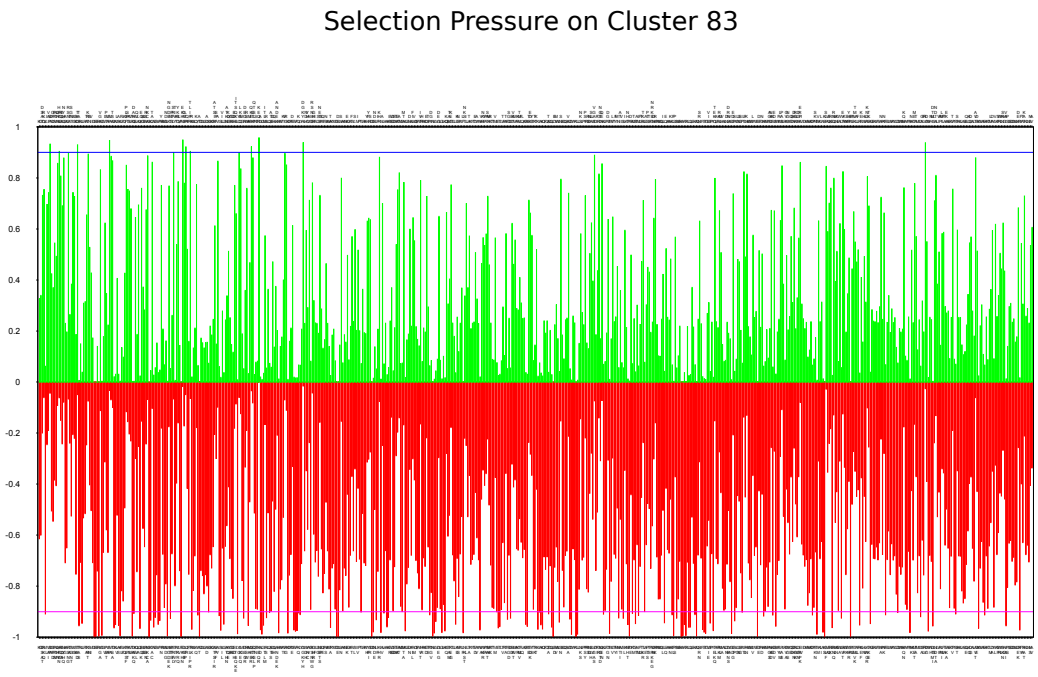

Figure I.100: Calculated codon level selection pressure on paralagous group 83. Levels above 0 are correspondent to positive selection pressure and levels below 0 are negative selection pressures. Anything over a selection pressure of ± 0.9 is considered significant.

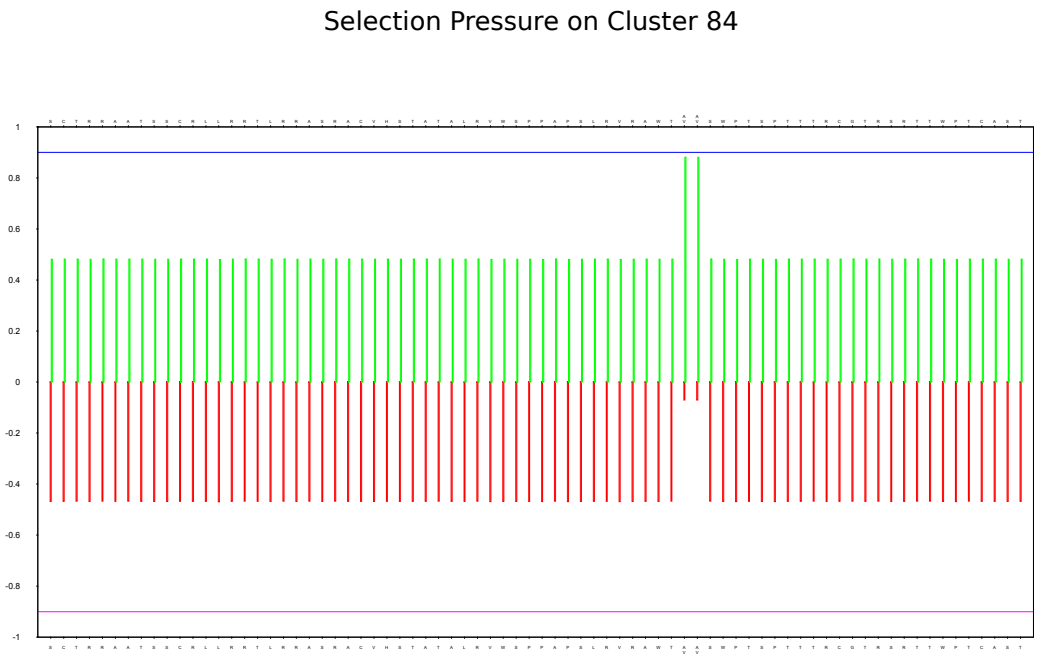

Figure I.101: Calculated codon level selection pressure on paralagous group 84. Levels above 0 are correspondent to positive selection pressure and levels below 0 are negative selection pressures. Anything over a selection pressure of ± 0.9 is considered significant.

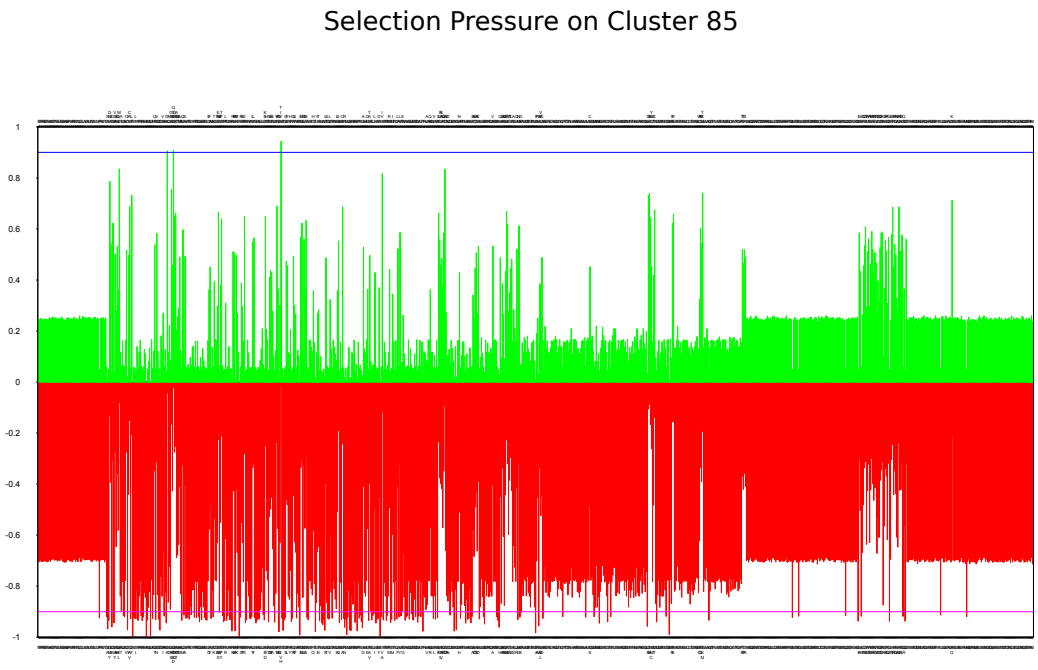

Figure I.102: Calculated codon level selection pressure on paralagous group 85. Levels above 0 are correspondent to positive selection pressure and levels below 0 are negative selection pressures. Anything over a selection pressure of ± 0.9 is considered significant.

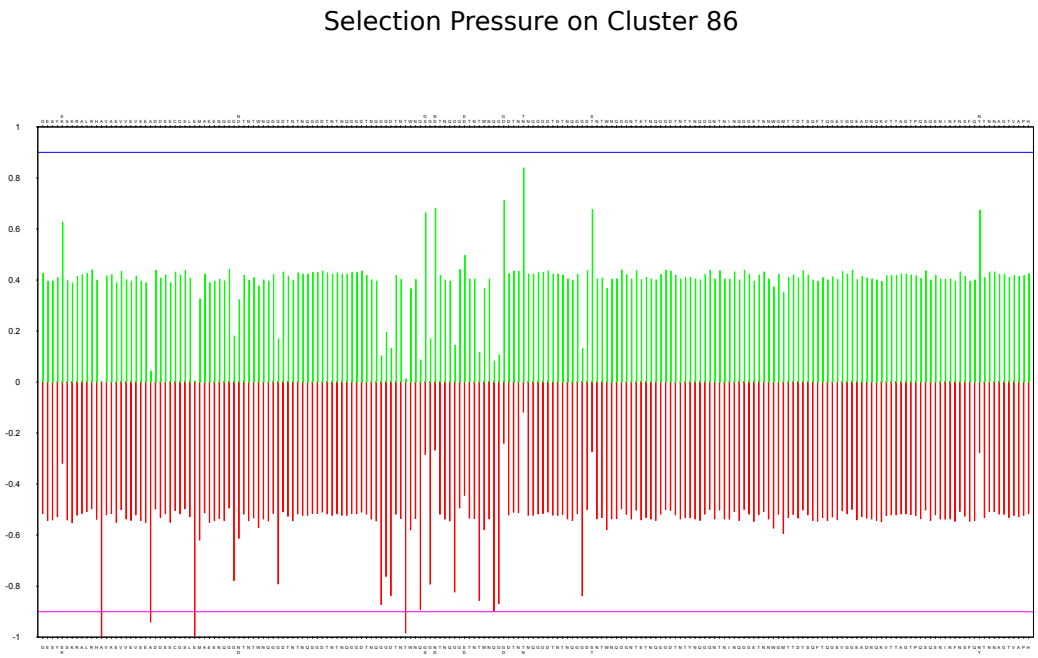

Figure I.103: Calculated codon level selection pressure on paralagous group 86. Levels above 0 are correspondent to positive selection pressure and levels below 0 are negative selection pressures. Anything over a selection pressure of ± 0.9 is considered significant.

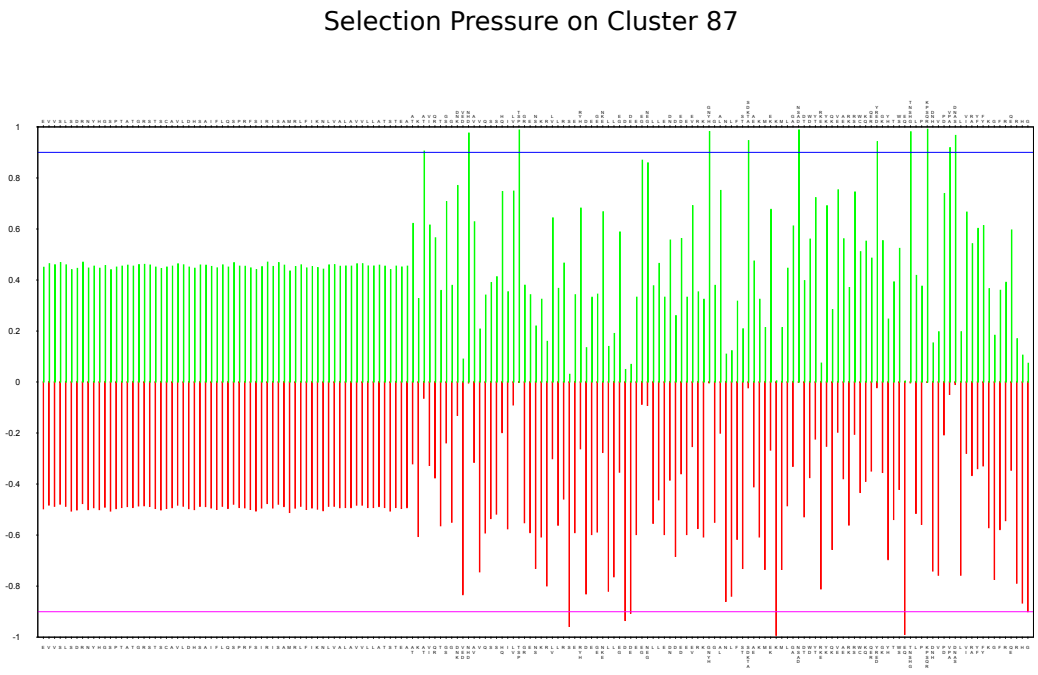

Figure I.104: Calculated codon level selection pressure on paralagous group 87. Levels above 0 are correspondent to positive selection pressure and levels below 0 are negative selection pressures. Anything over a selection pressure of ± 0.9 is considered significant.

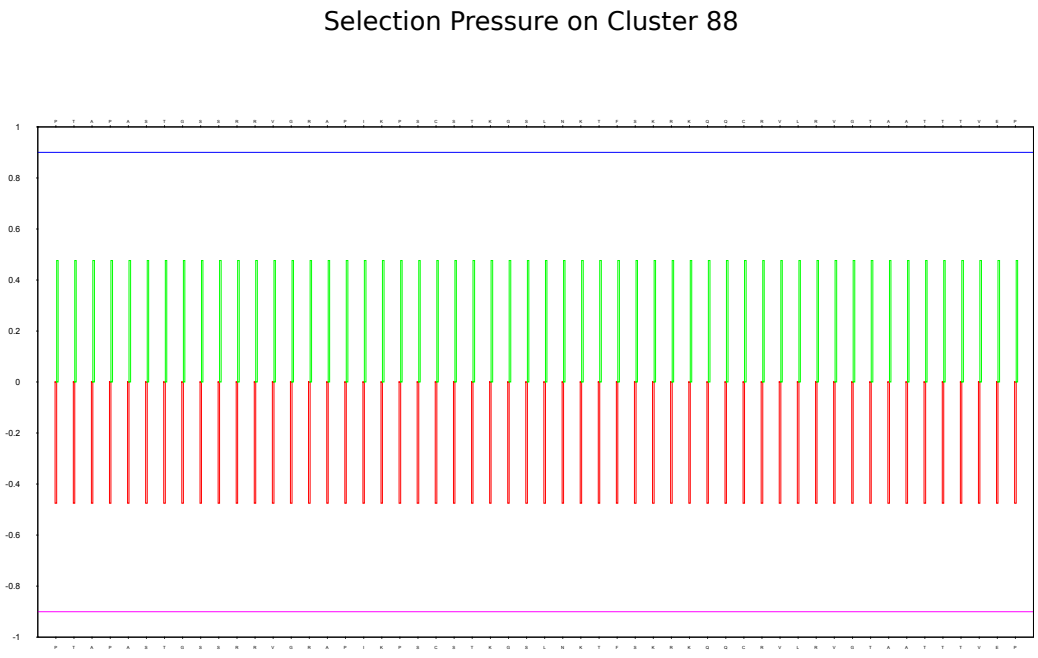

Figure I.105: Calculated codon level selection pressure on paralagous group 88. Levels above 0 are correspondent to positive selection pressure and levels below 0 are negative selection pressures. Anything over a selection pressure of ± 0.9 is considered significant.

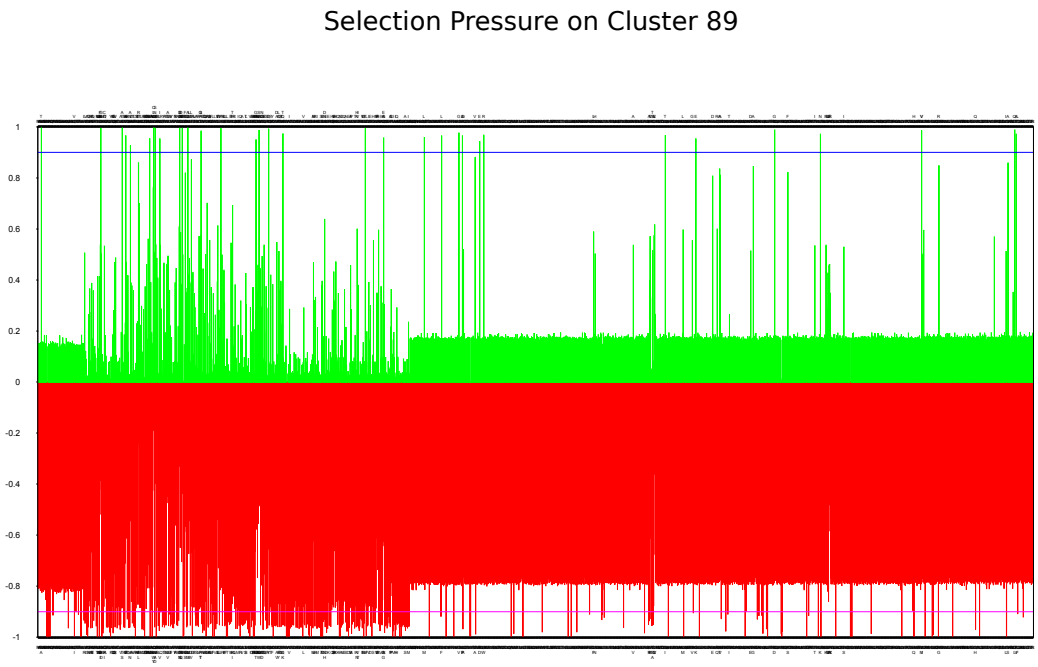

Figure I.106: Calculated codon level selection pressure on paralagous group 89. Levels above 0 are correspondent to positive selection pressure and levels below 0 are negative selection pressures. Anything over a selection pressure of ± 0.9 is considered significant.

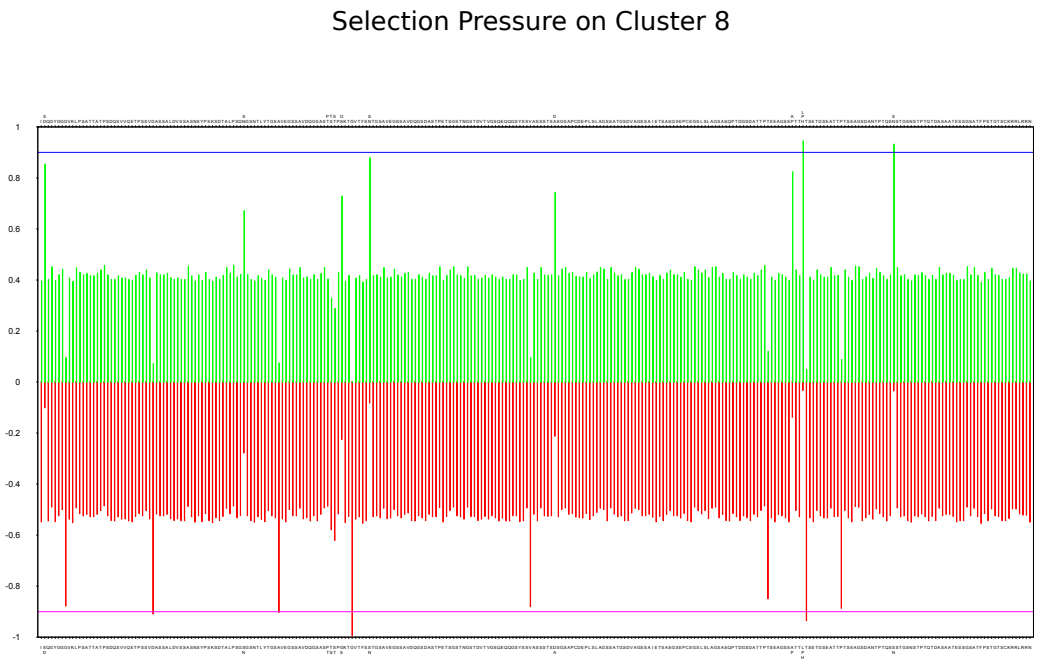

Figure I.107: Calculated codon level selection pressure on paralagous group 8. Levels above 0 are correspondent to positive selection pressure and levels below 0 are negative selection pressures. Anything over a selection pressure of ± 0.9 is considered significant.

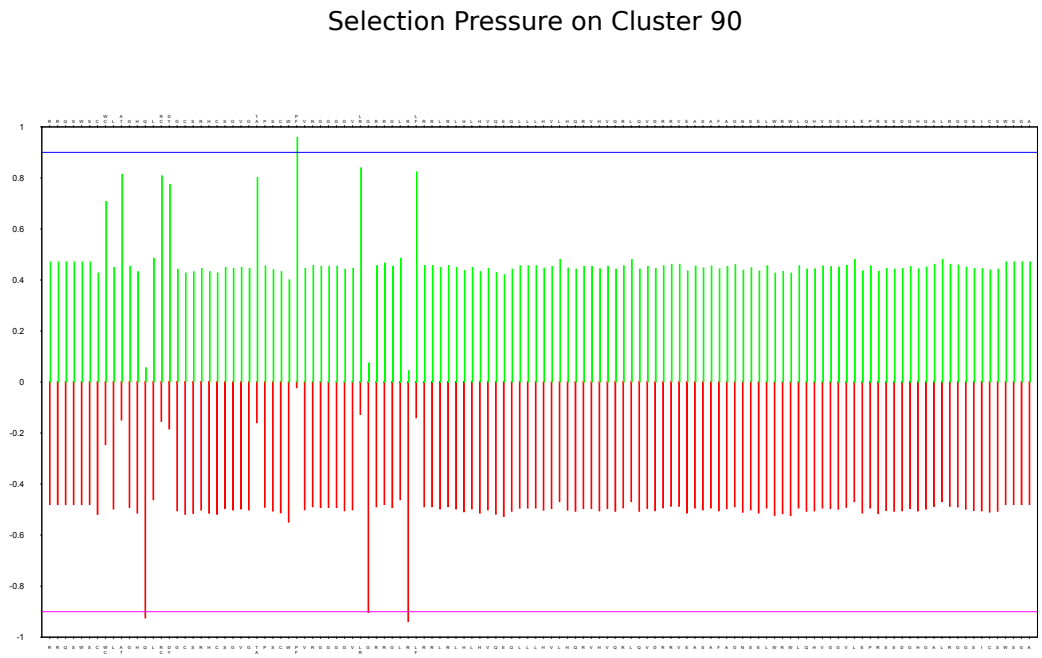

Figure I.108: Calculated codon level selection pressure on paralagous group 90. Levels above 0 are correspondent to positive selection pressure and levels below 0 are negative selection pressures. Anything over a selection pressure of ± 0.9 is considered significant.

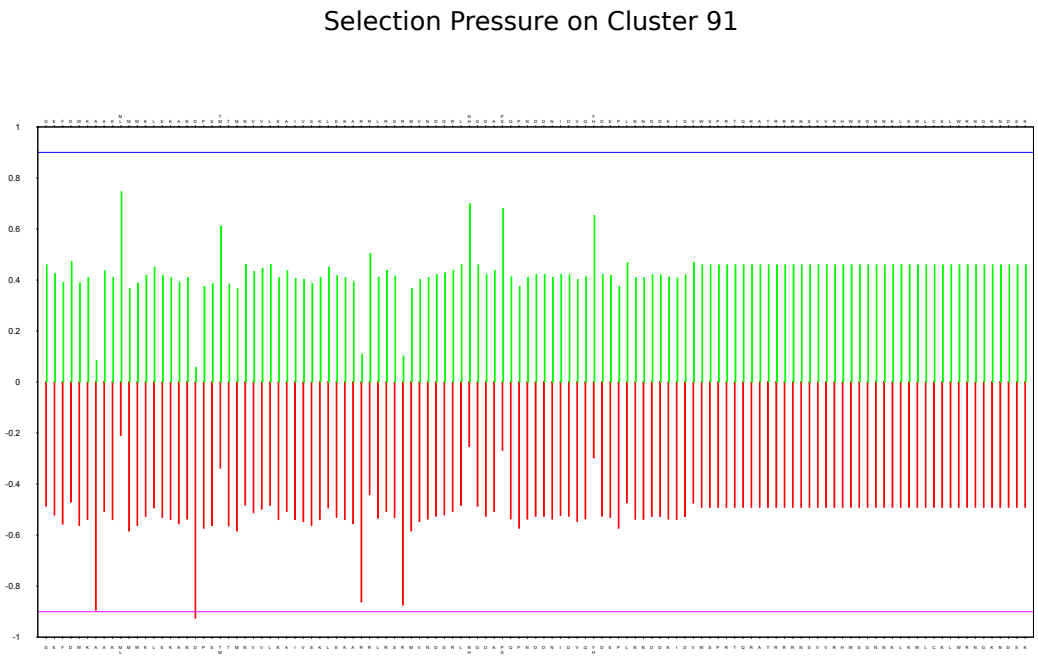

Figure I.109: Calculated codon level selection pressure on paralagous group 91. Levels above 0 are correspondent to positive selection pressure and levels below 0 are negative selection pressures. Anything over a selection pressure of ± 0.9 is considered significant.

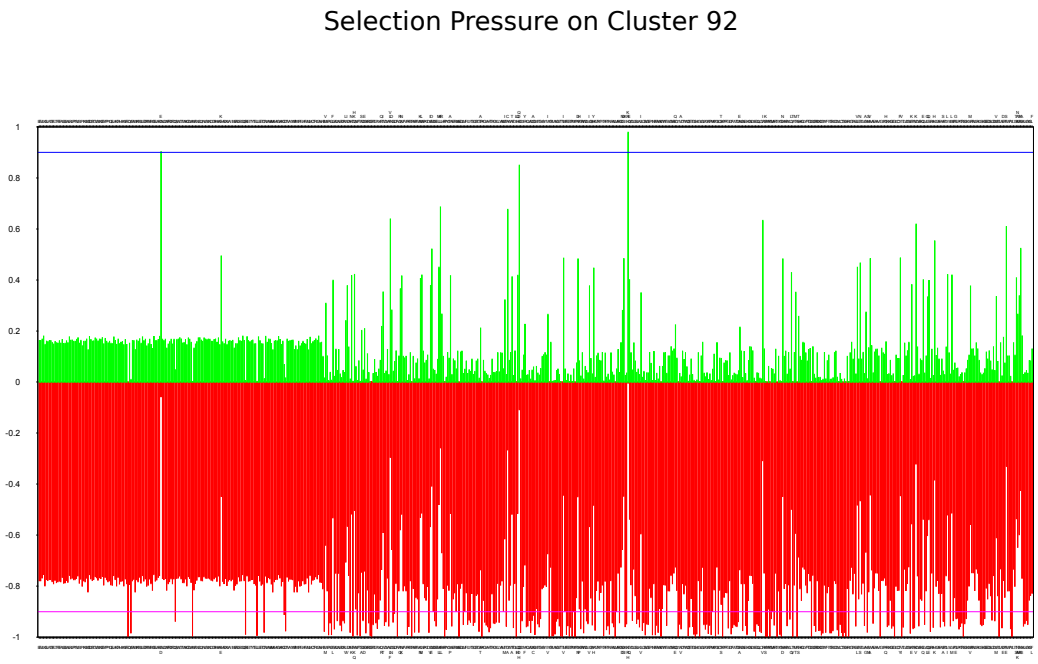

Figure I.110: Calculated codon level selection pressure on paralagous group 92. Levels above 0 are correspondent to positive selection pressure and levels below 0 are negative selection pressures. Anything over a selection pressure of ± 0.9 is considered significant.

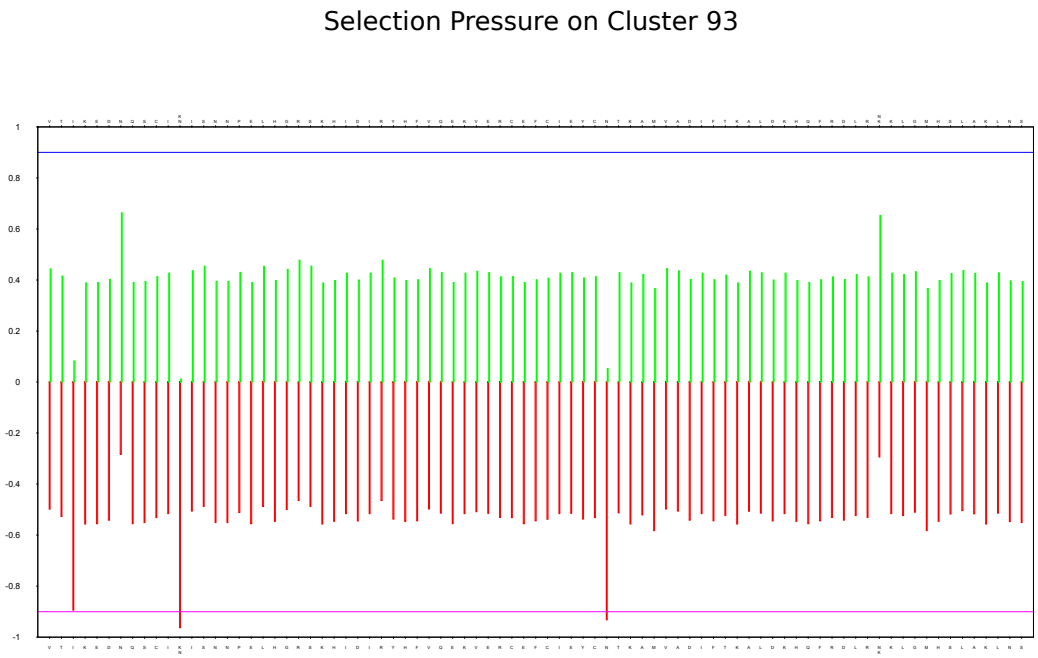

Figure I.111: Calculated codon level selection pressure on paralagous group 93. Levels above 0 are correspondent to positive selection pressure and levels below 0 are negative selection pressures. Anything over a selection pressure of ± 0.9 is considered significant.

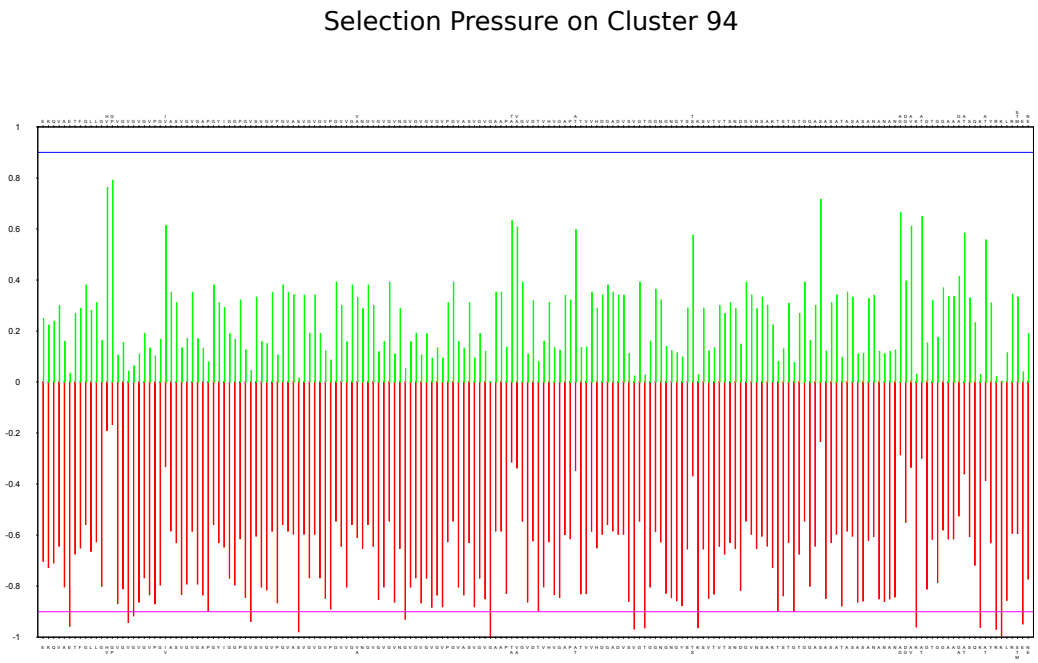

Figure I.112: Calculated codon level selection pressure on paralagous group 94. Levels above 0 are correspondent to positive selection pressure and levels below 0 are negative selection pressures. Anything over a selection pressure of ± 0.9 is considered significant.

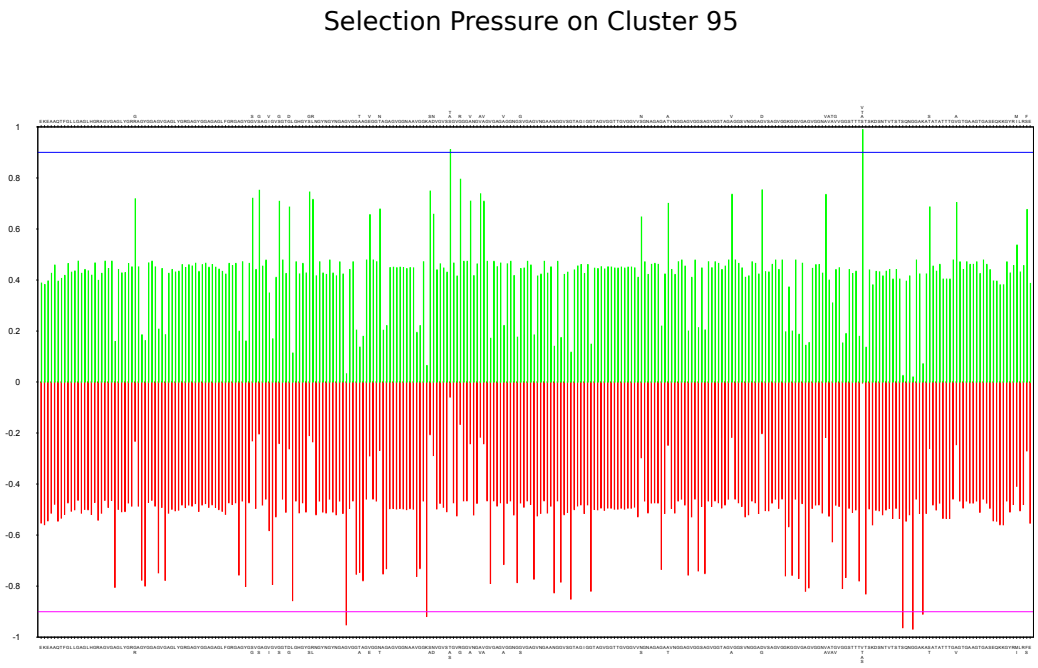

Figure I.113: Calculated codon level selection pressure on paralagous group 95. Levels above 0 are correspondent to positive selection pressure and levels below 0 are negative selection pressures. Anything over a selection pressure of ± 0.9 is considered significant.

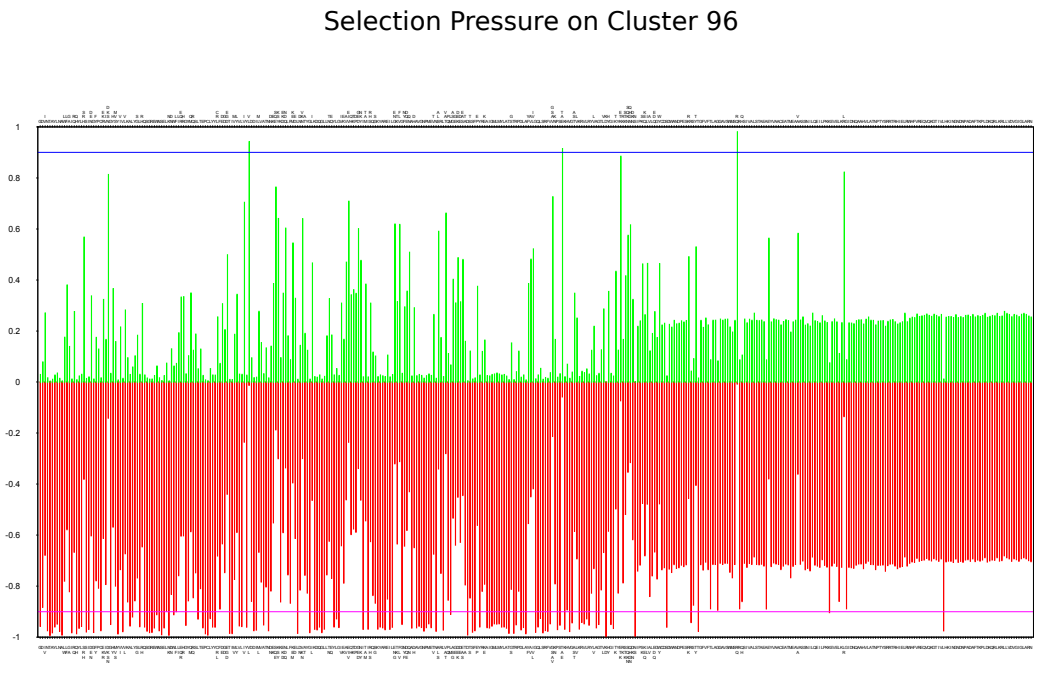

Figure I.114: Calculated codon level selection pressure on paralagous group 96. Levels above 0 are correspondent to positive selection pressure and levels below 0 are negative selection pressures. Anything over a selection pressure of ± 0.9 is considered significant.

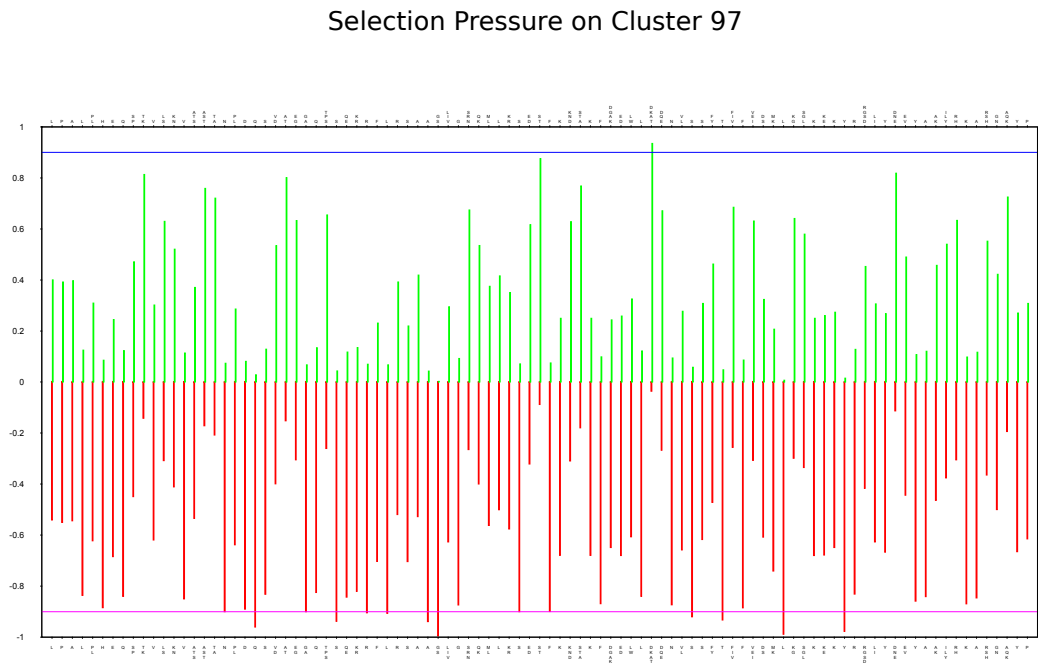

Figure I.115: Calculated codon level selection pressure on paralagous group 97. Levels above 0 are correspondent to positive selection pressure and levels below 0 are negative selection pressures. Anything over a selection pressure of ± 0.9 is considered significant.

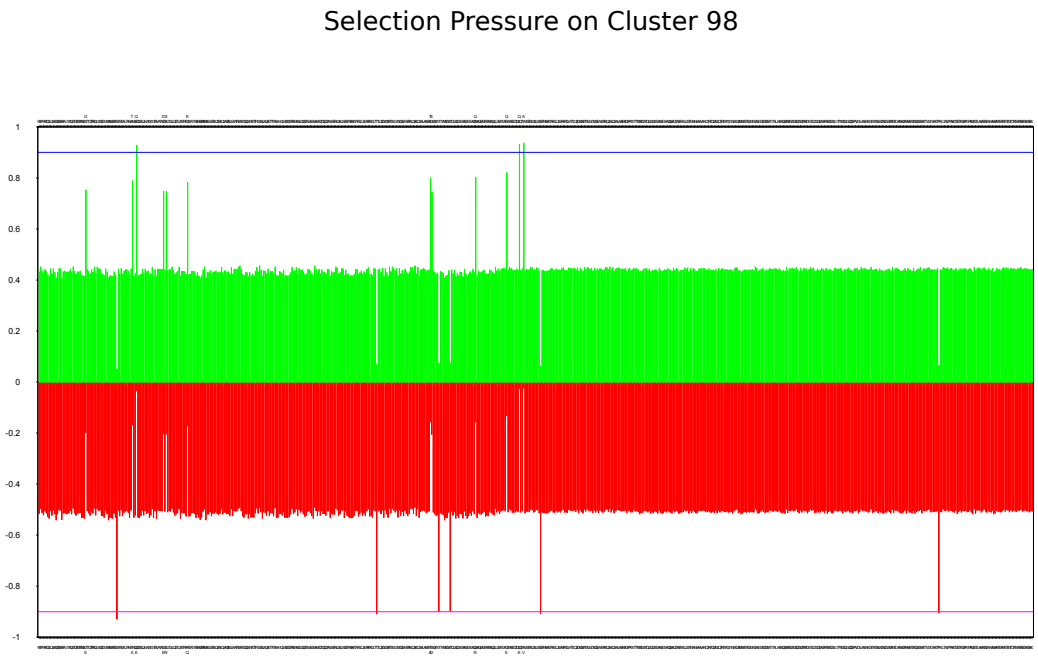

Figure I.116: Calculated codon level selection pressure on paralagous group 98. Levels above 0 are correspondent to positive selection pressure and levels below 0 are negative selection pressures. Anything over a selection pressure of ± 0.9 is considered significant.

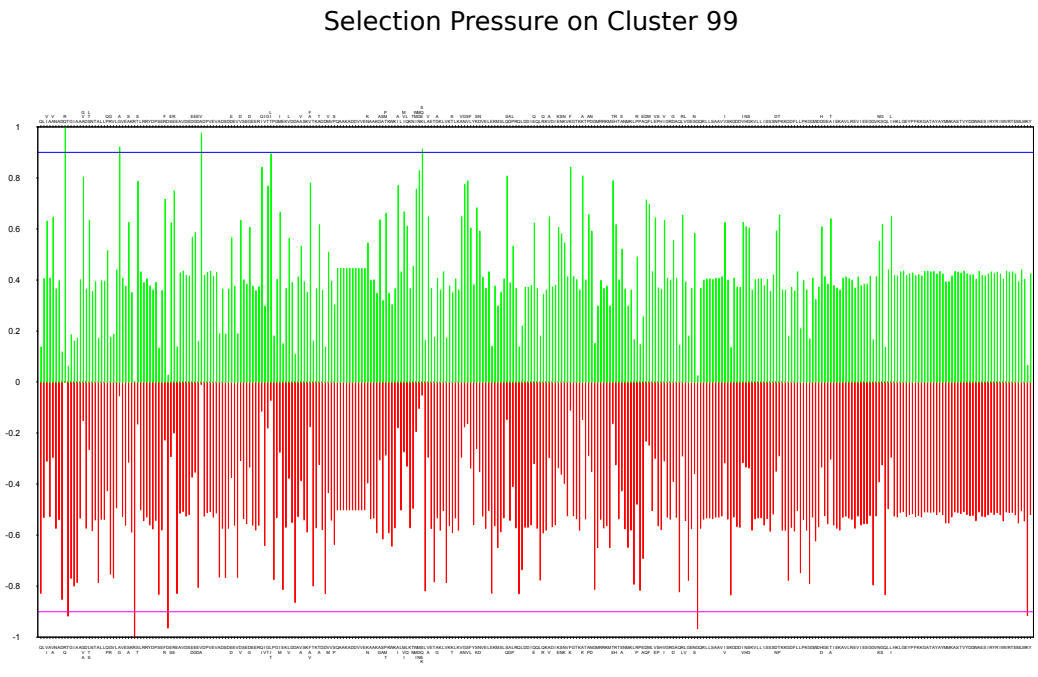

Figure I.117: Calculated codon level selection pressure on paralagous group 99. Levels above 0 are correspondent to positive selection pressure and levels below 0 are negative selection pressures. Anything over a selection pressure of ± 0.9 is considered significant.

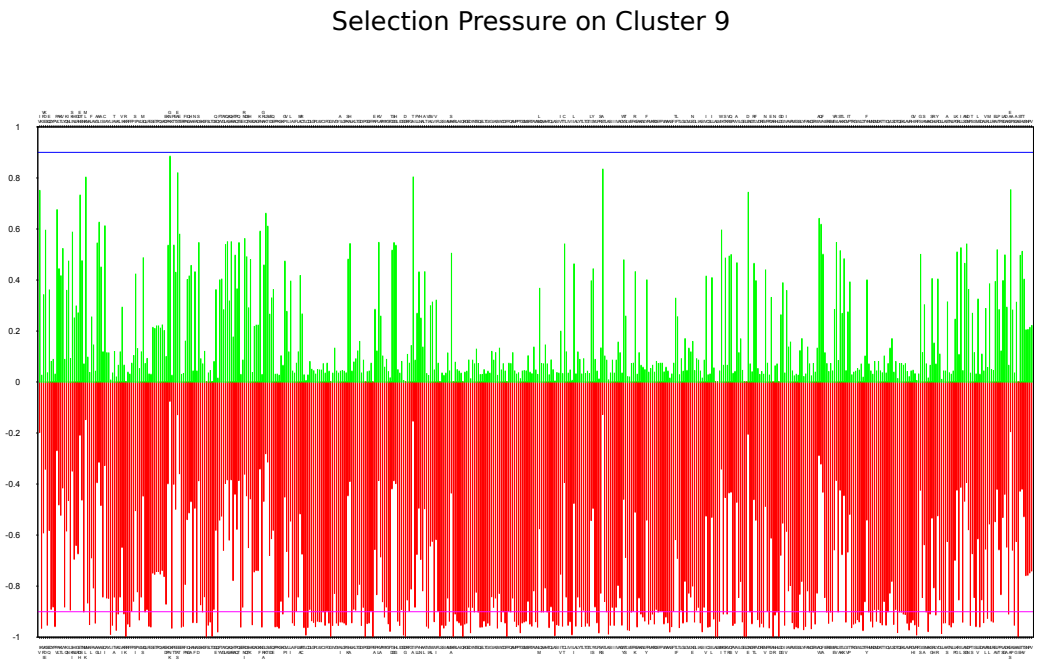

Figure I.118: Calculated codon level selection pressure on paralagous group 9. Levels above 0 are correspondent to positive selection pressure and levels below 0 are negative selection pressures. Anything over a selection pressure of ± 0.9 is considered significant.

Appendix J

Calculated Selection Pressures on Paralagous CRN Groups

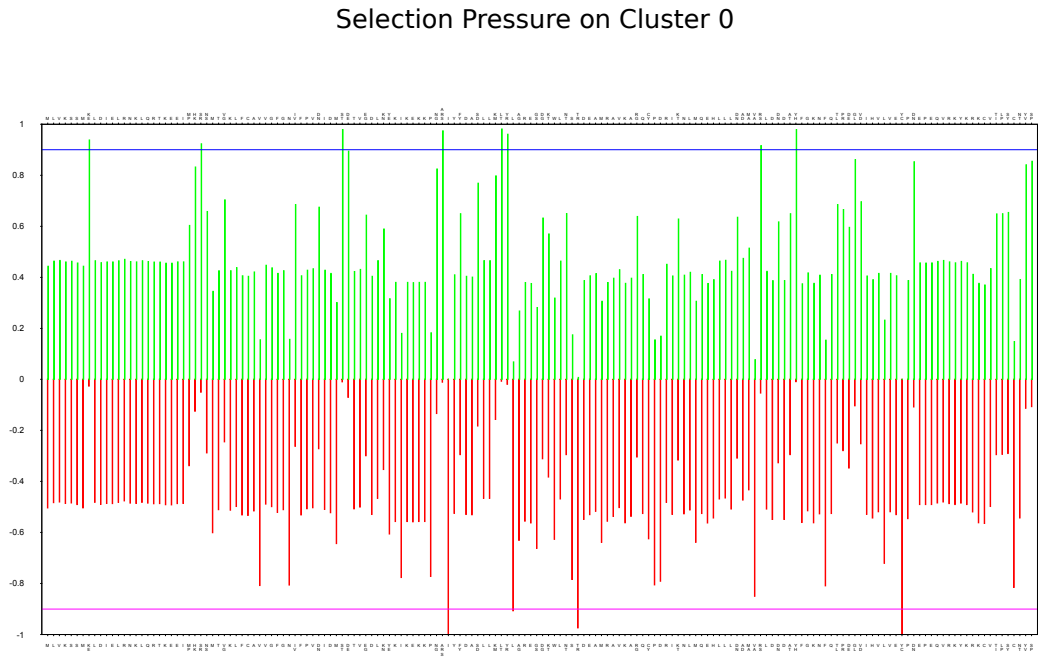

Figure J.1: Calculated codon level selection pressure on paralagous group 0. Levels above 0 are correspondent to positive selection pressure and levels below 0 are negative selection pressures. Anything over a selection pressure of ± 0.9 is considered significant.

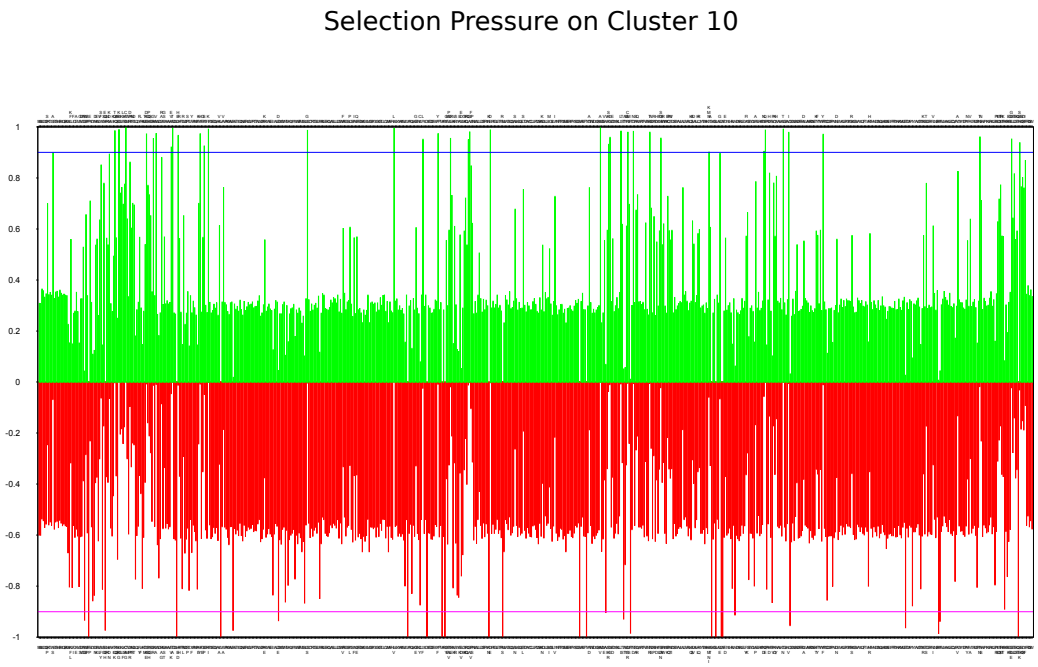

Figure J.2: Calculated codon level selection pressure on paralagous group 10. Levels above 0 are correspondent to positive selection pressure and levels below 0 are negative selection pressures. Anything over a selection pressure of ± 0.9 is considered significant.

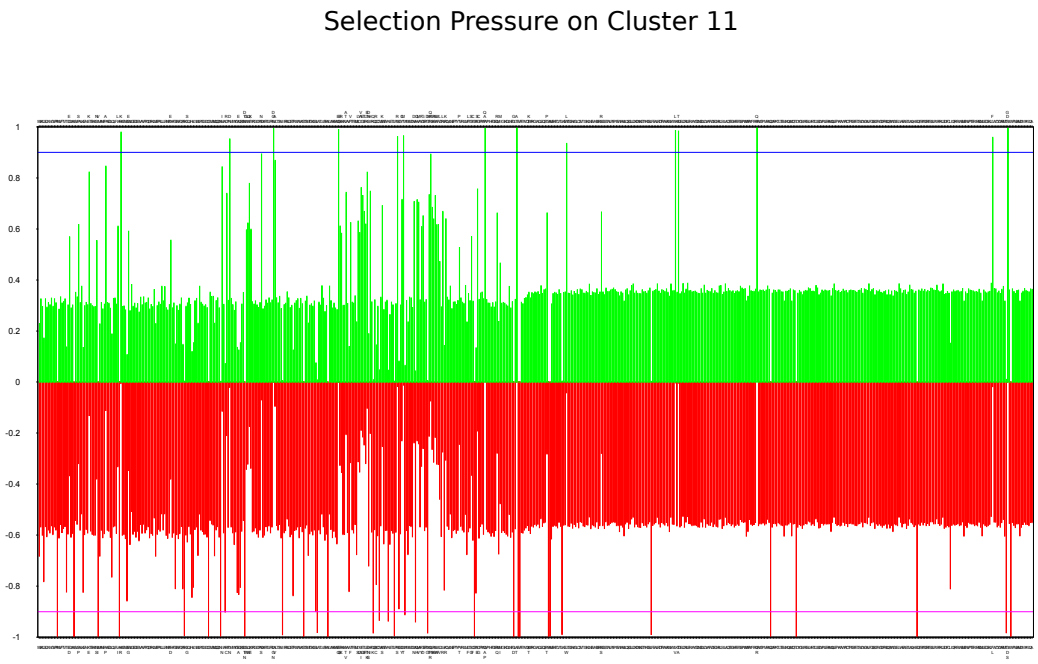

Figure J.3: Calculated codon level selection pressure on paralagous group 11. Levels above 0 are correspondent to positive selection pressure and levels below 0 are negative selection pressures. Anything over a selection pressure of ± 0.9 is considered significant.

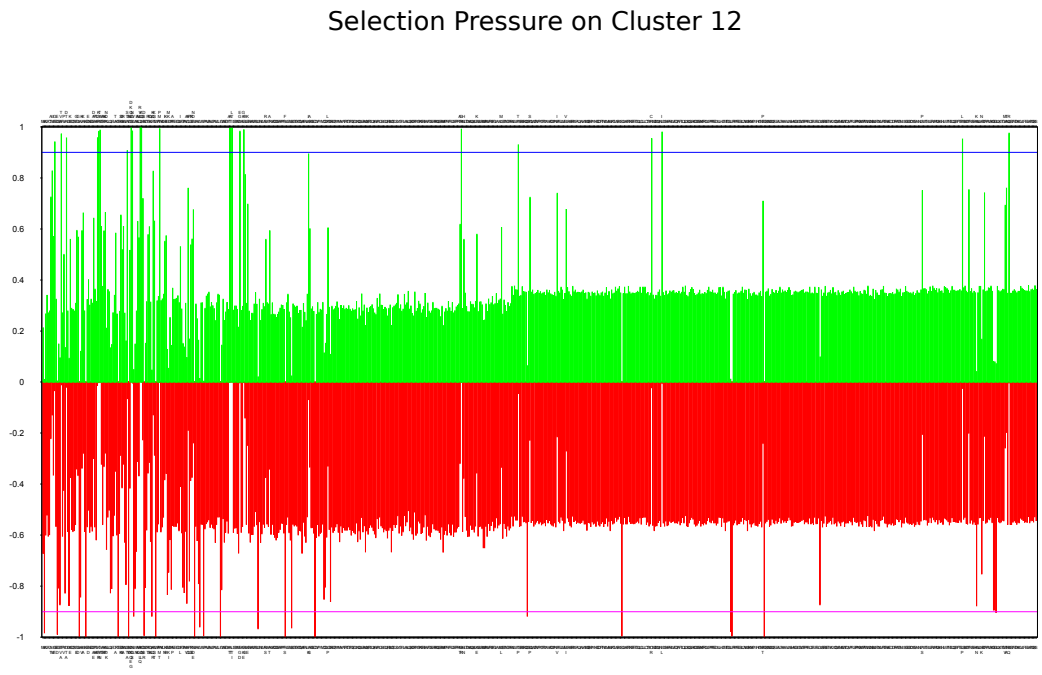

Figure J.4: Calculated codon level selection pressure on paralagous group 12. Levels above 0 are correspondent to positive selection pressure and levels below 0 are negative selection pressures. Anything over a selection pressure of ± 0.9 is considered significant.

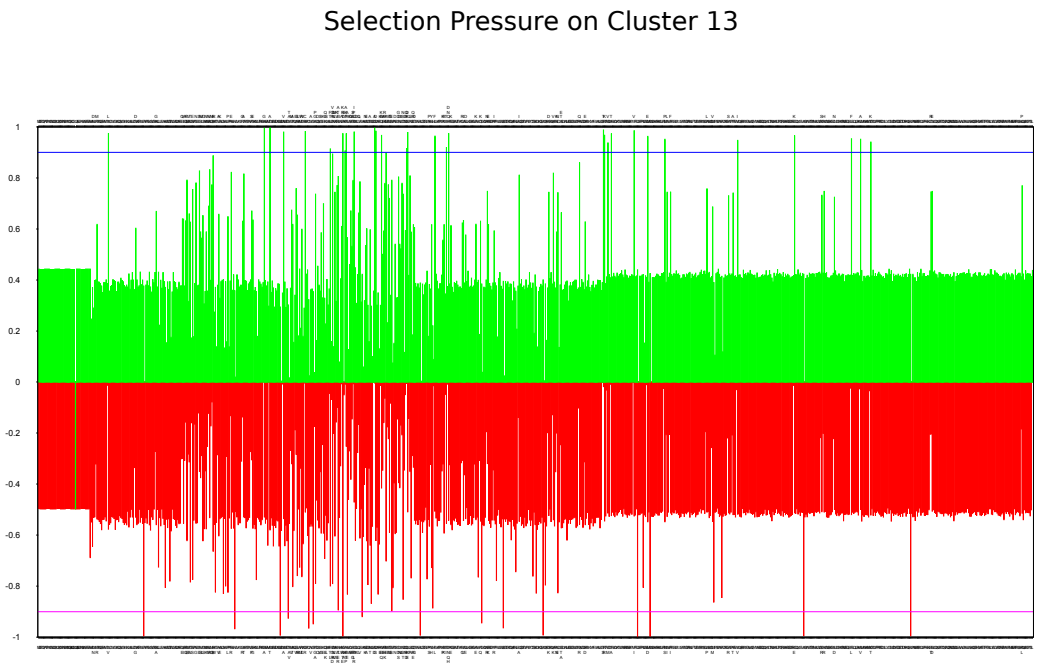

Figure J.5: Calculated codon level selection pressure on paralagous group 13. Levels above 0 are correspondent to positive selection pressure and levels below 0 are negative selection pressures. Anything over a selection pressure of ± 0.9 is considered significant.

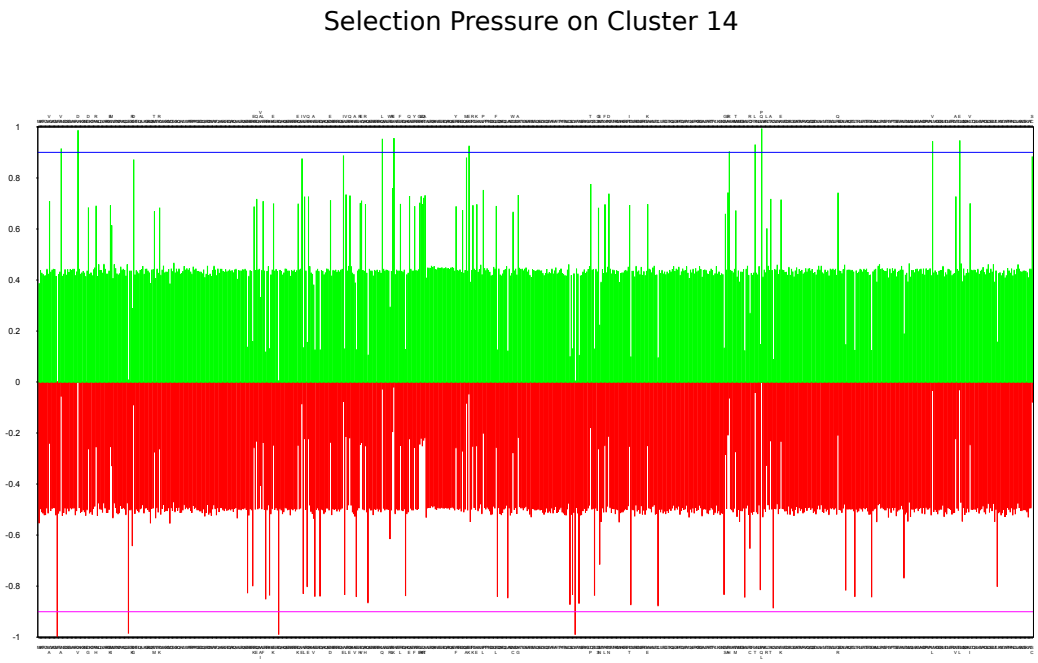

Figure J.6: Calculated codon level selection pressure on paralagous group 14. Levels above 0 are correspondent to positive selection pressure and levels below 0 are negative selection pressures. Anything over a selection pressure of ± 0.9 is considered significant.

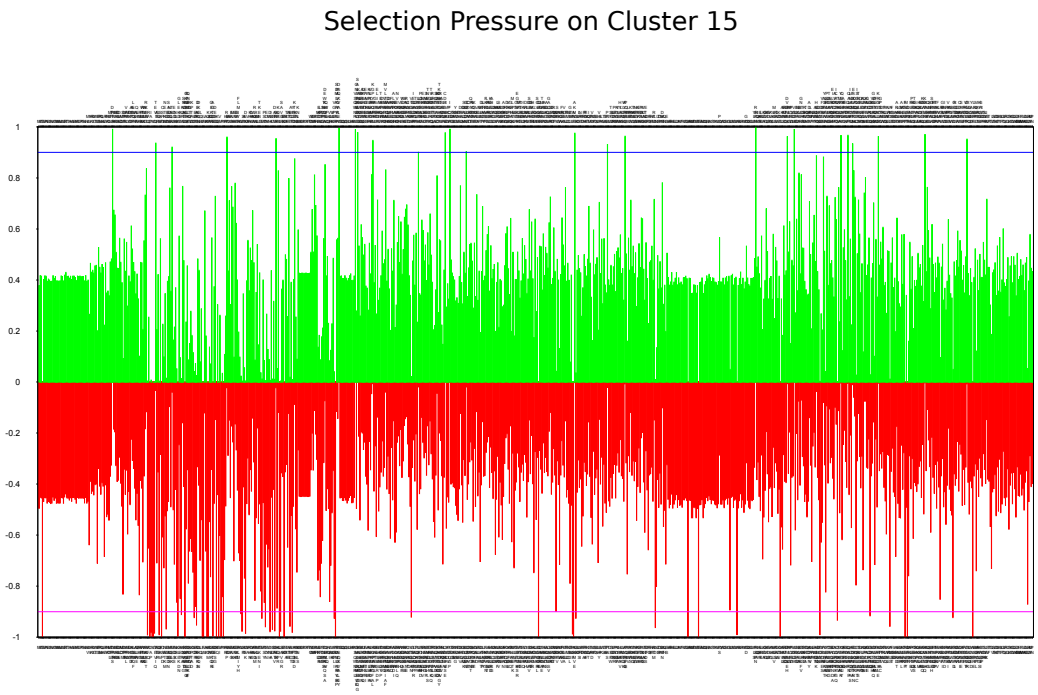

Figure J.7: Calculated codon level selection pressure on paralagous group 15. Levels above 0 are correspondent to positive selection pressure and levels below 0 are negative selection pressures. Anything over a selection pressure of ± 0.9 is considered significant.

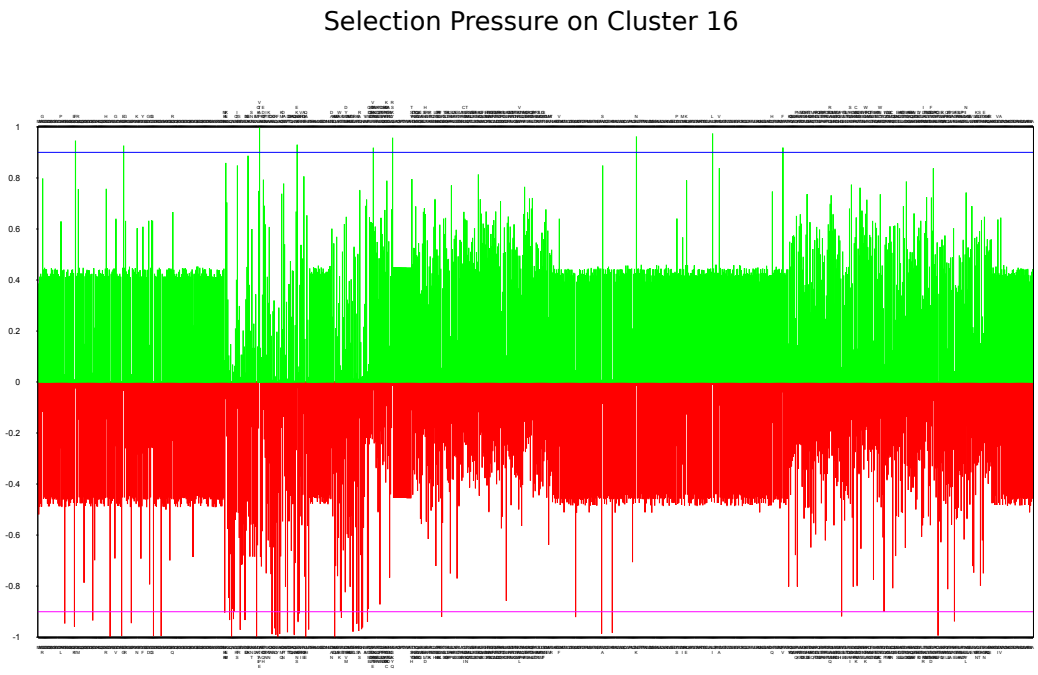

Figure J.8: Calculated codon level selection pressure on paralagous group 16. Levels above 0 are correspondent to positive selection pressure and levels below 0 are negative selection pressures. Anything over a selection pressure of ± 0.9 is considered significant.

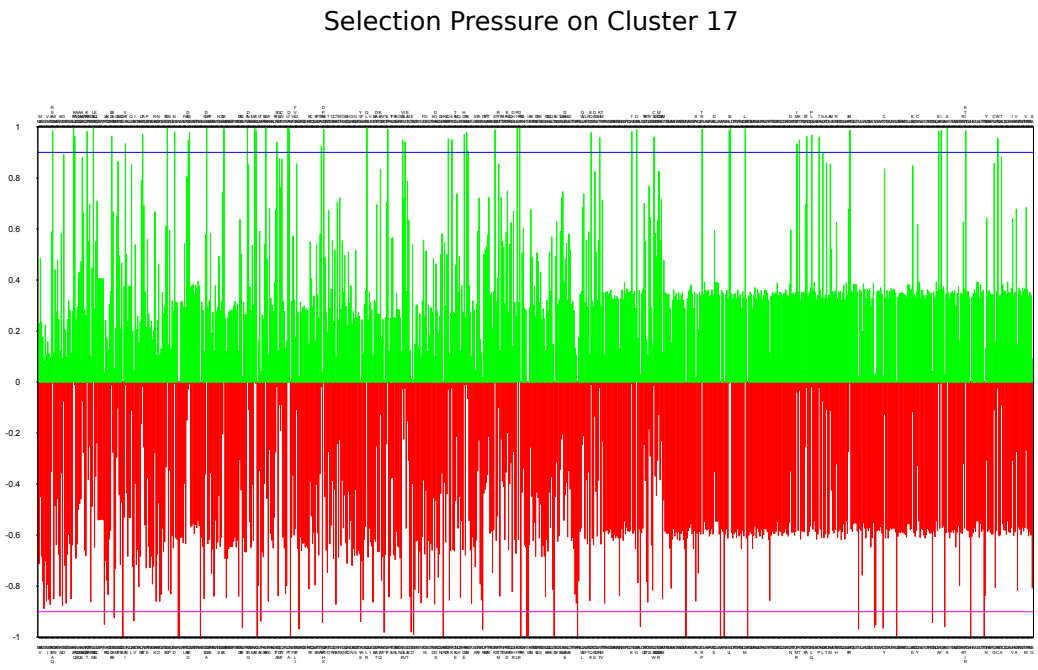

Figure J.9: Calculated codon level selection pressure on paralagous group 17. Levels above 0 are correspondent to positive selection pressure and levels below 0 are negative selection pressures. Anything over a selection pressure of ± 0.9 is considered significant.

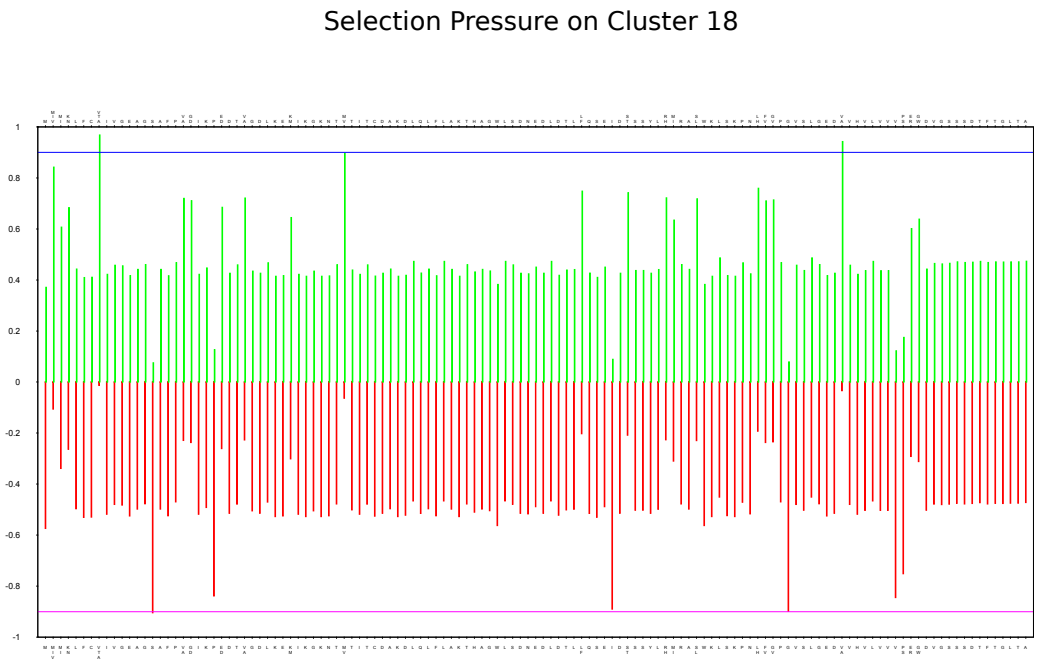

Figure J.10: Calculated codon level selection pressure on paralagous group 18. Levels above 0 are correspondent to positive selection pressure and levels below 0 are negative selection pressures. Anything over a selection pressure of ± 0.9 is considered significant.

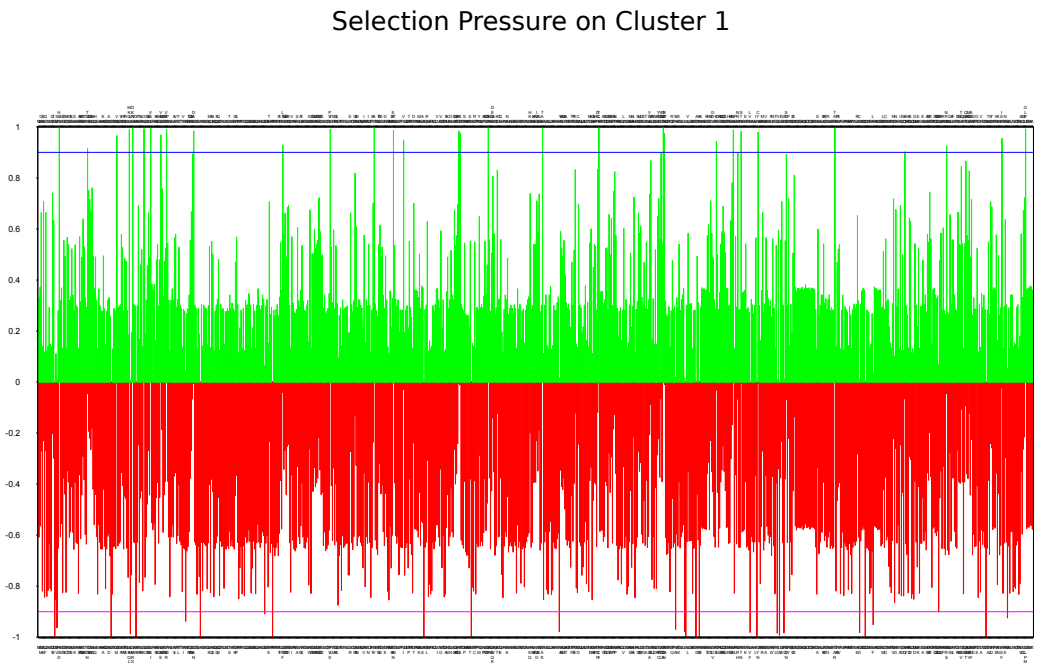

Figure J.11: Calculated codon level selection pressure on paralagous group 1. Levels above 0 are correspondent to positive selection pressure and levels below 0 are negative selection pressures. Anything over a selection pressure of ± 0.9 is considered significant.

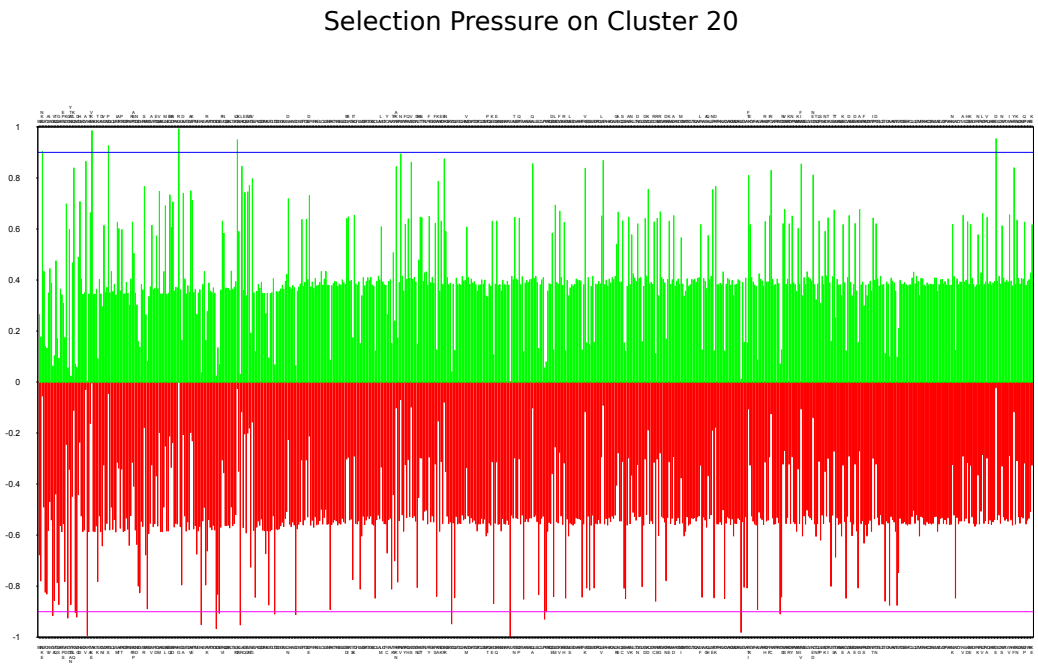

Figure J.12: Calculated codon level selection pressure on paralagous group 20. Levels above 0 are correspondent to positive selection pressure and levels below 0 are negative selection pressures. Anything over a selection pressure of ± 0.9 is considered significant.

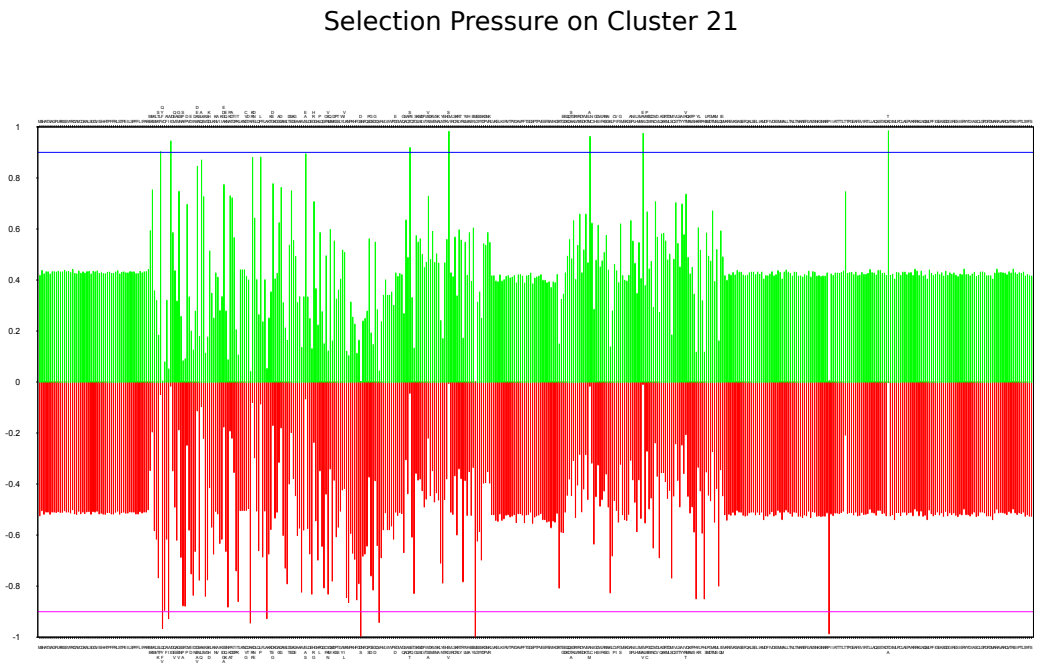

Figure J.13: Calculated codon level selection pressure on paralagous group 21. Levels above 0 are correspondent to positive selection pressure and levels below 0 are negative selection pressures. Anything over a selection pressure of ± 0.9 is considered significant.

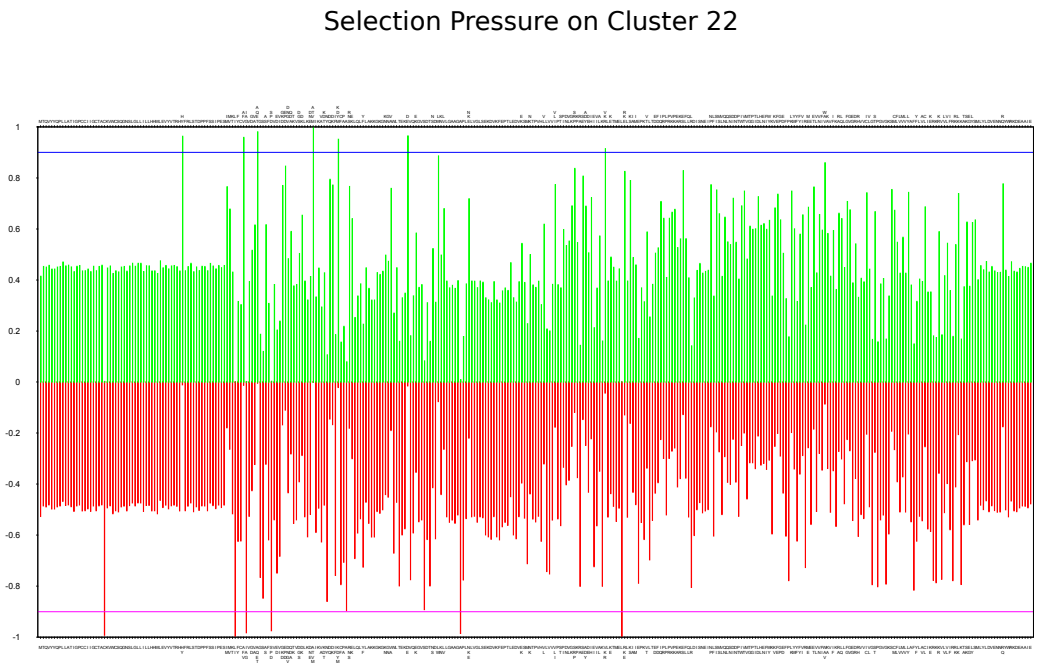

Figure J.14: Calculated codon level selection pressure on paralagous group 22. Levels above 0 are correspondent to positive selection pressure and levels below 0 are negative selection pressures. Anything over a selection pressure of ± 0.9 is considered significant.

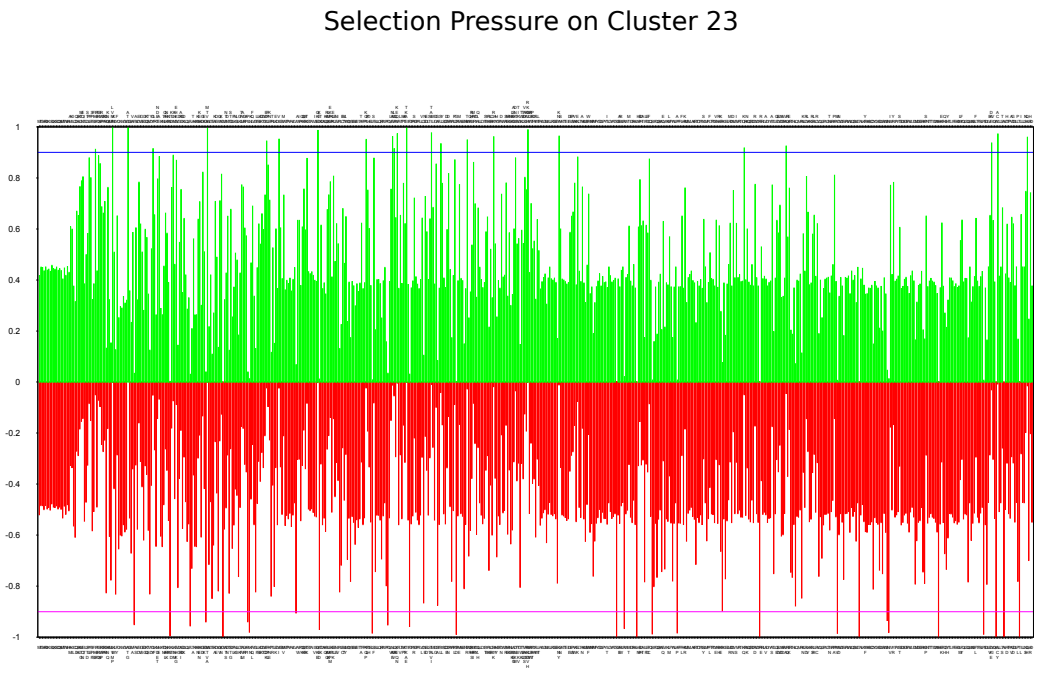

Figure J.15: Calculated codon level selection pressure on paralagous group 23. Levels above 0 are correspondent to positive selection pressure and levels below 0 are negative selection pressures. Anything over a selection pressure of ± 0.9 is considered significant.

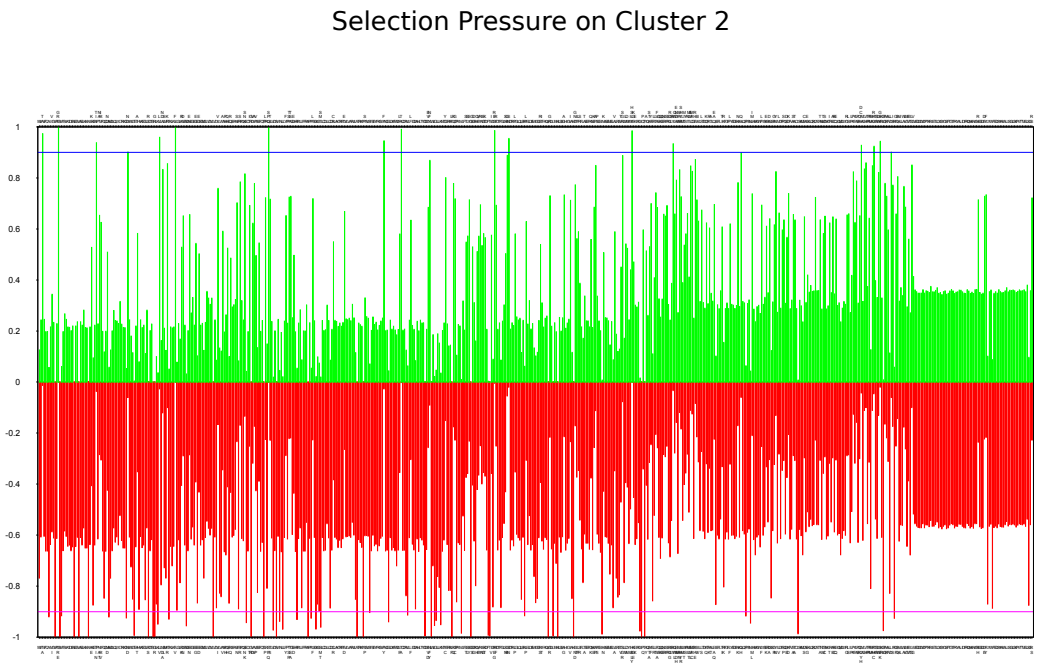

Figure J.16: Calculated codon level selection pressure on paralagous group 2. Levels above 0 are correspondent to positive selection pressure and levels below 0 are negative selection pressures. Anything over a selection pressure of ± 0.9 is considered significant.

Figure J.17: Calculated codon level selection pressure on paralagous group 3. Levels above 0 are correspondent to positive selection pressure and levels below 0 are negative selection pressures. Anything over a selection pressure of ± 0.9 is considered significant.

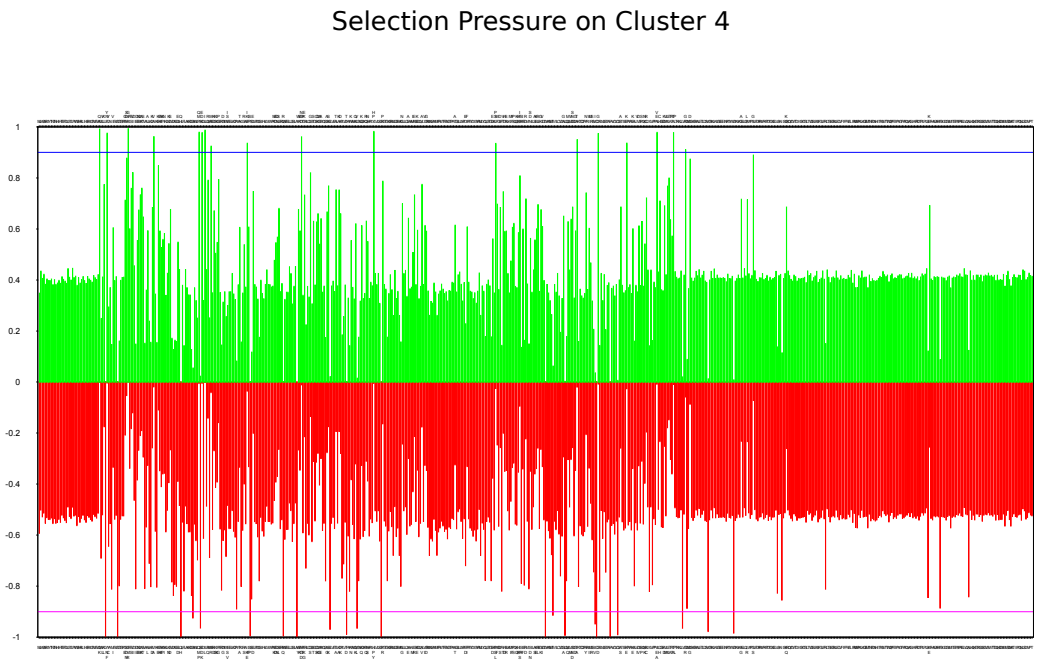

Figure J.18: Calculated codon level selection pressure on paralagous group 4. Levels above 0 are correspondent to positive selection pressure and levels below 0 are negative selection pressures. Anything over a selection pressure of ± 0.9 is considered significant.

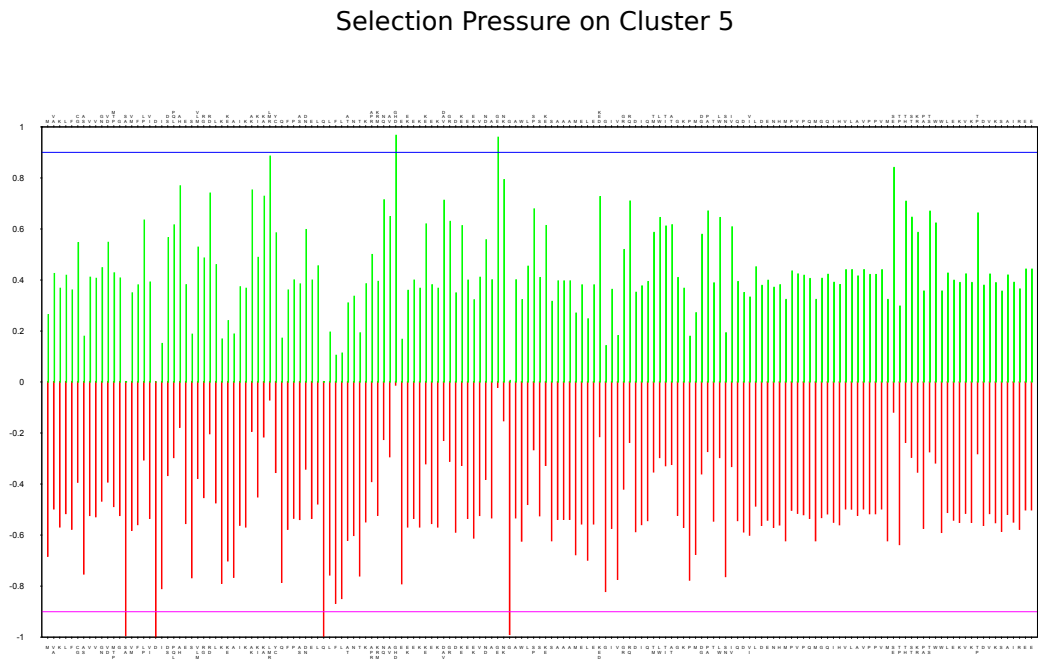

Figure J.19: Calculated codon level selection pressure on paralagous group 5. Levels above 0 are correspondent to positive selection pressure and levels below 0 are negative selection pressures. Anything over a selection pressure of ± 0.9 is considered significant.

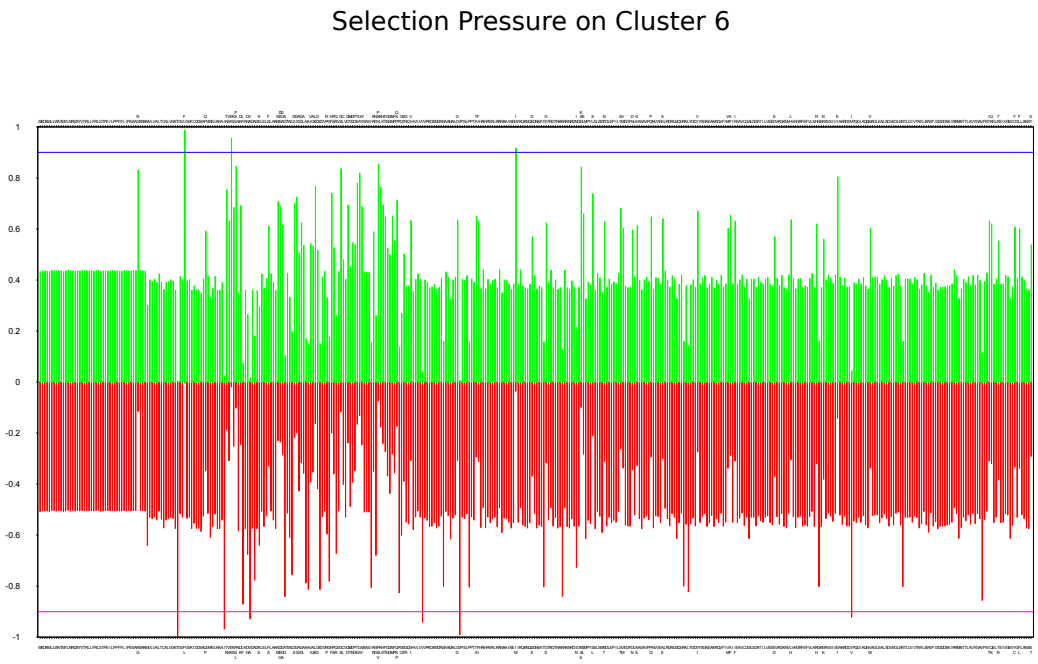

Figure J.20: Calculated codon level selection pressure on paralagous group 6. Levels above 0 are correspondent to positive selection pressure and levels below 0 are negative selection pressures. Anything over a selection pressure of ± 0.9 is considered significant.

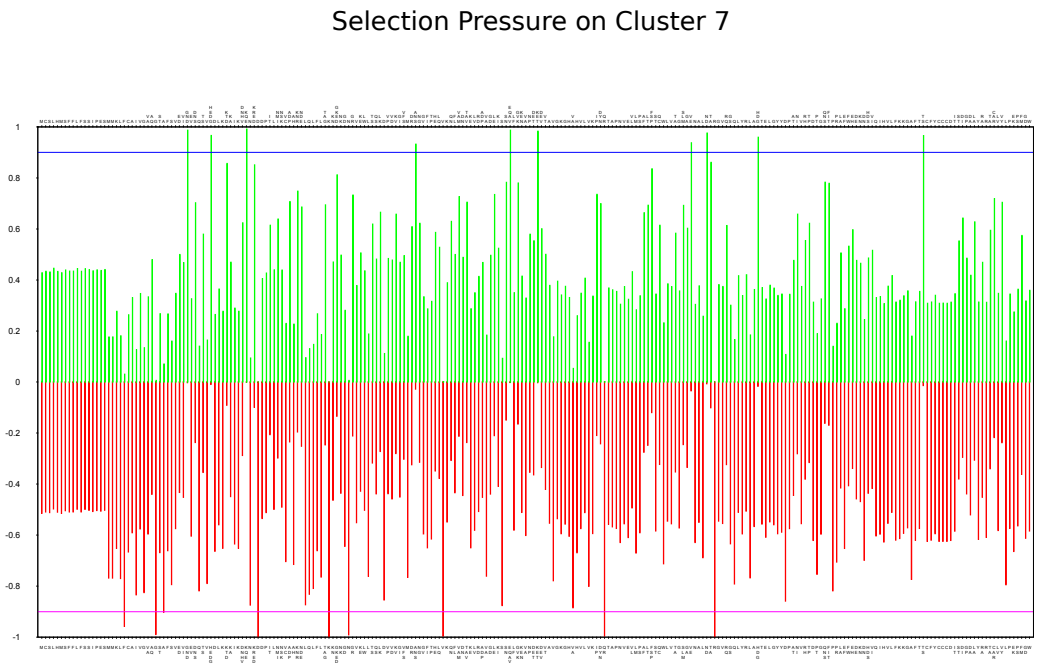

Figure J.21: Calculated codon level selection pressure on paralagous group 7. Levels above 0 are correspondent to positive selection pressure and levels below 0 are negative selection pressures. Anything over a selection pressure of ± 0.9 is considered significant.

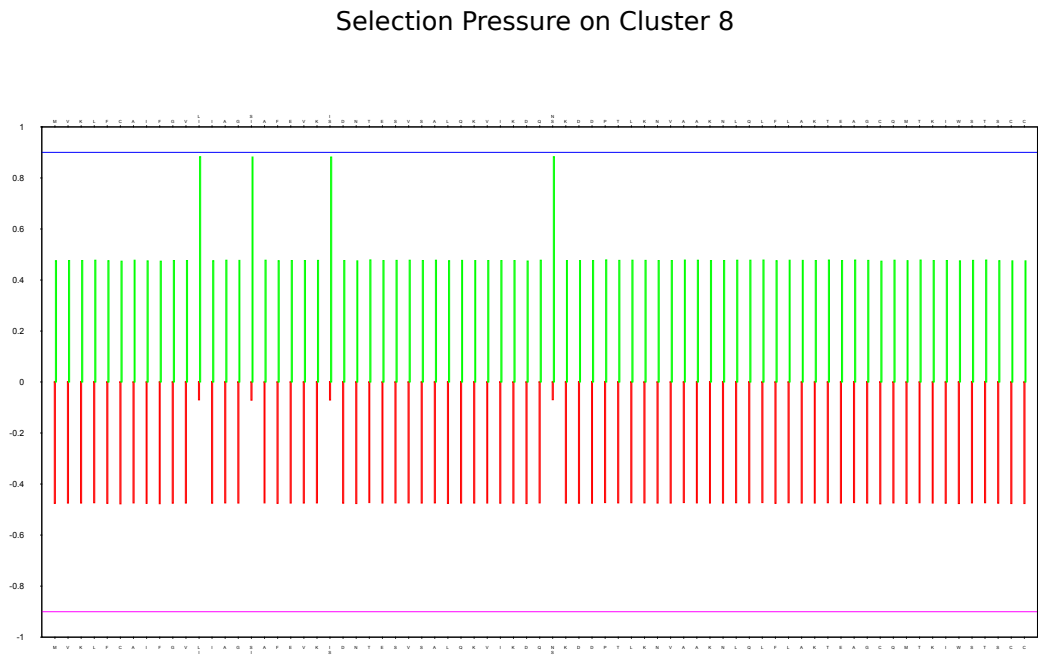

Figure J.22: Calculated codon level selection pressure on paralagous group 8. Levels above 0 are correspondent to positive selection pressure and levels below 0 are negative selection pressures. Anything over a selection pressure of ± 0.9 is considered significant.

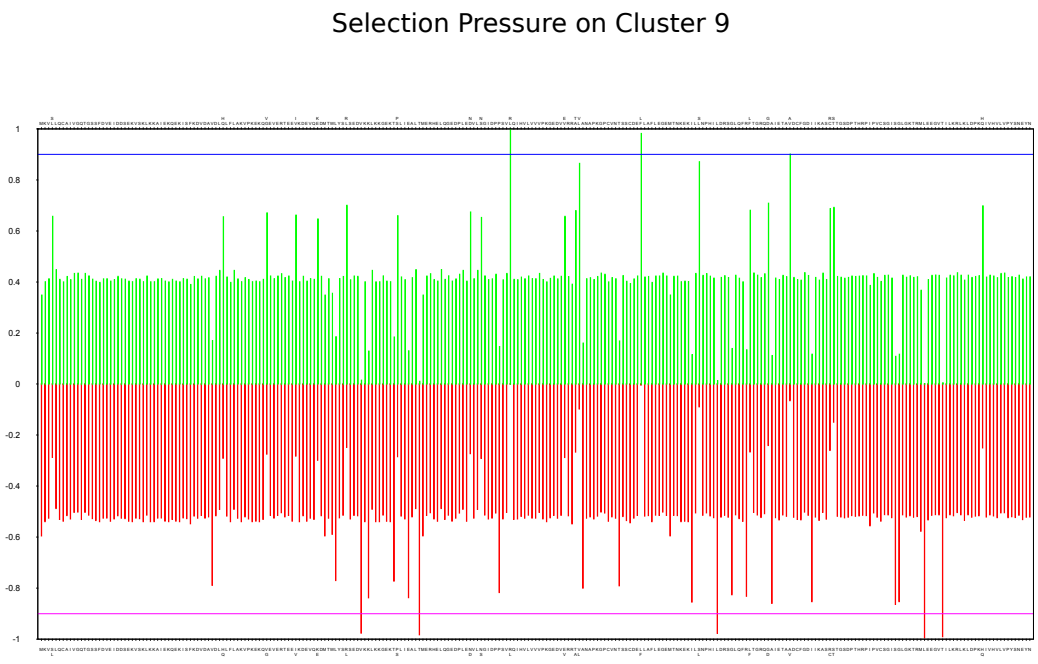

Figure J.23: Calculated codon level selection pressure on paralagous group 9. Levels above 0 are correspondent to positive selection pressure and levels below 0 are negative selection pressures. Anything over a selection pressure of ± 0.9 is considered significant.

Vita

Dylan Bobby Storey, only child of Robert and Diane, began his collegiate education at California State University, Fresno where he received a Bachelor of Science in Biology with a concentration in Molecular Cellular and Developmental biology. He then continued his education in the lab of Dr. Jim Prince at the same institution where he received his Masters of Science in Biology for his work on integrating linkage maps of *Capsicum annuum*.

He entered the University of Tennessee's Genome Science and Technology program in 2009 as an NSF IGERT trainee. In 2012 he was awarded a USDA-NIFA pre-doctoral fellowship for his proposed work on the application of novel graph theory algorithms to RNA-Seq data. His dissertation work while in the lab of Dr. Kurt Lamour has centered around the application of next generation sequencing technologies to assess and measure genomic levels of variation in the plant pathogens *P. capsici* and *P. tropicalis*.